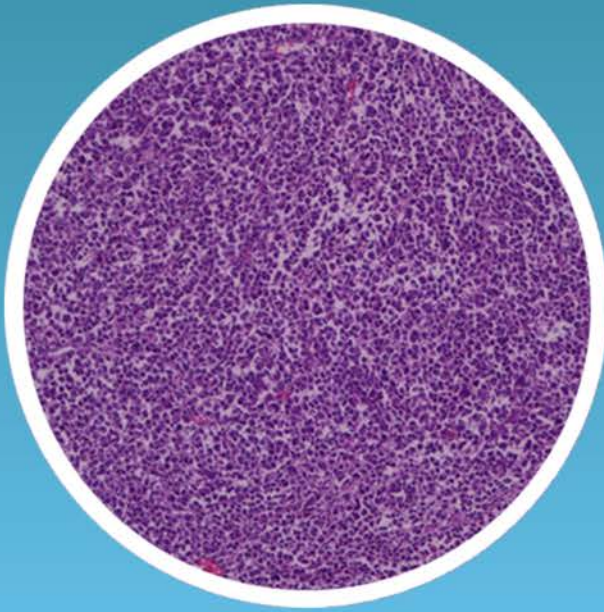




Volume 9 · Issue 3 · May 2023

e-ISSN: 2149-3189

The European Research Journal



Copyright © 2023 by Prusa Medical Publishing
Available at <http://dergipark.org.tr/eurj>



The European Research Journal

Aim and Scope

The European Research Journal (EuRJ) is an international, independent, double-blind peer reviewed, Open Access and online publishing journal, which aims to publish papers on all the related areas of basic and clinical medicine.

Editorial Board of the European Research Journal complies with the criteria of the International Council of Medical Journal Editors (ICMJE), the World Association of Medical Editors (WAME), and Committee on Publication Ethics (COPE).

The journal publishes a variety of manuscripts including original research, case reports, invited review articles, technical reports, how-to-do it, interesting images and letters to the editor. The European Research Journal has signed the declaration of the Budapest Open Access Initiative. All articles are detected for similarity or plagiarism. Publication language is English. The journal does not charge any article submission or processing charges.

EuRJ recommends that all of our authors obtain their own ORCID identifier which will be included on their article.

The journal is published bimonthly (January, March, May, July, September, and November).

Abstracting and Indexing

The journal is abstracted and indexed with the following: ULAKBİM TR Index (ULAKBİM TR DİZİN), NLM Catalog (NLM ID: 101685727), Google Scholar (h-index: 10), Index Copernicus (ICV 2021: 100), EMBASE, ProQuest Central, EBSCO Academic Search Ultimate, ROAD, SciLit, MIAR (ICDS 2021: 3.8), J-Gate, SHERPA/RoMEO, BASE, EZB, CrossRef, JournalTOCs, WorldCat, TURK MEDLINE, Turkish Citation Index, EuroPub, OpenAIRE, ResearchGate, SOBIAD, Advanced Science Index, ScienceGate, OUCI, Publons, (Clarivate Web of Science)

Publisher

The European Research Journal (EuRJ)
Prusa Medical Publishing
Konak Mh. Kudret Sk. Şenyurt İş Mrk. Blok No:6 İç kapı no: 3
Nilüfer/Bursa-Turkey
info@prusamp.com

www.dergipark.org.tr/eurj/
<http://www.prusamp.com>



e-ISSN: 2149-3189

The European Research Journal, hosted by Turkish JournalPark ACADEMIC, is licensed under a Creative Commons Attribution-NonCommercial-NoDerivatives 4.0 International License.



EDITORIAL BOARD

EDITOR-IN-CHIEF

Senol YAVUZ, MD,

Professor,

University of Health Sciences, Bursa Yuksek Ihtisas Training & Research Hospital,
Department of Cardiovascular Surgery,
Bursa, Turkey,

MANAGING EDITORS

Nizameddin KOCA, MD,

Associate Professor,

University of Health Sciences, Bursa Şehir Training & Research Hospital,
Department of Internal Medicine,
Bursa, Turkey

Soner CANDER, MD

Professor,

Uludag University Medical School,
Department of Endocrinology and Metabolism
Bursa, Turkey

Mesut ENGİN, MD,

Associate Professor,

University of Health Sciences, Bursa Yuksek Ihtisas Training & Research Hospital,
Department of Cardiovascular Surgery,
Bursa, Turkey

FOUNDING EDITOR

Rustem ASKIN, MD,

Professor of Psychiatry

İstanbul Ticaret University, Department of Psychology
İstanbul, Turkey

EDITORIAL ASSISTANT

Ugur BOLUKBAS

EDITORS

Omer SENORMANCI, MD

Professor,

Beykent University, Faculty of Arts-Sciences
Department of Psychology,
İstanbul, Turkey

Mahmut KALEM, MD,
Associate Professor,
Ankara University Medical School,
Department of Orthopedics and Traumatology,
Ankara, Turkey

Meliha KASAPOGLU AKSOY, MD
Associate Professor,
University of Health Sciences, Bursa Yuksek Ihtisas Training & Research Hospital,
Department of Physical Therapy and Rehabilitation,
Bursa, Turkey

Burcu DİNÇGEZ, MD
Associate Professor,
University of Health Sciences, Bursa Yuksek Ihtisas Training & Research Hospital,
Department of Gynecology and Obstetrics,
Bursa, Turkey

Arda ISIK, MD
Associate Professor,
Medeniyet University School of Medicine,
Department of General Surgery,
Istanbul, Turkey

Melih CEKINMEZ, MD
Professor,
University of Health Sciences, Adana City Training & Research Hospital,
Department of Neurosurgery,
Adana, Turkey

Kadir Kaan OZSIN, MD
Associate Professor,
University of Health Sciences, Bursa Yuksek Ihtisas Training & Research Hospital,
Department of Cardiovascular Surgery,
Bursa, Turkey

Alper KARAKUS, MD
Associate Professor,
University of Health Sciences, Bursa Yuksek Ihtisas Training & Research Hospital,
Department of Cardiology,
Bursa, Turkey

Onur KAYGUSUZ, MD.,
Associate Professor,
Uludag University School of Medicine,
Department of Urology,
Bursa, Turkey

Sayad KOCAHAN, PhD,
Professor,
University of Health Sciences, Gülhane Medical Faculty,
Department of Physiology,
Ankara, Turkey

Gokhan OCAKOGLU, Ph.D.,
Associate Professor,
Uludag University School of Medicine,
Department of Biostatistics,
Bursa, Turkey

Nurullah DOGAN, MD,
Associate Professor,
Doruk Nilüfer Hospital,
Department of Radiology,
Bursa, Turkey

INTERNATIONAL EDITORIAL BOARD MEMBERS

Ahmet KIZILAY, MD
Professor,
Inönü University School of Medicine,
Department of Otorhinolaryngology,
Malatya, Turkey

Aron Frederik POPOV, MD
Professor,
University of Frankfurt,
Department of Cardiothoracic Surgery,
Frankfurt, Germany

Cristina FLORESCU, MD
Associate Professor,
University of Craiova,
Department of Medicine and Pharmacy,
Romania

Elif EKINCI, MD
MBBS, FRACP, PhD
University of Melbourne
Department of Medicine,
Melbourne, Australia

Essam M MAHFOUZ, MD
Professor,
University of Mansoura School of Medicine
Department of Cardiology,
Mansoura, Egypt

Francesco CARELLI, MD
Professor,
University of Milan School of Medicine,
Department of Family Medicine,
Milan, Italy

Gary TSE, MD, PhD

Assistant Professor,
The Chinese University of Hong Kong,
Department of Medicine and Therapeutics,
Hong Kong, China

Kendra J. GRUBB, MD, MHA, FACC

Assistant Professor,
Emory University School of Medicine,
Department of Cardiovascular Surgery,
Atlanta, GA, USA

Muzaffer DEMIR, MD

Professor,
Trakya University School of Medicine,
Department of Hematology,
Edirne, Turkey

Nader D NADER, MD

Professor,
University of Buffalo School of Medicine
Department of Anesthesiology,
NY, USA

Sait Ait BENALI, MD

Professor,
Cadi Ayyad University School of Medicine,
Department of Neurosurgery,
Marrakech, Morocco

Sedat ALTIN, MD

Professor,
University of Health Sciences, Yedikule Training & Research Hospital,
Department of Chest Diseases,
Istanbul, Turkey

Semih HALEZEROGLU, MD, FETCS

Professor,
Acibadem University School of Medicine,
Department of Thoracic Surgery,
Istanbul, Turkey

Veysel TAHAN, MD, FACP, FACG, FESBGH

Assistant Professor,
University of Missouri,
Division of Gastroenterology and Hepatology,
Columbia, Missouri, USA

Yenal DUNDAR, MD

Consultant Psychiatrist
Central Queensland Hospital and Health Service,
QLD, Australia

Table of Contents

Original Articles

- Can tolvaptan usage cause cytotoxicity? An in vitro study** 454-460
Beril ERDEM TUNÇDEMİR
- Comparing the closure of hepatocaval ligament using stapler or suturing in liver surgery** 461-467
Imam Bakır BATI, Umut TÜYSÜZ
- Are body mass index and the systemic immune-inflammation index risk factors for carpal tunnel syndrome?** 468-476
Meltem KARACAN GÖLEN, Dilek YILMAZ OKUYAN
- GSTM1, GSTP1, p53 as some probable predictors of prognosis in primary and metastatic epithelial ovarian cancer** 477-483
Gizem ÖZER, Pınar KAYGIN, Onur DİRİCAN, Serpil OĞUZTÜZÜN, Sezen YILMAZ SARIALTIN, Gülçin GÜLER ŞİMŞEK, Ayşegül ERDEM, Murat KILIÇ, Tülay ÇOBAN
- Determination of anti-HCV signal to cut-off value in patients with hepatitis C virus infection and the variety of antibody responses** 484-494
Murat OCAL, Mehmet Emin BULUT
- Is primary dysmenorrhea affected by gray matter volumetric changes in the brain?** 495-501
Ela KAPLAN, Selçuk KAPLAN
- Importance of paravertebral muscle quality in the etiology of degenerative lumbar spinal stenosis** 502-510
İsmail KAYA
- Percutaneous nephrostomy experience in pediatric patients: comparison of fine and thick needle techniques** 511-516
Omer Fatih NAS, Muhammet OZTEPE, Selman CANDAN, Sedat Giray KANDEMİRLİ, Cem BİLGİN, Mehmet Fatih İNECİKLİ, Güven ÖZKAYA, Gokhan ONGEN, Cüneyt ERDOĞAN
- Expression and prognostic value of ING3 in advanced laryngeal squamous cell carcinoma** 517-528
Neslişah BARLAK, Gülnur KUŞDEMİR, Rasim GUMUS, Abdulkadir ŞAHİN, Betül GÜNDOĞDU, Ömer Faruk KARATAS, Arzu TATAR
- Evaluation of hematopoietic- and neurologic-expressed sequence 1-like (HN1L) protein levels in tissue and plasma of breast cancer patients** 529-535
Elif ERTURK, Mehmet SARİMAHMUT, Mustafa Şehsuvar GÖKGÖZ, Sahsine TOLUNAY
Sayfa: 529-535
- Information, attitudes and behaviors of mothers about breastfeeding behavior during the COVID-19 pandemic process** 536-542
Mehmet Emin PARLAK, Osman KÜÇÜKKELEPÇE, Dilek ENER, Erdoğan ÖZ, Volkan BAYAR
- Immunohistochemical approach to obesity disease in terms of expression levels of glutathione s-transferase (sigma, zeta, theta) isozymes** 543-554
Mahammad DAVUDOV, Hakan BULUŞ, Onur DİRİCAN, Pınar KAYGIN, Gülçin GÜLER ŞİMŞEK, Sezen YILMAZ SARIALTIN, Fatıma Nurdan GÜRBÜZ, Serpil OĞUZTÜZÜN

Investigation of general surgery consultations in COVID-19 patients treated in a tertiary hospital	555-560
<i>Mehmet Eşref ULUTAŞ, Kemal ARSLAN</i>	
Evaluation of the uric acid and hematological parameters in patients with nodal hand osteoarthritis	561-566
<i>Ayşe ÜNAL ENGİNAR</i>	
Protective effects of methylprednisolone in kidney: aortic occlusion-reperfusion model in rats	567-573
<i>Serkan SEÇİCİ, Kadir Kaan ÖZSİN, M.özgür ÖZYİĞİT, Omer ARDA, Yasemin ÜSTÜNDAĞ</i>	
Evaluation of organ donation process and affecting factors in COVID-19 pandemic	574-581
<i>Gökhan KILINÇ, Fuat ÇÖKEN</i>	
Evaluation of novel ventricular repolarization parameters in patients with acromegaly	582-590
<i>Hayati EREN, Selin GENÇ, Bahri EVREN, İbrahim ŞAHİN</i>	

Reviews

The mechanism of mindfulness meditation on pain by functional magnetic resonance imaging method	591-599
<i>Yasemin YILDIZ, Sayad KOCAHAN, Alp Eren ÇELENLİOĞLU, Mehmet ÖZLER</i>	

Case Report

Primary bone diffuse B cell lymphoma of the thoracic spine: a rare entity	600-604
<i>Emrah AKÇAY, Hüseyin Berk BENEK, Hakan YILMAZ, Alper TABANLI, Alaattin YURT</i>	
Ovarian malignant melanoma metastasized from skin mimicking a benign cyst: a rare case report and mini-review of the literature	605-610
<i>Fatma KETENCİ GENCER, Bülent BABAOĞLU, Zeynep Kübra USTA KURT, Hatice YAŞAT NACAR, Sibel BEKTAŞ</i>	
Surgical approach to neglected giant cervical fibroids	611-617
<i>Cagdas Nurettin EMEKLİOĞLU, Emine AYDİN, Merve KONAL, Hicran ŞİRİNOĞLU, Erhan AKTÜRK, Ozgur AKBAYİR</i>	

Can tolvaptan usage cause cytotoxicity? An in vitro study

Beril Erdem Tunçdemir^{ORCID}

Department of Biology, Molecular Biology Section, Hacettepe University, Faculty of Science, Ankara, Turkey

ABSTRACT

Objectives: Tolvaptan is a nonpeptide V2 (vasopressin) receptor antagonist which is commonly used for treatment of hypernatremia. Besides it is mostly used for rescue strategies of mutant V2 receptors which are responsible for congenital type of Nephrogenic Diabetes insipidus (NDI) as a pharmacological chaperone (PC) treatment. Tolvaptan is metabolized by CYP3A4 and usage of tolvaptan may cause cytotoxicity which can be prevented by antioxidants. The aim of this study is investigating cytotoxic effect of tolvaptan on COS-1 cells and preventing it via antioxidants such as Vitamin C and N-acetyl cysteine (NAC).

Methods: To measure cytotoxicity of tolvaptan, COS-1 cells were separated in three groups; tolvaptan, tolvaptan+Vitamin C and tolvaptan+NAC. 24 h after cells were seeded in 96-well plates, they were treated with different concentrations of tolvaptan, tolvaptan+Vitamin C and tolvaptan+NAC. After 24 h incubation, the (3-(4,5-Dimethylthiazol-2-yl)-2,5-diphenyltetrazolium bromide) [MTT] analysis were performed and GraphPad Prism 5.01 for Windows was used for statistical analysis.

Results: According to results of MTT assay, treatment with tolvaptan did not decrease cell viability except that treatment of 10^{-5} M tolvaptan showed significantly decrease on cell viability compared to control group. At the concentration of 10^{-9} M, there was significantly different cell viability between treated with tolvaptan and tolvaptan+Vitamin C.

Conclusions: Tolvaptan may show its cytotoxic effects when it is used for the treatment of hyponatremia than its usage of as a PC. Since low concentrations of tolvaptan for a short time treatment is enough for its PC role, it may not show any cytotoxic effect on cells which is coherent with our results.

Keywords: Tolvaptan, cytotoxicity, cell culture, hyponatremia, nephrogenic diabetes insipidus, pharmacological chaperone

Arginine vasopressin (AVP) is a small peptide hormone that plays a critical role in body water and sodium homeostasis and also regulating serum osmolality [1]. AVP shows its effects on V1a, V1b and V2 receptors (vasopressin receptors) which are mainly seen in the heart and blood vessels, anterior pituitary

and collecting ducts in the kidney, respectively. In physiological conditions, when urine osmolality increase and plasma serum level decrease, AVP is secreted from posterior pituitary which causes increased water reabsorption resulting in an increase of total body water. AVP levels are excessively increased in several clinical



e-ISSN: 2149-3189

Received: January 16, 2022; Accepted: April 27, 2022; Published Online: August 20, 2022

How to cite this article: Erdem Tunçdemir B. Can tolvaptan usage cause cytotoxicity? An in vitro study. Eur Res J 2023;9(3):454-460. DOI: 10.18621/eurj.1058030

Address for correspondence: Beril Erdem Tunçdemir, PhD., Hacettepe University, Faculty of Science, Department of Biology, Molecular Biology Section, Beytepe Campus, 06800 Ankara, Turkey. E-mail: beril@hacettepe.edu.tr, Phone: +90 312 297 80 00, Fax: +90 312 299 20 28
Copyright © 2022 by Prusa Medical Publishing



©Copyright © 2023 by Prusa Medical Publishing
Available at <http://dergipark.org.tr/eurj>
info@prusamp.com

cal situations such as syndrome of inappropriate antidiuretic hormone (SIADH), polycystic kidney disease (PKD), liver cirrhosis and heart failure [2, 3]. Hyponatremia is seen as the most common electrolyte disorder in hospitalized patients [4, 5] and many studies showed that hyponatremia can increase mortality in patients with liver cirrhosis, congestive heart failure and neurological diseases [6-9]. Traditional treatment of hyponatremia is fluid restriction with or without the usage of lithium, demeclocycline and urea can be remained incomplete in clinical practice because different pathophysiological mechanisms have multiple causes [3, 10]. Usage of vasopressin antagonists known as vaptans can induce electrolyte free excretion of water; therefore, they provide a more effective option to treat hyponatremia [3, 4, 10, 11]. Vaptans are non-peptide vasopressin receptor antagonists which can be usable both orally and intravenously. Tolvaptan, which is a selective V2 receptor antagonist, is an orally active molecule that is commonly used for the treatment of hyponatremia. Tolvaptan was evaluated in many studies such as "Study of Ascending Levels of Tolvaptan in Hyponatremia" (SALT-1 and 2), "The Efficacy of Vasopressin Antagonism in Heart Failure Outcome Study with Tolvaptan" (EVEREST) and autosomal dominant PKD [5, 11-14]. On the other hand, V2 vasopressin antagonists mostly have been studied in functional analysis studies on Nephrogenic Diabetes insipidus which is characterized imbalance of body water homeostasis that is a related pathway mentioned above. V2 receptor mutations can affect maturation of receptor protein and they can be trapped by Endoplasmic reticulum (ER) quality control mechanism in the cell. Therefore, they cannot perform their function properly in the kidney. Last years, many vasopressin agonists and antagonists (tolvaptan belong to this group) have been used as a pharmacological chaperone (PC) to rescue these mutant receptors from ER. PCs are small cell-permeable molecules that bind specifically to a misfolded protein and help its stabilization throughout decreasing the folding energy barrier [15, 16]. As a PC, tolvaptan has a potential to rescue ER-trapped misfolded protein and helps it to become functional again [17-19]. Studies of functional analysis and PC rescue about GPCRs mostly use COS-1 or COS-7 cell lines which were derived from the CV-1 fibroblast cell line (kidney cell of an adult African green monkey) in addition to other cell line

types, and COS-1 and COS-7 are different from each other in terms of early region of SV40 DNA [15, 17, 20-26]. COS cell line was used in this study because we have been functionally analyzed and showed rescue potential of mutant V2 receptors via PCs in our previous and ongoing studies and therefore it was aimed to show cytotoxic effects of tolvaptan on COS-1 cells. In addition to PC studies, many of the other studies showed that tolvaptan is successful to increase serum sodium levels in patients with hyponatremia related with heart failure, cirrhosis and SIADH [27, 28]. On the contrary, in the present time, tolvaptan are not recommended for routine use in patients with PKD. Also, FDA restricts the maximum usage period of tolvaptan as 30 days because of the increased level of liver enzymes may cause hepatic toxicity with prolonged use [11, 29, 30]. PC studies show that small concentrations of tolvaptan can be enough to rescue mutant protein [18]. Even so it could cause toxicity in the cell. For this reason, it is important to decrease cytotoxicity of tolvaptan when it is used as a PC in case it has a toxic effect. Consequently, the aim of this study is to show cytotoxic effects of tolvaptan on cell viability and to prevent these effects by antioxidants such as vitamin C and N-acetyl cysteine (NAC) in case it shows cytotoxicity.

METHODS

Chemicals

Tolvaptan (Sigma-Aldrich) were prepared as 1 mM stock solution in DMSO (Cell culture grade, AppliChem GmbH). Vitamin C (Basel Kimyevi Mad. ve İlaç San. Tic. A.Ş.) was prepared from 500 mg/ml injection solution as 1 mM in DMEM and NAC (Bayer Türk Kimya San. Ltd. Şti.) was prepared from 600 mg effervescent tablet which was first dissolved in 50 ml cell culture grade water then, was made as 1 mM stock solution in DMEM. Stock solutions of Vitamin C and NAC were freshly prepared before usage. Dulbecco's modified Eagle's medium (DMEM) High Glucose with stable Glutamine and sodium pyruvate (Biowest SAS France facility) supplemented with 10% fetal bovine serum (originated in South America), 100 U/ml penicillin and 10 µg/ml streptomycin was used as a medium in the cell culture.

Cell Culture Studies

COS-1 cell line was purchased from AddexBio Technologies (T0014001, Lot number: 0013255) in 2017 for our previous studies and they have been kept as stocks in liquid nitrogen. For this study, they cells were grown in DMEM supplemented with 10% FBS, 100 U/ml penicillin and 10 µg/ml streptomycin, in 5% CO₂ in air, at 37°C. Cells were seeded on 96-well plates as 50.000 cells/well as a three group. After 24 h, media were removed and one group was treated with only tolvaptan in different concentrations (between 10⁻⁵ and 10⁻⁹ M). Other two groups were treated as tolvaptan together with Vitamin C, and tolvaptan together with NAC (as the same concentrations of both). After 24 h incubation, the (3-(4,5-Dimethylthiazol-2-yl)-2,5-diphenyltetrazolium bromide) [MTT] assay was performed.

MTT Assay

MTT is a reagent that is commonly used to define cell viability in cell culture studies. Formation of MTT formazan crystals is used to determine viable cells in this colorimetric method [28]. To measure the viability of the cells, after the incubation with tolvaptan and antioxidants of the cells, medium was removed and freshly prepared 100 µl 0.5 mg/ml MTT was added to the well and plates were incubated for 4 hours in 37°C in dark. Then, the MTT reagent was removed and replaced with 100 µl isopropanol to solubilize the converted purple dye in wells. Absorbance at 570 nm was measured with EnSight Multimode Plate Reader (Perkin Elmer).

Statistical Analysis

For statistical analysis, tolvaptan treatment was compared with control group, tolvaptan+Vitamin C group and tolvaptan+ NAC group, separately. Two-way ANOVA was used as a statistical analysis to determine the prevention of cytotoxicity of tolvaptan with using Vitamin C and NAC. The level of significance was taken as $p < 0.05$ in all instances. Statistical analysis was performed by using GraphPad Prism 5.01 for Windows (GraphPad Software).

RESULTS

For all comparisons, untreated COS-1 cells were set to 100% as a control group. According to the percentages of MTT assay results, it was seen that increased tolvaptan treatment caused increased cytotoxicity since the percentages of cell viability decreased (Table 1). In addition, Vitamin C and NAC treatment did not increase the cell viability when it is compared with the group of only treated with tolvaptan. In other words, the percentage values were not increased with the treatment of antioxidants (Table 1). However, when these results were statistically analyzed, it was seen that cells treated only with 10⁻⁵ M tolvaptan showed significantly decreased cell viability compared to the control group ($p = 0.0023$) (Table 2). Also, at the concentration of 10⁻⁹ M, there was significantly different cell viability between treated with tolvaptan and tolvaptan together with Vitamin C ($p = 0.0129$) (Table 2).

Table 1. MTT assay results as percentages are seen

Concentration	Tolvaptan		Tolvaptan + Vitamin C		Tolvaptan + NAC	
	Mean (%)	SD	Mean (%)	SD	Mean (%)	SD
10 ⁻⁵ M	67.9	2.7	68.3	6.8	63.0	5.2
10 ⁻⁶ M	79.5	9.9	77.0	11.1	78.3	15.8
10 ⁻⁷ M	88.1	6.5	83.5	6.2	84.9	5.7
10 ⁻⁸ M	89.5	9.5	89.5	8.8	87.2	13.3
10 ⁻⁹ M	92.5	3.5	97.3	2.9	94.5	7.7

The data are given as mean ± S.D. of independent experiments (n = 3). For all concentrations, untreated sample of COS-1 cells was set to 100% as a control. MTT = the 3-(4,5-dimethylthiazol-2-yl)-2,5-diphenyl tetrazolium bromide, NAC = N-acetyl cysteine, SD = standard deviation

Table 2. Comparison of groups

Groups	p value
10 ⁻⁵ M Tolvaptan vs Control	0.0023
10 ⁻⁹ M Tolvaptan vs 10 ⁻⁹ M Tolvaptan + Vitamin C	0.0129

Significant p values between the groups were analyzed. All groups were compared between each other and also with the control group using with two-way ANOVA and only significant P values were presented in this table. The level of significance was taken as $p < 0.05$ in all instances. Statistical analysis was performed by using GraphPad Prism 5.01 for Windows (GraphPad Software).

DISCUSSION

Vaptans are nonpeptide V2 receptor antagonists and they are resembling AVP. Tolvaptan, one of these vaptans, is an orally usable and non-peptide V2 receptor antagonist [3]. It has approximately 2-fold greater affinity to V2 receptor than its specific ligand, AVP [31]. Tolvaptan has an ability to increase urine free water excretion causing decreased urine osmolality and increased sodium level [31].

At the first double-blind study, the effects of 30 mg, 45 mg and 60 mg of tolvaptan usage once in a daily for 25 days was investigated in patients with chronic heart failure (CHF) and it was found that CHF patients tolerated tolvaptan well and their serum sodium levels were normalized compared to the placebo group [32]. According to the SALT-1 and SALT-2 trials, which were about evaluation of tolvaptan usage effects on hyponatremia associated with congestive heart failure, cirrhosis of the liver and SIADH, serum sodium levels of patients were improved but after one week of discontinuation, reverted to hyponatremic conditions [5]. Prolonged use of tolvaptan (804 days) caused normalization of serum sodium levels [33]. The results of the EVEREST trials showed that tolvaptan usage made normalize of serum sodium levels in patients with congestive heart failure but it did not demonstrate any survival benefit for patients [12, 34-36]. At the TEMPO trials which were about evaluation of tolvaptan treatment in patients with autosomal dominant PKD, progression of PKD was delayed but transaminases were seen as increased more than 3 times in patients with tolvaptan group [2]. After that, US Food Drug Administration (FDA) restricted the usage of tolvaptan more than 30 days be-

cause of the probability of liver toxicity. At all those trials, the doses of tolvaptan were approximately between 15 mg and 60 mg in a day. Above this dosage and also prolonged usage were reported to cause liver dysfunction via toxicity because tolvaptan is mainly metabolized by CYP3A4 [11, 37]. All these trials were conducted with higher concentrations of tolvaptan treatment in patients; therefore, our results of cellular toxicity cannot be compared with these trials because our results are more meaningful for very small dosages of tolvaptan which could be measured in the cell culture system. A study about determining the mechanism of hepatotoxicity of tolvaptan in HepG2 cells showed that tolvaptan inhibited cell cycle progression, induced DNA damage and executed apoptosis [9]. Also, they found that tolvaptan affected many signaling pathways that cause cytotoxicity [9]. 24 h treatment of HepG2 cells with different tolvaptan concentrations from 1.56 to 100 μ M showed that short time as a 24 h-treatment slightly decreased cell viability. The most obvious decrease which was about 40-50% was seen in 100 μ M concentration of tolvaptan [9]. During 24 h treatment, cell viability decrease was seen at 25 μ M concentration which can be compatible with the results of this study because the difference between even in 10 μ M-treated cells and the control group of cell viability was found significant ($p = 0.0023$) (Table 2). More than 10⁻⁵ M concentration of tolvaptan could cause cytotoxicity with more than 24 h which is known through the clinical studies. However, in this study the experiments were performed for only 24 h because PC studies (which were mentioned in detailed below) mostly treat cells with PCs for 18-24 h and short-time treatment is mostly enough to rescue of mutant protein using with PCs [18, 38].

The disease nephrogenic syndrome of inappropriate antidiuresis (NSIAD) is caused by gain-of-function mutations in the V2 receptor gene (arginine vasopressin receptor 2, AVPR2) [39]. Mutations of Phe229 and Arg137 in AVPR2 were found that cause gain-of-function in the V2 receptor and consequently, it was reported that infants who had these mutations showed clinical symptoms related with hyponatremia [39]. In another study showed that I130N mutation in AVPR2 cause gain-of-function in the V2 receptor which is responsible of constitutive activity of cAMP production [40]. They showed that tolvaptan blocked this basal activity of cAMP production through its inverse ago-

nist property and they proposed that tolvaptan could be a treatment for hyponatremia in patients with NSIAD who have I130N mutation in AVPR2 [40]. On the other hand, many studies showed that loss-of-function mutations in AVPR2 are responsible of NDI. NDI is characterized as an imbalance of body water homeostasis which is normally controlled by antidiuretic hormone AVP via kidney [41]. Functional analysis studies about these loss-of-function mutations in patients with NDI revealed that presence of a mutation may show its effect on function at different levels. Instead, it can cause the mutant V2 receptor is retained in the ER quality control mechanism. Therefore, even if these mutant V2 receptors are functional, they cannot escape from the ER and locate on plasma membrane where they function [18, 38]. To correct this trafficking problem and make mutant V2 receptors functional again, PCs can be used because they are nonpeptide and cell-permeable ligands that bind specifically to the mutant receptor and stabilize receptors conformation [42]. In this way, PCs help mutant V2 receptors to be rescued and located where they are functional again [38, 43, 44]. Tolvaptan is a kind of PC that commonly used in these studies because its rescue potential which was reported by many researches has an importance on to develop new treatment strategies for NDI [17-19]. The treatment dosages of tolvaptan were mostly 1 μM or 10 μM at these studies and they all reported that this low level of tolvaptan usage (and also for a short time like 24 h, etc.) was enough to rescue and make functional mutant V2 receptor. They did not report any cytotoxic effect of tolvaptan in cell culture studies [17-19]. In this study, the maximum concentration of tolvaptan was 10 μM and it was seen just a slight decrease on cell viability (Table 1). Therefore; it can be said that tolvaptan is not cytotoxic for the cells when it is used as a low dose-PC to rescue mutant V2 receptors. Because of this result, treatment of equimolar dose of Vitamin C and NAC with tolvaptan did not show any significant difference about cell viability than treated with only tolvaptan, except the treatment of equimolar dose of 10^{-9} M Vitamin C and tolvaptan ($p = 0.0129$) (Table 2). If it was seen very low cell viability in the group of treated with just tolvaptan, it could be said that tolvaptan treatment might show its cytotoxic effects through the oxidative stress. Since the tolvaptan is metabolized by the cytochrome P450 system, it

might be said that reactive oxygen species (ROS) could be occurred and consequently oxidative stress might show itself [10, 45, 46]. At these kinds of situations, antioxidants such as Vitamin C and NAC may help to reduce oxidative stress in the cell. Vitamin C and NAC may mediate their antioxidant roles via scavenging ROS [45]. Thus, Vitamin C and NAC could be used as antioxidants if it was found a significant cytotoxic effect of tolvaptan. However, there was no cytotoxicity observed. Just at very low concentration (10^{-9} M) of tolvaptan and Vitamin C treatment together, it was seen a significant antioxidant effect of Vitamin C compared to the only tolvaptan treated group ($p = 0.0129$) (Table 2). Even if it was found a significant difference between the group of treated with tolvaptan only and the group of treated with tolvaptan and Vitamin C together, according to the results, it was concluded that the usage of low concentration of tolvaptan did not show any significant effect on cytotoxicity. However, prevention of the cytotoxicity of high dosages of tolvaptan usage, which is known through the clinical studies, using with antioxidants such as Vitamin C and NAC will shed light into the future studies.

CONCLUSION

As a conclusion, tolvaptan is a very successful V2 receptor antagonist for treatment of the hyponatremia. It also can be used as a PC to rescue of misfolded mutant V2 receptor protein from ER to the plasma membrane of the kidney where it shows its function. Tolvaptan may show its cytotoxic effects when it is used for the treatment of hyponatremia than its usage of as a PC. Since low concentrations of tolvaptan for a short time treatment is enough for its PC role, it may not show any cytotoxic effect on the cells which is coherent with our results. In accordance with that, it was seen in this study, the cytotoxic effects of higher concentrations of tolvaptan cannot be prevented by Vitamin C and NAC. However, when tolvaptan was used as low concentration as like a PC, we showed that cytotoxicity of the tolvaptan was significantly decreased with using Vitamin C.

Authors' Contribution

Study Conception: BET; Study Design: BET; Su-

pervision: BET; Funding: BET; Materials: BET; Data Collection and/or Processing: BET; Statistical Analysis and/or Data Interpretation: BET; Literature Review: BET; Manuscript Preparation: BET and Critical Review: BET.

Conflict of interest

The authors disclosed no conflict of interest during the preparation or publication of this manuscript.

Financing

The authors disclosed that they did not receive any grant during conduction or writing of this study.

REFERENCES

1. Ali F, Guglin M, Vaitkevicius P, Ghali JK. Therapeutic potential of vasopressin receptor antagonists. *Drugs* 2007;67:847-58.
2. Torres VE. Vasopressin receptor antagonists, heart failure, and polycystic kidney disease. *Annu Rev Med* 2015;66:195-210.
3. Yi JH, Shin HJ, Kim HJ. V2 receptor antagonist; tolvaptan. *Electrolyte Blood Press* 2011;9:50-4.
4. Bichet DG. What is the role of vaptans in routine clinical nephrology? *Clin J Am Soc Nephrol* 2012;7:700-3.
5. Schrier RW, Gross P, Gheorghiade M, Berl T, Verbalis JG, Czerwiec FS, et al. Tolvaptan a selective oral vasopressin v2 receptor antagonist for hyponatremia. *N Engl J Med* 2006;355:2099-112.
6. Bhardwaj A. Neurological impact of vasopressin dysregulation and hyponatremia. *Ann Neurol* 2006;59:229-36.
7. De Luca L, Klein L, Udelson JE, Orlandi C, Sardella G, Fedele F, et al. Hyponatremia in patients with heart failure. *Am J Cardiol* 2005;96:19L-23L.
8. Goldberg A, Hammerman H, Petcherski S, Nassar M, Zdoroviyak A, Yalonetsky S, et al. Hyponatremia and long-term mortality in survivors of acute ST-elevation myocardial infarction. *Arch Intern Med* 2006;166:781-6.
9. Wu Y, Beland FA, Chen S, Liu F, Guo L, Fang JL. Mechanisms of tolvaptan-induced toxicity in HepG2 cells. *Biochem Pharmacol* 2015;95:324-36.
10. Zmily HD, Daifallah S, Ghali JK. Tolvaptan, hyponatremia, and heart failure. *Int J Nephrol Renovasc Dis* 2011;4:57-71.
11. Rangarajan B, Binoy V, Hingmire SS, Noronha V. Tolvaptan. *South Asian J Cancer* 2014;3:182-4.
12. Gheorghiade M, Konstam MA, Burnett JC, Grinfeld L, Maggioni A, Swedberg K, et al. Short-term clinical effects of tolvaptan, an oral vasopressin antagonist, in patients hospitalized for heart failure: the EVEREST Clinical Status Trials. *JAMA* 2007;297:1332-43.
13. Gheorghiade M, Orlandi C, Burnett JC, Demets D, Grinfeld L, Maggioni A, et al. Rationale and design of the multicenter, randomized, double-blind, placebo-controlled study to evaluate the Efficacy of Vasopressin antagonism in Heart Failure: Outcome Study with Tolvaptan (EVEREST). *J Card Fail* 2005;11:260-9.
14. Konstam MA, Gheorghiade M, Burnett JC, Grinfeld L, Maggioni AP, Swedberg K, et al. Effects of oral tolvaptan in patients hospitalized for worsening heart failure: the EVEREST Outcome Trial. *JAMA* 2007;297:1319-31.
15. Erdem Tuncdemir B, Mergen H, Saglar Ozer E. Evaluation of pharmacochaperone mediated rescue of mutant V2 receptor proteins. *Eur J Pharmacol* 2019;865:172803.
16. Tao YX, Conn PM. Pharmacoperones as novel therapeutics for diverse protein conformational diseases. *Physiol Rev* 2018;98:697-725.
17. Prosperi F, Suzumoto Y, Marzuillo P, Costanzo V, Jelen S, Iervolino A, et al. Characterization of five novel vasopressin V2 receptor mutants causing nephrogenic diabetes insipidus reveals a role of tolvaptan for M272R-V2R mutation. *Sci Rep* 2020;10:16383.
18. Robben JH, Sze M, Knoers NV, Deen PM. Functional rescue of vasopressin V2 receptor mutants in MDCK cells by pharmacochaperones: relevance to therapy of nephrogenic diabetes insipidus. *Am J Physiol Renal Physiol* 2007;292:F253-60.
19. Takahashi K, Makita N, Manaka K, Hisano M, Akioka Y, Miura K, et al. V2 vasopressin receptor (V2R) mutations in partial nephrogenic diabetes insipidus highlight protean agonism of V2R antagonists. *J Biol Chem* 2012;287:2099-106.
20. Eichel K, Jullié D, Barsi-Rhyne B, Latorraca NR, Masureel M, Sibarita J-B, et al. Catalytic activation of β -arrestin by GPCRs. *Nature* 2018;557:381-6.
21. Schulz A, Sangkuhl K, Lennert T, Wigger M, Price DA, Nuuja A, et al. Aminoglycoside pretreatment partially restores the function of truncated V(2) vasopressin receptors found in patients with nephrogenic diabetes insipidus. *J Clin Endocrinol Metab* 2002;87:5247-57.
22. Sangkuhl K, Schulz A, Rompler H, Yun J, Wess J, Schoneberg T. Aminoglycoside mediated rescue of a disease-causing nonsense mutation in the V2 vasopressin receptor gene in vitro and in vivo. *Hum Mol Genet* 2004;13:893-903.
23. Groeneweg S, van den Berge A, Meima ME, Peeters RP, Visser TJ, Visser WE. Effects of chemical chaperones on thyroid hormone transport by MCT8 mutants in patient-derived fibroblasts. *Endocrinology* 2018;159:1290-302.
24. Kamijima S, Sekiya A, Takata M, Nakano H, Murakami M, Nakazato T, et al. Gene analysis of inherited antithrombin deficiency and functional analysis of abnormal antithrombin protein (N87D). *Int J Hematol* 2018;107:490-4.
25. Leanos-Miranda A, Ulloa-Aguirre A, Janovick JA, Conn PM. In vitro coexpression and pharmacological rescue of mutant gonadotropin-releasing hormone receptors causing hypogonadotropic hypogonadism in humans expressing compound heterozygous alleles. *J Clin Endocrinol Metab* 2005;90:3001-8.
26. Janovick JA, Goulet M, Bush E, Greer J, Wettlaufer DG, Conn PM. Structure-activity relations of successful pharmacologic chaperones for rescue of naturally occurring and manufactured mutants of the gonadotropin-releasing hormone receptor. *J Pharmacol Exp Ther* 2003;305:608-14.
27. Gunderson EG, Lillyblad MP, Fine M, Vardeny O, Berei TJ. Tolvaptan for volume management in heart failure. *Pharma-*

cotherapy 2019;39:473-85.

28. Hitomi Y, Nagatomo Y, Yukino M, Yumita Y, Kagami K, Yasuda R, et al. Characterization of tolvaptan response and its impact on the outcome for patients with heart failure. *J Cardiol* 2021;78:285-93.

29. Beaudoin JJ, Brock WJ, Watkins PB, Brouwer KLR. Quantitative systems toxicology modeling predicts that reduced biliary efflux contributes to tolvaptan hepatotoxicity. *Clin Pharmacol Ther* 2021;109:433-42.

30. Carmichael J, DeGraff WG, Gazdar AF, Minna JD, Mitchell JB. Evaluation of a tetrazolium-based semiautomated colorimetric assay: assessment of chemosensitivity testing. *Cancer Res* 1987;47:936-42.

31. Costello-Boerrigter LC, Boerrigter G, and Burnett JC, Jr. Pharmacology of vasopressin antagonists. *Heart Fail Rev* 2009;14:75-82.

32. Gheorghide M, Niazi I, Ouyang J, Czerwiec F, Kambayashi J, Zampino M, et al. Vasopressin V2-receptor blockade with tolvaptan in patients with chronic heart failure: results from a double-blind, randomized trial. *Circulation* 2003;107:2690-6.

33. Reilly T, Chavez B. Tolvaptan (Samsca) for hyponatremia: is it worth its salt? *PT* 2009;34:543-547.

34. Gheorghide M, Abraham WT, Albert NM, Gattis Stough W, Greenberg BH, O'Connor CM, et al. Relationship between admission serum sodium concentration and clinical outcomes in patients hospitalized for heart failure: an analysis from the OPTIMIZE-HF registry. *Eur Heart J* 2007;28:980-8.

35. Gheorghide M, Rossi JS, Cotts W, Shin DD, Hellkamp AS, Pina IL, et al. Characterization and prognostic value of persistent hyponatremia in patients with severe heart failure in the escape trial. *Arch Intern Med* 2007;167:1998-2005.

36. Konstam MA, Kiernan M, Chandler A, Dhingra R, Mody FV, Eisen H, et al. Short-term effects of tolvaptan in patients with acute heart failure and volume overload. *J Am Coll Cardiol*

2017;69:1409-19.

37. Bellos I. Safety profile of tolvaptan in the treatment of autosomal dominant polycystic kidney disease. *Ther Clin Risk Manag* 2021;17:649-56.

38. Szalai L, Sziraki A, Erdelyi LS, Kovacs KB, Toth M, Toth AD, et al. Functional rescue of a nephrogenic diabetes insipidus causing mutation in the V2 vasopressin receptor by specific antagonist and agonist pharmacochaperones. *Front Pharmacol* 2022;13:811836.

39. Feldman BJ, Rosenthal SM, Vargas GA, Fenwick RG, Huang EA, Matsuda-Abedini M, et al. Nephrogenic syndrome of inappropriate antidiuresis. *N Engl J Med* 2005;352:1884-90.

40. Erdelyi LS, Mann WA, Morris-Rosendahl DJ, Gross U, Nagel M, Varnai P, et al. Mutation in the V2 vasopressin receptor gene, AVPR2, causes nephrogenic syndrome of inappropriate diuresis. *Kidney Int* 2015;88:1070-8.

41. Morello JP, Bichet DG. Nephrogenic diabetes insipidus. *Annu. Rev. Physiol* 2001;63:607-30.

42. Mubeen MF. Pharmacoperones role in nephrogenic diabetes insipidus. *Glob Acad J Pharm Drug Res* 2020;2:34-28.

43. Bernier V, Bichet DG, Bouvier M. Pharmacological chaperone action on G-protein coupled receptors. *Curr Opin Pharmacol* 2004;4:528-33.

44. Ulloa-Aguirre A, Janovick JA, Brothers SP, Conn PM. Pharmacologic rescue of conformationally-defective proteins: implications for the treatment of human disease. *Traffic* 2004;5:821-37.

45. Durukan AB, Erdem B, Durukan E, Sevim H, Karaduman T, Gurbuz HA, et al. May toxicity of amiodarone be prevented by antioxidants? A cell culture study. *J Cardiothorac Surg* 2012;7:61.

46. Fujiki T, Ando F, Murakami K, Isobe K, Mori T, Susa K, et al. Tolvaptan activates the Nrf2/HO-1 antioxidant pathway through PERK phosphorylation. *Sci Rep* 2019;9:9245.



This is an open access article distributed under the terms of Creative Commons Attribution-NonCommercial-NoDerivatives 4.0 International License.

Comparing the closure of hepatocaval ligament using stapler or suturing in liver surgery

Imam Bakır Batı¹, Umut Tüysüz²

¹Department of Transplant Surgery, Acibadem University, Faculty of Medicine, İstanbul, Turkey; ²Department of Liver Transplant surgery, Şişli Etfal Hamidiye Training and Research Hospital, İstanbul, Turkey

ABSTRACT

Objectives: Hepatocaval ligament is localized on the posterior and lateral side of the retrohepatic Inferior Vena Cava (IVC), above the right adrenal vein. Bleeding due to retro-hepatic cava injury could sometimes occur during the dissection and closure of hepatocaval ligament (HCL). We aim to determine closing methods of HCL in terms of cost, ease of application and safety.

Methods: The study population included 90 recipient hepatectomy patients who had cadaveric and live-donor liver transplantation at Organ Transplant Center of Acibadem Hospital between 2017 and 2019. The patients were divided into two groups. The first group contained 40 patients who were closed with 25 mm EndoTA 30 stapler. The second group contained 50 patients who were closed by continuous double-layer suturing with 5/0 propylene.

Results: In the group closed by endovascular stapler, reinforcement suturing was performed in eight patients (20%) using 5/0 propylene suture due to mild blood leakage in the closing line. In two patients (5%), on the other hand, the staple device could not be used due to the fact that HCL was very close to the right hepatic vein and the distance between the liver and the vena cava was short. There were no perioperative and postoperative HCL-associated liver and vena cava bleeding complications in both groups. However, the cost was significantly higher in the stapler group than in the suturing group.

Conclusions: The present study is the first to compare the stapler or suturing techniques for closing HCL in the receiver hepatectomy of liver transplantation. The results indicated that the closure with suturing was at least as useful and convenient in terms of cost, ease of application and safety.

Keywords: Liver transplantation, hepatocaval ligament, hepatectomy, suture, stapler

Major hepatic resection is more complicated due to blood loss of high volumes and associated mortality and morbidity. Although bleeding could arise during liver transection and control of hilar vessels, hepatic vein and retro-hepatic vena cava injuries are the most common mortality cause of major intraoperative bleeding. Bleeding due to retro-hepatic cava

injury could sometimes occur during the dissection and closure of hepatocaval ligament (HCL). During embryogenesis, inferior vena cava (IVC) is surrounded by hepatic parenchyma. At the end of embryogenesis, the parenchymal bridge connecting the right and left liver behind the IVC starts to atrophy and turns into a hepatocaval ligament [1, 2].



e-ISSN: 2149-3189

Received: March 22, 2022; Accepted: October 9, 2022; Published Online: January 10, 2023

How to cite this article: Batı IB, Tüysüz U. Comparing the closure of hepatocaval ligament using stapler or suturing in liver surgery. Eur Res J 2023;9(3):461-467. DOI: 10.18621/eurj.1091092

Address for correspondence: Umut Tüysüz, MD., Şişli Etfal Hamidiye Training and Research Hospital, Department of Liver Transplant Surgery, İstanbul, Turkey. E-mail: umutuysuz@gmail.com, Phone: +90 212 338 63 00



©Copyright © 2023 by Prusa Medical Publishing
Available at <http://dergipark.org.tr/eurj>
info@prusamp.com

In the 1950s, some liver surgeons were aware of the existence and importance of HCL, describing it as the posterior bed of the IVC, which allows control of small retrohepatic veins. This is a structure that always completely envelops Vena cava inferior and extends to its posterior [3, 4]. This ligament, which covers the retrohepatic IVC, makes it difficult to expose the hepatic veins without cutting the hepatic parenchyma. HCL is localized on the posterior and lateral side of the retrohepatic IVC, above the right adrenal vein. It partially or completely blocks the entry of right hepatic vein (RHV) into IVC. Especially with the development of liver surgery with total vascular exclusion and microsurgical techniques, surgical interest in HCL and its relationship with hepatic veins have increased in recent years. In addition to its relationships with IVC and RHV, relationships of HCL with techniques in liver surgery, especially with elective vascular exclusion, during right hemi-liver and recipient hepatectomy surgery have gained importance.

METHODS

This study was conducted retrospective and one center study. The study population included consecutively 90 recipient hepatectomy patients who had cadaveric and live-donor liver transplantation at Organ Transplant Center of Bursa Acibadem Hospital between 2017 and

2019. Hepatocaval ligament (HCL) was dissected and closed safely during the hepatectomy in these patients (Fig. 1). Two different methods were used to close the HCL larger than 10 mm width. The patients were divided into two groups. The first group contained 40 patients who were closed with 25 mm EndoTA 30 stapler (Group I). The second group contained 50 patients who were closed by continuous double-layer suturing with 5/0 propylene (Group II). We defined morbidity and death which occurred within 90 days after surgery as postoperative complications and mortality, respectively. We also defined mild, moderate and severe estimated blood loss. Patient short-term outcomes evaluated at 30 days postoperatively. Postoperative complications were classified according to the Dindo-Clavien classification [5]. The hospital reimbursement is calculated considering all issues in a liver transplantation settings as operating time, ITU (intensive therapy unit) stay, hospital stay, etc. as fixed fee policy our hospital. Safety and applicability, cost, perioperative and postoperative estimated blood loss on the closed line were evaluated among the groups.

The study was approved by the Acibadem University Ethical Review Board. For the present study. No informed consent was required.

Statistical Analysis

Mean, standart deviation, median, minimum, maximum value frequency and percentage were used for

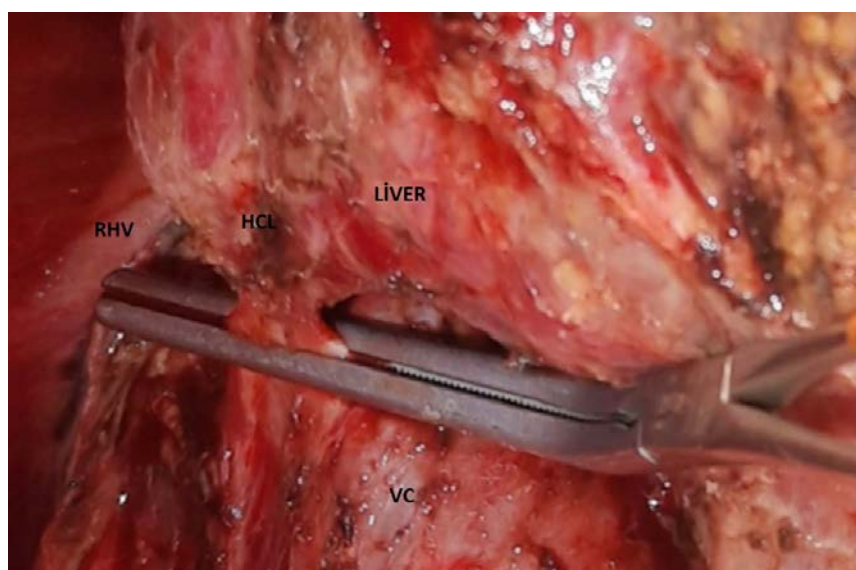


Fig. 1. Right lateral view to the liver during the dissection of the HCL, IVC and the RHV.

Table 1. Demographic and clinical characteristics of recipients at transplantation

	n (%)	Median (min-max)	Mean ± SD
Age (years)		57.0 (41.0-69.0)	56.9 ± 7.3
Gender			
Female	26 (26.0)		
Male	64 (64.0)		
Primary disease			
Budd-Chiari	3 (3.0)		
Alcohol-related	13 (13.0)		
HBV	33 (33.0)		
HCC	9 (9.0)		
HCV	12 (9.0)		
Kriptogenic	15 (15.0)		
NASH	4 (4.0)		
PBS	1 (1.0)		
Procedure time (s)			
Hepatectomy time (min)			
MELD score			
LT		58.0 (45.0-70.0)	57.7 ± 7.3
DDLT	21 (21.0)	240.0 (190.0-300.0)	239.9 ± 26.0
LDLT	69 (69.0)	22.0 (12.0-28.0)	21.7 ± 3.8
Perioperative blood loss			
(-)	82 (82.0)		
(+)	8 (8.0)		
Postoperative blood loss			
(+)	0 (0.0)		
(-)	100 (100.0)		
Clavien-Dindo (grade)			
I	50 (50.0)		
II	33 (33.0)		
IIIA	4 (4.0)		
IIIB	3 (3.0)		
Mortality			
(-)	88 (88.0)		
(+)	2 (2.0)		
Cost (\$)		2.0 (2.0-152.0)	68.0 ± 74.2

HBV = Hepatit B Virus, HCC = Hepatocellular carcinoma, HCV = Hepatit C virüs, NASH = Nonalcoholic Steatohepatitis, PBS = Primary biliary sclerosis, LT = Liver transplantation, DDLT = Deceased donor liver transplantation, LDLT = Living donor liver transplantation, Cost = Cost of surgery. Postoperative blood loss was determined as a complication including clavien-dindo grade IIIA and IIIB

descriptive statistics. The distribution of variables was checked with kolmogorov-simirnov test. Independent Samples t test and Mann - Whitney U test were used for the comparison of quantitative data. Chi-square test was used for the comparison of the comparison of qualitative data. SPSS 27.0 was used for statistical analyses.

RESULTS

Sixty-four percent of the hepatectomy patients were male and 26% were female. Median age was 57 years (range: 41-69 years). All patients underwent total hepatectomy shows the baseline characteristics of the 40 Group I and 50 Group II recipients. No significant differences existed between the groups in terms of recipient age, gender, model for end-stage liver disease (MELD) score and underlying cause of cirrhosis (Table 1).

Postoperative morbidity and mortality were similar in both groups. Operation time was significantly higher in the Group II than in the Group I. But hepatectomy time was similar in both groups. The DLDT rate in Group II was significantly higher than the DLDT rate Group I. In the group closed by endovascular stapler, reinforcement suturing was performed in eight patients (20%) using 5/0 propylene suture due to mild blood leakage (1-5 mL) in the closing line. In two patients (5%), on the other hand, the staple device could not be used due to the fact that HCL was very close to the right hepatic vein and the distance between the liver and the vena cava was short. Two of patients died from sepsis within one month. There were no perioperative and postoperative HCL-associated liver and vena cava moderate and severe bleeding complications in both groups. However, the cost was significantly higher in the stapler group than in the suturing group (Table 2).

DISCUSSION

Detailed anatomical knowledge of HCL and its relationship with IVC and hepatic veins is important in split liver and live donor transplantations as well as in hepatic resections. The safe dissection and closure of HCL relieves elective vascular control while maintain-

ing the IVC flow. Makuuchi *et al.* [6] reported for the first time that RHV control was possible in 89% of cases whose HCL ligament was resected during the right hepatic resection. HCL could not be resected only in 34% of cases. During the right hepatectomy with elective vascular control, it was anatomically possible in 85% of cases HCL should be dissected in 85/77% of livers with HCL. This was challenging or impossible in 15% of cases [7]. The presence of HCL is also important during the liver bi- or tri-partitioning and in control and pediculation of hepatic veins in split liver transplantations and live donor transplantations. The dissection and ligation of HCL exposes the retrohepatic part of IVC and the terminal parts and entrances of the main hepatic veins. One study found HCL in livers of 33 patients out of 43 (77%), but it was not observed in 20% of the cases. Only 3% of the cases had parenchymatous bridge in IVC posterior.

HCL was different in all cases. The average length was 22 ± 10 mm (range: 12-35 mm), while the average width was 8 ± 5 mm (range: 3-18 mm), and its thickness was approximately 0.5-2 mm. In two cases (5%), it contained small retrohepatic veins larger than 1 mm in diameter [7]. At the same time, reports from Gadzi-jev *et al.* [8] that HCL was of hepatic origin and that bile ducts were found in the ligament were supported by the similar studies of Mackenzie *et al.* [9]. Rosset *et al.* [10] showed that in 25% of cases hepatocytes were present in HCL. In order to prevent an unexpected bleeding in an associated caudate vein, which exists in 69% of the cases, control of the ligament with clips or suture ligation is necessary [9]. However, during the closure of the large HCL without ligament, there could be uncontrollable bleeding if they are dislocated or do not overlap. This could be important in terms of cutting and closing the HCL near the retrohepatic cava during the cancer surgery. Details of both methods were clearly stated in our surgical records.

Therefore it is not difficult to compare the surgical outcome in using between endostapler and suturing because of the different background in the retrospective study. With the combination of advances in intra- and post-operative methods including surgical technique, the use of microsurgery and vascular closure instruments as well as advances in blood transfusion, liver surgery has been a safer and more effective procedure. The average blood loss was reported to be 848 ± 972 mL (range: 40 to 9000 mL) in a review which

Table 2. Operative outcomes of the matched Group I and Group II

	Group I		Group II		p value
	Mean ± SD/ n (%)	median	Mean ± SD/ n (%)	median	
Age (years)	56.5 ± 7.2	56.0	57.3 ± 7.4	57.5	0.636 ^t
Gender					0.499 ^{x²}
Female	13 (32.5)		13 (21.7)		
Male	27 (67.5)		37 (61.7)		
Procedure time (s)	52.5 ± 4.6	54.0	61.8 ± 5.0	62.5	0.000^t
Hepatectomy time (min)	243.7 ± 27.8	244.0	236.9 ± 24.4	237.5	0.290 ^m
MELD Score	22.6 ± 3.6	24.0	21.0 ± 3.8	20.0	0.041^m
LT					0.019^{x²}
DDLTL	14 (35.0)		7 (11.7)		
LDLT	26 (65.0)		43 (71.7)		
Perioperative Blood Loss					0.001^{x²}
(-)	32 (80.0)		50 (83.3)		
(+)	8 (20.0)		0 (0.0)		
Postoperative Blood Loss					1.000 ^{x²}
(+)	0 (0.0)		0 (0.0)		
(-)	40 (60.0)		60 (100)		
Clavien-Dindo (Grade)					0.568 ^{x²}
I	23 (57.5)		27 (45.0)		
II	14 (35.0)		19 (31.7)		
IIIA	2 (5.0)		2 (3.3)		
IIIB	1 (2.5)		2 (3.3)		
Mortality					1.000 ^{x²}
(-)	39	97.5%	49	81.7%	
(+)	1	2.5%	1	1.7%	
Cost (\$)	150.4 ± 0.8	150	2.0 ± 0.0	2.0	0.000^m

LT = Liver transplantation, DDLT = Deceased donor liver transplantation, LDLT = Living donor liver transplantation, Cost = Cost of surgery. Perioperative blood loss determined.

^tt test /^mMann-whitney u test/^{x²} Chi-square test

included major liver resections performed at Memorial Sloan-Kettering cancer center between 1991 and 1997. More than 13% of the patients had blood loss of more than a quarter of their estimated blood volumes during surgery [10]. Even in a more contemporary major hepatectomy series, an average blood loss of 700 mL (range: 400-1050 mL) was observed [11]. It was reported that 30-47% of patients received allogenic

blood components during major hepatectomy or within the first 24 hours [11, 12]. This is not a benign intervention. What's more, the immunomodulatory effect of blood transfusion can lead to increased infection predisposition and a decrease in cancer-free disease survival [13, 14]. Since all of the patients in the present study had cirrhosis and had different amounts of acid, there were different degrees of adhe-

sion between the liver and the diaphragm and the retrohepatic cava. Moreover, in those who are subjected to the receiver hepatectomy due to Budd-Chiari syndrome, fibrous thickening could also be observed in vena cava around HCL. In this case, the dissection, closure and cutting of HCL, an important step in the mobilization of the liver to reach hepatic veins, can often be difficult. In cases where HCL is wide and short, the increased risk of massive retrohepatic hemorrhage makes it imperative to perform this dissection and subsequent cutting and closing more carefully and meticulously. We carried out extensive hepatic mobilization through exposing the major hepatic veins before we engaged in the major hepatic resection. This procedure facilitates the control of veins in challenging cases with intraoperative bleeding and provides the necessary exposure in major hepatic resection and receiver hepatectomy. On the other hand, in order to ensure a sufficient tumor cleaning with an adequate bleeding control in tumors of central location which is close to inferior vena cava (IVC) and hepatic vein confluence, the dissection and safe closure of HCL with subsequent hepatic vein control and isolation is especially critical. In addition to the right hepatic vein, the complete exposure of the retrohepatic vena cava necessitates the splitting of vena cava ligament, which generally contains fibrous tissue but could also include liver tissue, bile ducts and small hepatic veins and which is adjacent to the right hepatic vein [7]. In addition, due to its connection with VCI, its dissection could lead to injury and breakage in VCI. Therefore, we chose to close especially the HCLs larger than 10 mm. Ramacciato *et al.* [15] proposed the use of vascular endostapler for controlling the inferior diaphragmatic vein of considerable size right adjacent to the ligament. In another study, Dudeja and Jarnagin [16] reported that they closed HCL successfully with endovascular stapler. In the present study, HCL was closed with a vascular endostapler during the receiver hepatectomy of 30 patients with underlying chronic liver disease. In eight of these patients (20%), slight blood leakage was observed on the closing line, and consequently reinforcement suturing was performed for these leaks. However, the use of endostapler was not technically possible in two patients (5%) because the HCL was short, wide or very close to the right hepatic vein. The duration of operation was extended due to additional suturing in eight patients. Dudeja and Jar-

nagin [16] reported that they mostly achieved successful closing of HCL with endovascular stapler. However, none of the patients who were closed with suturing technique had any leaks that would require additional control. Besides, the cost was significantly higher in the group closed with stapler. There were no bleeding or bleeding-associated complications during surgery or in the postoperative early periods in any groups. In the endovascular stapler group, the procedure time was slightly, though not significantly, longer in eight patients (20%) who needed additional suturing.

Stapler could not be used in two patients due to the anatomical and technical difficulties. In terms of cost-benefit balance, the closure with suturing was more advantageous. This method can be used as a more viable, effective and safe method for the closure of the HCLs wider than 1 cm during liver transplantation with live donors in which the receiver hepatectomy is performed as open surgery, during right hepatectomy and during tumor-related major hepatectomies. The mild perioperative bleeding seen in the stapler closure group is due to the stapler not firmly attaching to the area between the vena cava and the HCL, as the HCL was thin and short.

Limitations

Our study had limitations because it was single-centered and retrospective. The study included patients receiving hepatectomy. The division of the major hepatic veins and the HCL using devices such as 'ENDO-PATH Stapler Echelon white cartridge' has currently become the standard and routine surgical procedure at least in Japan during not only laparoscopic but also open surgical hepatectomy. Therewithal, the vast majority of North American Centers use a laparoscopic stapler (EndoGIA 30mm for example) given its ease of use and slim profile. Although the present study had homogeneity, more prospective studies should be performed in patients with the right liver surgery with normal liver structure.

CONCLUSION

Safe and effective control of intraoperative bleeding and blood loss has been the challenging side of liver surgery. Numerous techniques have been developed to

minimize the bleeding. HCL is a common anatomical structure. Dissection of the HCL exposes the terminal extrahepatic part of RHV, and provides elective vascular control during the receiver hepatectomy surgery in the right hemi-liver and liver transplantation. In some cases where HCLs greater than 1 cm are not closed, retrohepatic hemorrhages that are difficult to control could develop. The present study is the first to compare the stapler or suturing techniques for closing HCL in the receiver hepatectomy of liver transplantation. The results indicated that the closure with suturing was at least as useful and convenient in terms of cost, ease of application and safety.

Authors' Contribution

Study Conception: UT; Study Design: İBB; Supervision: İBB, UT; Funding: N/A; Materials: İBB, UT; Data Collection and/or Processing: İBB; Statistical Analysis and/or Data Interpretation: UT; Literature Review: UT; Manuscript Preparation: İBB, UT and Critical Review: İBB.

Conflict of interest

The authors disclosed no conflict of interest during the preparation or publication of this manuscript.

Financing

The authors disclosed that they did not receive any grant during conduction or writing of this study.

Acknowledgements

The preliminary findings were presented at the Annual Congress of the Korean Association of HBP Surgery in Seoul, Korea, March 2021.

REFERENCES

- Langman J. Medical embryology, ed 3. Baltimore, Williams & Wilkins. 1975.
- Heloury Y, Leborgne J, Rogez JM, Robert R, Barbin JY, Hureau J. The caudate lobe of the liver. *Surg Radiol Anat* 1988;10:83-91.
- Lortat-Jacob JL, Robert HG. Un cas d'hépatectomie droite réglée. *Mem Acad Chir* 1952;78:224-52.
- Couinaud C. Le foie, études anatomiques et chirurgicales, Paris, Masson. 1957.
- Dindo D, Demartines N, Clavien PA. Classification of surgical complications : a new proposal with evaluation in a cohort of 6336 patients and results of a survey. *Ann Surg* 2004;240:205-13.
- Makuuchi M, Hasegawa H, Yamazaki S, Takayasu K. Four new hepatectomy procedures for resection of the right hepatic vein and preservation of the inferior right hepatic vein. *Surg Gynecol Obstet* 1987;164:68-72
- Morjane A, Dahmane R, Ravnik D, Hribernik M. Anatomy and surgical relevance of the hepato-caval ligament. A study on cadaveric livers. *Cells Tissues Organs* 2008;187:243-6.
- Gadžijev E, Stanisavljević RD, Trotovšek B. Venous drainage of the dorsal sector of the liver: differences between segments I and IX. A study on corrosion casts of the human liver. *Surg Radiol Anat* 1997;19:79-83.
- Mackenzie S, Dixon E, Bathe O, Sutherland F. Intermittent hepatic vein – total vascular exclusion during liver resection: anatomic and clinical studies. *J Gastrointest Surg* 2005;9:658-66.
- Rosset E, Brunet C, Meunier B, Marie PA, DiMarino V, Argeme M, et al. Anatomic basis of the liver for the development of a perihepatic prosthesis. *Surg Radiol Anat* 1995;17:1-5.
- Melendez JA, Arslan V, Fischer ME, Wuest D, Jarnagin WR, Fong Y, et al. Perioperative outcomes of major hepatic resections under low central venous pressure anesthesia: blood loss, blood transfusion, and the risk of postoperative renal dysfunction. *J Am Coll Surg* 1998;187:620-5.
- Correa-Gallego C, Gonen M, Fischer M, Grant F, Kemeny NE, Arslan-Carlon V, et al. Perioperative complications influence recurrence and survival after resection of hepatic colorectal metastases. *Ann Surg Oncol* 2013;20:2477-84.
- Amato A, Pescatori M. Perioperative blood transfusions for the recurrence of colorectal cancer. *Cochrane Database Syst Rev* 2006;1:CD005033.
- Kooby DA, Stockman J, Ben-Porat L, Gonen M, Jarnagin WR, Dematteo RP, et al. Influence of transfusions on perioperative and long-term outcome in patients following hepatic resection for colorectal metastases. *Ann Surg* 2003;237:860-9.
- Ramacciato G, Balesh AM, Fornasari V. Vascular endostapler as an aid to hepatic vein control during hepatic resections. *Am J Surg* 1996;172:358-62.
- Dudeja V, Jarnagin W. Massive Intraoperative Hemorrhage During Hepato-Biliary and Pancreatic Surgery. In: Pawlik T, Maithel S, Merchant N. (eds) *Gastrointestinal Surgery*. Springer:New York, NY. 2015: pp. 201-15.



This is an open access article distributed under the terms of [Creative Commons Attribution-NonCommercial-NoDerivatives 4.0 International License](https://creativecommons.org/licenses/by-nc-nd/4.0/).

Are body mass index and the systemic immune-inflammation index risk factors for carpal tunnel syndrome?

Meltem Karacan Gölen[✉], Dilek Yılmaz Okuyan[✉]

Department of Neurology, Konya State Hospital, Konya, Turkey

ABSTRACT

Objectives: Carpal tunnel syndrome (CTS) is the most common entrapment neuropathy of the upper extremity that affects activities of daily living. In our study, we aimed to reveal the relationship between CTS and BMI, and to evaluate symptom severity and functionality in these patients by using the Boston CTS questionnaire.

Methods: In this study, 300 patients with CTS and 100 healthy individuals without CTS whose EMG was performed in our neurology clinic electrophysiology laboratory between June 2021 and December 2021, were included. BMI, SII index, and Boston CTS questionnaire findings were compared between patients diagnosed as having mild, moderate, and severe CTS (according to electrophysiologic evaluations) and a control group consisting of healthy individuals.

Results: In our study, a statistically significant difference was observed between the CTS and control groups in terms of mean age ($p < 0.001$). When the increased BMI and SII parameters were compared, a statistically significant difference was observed between the control and CTS groups ($p < 0.001$ for both). In the multivariate logistic regression analysis, it was observed that the risk of CTS increased 1.566 times as BMI increased, and the risk of CTS increased 1.005 times as the SII index increased ($p < 0.001$ for both).

Conclusions: We observed that increased BMI and advanced age were risk factors for CTS. In our study, in which the relationship between the SII index and CTS was evaluated for the first time, according to our findings, inflammation was thought to play a role in the pathophysiology of CTS.

Keywords: Carpal tunnel syndrome, body mass index, nerve conduction study, inflammation, systemic immune-inflammation index

Carpal tunnel syndrome (CTS) is the most common entrapment neuropathy of the upper extremity, which causes functional disability in clinical practice and affects daily life activities [1]. It presents with localized paresthesia in the hands, especially in the palms and 1st-3rd fingers, and increasing pain at night, which develops as a result of compression of

the median nerve at the wrist level. It has been reported to be more common in females and the 3rd and 5th decades [2]. Apart from this, advanced age, pregnancy, connective tissue diseases, hypothyroidism, diabetes mellitus, occupational diseases are other common predisposing factors [2]. In the electrophysiology laboratory, the diagnosis of CTS is made

Received: May 29, 2022; Accepted: December 19, 2022; Published Online: January 17, 2023



How to cite this article: Karacan Gölen M, Yılmaz Okuyan D. Are body mass index and the systemic immune-inflammation index risk factors for carpal tunnel syndrome? *Eur Res J* 2023;9(3):468-476. DOI: 10.18621/eurj.1120577

e-ISSN: 2149-3189

Address for correspondence: Meltem Karacan Gölen, MD., Konya State Hospital, Department of Neurology, Hospital Street, 42060 Selçuklu, Konya, Turkey. E-mail: drmeltemkaracan@hotmail.com, Phone: +90 332 235 45 00



©Copyright © 2023 by Prusa Medical Publishing
Available at <http://dergipark.org.tr/eurj>
info@prusamp.com

through motor and sensory nerve conduction studies of the median nerve. The motor and sensory conduction velocities of the median nerve and motor distal latency are evaluated, and severity classification is made according to the level of symptoms [3, 4].

Considering the predisposing factors, it is obvious that multifactorial processes are dominant in the etiopathogenesis of CTS. Although the underlying mechanisms are not fully understood, it is thought that the common result of all these processes is compression in the channel where the median nerve travels and an increase in pressure secondary to the increase in fat tissue in individuals with obesity. Axonal damage to the median nerve develops as a result of compression of the median nerve in the carpal tunnel, and ischemia in the median nerve develops as a result of damage to the vascular structures in the perineum. Repetitive compression leads to tenosynovial thickening, the pressure becomes continuous, and the median nerve is pressed in the canal [5]. Studies in the literature on whether inflammation affects these processes are limited. We aimed to reveal the relationship between the systemic immune-inflammation index (SII), which was shown as an inflammation marker in various diseases recently, and the severity of CTS [6, 7]. We believe our study is the first to investigate this relationship because we have not come across a similar study in the literature. It is known that individuals with obesity are prone to CTS, and it has been shown in various studies that there is a relationship between an increase in body mass index (BMI) and the development of CTS [1, 8]. It has been reported that the development of CTS in individuals with obesity may be associated with an increase in adipose tissue or an increase in hydrostatic pressure in the canal where the median nerve travels [9].

In our study, we aimed to reveal the relationship between CTS and BMI and the SII in patients with CTS detected in our electrophysiology laboratory and evaluate severity and functionality in these patients using the Boston CTS questionnaire.

METHODS

In this study, 300 patients with CTS and 100 healthy individuals without CTS who were evaluated in our electrophysiology laboratory between June 2021 and

December 2021 were included. The nerve conduction studies and clinical diagnostic findings of the patients with clinical and electrophysiologic diagnoses of CTS and a control group were recorded. The study was approved by the local ethics committee (2021/025). Informed consent forms were obtained from the patients with CTS and the control group.

Electrophysiologic examinations of the patients were performed using a Nihon Kohden Corp. device by the same person, in the same place. Standardization was achieved by paying attention to the body temperature and room temperature of the patients.

Median nerve motor and sensory conduction studies were performed on patients who were admitted to the electromyography (EMG) laboratory with entrapment neuropathy. In addition, ulnar nerve motor and sensory conduction studies and concentric needle EMG were included in the study to exclude polyneuropathy and radiculopathy.

In the median nerve motor nerve conduction study, the superficial electrodes and the recording electrode were placed on the abductor pollicis brevis (APB) muscle, and then the recording was made by stimulating the median nerve 5 cm proximal to the active electrode on the wrist, along the fold between the hyper- and hypothenar muscles in the middle of the wrist, and by stimulating the median nerve in the elbow bend near the brachial artery pulse, as the second stimulation point. Motor distal latency, motor conduction velocity, and compound muscle action potential (CMAP) were recorded. Distal latency ≥ 3.98 ms, CMAP ≤ 4 mV, or conduction velocity ≤ 49.7 m/s was considered abnormal. The ulnar nerve was stimulated 5 cm proximal to the recording electrode and 4 cm distal to the elbow for motor conduction. It was considered abnormal if the ulnar nerve distal latency was above 3.3 ms, its velocity was below 49.9 m/s, or the CMAP amplitude was below 7.0 mV.

For the sensory nerve conduction study of the median nerve, recordings were made on 1st, 2nd, and 3rd fingers after stimulating from the wrist, palm-wrist segment, and wrist-elbow segment, respectively. For the sensory nerve conduction study of the ulnar nerve, a recording was made on the 5th finger. According to the normal levels of our laboratory, the velocity of the sensory potential obtained from the negative peak is considered abnormal if it is < 32.92 m/s for the 1st finger, < 39.4 m/s for the 2nd finger, < 39.65 m/s for the

3rd finger, < 35.2 m/s for palm-wrist, < 49.0 m/s for wrist-elbow, and < 37.3 m/s for 5th finger [10].

For the diagnosis of CTS; median motor nerve distal latency (mMDL), median motor nerve conduction velocity (mMNCV), median nerve motor compound muscle action potential (mCMAP), second finger median sensory nerve conduction velocity (mSNCV), median sensory nerve distal latency (mSDL), median sensory nerve action potential amplitude (mSNAP), ulnar motor nerve distal latency (uMDL), ulnar motor nerve conduction velocity (uMNCV), ulnar motor nerve compound muscle action potential (uCMAP), fifth finger median sensory nerve conduction velocity (uSNCV), ulnar sensory nerve distal latency (uSDL), and ulnar sensory nerve action potential amplitude (uSNAP) were evaluated and recorded.

Using concentric needle electrodes, needle EMG was usually applied to the abductor pollicis brevis muscle and if necessary, according to the findings, it was applied to the pronator teres and flexor pollicis longus muscles, which were more proximal muscles. When necessary, needle EMG was performed on abductor digiti minimi and extensor indicis proprius muscles to exclude radiculopathy from polyneuropathy [4].

Bandpass filters were set at 20-20,000 Hz for motor nerve conduction, 20-2000 Hz for sensory nerve conduction, and 10-10,000 Hz for needle EMG. Body temperature was measured and corrected to 31°C according to the conversion table; 1 m/s was added to motor and sensory nerve conduction velocities in participants aged over 60 years.

Participants included in the study were grouped according to their electrophysiologic findings as mild CTS, moderate CTS, severe CTS, and the control group. Both hands were studied in all participants and patients were classified electrophysiologically according to the following criteria. Mild CTS: Decreased sensory conduction velocity and amplitude in the median nerve finger-wrist segment and palm-wrist segment. Moderate CTS: Prolongation of the distal latency of the median motor nerve (> 4.0 msec) and decrease in the median nerve sensory conduction velocity and amplitude. Severe CTS: Failure to obtain uCMAP, decreased median motor nerve amplitude, prolongation of the distal latency of the median motor nerve, or failure to obtain mCMAP [11].

Patients with hereditary polyneuropathy, diabetic

polyneuropathy, cervical radiculopathy, brachial plexopathy, malignancy, traumatic nerve damage, connective tissue disease, rheumatological disease, hereditary neuropathy with liability to pressure palsy (HNPP), chronic renal failure, and patients in the infectious process were not included. Chronic diseases of the patients were recorded.

Among the laboratory markers, white blood cell (WBC), neutrophil, lymphocyte, and platelet counts were recorded. $NLR = \text{neutrophil count} / \text{lymphocyte count}$ and $SII = \text{neutrophil count} \times \text{platelet count} / \text{lymphocyte count}$ were calculated.

Height (cm) and weight (kg) measurements of the patients were made. BMI was calculated using the formula $\text{weight} / \text{height}^2$ (kg/m^2). Patients with BMI < 25 kg/m^2 were considered normal-weight, patients with BMI 25-30 kg/m^2 were considered overweight, patients with BMI 30-35 kg/m^2 were considered as having class 1 obesity, and patients with BMI > 35 kg/m^2 were considered as having class 2 obesity [12].

The Boston Carpal Tunnel Syndrome Questionnaire (BCTQ), consisting of two parts, was completed independently by the patients to evaluate their functional limitation and symptom severity. The symptom severity scale consists of 11 multiple-choice questions and the functional status scale consists of eight questions. Responses are scored from 1 (mildest) to 5 points [13]. The validity and reliability studies of the Turkish adaptation of BCTQ were carried out. [14].

Statistical Analysis

Data were analyzed using the IBM SPSS V23 software package. Conformity to normal distribution was evaluated using the Kolmogorov-Smirnov test. The Chi-square test and Fisher's exact test were used to compare categorical variables between the groups. The Mann-Whitney U test was used to compare data that were not normally distributed between two groups. The Kruskal-Wallis test was used to compare data that were not normally distributed between three or more groups, and multiple comparisons were analyzed using the Dunn test. Binary logistic regression analysis was used to examine the risk factors affecting the formation of CTS. Quantitative data results are given as mean \pm standard deviation and median (minimum-maximum). Categorical data results are given as frequency (percentage). The significance level was accepted as $p < 0.050$.

RESULTS

Our study included 300 patients with CTS who were diagnosed in our electrophysiology laboratory, and 100 healthy controls. One hundred eighty patients were not included in the study due to exclusion criteria. Patients diagnosed as having CTS were divided into three groups according to their electrophysiologic classification as mild, moderate, and severe CTS.

In Table 1, the demographic characteristics of the groups are shown. There was no statistically significant difference between the mild, moderate, severe CTS groups and the control group in terms of sex distribution ($p > 0.050$).

Considering the age distribution between the groups, the mean age of the control group was 42.0 ± 15.0 years, and the mean age of the CTS group was 51.0 ± 14.4 years; there was a statistically significant difference between the groups in terms of mean age ($p < 0.001$).

Considering weight distribution, it was observed that there was a statistically significant difference in terms of the median weight values between the control group and CTS groups ($p < 0.001$). In addition, a statistically significant difference was observed in terms of BMI between the control group and CTS groups ($p < 0.001$). There was no statistically significant difference between the groups in terms of chronic diseases (Table 1).

When the laboratory parameters were examined, a statistically significant difference was observed be-

tween the groups in terms of the median counts of lymphocytes and platelets ($p < 0.001$ for both). When the median SII index values were compared, the median SII index in the control group, mild CTS group, moderate CTS group, and severe CTS group was 469.5 ± 167 , 747.1 ± 329.5 , 824.1 ± 810.4 , and 774.0 ± 275.4 , respectively. A statistically significant difference was found between the groups ($p < 0.001$). No statistically significant difference was found in terms of the distributions of monocytes and neutrophils between the groups ($p > 0.050$) (Table 1, Fig. 1).

The BCTQ, consisting of two parts, was administered to patients diagnosed as having CTS. Accordingly, a statistically significant difference was found in terms of the median values of the Boston Symptom Severity Scale and Boston Functional Status Scale between the CTS groups ($p < 0.001$ for both) (Table 2).

Risk factors affecting CTS were analyzed using binary logistic regression analysis as univariate and multivariate models. Considering the multivariate logistic regression analysis, CTS risk increased 1.566 times ($p < 0.001$) as BMI increased, and CTS risk increased 1.005 times as SII increased ($p < 0.001$) (Table 3).

DISCUSSION

In our study, we evaluated whether BMI and the SII index, which was recently associated with an inflammatory process, was associated with CTS.

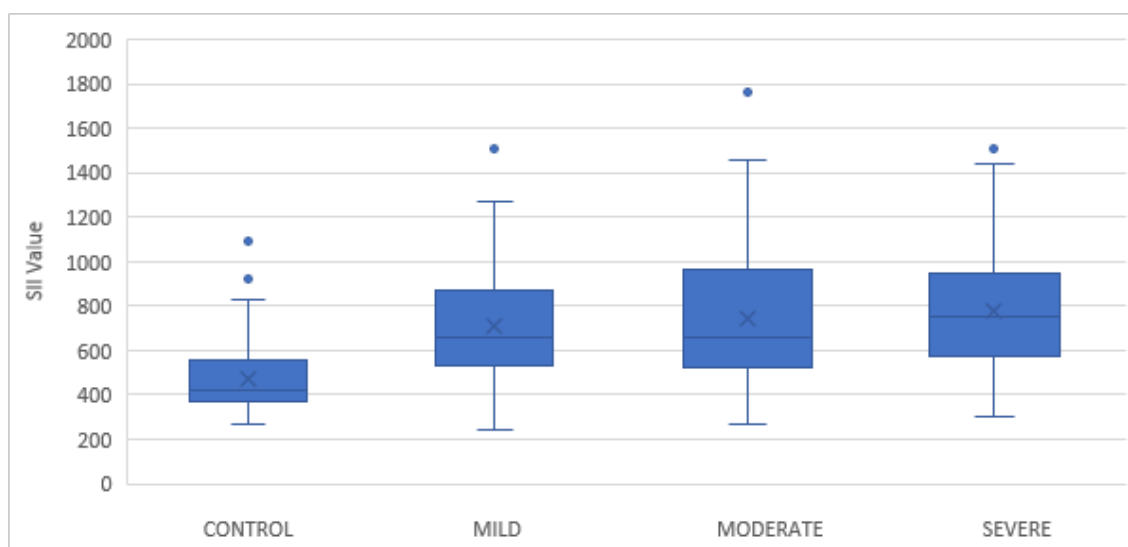


Fig. 1. Box plot of SII values.

Table 1. Comparison of demographic data and laboratory parameters between groups

	Control	Mild	Moderate	Severe	Total	Test statistics	p value
Gender, n (%)							
F	78 (78)	76 (76)	84 (84)	66 (66)	304 (76)	4.605	0.203*
M	22 (22)	24 (24)	16 (16)	34 (34)	96 (24)		
Age (years)	42.0 ± 15.0	52.8 ± 12.1	53.0 ± 13.5	56.0 ± 13.2	51.0 ± 14.4	22.862	< 0.001*
	42.0 (15.0 - 68.0) ^a	52.5 (29.0 - 72.0) ^b	54.0 (23.0 - 85.0) ^b	57.0 (27.0 - 81.0) ^b	51.5 (15.0 - 85.0)		
Height (cm)	166.1 ± 7.1	163.3 ± 9.2	162.4 ± 9.0	161.1 ± 6.8	163.3 ± 8.3	11.272	0.060**
	165.0 (155.0 - 182.0) ^b	160.0 (150.0 - 185.0) ^{ab}	160.0 (150.0 - 192.0) ^{ab}	160.0 (150.0 - 175.0) ^a	161.5 (150.0 - 192.0)		
Weight (kg)	68.8 ± 7.9	82.2 ± 12.7	79.1 ± 12.7	79.2 ± 12.5	77.3 ± 12.6	34.815	< 0.001**
	69.0 (50.0 - 85.0) ^a	80.0 (60.0 - 115.0) ^b	76.5 (51.0 - 110.0) ^b	78.0 (49.0 - 105.0) ^b	75.0 (49.0 - 115.0)		
BMI (kg/m ²)	24.6 ± 4.3	30.9 ± 4.9	30.2 ± 3.7	30.6 ± 4.5	29.0 ± 5.1	66.865	< 0.001*
	25.1 (0.0 - 29.8) ^a	29.8 (22.0 - 45.8) ^b	29.0 (24.3 - 39.1) ^b	30.1 (21.8 - 43.7) ^b	28.1 (0.0 - 45.8)		
HT							
No	88 (88)	72 (72)	76 (76)	72 (72)	308 (77)	4.856	0.183*
Yes	12 (12)	28 (28)	24 (24)	28 (28)	92(23)		
DM							
No	86 (86)	70 (70)	86 (86)	70 (70)	312 (78)	7.459	0.059*
Yes	14 (14)	30 (30)	14 (14)	30 (30)	88 (22)		
Hpl							
No	100 (100)	90 (90)	92 (92)	92 (92)	374 (93.5)	4.854	0.183*
Yes	0 (0)	10 (10)	8 (8)	8 (8)	26 (6.5)		
Neutrophil ×10 ³ /µL	4.2 ± 0.8	4.4 ± 1.2	4.5 ± 1.4	4.7 ± 1.2	4.4 ± 1.2	4.634	0.201*
	4.0 (2.6 - 6.2)	4.3 (2.3 - 6.7)	4.2 (2.6 - 10.3)	4.5 (2.6 - 7.4)	4.3 (2.3 - 10.3)		
Lymphocyte ×10 ³ /µL	2.55 ± 0.48	2.02 ± 0.54	2.03 ± 0.52	2.04 ± 0.36	2.16 ± 0.53	38.926	< 0.001
	2.59 (1.60 - 3.85) ^a	1.90 (1.00 - 3.66) ^b	2.00 (1.08 - 3.71) ^b	2.10 (1.30 - 2.86) ^b	2.10 (1.00 - 3.85)		
Platelet ×10 ³ /µL	278.6 ± 47.7	317.4 ± 56.6	372.6 ± 449.2	329.1 ± 50.4	324.4 ± 229.7	27.412	< 0.001*
	278.0 (189.0-451.0) ^a	326.5 (189.0 - 423.0) ^b	302.0 (190.0-3455.0) ^b	341.5 (190.0-431.0) ^b	304.5 (189.0-3455.0)		
Monocyte ×10 ³ /µL	0.79 ± 0.76	0.64 ± 0.18	0.70 ± 0.17	0.70 ± 0.18	0.71 ± 0.41	3.844	0.279*
	0.67 (0.27 - 5.90)	0.62 (0.30 - 1.00)	0.70 (0.43 - 1.00)	0.70 (0.32 - 1.02)	0.67 (0.27 - 5.90)		
SII ×10 ³ /µL	469.5 ± 167.7	747.1 ± 329.5	824.1 ± 810.4	774.0 ± 275.4	703.7 ± 482.9	46.036	< 0.001*
	422.9 (264.1-1095.3) ^a	657.2 (265.8-1762.6) ^b	674.3 (242.0-6158.9) ^b	755.1 (299.9-1508.5) ^b	613.7 (242.06158.9)		

Data are given as mean ± standard deviation or median (minimum – maximum) or n (%). F = Female, M = Male, BMI = Body mass index, HT = Hypertension, DM = Diabetes mellitus, Hpl = Hyperlipidemia, SII = Systemic immune-inflammation index, *Chi-square test, **Kruskal-Wallis test, **Kruskal-Wallis test, ab No difference between groups with the same letter.

Table 2. Comparison of Boston Symptom Severity Scale and Boston Functional Status Scale parameters between the groups

	Mild	Moderate	Severe	Total	Test statistics	p value
Boston Symptom Severity Scale	15.6 ± 3.4	23.9 ± 3.2	39.2 ± 7.9	26.2 ± 11.1	131.628	< 0.001
	16.0 (11.0 – 20.0) ^a	23.0 (20.0 – 30.0) ^b	37.5 (30.0 – 55.0) ^c	23.0 (11.0 – 55.0)		
Boston Functional Status Scale	7.6 ± 1.4	18.3 ± 2.8	30.2 ± 5.1	18.7 ± 9.9	131.569	< 0.001
	8.0 (5.0 – 10.0) ^a	18.0 (15.0 – 25.0) ^b	29.0 (23.0 – 40.0) ^c	18.0 (5.0 – 40.0)		

Data are given as mean ± standard deviation or median (minimum – maximum) or n (%). Kruskal-Wallis test, ^{ac}No difference between groups with the same letter,

In our study, it was found that the mean age of patients with CTS was statistically significantly higher than the control group. The increased risk with age might be associated with prolonged exposure to repetitive physical movements that strained the wrist. In addition, axon loss and vascular abnormalities that develop in nerves with age may explain the relationship between age and CTS [15-16]. Becker *et al.* [17] evaluated 791 patients with CTS and emphasized that female sex, BMI > 30, age 41-60 years, and DM were independent risk factors for CTS.

It has been suggested that the hydrostatic pressure, which occurs as a result of the increase in the adipose tissue around the median nerve in individuals with obesity with increased BMI, causes a slowdown in the median nerve sensory conduction. In our study, when we compared the mild, moderate, and severe CTS groups with the control group in terms of BMI, we observed a statistically significant relationship between increased BMI and CTS. In the epidemiologic study conducted by Vessey *et al.* [18], a significant relationship was observed between BMI and CTS, similar to our study. In other study, in which the relationship between CTS and obesity was discussed from a different perspective, the relationship between abdominal obesity and CTS was investigated by measuring waist circumference-waist-hip ratio, and it was suggested that abdominal obesity might be a risk factor for CTS [19].

In another study, it was reported that there was an increase in the risk of CTS in addition to the increases in the risk of development of cardiovascular disease and type 2 DM in patients with obesity with metabolic syndrome [20]. Besides BMI being a risk factor for CTS, no relationship was found between the increase in BMI and the severity of CTS [9]. In the study of Kouyoumdjian *et al.* in which 210 patients with symptomatic CTS and 320 controls were compared, it was reported that there was a significant relationship between CTS and BMI, and CTS-wrist index. They also reported that although age and wrist index were associated with the severity of CTS, BMI was not associated with the CTS severity [21]. When the multivariate model analysis results of our study were examined, we observed that each 1 unit increase in BMI increased the risk of CTS by 1.566 times (p < 0.001). In other words, according to the results of our study, it can be concluded that the risk of developing CTS increases as BMI increases.

Table 3. Examination of risk factors affecting the disease

	Univariate		Multivariate (enter) ¹		Multivariate (wald) ²	
	OR (95 % CI)	p value	OR (95 % CI)	p value	OR (95 % CI)	p value
Gender (male)	1.161 (0.540-2.495)	0.702	2.210 (0.733-6.664)	0.159		
Ht	0.375 (0.148-0.947)	0.038	1.765 (0.367-8.495)	0.478		
Dm	0.497 (0.206-1.200)	0.120	0.741 (0.188-2.930)	0.670		
Age	1.066 (1.038-1.095)	< 0.001	1.034 (0.995-1.074)	0.085	1.037 (1.001-1.074)	0.046
BMI	1.849 (1.509-2.265)	< 0.001	1.611 (1.307-1.985)	< 0.001	1.566 (1.285-1.907)	< 0.001
SII	1.006 (1.004-1.008)	< 0.001	1.005 (1.002-1.008)	< 0.001	1.005 (1.002-1.008)	< 0.001

BMI = Body mass index, HT = Hypertension, DM = Diabetes mellitus, SII = Systemic immune inflammation index. Cox&Snell R² = 0,3419; Nagelkerke R² = 0,621; Hosmer and Lemeshow Chi Square = 8,304, Accuracy= 0,850¹, Cox&Snell R² = 0,412; Nagelkerke R² = 0,610; Hosmer and Lemeshow Chi Square = 7.926, Accuracy = 0,850²

Investigations on the pathophysiologic mechanisms that cause compression and traction of the median nerve are still ongoing, and studies aimed at investigating the role of chronic inflammation and elucidating the pathophysiology attract attention [22]. It is known that fibrosis develops as a result of compression in the canal where the median nerve is located. The release of interleukins (IL-1, IL-2, and IL-6) increases with the increase in pressure caused by the effect of compression. Increased interleukins trigger the formation of fibrosis by increasing the release of growth factors such as vascular endothelial growth factor (VEGF) and transforming growth factor-beta (TGF-β). Subclinical systemic inflammation may also play a role in the development of fibrosis by triggering the release of cytokines and growth factors [23]. The SII index is a marker that has been shown to be associated with inflammation in many studies in different disease groups. Because we could not find a similar study evaluating its relationship with CTS in the literature, we believe ours is the first on this subject. In our study, when the patients with CTS were compared with the control group, we observed that there was a statistically significant relationship between the SII index and the development of CTS, and the risk of CTS increased 1.005 times as the SII index increased

(*p* < 0.001).

In the study of Tepe *et al.* [24], C-reactive protein (CRP) and CRP/albumin ratios were evaluated in 50 controls and 50 patients with CTS, and no statistically significant difference supporting inflammation was detected, but it was suggested that re-evaluation of this hypothesis by increasing the number of patients with acute CTS might lead to decide anti-inflammatory treatment options in the treatment [24]. To investigate the contribution of the SII index to inflammation, its relationship with many different disease groups such as solid tumors, colorectal cancers, cerebrovascular diseases, and sinus vein thrombosis was evaluated, and it was emphasized that the SII index was a predictor of inflammation as a common result of the studies [25, 26]. In a study comparing inflammation markers in patients undergoing dialysis with and without CTS, it was shown that IL-1, tumor necrosis factor-alpha (TNF-α), and IL-6 levels were significant in patients with CTS and that inflammation had an effect on the process [27].

In a different study investigating the relationship of inflammation with CTS, 407 patients with CTS were compared with 206 controls. The correlation between CTS and NLR and PLR was evaluated. As a result of the study, it was reported that a 1 unit increase

in NLR level increased the risk of CTS by 1.7 times, and accordingly it was shown that the NLR level increased in severe CTS. In addition, it was suggested that subclinical systemic inflammation might cause CTS by increasing cytokines and growth factors and by causing fibrosis [28]. The contribution of inflammation in the pathophysiologic process of CTS has been demonstrated in many studies, but this evidence should be supported by studies with large case series.

When we compared the Boston symptom severity scale and functional status scale, a statistically significant difference was observed between the CTS groups ($p < 0.001$). This made us think that as the severity of compression increased in patients with CTS, the functionality of the patients might decrease and their quality of life might be adversely affected.

Studies have reported that there is a correlation between the increase in compression severity and the Boston functional score and that this relationship becomes stronger, especially in patients in whom deterioration in motor functions is evident. It has been suggested that the use of the Boston functional status scale in CTS would reflect the level of compression severity more effectively than grip strength in terms of assessing hand functions [29, 30].

Limitations

Our study had some limitations such as the limited number of patients, the inability to follow up for a long time, and the fact that the patients were not re-evaluated after the treatment.

CONCLUSION

In conclusion, we found a significant relationship between age, increased BMI, and the SII index and CTS in our study. In light of previous studies and the information obtained in our study, it was thought that advanced age and increased BMI were risk factors in CTS. According to the results of our study, in which the relationship between the SII index and CTS was evaluated for the first time, inflammation may play a role in the pathophysiology of CTS, and this suggests that systemic anti-inflammatory drugs could be beneficial in the treatment. However, to confirm the role of systemic inflammation in CTS, this hypothesis should be supported by multicenter randomized controlled

prospective studies with a large number of patients.

Authors' Contribution

Study Conception: MKG, DYO; Study Design: MKG, DYO; Supervision: MKG, DYO; Funding: N/A; Materials: N/A; Data Collection and/or Processing: MKG; Statistical Analysis and/or Data Interpretation: MKG, DYO; Literature Review: MKG; Manuscript Preparation: SMKG, DYO and Critical Review: MKG, DYO.

Conflict of interest

The authors disclosed no conflict of interest during the preparation or publication of this manuscript.

Financing

The authors disclosed that they did not receive any grant during conduction or writing of this study.

REFERENCES

1. Miyamoto H, Morizaki Y, Kashiyama T, Tanaka S. Grey-scale sonography and sonoelastography for diagnosing carpal tunnel syndrome. *World J Radiol* 2016;8:281-7.
2. Kurt S, Karaer H, Kaplan Y, Etikan İ et al. [The relationship between carpal tunnel syndrome and body mass index, age and gender]. *Turk J Phys Med Rehab* 2006;52:154-7. [Article in Turkish]
3. Newington L, Harris EC, Walker-Bone K. Carpal tunnel syndrome and work. *Best Pract Res Clin Rheumatol* 2015;29:440-53.
4. Cranford CS, Ho JY, Kalainov DM, Hartigan BJ. Carpal tunnel syndrome. *J Am Acad Orthop Surg* 2007;15:537-48.
5. Neal NC, McManners J, Stirling GA. Pathology of the flexor tendon sheath in the spontaneous carpal tunnel syndrome. *J Hand Surg Br* 1987;12:229-32.
6. Yang Y, Han Y, Sun W, Zhang Y. Increased systemic immune-inflammation index predicts hemorrhagic transformation in anterior circulation acute ischemic stroke due to large-artery atherosclerotic. *Int J Neurosci* 2021. doi: 10.1080/00207454.2021.1953021.
7. Hu B, Yang XR, Xu Y, Sun YF, Sun C, Guo W, et al. Systemic immune-inflammation index predicts prognosis of patients after curative resection for hepatocellular carcinoma. *Clin Cancer Res* 2014;20:6212-22.
8. Habib SS, Alanazy MH. Predictive value of markers of adiposity in carpal tunnel syndrome: a clinical and electrophysiological evaluation. *J Coll Physicians Surg Pak* 2020;30:828-32.
9. Werner RA, Albers JW, Franzblau A, Armstrong TJ.. The relationship between body mass index and the diagnosis of carpal tunnel syndrome. *Muscle and Nerve* 1994;17:632-6.
10. Lee DH, Claussen GC, Oh S. Clinical nerve conduction and

needle electromyography studies. *J Am Acad Orthop Surg* 2004;12:276-87.

11. Padua L, LoMonaco M, Gregori B, Valente EM, Padua R, Tonali P. Neurophysiological classification and sensitivity in 500 carpal tunnel syndrome hands. *Acta Neurol Scand* 1997;96:211-7.

12. Garrow JS, Webster J. Quetelet's index (W/H²) as a measure of fatness. *Int J Obes* 1985;9:147-53.

13. Levine DW, Simmons BP, Koris MJ, Daltroy LH, Hohl GG, Fossel AH, et al. A self-administered questionnaire for the assessment of severity of symptoms and functional status in carpal tunnel syndrome. *J Bone Joint Surg Am* 1993;75:1585-92.

14. Sezgin M, İncel NA, Sevim S, Camdeviren H, As İ, Erdogan C. Assessment of symptom severity and functional status in patients with carpal tunnel syndrome: reliability and validity of the Turkish version of the Boston Questionnaire. *Disabil Rehabil* 2006;28:1281-5.

15. Kouyoumdjian JA. Carpal tunnel syndrome. Age, nerve conduction severity and duration of symptomatology. *Arq Neuropsiquiatr* 1999;57:382-6.

16. Kommalage M, Pathirana KD. Influence of age and the severity of median nerve compression on forearm median motor conduction velocity in carpal tunnel syndrome. *J Clin Neurophysiol* 2011;28:642-6.

17. Becker J, Nora DB, Gomes I, Stringari FF, Seitensus Panosso JS, et al. An evaluation of gender, obesity, age and diabetes mellitus as risk factors for carpal tunnel syndrome. *Clin Neurophysiol* 2002;13:1429-34.

18. Vessey MP, Villard-Mackintosh L, Yeates D. Epidemiology of carpal tunnel syndrome in women of childbearing age. Findings in a large cohort study. *Int J Epidemiol* 1990;19:655-9.

19. Uzar E, İlhan A, Ersoy A. [Association between carpal tunnel syndrome and abdominal obesity]. *Turk J Neurol* 2010;16:187-92. [Article in Turkish]

20. Aydemir ŞU, Tekeşin A, Yıldırım A. [Relationship between carpal tunnel syndrome and metabolic syndrome]. *Bakırköy Tıp*

Dergisi 2019;15:250-8. [Article in Turkish]

21. Kouyoumdjian JA, Zanetta DMT, Morita MP. Evaluation of age, body mass index, and wrist index as risk factors for carpal tunnel syndrome severity. *Muscle Nerve* 2002;25:93-7.

22. Altun Y, Tak AZA. Can serum C-reactive protein and procalcitonin levels associate with carpal tunnel syndrome? *Medical Science and Discovery* 2019;6:18-23.

23. Chikenji T, Gingery A, Zhao C, Passe SM, Ozasa Y, Larson D, et al. Transforming growth factor- β (TGF- β) expression is increased in the subsynovial connective tissues of patients with idiopathic carpal tunnel syndrome. *J Orthop Res* 2014;32:116-22.

24. Tepe N, Gülçen B. The role of CRP/albumin ratio in the carpal tunnel syndrome. *Balıkesir Med J* 2020;4:19-23.

25. Zhong JH, Huang DH, Chen ZY. Prognostic role of systemic immune-inflammation index in solid tumors: a systematic review and meta-analysis. *Oncotarget* 2017;8:75381-8.

26. Li LH, Chen CT, Chang YC, Chen YJ, Lee IH, How CK. Prognostic role of neutrophil-to-lymphocyte ratio, platelet-to-lymphocyte ratio, and systemic immune inflammation index in acute ischemic stroke: A STROBE-compliant retrospective study. *Medicine (Baltimore)* 2021;100:e26354.

27. Takasu S, Takatsu S, Kunitomo Y. Serum hyaluronic acid and interleukin-6 as possible markers of carpal tunnel syndrome in chronic hemodialysis patients. *Artif Organs* 1994; 18:420-4.

28. Güneş M, Büyükgöl H. Correlation of neutrophil/lymphocyte and platelet/lymphocyte ratios with the severity of idiopathic carpal tunnel syndrome. *Muscle Nerve* 2020;61:369-74.

29. Umay E, Karahmet Z, Avluk Ö, Ünlü E, Çakçı A. [Relationship between the severity of compression and clinical symptoms, physical, functional and quality of life findings in patients with carpal tunnel syndrome] *Turk J Phys Med Rehab* 2011;57:93-200. [Article in Turkish]

30. De Kleermaeker FGCM, Boogaarts HD, Meulstee J, Verhagen VIM. Minimal clinically important difference for the Boston Carpal Tunnel Questionnaire: new insights and review of literature. *J Hand Surg Eur Vol* 2019;44:283-9.



This is an open access article distributed under the terms of [Creative Commons Attribution-NonCommercial-NoDerivatives 4.0 International License](https://creativecommons.org/licenses/by-nc-nd/4.0/).

GSTM1, GSTP1, p53 as some probable predictors of prognosis in primary and metastatic epithelial ovarian cancer

Gizem Özer¹, Pınar Kaygın¹, Onur Dirican², Serpil Oğuztüzün¹, Sezen Yılmaz Sarialtın³, Gülçin Güler Şimşek⁴, Ayşegül Erdem⁵, Murat Kılıç⁶, Tülay Çoban³

¹Department of Biology, Kırıkkale University, Faculty of Art and Sciences, Kırıkkale, Turkey; ²Department of Pathology Laboratory Techniques, Istanbul Gelişim University, Vocational School of Health Services, Istanbul, Turkey; ³Department of Pharmaceutical Toxicology, Ankara University, Faculty of Pharmacy, Ankara, Turkey; ⁴Department of Pathology, University of Health Sciences, Gülhane Training and Research Hospital, Ankara, Turkey; ⁵Department of Pathology, University of Health Sciences, Keçiören Training and Research Hospital, Ankara, Turkey; ⁶Department of Pharmacy Services, Ankara University, Vocational School of Health Services, Ankara, Turkey

ABSTRACT

Objectives: Ovarian carcinomas are responsible for the death of more women than all other gynecologic malignancies in the Western world. Ovarian carcinomas are detected in an advanced stage of the disease in approximately 80% of the patients. Glutathione S-transferases (GSTs) are an important family involved in the detoxification of several xenobiotics. Thus, this mechanism protects tissues from the harmful effects of oxidative stress and chemical-induced damages. The expression of them may contribute to the characteristics of ovarian carcinoma as they can metabolise both exogenous and endogenous compounds, which are implicated in the development of ovarian cancer. Therefore, our aim was to determine the expressions of GST Mu 1 (GSTM1), GST Pi 1 (GSTP1), and also p53, which is a tumor suppressor gene, in benign and malign ovarian tumors and metastasis tissues.

Methods: A total of the 99 patients with ovarian tumor enrolled in the study. Thirty-one of the tissues was benign tumor, 17 was malign tumor and 51 was metastasis. The immunohistochemical GSTM1, GSTP1, and p53 staining characteristics of these tissues were investigated.

Results: The highest GSTM1, GSTP1, and p53 expression was noted in the malignant group followed by the metastasis group. GSTP1 expression was significantly higher in malignant tissues than benign ones ($p = 0.015$). No statistically significant difference was observed in the level of GSTM1 expression between groups ($p = 0.524$). p53 expression was significantly higher in the metastasis and malignant tissues than the benign ones ($p < 0.001$).

Conclusions: The higher expressions of GSTP1 and p53 in malignant and metastasis tissues than benign ones indicate that these expressions could be important biomarkers in ovarian cancer development and progression. Further studies with more cases are required to confirm the results of our present study.

Keywords: Ovary carcinoma, glutathione-S-transferase, p53, immunohistochemistry

Received: May 5, 2022; Accepted: December 30, 2022; Published Online: January 15, 2023



e-ISSN: 2149-3189

How to cite this article: Özer G, Kaygın P, Dirican O, Oğuztüzün S, Yılmaz Sarialtın S, Güler Şimşek G, et al. GSTM1, GSTP1, p53 as some probable predictors of prognosis in primary and metastatic epithelial ovarian cancer. Eur Res J 2023;9(3):477-483. DOI: 10.18621/eurj.1112116

Address for correspondence: Onur Dirican, MD., Istanbul Gelişim University, Vocational School of Health Services, Department of Pathology Laboratory Techniques, Cihangir Mah., Şehit Jandarma Komando Er Hakan Öner Sk., No:1, 34310 Avcılar, Istanbul, Turkey

E-mail: onurdirican@hotmail.com, Phone: +90 212 422 70 00, Fax: +90 212 422 74 01



©Copyright © 2023 by Prusa Medical Publishing
Available at <http://dergipark.org.tr/eurj>
info@prusamp.com

Ovarian cancer is a type of cancer that starts in the ovaries and generally spreads throughout the body [1]. It is a heterogeneous disease with a low survival rate and rapid spread, and is the most important cause of death from gynecological cancer [2]. Different types of tumors can develop from each cell type. These tumors are epithelial tumors, germ cell tumors (originating from ovarian cell and follicle) and stromal tumors. Epithelial tumors arise from epithelial cells that cover the outer surface of the ovary. Germ cell tumors are derived from the ovary. Stromal tumors, on the other hand, consist of structural cells that hold the ovarian cells together and produce female hormones, progesterone and estrogen. Most of these tumors are benign and do not spread beyond the ovary [3]. Tumors originating from nonspecific connective tissue cells and tumors originating from another organ by metastasis [1].

The metabolism of xenobiotics is a two-phase process. Phase I reaction is mostly carried out in the liver by the microsomal enzyme system. Phase I reaction may also occur in the lung, kidney, intestine, skin, testis, placenta, and adrenal gland limitedly. Lipid-soluble xenobiotics become more polar by the phase I reactions [4, 5]. Phase II reactions are conjugation reactions carried out by many cytosolic enzymes. Polar metabolites, which are formed as a result of detoxification, combine with endogenous substances by conjugation reactions and are eliminated inactively [6]. Reactive species formed by the Phase I enzymes with glutathione enter into conjugation and eventually bind with cell macromolecules (DNA, RNA, protein), preventing cell damage [7].

Glutathione S-transferases (GSTs) is a family of Phase II detoxification enzymes responsible for the metabolism of chemotherapeutic agents, reactive oxygen molecules and xenobiotics including environmental carcinogens. GSTs catalyze the reactions between various electrophilic compounds and glutathione. GSTs protect DNA from alkylation by conjugation of active metabolites with glutathione. GSTs are dimeric enzymes that inactivate electrophilic xenobiotics and enable their conjugation for removal from the body. Glutathione protects the organism against reactive chemical compounds by binding to compounds with its nucleophilic sulfhydryl group [8]. GSTM1 isoenzymes are predominantly expressed in the liver and a lesser extent in the lung while GSTM3 is an important

isoenzyme in lung tissue [9]. GSTP1-1 enzymes show resistance to chemotherapy and radiotherapy applied in many different cancers [10]. It is estimated that half of all cancer cases are associated with mutations in the p53 gene. This prediction suggests that p53 controls a key event in cell proliferation and that this regulation is not cell- or tissue-specific [11]. Since different mutations of p53 cause the structure of the protein to change, it cannot bind to DNA [12]. Mutation occurring in a single allele of the gene behaves as if there is no functional p53 protein in the cell. Homozygous loss of this gene results in non-repairing of DNA damage and the cell undergoes malignant transformation [13]. In our study, we aimed to investigate the differences in the expressions of GSTM1 and GSTP1, which play essential roles in xenobiotic metabolism, and p53, a tumor suppressor gene, in benign and malignant ovarian tumor tissues. Our other goal was to determine the GSTM1, GSTP1, and p53 expressions in metastatic tissues and assess whether these proteins have a role in the progression of the disease. Moreover, the relationship of these expressions with age was also aimed to investigate.

METHODS

We investigated the immunohistochemical staining characteristics of GSTM1, GSTP1, and p53 in malignant (n = 17), benign (n = 31), and metastasis (n = 51) ovarian tumor tissues from 99 patients in Ankara Keçiören Training and Research Hospital. The expression patterns of the tissues were compared based on immunohistochemical staining intensity. Ethics committee approval was provided by the decision of the Ankara Keçiören Training and Research Hospital Clinical Research Ethics Committee, with the decision number of 2012-KAEK-15/2215 (09.02.2021).

Immunohistochemical Staining

The GSTM1, GSTP1, and p53 were studied by immunohistochemical staining in the tumor tissues of the patients. For immunohistochemistry, the formalin-fixed tissue sections dewaxed in xylene and rehydrated in ethanol sections were washed with distilled water for 3 min. The sections were peroxidase-incubated for 10 minutes using 3% hydrogen peroxide in methanol (v/v). Subsequently, the sections were washed with

distilled water for 3 min and antigen retrieval was performed for 3 min using a 0.01M citrate buffer, pH 6.0 in a domestic pressure cooker. Sections were placed in Tris-buffered saline (TBS) containing 0.15M sodium chloride and 0.05 M Tris-HCL pH 7.6. Sections were incubated at room temperature for 10 min with superblock (SHP125; Scy Tek laboratories, west logan, UT). The primary antibody was diluted through a diluting solution, based on the manufacturer company instructions. After sections were incubated with the primary antibody for anti-GSTP1 (Sc-28,494; Santa Cruz Biotechnology, Inc) diluted 1:500, anti-p53 (M00001-4, Boster Biological Technology) diluted 1:300, anti-GSTM1 (Sc-517262; Santa Cruz Biotechnology, Inc) diluted 1:100. The sections were incubated at room temperature with a biotinylated link antibody (SHP125; ScyTek Laboratories) followed by streptavidin/HRP complex (SHP125; ScyTek laboratories). After washing with TBS for 15 min, the sections were incubated at room temperature with biotinylated link antibody (SHP125; ScyTek Laboratories) then diaminobenzidine was used to visualize peroxidase activity in tissues. Nuclei were lightly counterstained with hematoxylin, and then the sections were dehydrated and mounted. Light microscopy and scoring of immunohistochemically stained sections were performed by a pathologist, who was unaware of the patients' clinical information scoring for each enzyme was: -, negative (no staining); 1, weak staining; 2, moderate staining; 3, strong staining.

Statistical Analysis

Statistical analyses were performed with the IBM SPSS software (Statistical Package for the Social Sciences, Version 25.0). Data were presented as mean \pm standard error of the mean (SEM) and minimum-maximum staining intensity. Homogeneity of variances was tested by Levene test. Normality of distribution was assessed via Shapiro-Wilk and Kolmogorov-Smirnov tests. The data were not normally distributed. Thus, the Kruskal-Wallis test was performed to compare differences between groups followed by the post hoc bonferonni correction. The point biserial correlation analysis was used to evaluate the correlation between data. The statistical significance level was defined as $p < 0.05$.

RESULTS

The study covers 99 female subjects with benign ovarian tumor ($n = 31$), malignant ovarian tumor ($n = 17$), and metastasis ($n = 51$). The mean age was 47.29 ± 2.87 years in benign ovarian tumor group, 60.56 ± 2.35 years in malignant ovarian tumor group and 61.02 ± 1.37 years in metastasis group (Fig. 1).

Immunohistochemical expression of GSTM1, GSTP1, and p53 was determined in benign ovarian tumor, malign ovarian tumor and metastasis tissues and the results were shown in Table 1. Some of the general images obtained for pathological microscopy ex-

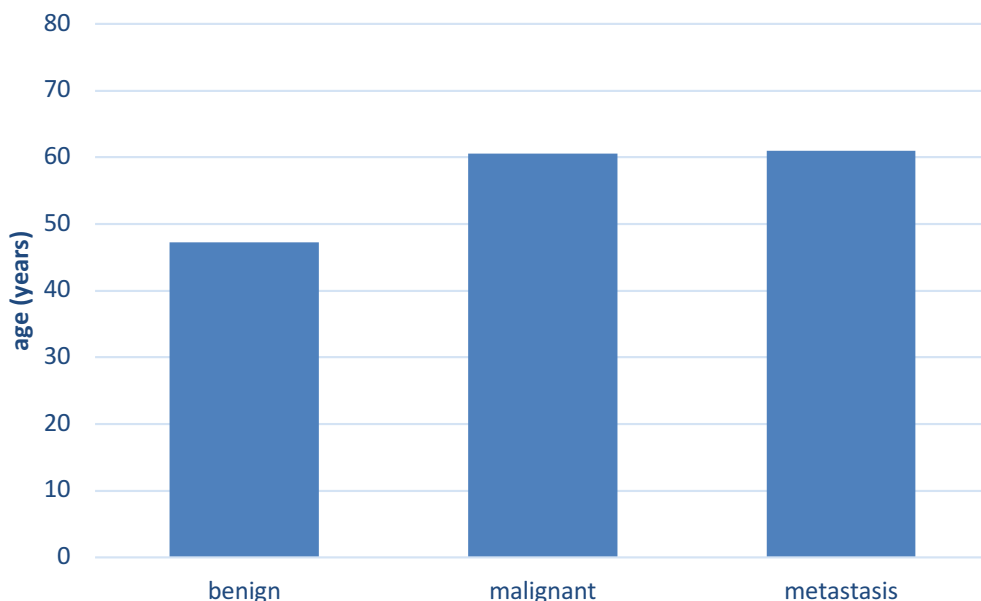


Fig. 1. Age distribution of patients according to benign, malignant and metastasis groups

Table 1. Expression levels of GSTM1, GSTP1, and p53 proteins in benign and malignant ovarian tumor samples and metastasis tissues

	Benign group (n = 31)	Malignant group (n = 17)	Metastasis group (n = 51)	p value
GSTM1				
Positive (1)	11/31 (35.48%)	7/17 (41.18%)	14/51 (27.45%)	0.524
Negative (0)	20/31 (64.52%)	10/17 (58.82%)	37/51 (72.55%)	
Mean	0.35 ± 0.09 (0-1)	0.41 ± 0.12 (0-1)	0.27 ± 0.06 (0-1)	
GSTP1				
Positive (1)	15/31 (48.39%)	15/17 (88.24%)	37/51 (72.55%)	0.010
Negative (0)	16/31 (51.61%)	2/17 (11.76%)	14/51 (27.45%)	
Mean	0.48 ± 0.09 (0-1)	0.88 ± 0.08 (0-1)	0.73 ± 0.06 (0-1)	
p53				
Positive (1)	0/31 (0%)	11/17 (64.71%)	26/51 (50.98%)	< 0.001
Negative (0)	31/31 (100%)	6/17 (35.29%)	25/51 (49.02%)	
Mean	0	0.65 ± 0.12 (0-1)	0.51 ± 0.07 (0-1)	

Data were presented as mean ± SEM and minimum-maximum staining intensity. The Kruskal-Wallis test was used for the statistical analysis. The statistical significance level was defined as $p < 0.05$.

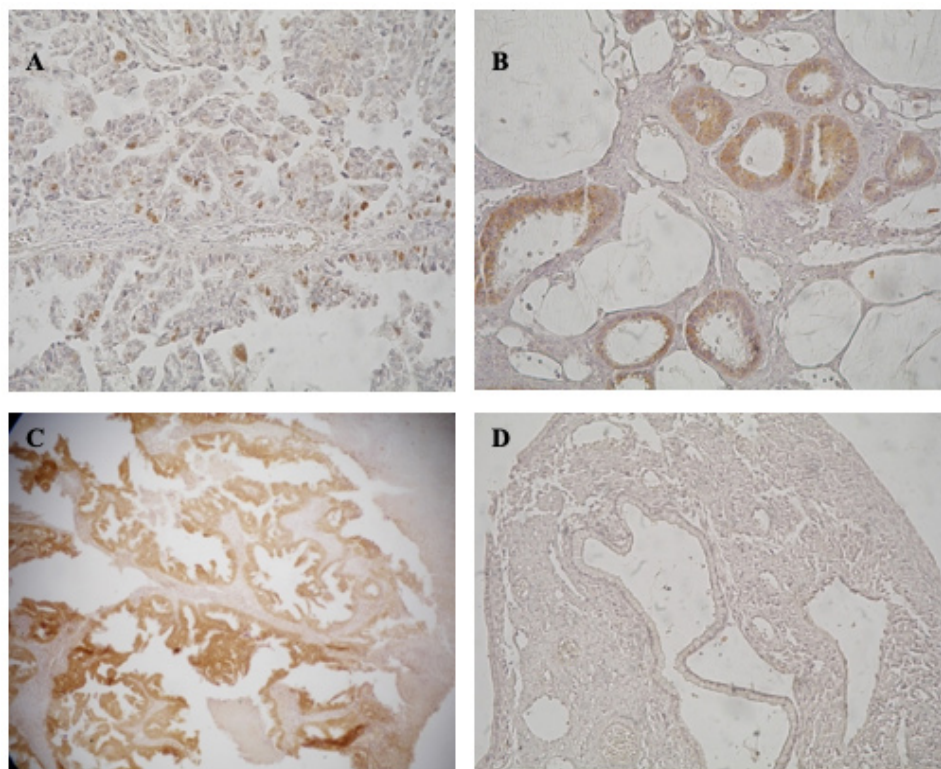


Fig. 2. Immunohistochemical expression of GSTM1 and GSTP1 isoenzymes, and p53 protein in ovarian benign and tumor tissues, (A) p53 protein expression on tumor tissue; (B) GSTP1 protein expression on tumor tissue; (C) GSTM1 protein expression on tumor tissue; and (D) GSTP1 protein expression on benign tissue.

amination of preparative tissues obtained as a result of immunohistochemical applications are given in Fig. 2.

The results showed that the highest GSTM1 expression was observed in the malignant group. GSTM1 was positively expressed in 35.48% of benign tissues, while 41.18% of malignant ones. Positive GSTM1 expression was found in 27.45% of metastasis tissues. However, there were no statistically significant differences between groups in terms of GSTM1 expression ($p = 0.524$).

There was a statistically significant GSTP1 expressions between groups ($p = 0.010$). The highest GSTP1 expression was noted in the malignant group followed by the metastasis group. Positive GSTP1 expression was observed in 88.24% of malignant, 72.55% of metastasis, and 48.39% of benign tissues. GSTP1 expression of malignant tissues was 1.83-times higher than that of benign tissues ($p = 0.015$). Metastasis tissues were exhibited 1.5-fold greater GSTP1 expression than that of benign tissues. There was no significant difference in GSTM1 expressions between malignant and metastatic tissues ($p = 0.700$). The highest p53 expression was noted in the malignant group followed by the metastasis group. 64.71% of malign tissues displayed positive p53 expression, while 50.98% of metastasis ones. None of the samples had positive p53 expression in the benign group. Both malignant and metastasis tissues exhibited statistically significantly higher p53 expression than benign tissues ($p < 0.001$). Malignant and metastasis tissues exhibited

similar p53 expression patterns. No significant difference in p53 expressions was found between the malignant and the metastasis groups ($p = 0.941$).

The point biserial correlation analysis was performed. The relationships between the patients's age and the expression levels were examined. Hex binned scatter plots of expressions versus age were shown in Fig. 4. The increase in expressions of p53 was observed to be positively correlated with the age in a ratio of 32.70% ($p = 0.001$). No significant correlation was observed between age and GSTM1 and GSTP1 expressions ($p = 0.422$ and $p = 0.427$, respectively).

DISCUSSION

It is now known that genes and proteins produced by the cell for different functions are also involved in the mechanism of this disease, rather than studies on target genes and proteins at the molecular level, in studies aimed at elucidating the mechanisms of cancer. Genes and proteins and their metabolism, which are not directly involved in cancer formation such as detoxification and drug metabolism, and intracellular immunity, but cause cancer as a result of structural deterioration, are also shown among the causes of cancer formation. Detoxification mechanisms are of great importance in protecting cells from carcinogenic effects. Detoxification (biotransformation) is the mechanisms of making harmful substances such as xenobiotics (toxic substances, metabolites, epoxides) harmless

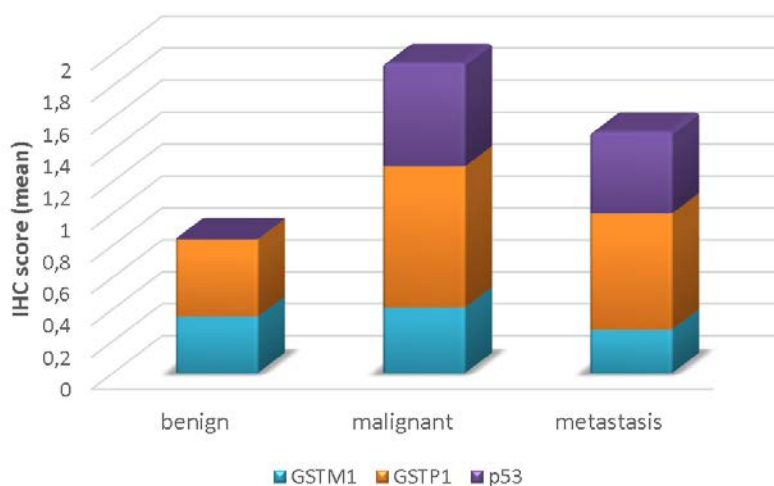


Fig. 3. Immunohistochemical staining scores of subjects in benign, malignant and metastasis groups. IHC = Immunohistochemical.

with the help of various enzymes or molecules and excreting them out of the body. Enzymes or molecules involved in these mechanisms also support this vital phenomenon. The GST enzyme family constitutes an enzyme system that creates Phase II reactions in detoxification metabolism. At the same time, GST enzymes have crucial roles in drug metabolism, elimination of intracellular oxidative damage, provide the detoxification of reactive intermediates and protect the cells from harmful effects such as cancer, necrosis, tissue and DNA damage. In light of this information, the roles of the members of this family have been explained in the literature in many studies such as normal intracellular antioxidant activity in cancer formation, drug resistance in drug metabolism, and detoxification metabolism. On the other hand, studies on the roles of GSTM1 and GSTP1 isozymes in cancer formation are very limited [8, 14, 15].

Similar to the results of our study, Marks *et al.* [16] found high levels of nuclear p53 protein expression in the malignant epithelium in 54 (50%) of 107 epithelial ovarian cancers in their study. Green *et al.* [17] reported that GSTP1 could not make a difference in 109 ovarian cancers (86 cancer and 23 normal) in normal and malignant tissues, but stained more intensely in the malignant epithelium. In patients resistant to chemotherapy, GSTP1 stained at higher intensity. GSTA1 and GSTM1 did not make a difference in malignant and benign cases, but stained with higher intensity in malignant [17].

In a study conducted in the southeast of England in 2001, GSTM1 mutation and null allele frequency were investigated in 293 ovarian cancer patients and 219 control group. The "null" allele frequency in the patient group (59%) compared to the "null" allele frequency in the control group (48.9%) and it was found to be significantly increased ($p=0.025$). With these results, it was observed that the GSTM1 "null" allele was not associated with endometriosis. Despite this, it has been reported to be a factor in endometriotic malignant transformation and clear-cell ovarian cancer [18].

In another study, similar to our study, while trying to determine the "null" allele frequency in the GSTM1 and GSTT1 gene regions with samples taken from 81 individuals with invasive ovarian tumors, it was determined whether p53 protein expression accompanies the null allele frequency in phase II enzymes in this

patient group. The situation where it did not work was compared with the data obtained after the immunohistochemical method. A significant relationship could only be established in the group of patients who received chemotherapy with the group of patients with GSTM1/GSTT1 "null" allele frequency ($p = 0.007$). No relationship could be established between p53 and all other parameters and conditions such as survival [19]. The relationship between polymorphisms in the GSTT1, GSTM1, and GSTP1 gene regions in the formation and course of the disease was investigated in 132 patients with epithelial ovarian cancer and 132 control. Considering the polymorphic situation in these gene regions and compared to the control group, the risk of encountering epithelial ovarian cancer was found 1.8-fold, 2.38-fold, and 11.28-fold higher in GSTP1 Ile/Ile, GSTM1 null plus GSTP1 Ile/Ile, and GSTM1 null plus GSTT1 null plus GSTP1 Ile/Ile than control [20].

CONCLUSION

The higher expressions of GSTP1 and p53 in malignant and metastasis tissues than benign ones indicate that these expressions could be important biomarkers in ovarian cancer development and progression. However, our study have some limitations. The tissues used in this study belong to patients who have not received chemotherapy and clinical data of the patients are not sufficient. Since GSTs are involved in drug metabolism, their expression in patients with ovarian tumor receiving chemotherapy needs to be investigated. Therefore, there is a need for new studies in which a larger number of patients and clinical data will be evaluated together in order to confirm our results.

Authors' Contribution

Study Conception: GÖ,SO; Study Design: GÖ,PK,SYS,SO; Supervision: SO; Funding: SO; Materials: GÖ,PK,SYS,SO; Data Collection and/or Processing: PK,OD,SYS,GGŞ,SO; Statistical Analysis and/or Data Interpretation: SYS,OD,SO; Literature Review: OD,MK; Manuscript Preparation: OD and Critical Review: AE,TÇ.

Conflict of interest

The authors disclosed no conflict of interest during

the preparation or publication of this manuscript.

Financing

The authors disclosed that they did not receive any grant during conduction or writing of this study.

REFERENCES

- Edmondson RJ, Monaghan JM. The epidemiology of ovarian cancer. *Int J Gynecol Cancer* 2001;11:423-9.
- Chu CS, Rubin SC. Screening for ovarian cancer in the general population. *Best Pract Res Clin Obstet Gynaecol* 2006;20:307-20.
- American Cancer Society, Ovarian Cancer, Global Cancer Fact & Figures American Cancer Society, Atlanta, GA, USA. 2011.
- Donald PJ. Marijuana smoking -- possible cause of head and neck carcinoma in young patients. *OtolaryngolHead Neck Surg* 1986;94:517-21.
- Guengerich FP. Characterization of human microsomal cytochrome P-450 enzymes. *Ann Rev Pharmacol Toxicol* 1989;29:241-64.
- Caldwell J. Conjugation reactions in foreign-compound metabolism: definition, consequences, and species variations. *Drug Metab Rev* 1982;13:745-77.
- Board P, Coggan M, Johnston P, Ross V, Suzuki T, Webb G. Genetic heterogeneity of the human glutathione transferases: a complex of gene families. *Pharmacol Ther* 1990;48:357-69.
- Commandeur JN, Stijntjes GJ, Vermeulen NP. Enzymes and transport systems involved in the formation and disposition of glutathione S-conjugates. Role in bioactivation and detoxication mechanisms of xenobiotics. *Pharmacol Rev* 1995;47:271-330.
- Di Pietro G, Magno LA, Rios-Santos F. Glutathione S-transferases: an overview in cancer research. *Expert Opin Drug Metab Toxicol* 2010;6:153-70.
- Moscow JA, Fairchild CR, Madden MJ, Ransom DT, Wieand HS, O'Brien EE, et al. Expression of anionic glutathione-S-transferase and P-glycoprotein genes in human tissues and tumors. *Cancer Res* 1989;49:1422-8.
- Ko LJ, Prives C. p53: puzzle and paradigm. *Genes Dev* 1996;10:1054-72.
- Lane DP, Benchimol S. p53: oncogene or anti-oncogene? *Genes Dev* 1990;4:1-8.
- Maity A, McKenna WG, Muschel RJ. The molecular basis for cell cycle delays following ionizing radiation: a review. *Radiother Oncol* 1994;31:1-13.
- Kupryjańczyk J, Thor AD, Beauchamp R, Merritt V, Edgerton SM, Bell DA, et al. p53 gene mutations and protein accumulation in human ovarian cancer. *Proc Natl Acad Sci U S A* 1993;90:4961-5.
- Cui J, Li G, Yin J, Li L, Tan Y, Wei H, et al. GSTP1 and cancer: expression, methylation, polymorphisms and signaling (Review). *IntJ Oncol* 2020;56:867-78.
- Marks JR, Davidoff AM, Kerns BJ, Humphrey PA, Pence JC, Dodge RK, et al. Overexpression and mutation of p53 in epithelial ovarian cancer. *Cancer Res* 1991;51:2979-84.
- Green JA, Robertson LJ, Clark AH. Glutathione S-transferase expression in benign and malignant ovarian tumours. *Br J Cancer* 1993;68:235-9.
- Baxter SW, Thomas EJ, Campbell IG. GSTM1 null polymorphism and susceptibility to endometriosis and ovarian cancer. *Carcinogenesis* 2001;22:63-6.
- Howells REJ, Holland T, Dhar KK, Redman CWE, Hand P, Hoban PR, et al. Glutathione S-transferase GSTM1 and GSTT1 genotypes in ovarian cancer: association with p53 expression and survival. *Int J Gynecol Cancer* 2001;11:107-12.
- Oliveira C, Lourenco GJ, Sagarra RAM, Derchain SFM, Segalla JG, Lima CSP. Polymorphisms of glutathione S-transferase Mu 1 (GSTM1), Theta 1 (GSTT1), and Pi 1 (GSTP1) genes and epithelial ovarian cancer risk. *Dis Markers* 2012;33:155-9.



This is an open access article distributed under the terms of [Creative Commons Attribution-NonCommercial-NoDerivatives 4.0 International License](https://creativecommons.org/licenses/by-nc-nd/4.0/).

Determination of anti-HCV signal to cut-off value in patients with hepatitis C virus infection and the variety of antibody responses

Murat Ocal[✉], Mehmet Emin Bulut[✉]

Department of Medical Microbiology, University of Health Sciences, Şişli Hamidiye Etfal Training and Research Hospital, İstanbul, Turkey

ABSTRACT

Objectives: The diagnosis of hepatitis C virus (HCV) infection starts with the detection of antibodies against recombinant or synthetic HCV proteins by Enzyme Immunoassay (EIA). Although EIA tests are highly sensitive, false positivity rates are not low. Positive anti-HCV results are generally confirmed with complementary tests such as Nucleic Acid Amplification Tests (NAAT), or Western Blot modifications.

Methods: The anti-HCV results of 199,516 individuals referred from various clinics between 2015 and 2019 were evaluated retrospectively at University of Health Sciences, Şişli Hamidiye Etfal Training and Research Hospital, Medical Microbiology Laboratory. From the 2039 samples, of which EIA tests resulted borderline and reactive, 1419 samples having Line Immunoassay (LIA) confirmatory test results were included in the study.

Results: LIA tests yielded positive, negative and indeterminate for 820 (57.8%), 519 (36.6%) and 80 (5.6%) of 1419 samples, respectively. The optimal threshold point for EIA anti-HCV signal to cut-off (S/Co) according to LIA was found to be 15.85 corresponded to diagnostic sensitivity, specificity, positive predictive value (PPV), negative predictive value (NPV) and accuracy of 94.9%, 94.8%, 96.6%, 92.1%, 94.9%, respectively. The most common proteins detected in LIA positive samples were C1 96.3%, C2 90.4%, and NS3 93.2%.

Conclusions: To prevent false positivities, confirmatory tests must be used for samples with low S/Co ratios. The use of S/Co value will make significant contribution to reducing both false-positive results and the LIA confirmatory test consumption. There was no correlation between the number of bands and EIA index values in LIA positive samples, while the relationship between the number of 3+ bands and index values was remarkable.

Keywords: Hepatitis C virus, signal to cut-off, enzyme immunoassay, line immunoassay, confirmatory test

Hepatitis C virus (HCV) is 40-50 nm in diameter, enveloped, single-stranded RNA virus classified in *Flaviviridae* family [1]. HCV is a chronic hepatitis agent with worldwide distribution which infects more than 170 million people posing a serious public health

threat, yet has no protective vaccine [2, 3]. It is estimated that 3% of the world population is infected with HCV, and the prevalence is between 0.5-1% in Turkey [4]. Although hepatitis C is usually in form of asymptomatic infection, it also becomes chronic at a rate of

Received: June 21, 2021; Accepted: December 19, 2021; Published Online: March 31, 2022



e-ISSN: 2149-3189

How to cite this article: Ocal M, Bulut ME. Determination of anti-HCV signal to cut-off value in patients with hepatitis C virus infection and the variety of antibody responses. *Eur Res J* 2023;9(3):484-494. DOI: 10.18621/eurj.945588

Address for correspondence: Mehmet Emin Bulut, MD., University of Health Sciences, Şişli Hamidiye Etfal Training and Research Hospital, Department of Medical Microbiology, İstanbul, Turkey. E-mail: eminbulut212@gmail.com, GSM: +90 532 353 77 41



©Copyright © 2023 by Prusa Medical Publishing

Available at <http://dergipark.org.tr/eurj>

info@prusamp.com

75-85%. Cirrhosis develops in approximately 20-30% of patients with HCV infection within 20 years and total of 1-4% of patients develop hepatocellular carcinoma [5]. Although a meta-analysis study showed that the global incidence of HCV infection decreased, mathematical models show that deaths due to secondary liver disease in HCV infection will continue to increase [6].

Laboratory diagnosis of HCV infection needs to be reliable [7]. False positivity is an important issue in terms of time, cost and patient's psychological state [7, 8]. Since there are no neutralizing antibodies against HCV, anti-HCV can be detected not only in chronic hepatitis C patients, but also in most HCV patients who recover. For this reason, it cannot be clearly differentiated whether anti-HCV positivity indicates current or past infection [8]. A positive anti-HCV result can indicate active (acute or chronic) or past HCV infection, as well as false positivity [8, 9]. The healthy carriers of HCV infection may show a specific antibody response to HCV antigens, which may play role in disease control. Detecting these antibodies may allow this response to be fully characterized, which can identify specific antibodies that have potential clinical value [10].

The structural proteins of HCV processed by cellular proteases are core proteins (C), envelope glycoproteins E1, E2, and non-structural NS2, NS3, NS4A, NS4B, NS5A, NS5B proteins, which are processed by viral proteases [11]. The diagnosis of HCV infection starts with the detection of antibodies against recombinant or synthetic HCV proteins by Enzyme Immunoassay (EIA) [12]. First-generation EIA tests are intended to detect the antibodies against the c100-3 epitopes from the NS4 region. Core and NS3 regions were added to the second generation tests, and NS5 region epitopes were added to the third generation EIA tests in addition to the core and NS3 regions. With the use of third-generation EIA anti-HCV test, the HCV infection has become detectable at 7-8th weeks after transmission [7, 8, 13].

Although EIA tests are highly sensitive, false positivity rates are not low. False positivity is more likely to occur in populations with low prevalence [14]. Positive anti-HCV results are generally confirmed with complementary tests [12]. Among the confirmatory or complementary tests, the most widely used tests are Nucleic Acid Amplification Tests (NAAT), or Western

Blot modifications, ie. Recombinant Immunoblot Assay (RIBA) and Line Immunoassay (LIA) tests [3, 15]. The U.S. Centers for Disease Control and Prevention (CDC) recommended a diagnostic algorithm in 2003, which included RIBA and NAAT to determine positivity in anti-HCV screening tests at signal to cut-off (S/Co) rates [16]. In 2013, an updated algorithm was released that included testing anti-HCV positive samples using only NAAT (9). A negative RIBA result usually indicates false positive anti-HCV screening test, except for the early stage of acute infection and immunosuppression, while a positive RIBA result indicates current or past infection [17]. Determining HCV-RNA with Polymerase Chain Reaction (PCR) is considered as the gold standard method to evaluate viremia in patients during antiviral treatment and follow-up and is used to confirm the diagnosis of HCV infection [14]. However, using only the NAAT testing, may lead to challenges in the diagnosis in patients with recovered/past HCV infection [8]. While both NAAT and antibody confirmatory tests (RIBA and LIA) are used in Europe as complementary tests, there are no Food and Drug Administration (FDA) approved confirmatory antibody test commercially available in United States (US) [18].

When anti-HCV S/Co ratios are evaluated, it has been suggested that low levels may be associated with false positive results while high levels may reflect actual infection status and can be used to predict HCV viremia [19, 20]. However, the optimal S/Co values showing the actual infection status might vary from one manufacturer to another. For this reason, during HCV diagnosis, differences in S/Co values that are found by using various commercial tests should be taken into account [14].

The purpose of the present study was to determine S/Co ratios in anti-HCV reactive individuals, to evaluate the predictive performance of EIA with LIA testing, and examine the diversity of antibody responses against various HCV proteins in individuals infected with HCV.

METHODS

Patients and Samples

The anti-HCV results of 199,516 individuals referred from various clinics between 2015 and 2019 were

evaluated retrospectively at University of Health Sciences, Şişli Hamidiye Etfal Training and Research Hospital, Medical Microbiology Laboratory. From the 2039 samples, of which EIA tests resulted borderline and reactive, 1419 samples having LIA confirmatory test results were included in the study, after exclusion of samples that were previously confirmed.

Serological Diagnosis

Enzyme Immunoassay (EIA) Method (Elecsys Anti-HCV II, Roche Diagnostics, Germany) was used for anti-HCV screening test. For EIA, in line with the manufacturer’s instructions, the samples with S/Co index value < 0.9 were considered nonreactive, those with ≥ 0.9 to < 1 were considered borderline, and ≥ 1 as reactive. The borderline or reactive results were retested with the same test kit. Confirmatory test was performed for the samples with S/Co index value ≥ 0.9.

The confirmatory test was performed by using the Semi-Quantitative LIA (INNO-LIA HCV Score, Innogenetics-Belgium). The INNO-LIA HCV Score Test is intended for detecting the antibodies from C1, C2 from the core area, E2 from the hypervariable region (HVR), NS3 from the helicase region, and NS4, NS5 region antigens. The band reactivity was evaluated with visual calibration against IgG control bands on each strip. The bands were evaluated as negative (no bands), +/-, level 1+, level 3+. The LIA results were interpreted as follows:

- 1-A sample is NEGATIVE for HCV antibodies:
 - if all HCV antigen lines have a negative reactivity rating,
 - if only one HCV antigen line has a reactivity of ±, except when the reactivity is observed for NS3.
- 2-A sample is POSITIVE for HCV antibodies:

- if at least two HCV antigen lines have a reactivity of ± minimum or higher.

3-A sample is considered INDETERMINATE for HCV antibodies:

- if one HCV antigen line has a reactivity rating of 1+ or higher,
- if the NS3 line reacts with a reactivity of ± or higher and all other antigen lines are negative.

Statistical Analysis

SPSS 15.0 for Windows was used for statistical analysis. The descriptive statistics were given as numbers and percentages for categorical variables; and as mean values, standard deviations, and minimum-maximum values for numeric variables. In independent groups, the comparisons of numeric variables were made with the Kruskal Wallis Test in more than two group comparisons since the normal distribution condition was not met. The subgroup analyses were made with the Mann Whitney U-test. The cut-off point was selected with the analysis of the “Received Operator Characteristic (ROC)” Curve. The sensitivity, specificity, positive predictive value, and negative predictive value calculations were made for the resulting cut-off value. The statistical alpha significance level was taken as $p < 0.05$.

RESULTS

From the 2039 samples, of which EIA tests resulted in borderline and reactive, 1419 samples were included in the study, after exclusion of samples that were previously confirmed. LIA tests yielded positive, negative and indeterminate for 820 (57.8%), 519 (36.6%) and 80 (5.6%) of the 1419 samples, respectively (Table 1).

Table 1. Numerical data of EIA index value and LIA

		Mean ± SD (Min - Max)	Median (IQR)
EIA Index Value		36.3 ± 39.4 (0.91-216.4)	26 (3.18-52)
n (%)			
EIA	S/Co 0.9 - 1.0	31 (2.2)	
	S/Co ≥ 1	1388 (97.8)	
LIA	Indeterminate	80 (5.6)	
	Negative	519 (36.6)	
	Positive	820 (57.8)	

EIA = Enzyme Immunoassay, LIA = Line Immunoassay, IQR = Interquartile range, S/co= signal to cut-off, SD = standard deviation, Min = minimum, Max = maximum

Table 2. The EIA S/Co values relative to LIA results

		EIA	
		Mean ± SD (Min-Max)	Median (IQR)
LIA	Indeterminate	26.3 ± 22.9 (2.8-117.5)	20.3 (7.3-40.1)
	Negative	4.39 ± 6.46 (0.91-59.69)	1.99 (1.29-4.23)
	Positive	57.4 ± 38.8 (3.1-216.4)	45.4 (30.4-71.8)
<i>p value</i>		< 0.001	
All subgroup comparisons <i>p</i> < 0.001			

EIA = Enzyme Immunoassay, LIA = Line Immunoassay, IQR = Interquartile range, SD = standard deviation, Min = minimum, Max = maximum

A total of 465 (56.7%) of the individuals who were found positive with LIA were female and 355 (43.3%) were male while the mean age of patients was 56.1 ± 18.3 years.

According to the confirmation test results, the mean S/Co value of the positive group was found to be significantly higher compared to the indeterminate and negative groups while mean value of the indeterminate group was significantly higher compared to the

negative group (all comparisons *p* < 0.001) (Table 2). EIA test minimum, maximum, 25-75% percentile, and median index values are shown in Fig. 1 along with LIA results.

Indeterminate results were excluded from the study, and the ROC curve was drawn to determine the optimal screening test cut-off value. The Area Under the Curve was 0.987 (SE:0.003) (Fig. 2). The optimal threshold point for EIA anti-HCV S/Co according to

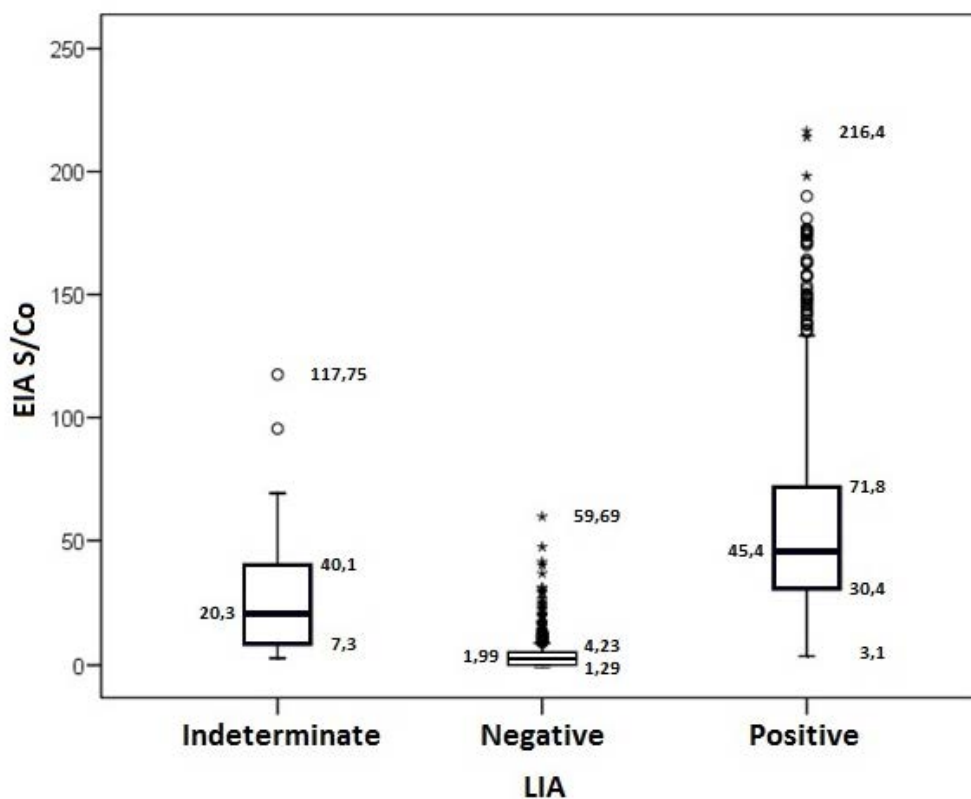


Fig. 1. Box-and-whisker plot for EIA anti-HCV S/Co levels relative to LIA test results. The horizontal line within each box represents median value, top and bottom of each box represent the 25th and 75th percentiles, respectively.

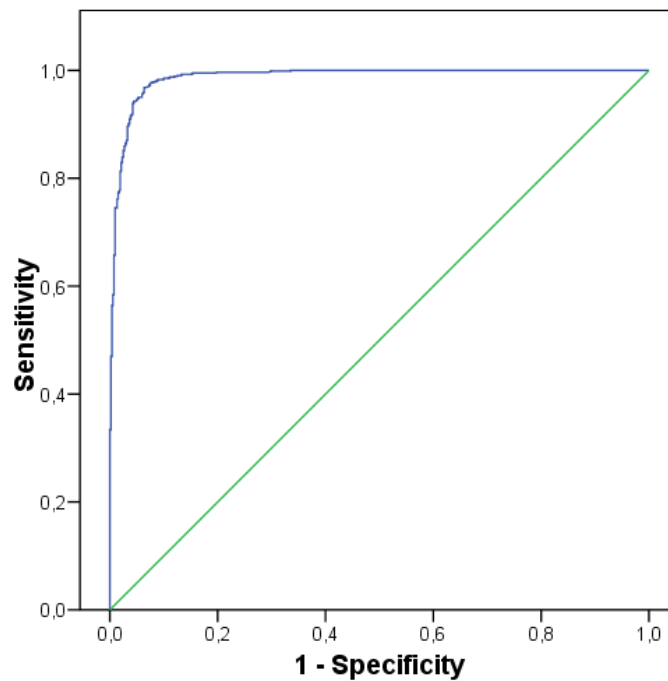


Fig. 2. LIA test ROC curve based on anti-HCV EIA results (AUC:0.987 (SE:0.003) 95% CI 0.982-0.992).

LIA was found to be 15.85 and following values were found for threshold point; sensitivity of 94.9%, specificity of 94.8%, positive predictive value (PPV) of 96.6%, negative predictive value (NPV) of 92.1%, ac-

curacy of 94.9%.

The C1, NS3 and C2 bands were most commonly detected among the positive samples, while NS3 was the most frequently detected HCV antigen band in in-

Table 3. Protein band counts and percentages in LIA-positive and indeterminate samples

LIA		C1	C2	E2	NS3	NS4	NS5
Positive	(n)	790	741	418	764	590	212
	%	96.3	90.4	51	93.2	71.9	25.8
Indeterminate	(n)	22	8	2	44	4	0
	%	27.5	10	2.5	55	5	0

LIA = Line Immunoassay

Table 4. S/Co mean values relative to positive band counts

Positive Band Counts	n	%	Mean S/Co
2	83	10.1	50
3	129	15.7	61
4	213	26	68
5	260	31.7	56
6	135	16.5	45
Total	820	100	

S/co = signal to cut-off

determinate samples (Table 3).

When multiple-band positivity was examined, 5-band positivity (31.7%) was the most common, followed by four-band (26%), six-band (16.5%), three-band (15.7%) and two-band (10.1%) positivity. The S/Co mean values by the number of positive bands are given in Table 4.

DISCUSSION

With the help of new technologies, significant progress was made in identifying patients who are infected with HCV. It is important to screen general population, blood and organ donors to prevent the spread of HCV. More than %95 of individuals infected with HCV can full recovery with correct diagnosis and new treatment methods. The complications of HCV can be significantly reduced as a result of a successful diagnosis and treatment [13]. With the help of new technologies, significant progress was made in identifying patients who are infected with HCV. It is important to screen general population, blood and organ donors to prevent the spread of HCV. More than %95 of individuals infected with HCV can full recovery with correct diagnosis and new treatment methods. The complications of HCV can be significantly reduced as a result of a successful diagnosis and treatment [13].

The addition of more antigens to third-generation EIA used as screening tests increased sensitivity, however, this also increased the false positivity rates. To prevent false positive results, confirmatory tests must be used on samples with low S/Co ratios [21]. CDC recommends determining anti-HCV S/Co values that reflect true positivity in individuals, in order to reduce false positive results, particularly in populations with low prevalence of HCV [22]. The actual positive S/Co ratio may differ for each manufacturer's products. Regardless of the prevalence, laboratories could determine their optimal S/Co ratios and use confirmatory tests accordingly [21, 23].

Researchers tried to find an anti-HCV threshold value by using different confirmatory tests. Altuğlu *et al.* [12] used Architect Anti-HCV assay (Abbott Laboratories) and confirmed the reactive EIA results with LIA and evaluated by ROC curve analysis. They stated that, when the S/Co ratio was 3.27, they could detect true antibody positivity in 94.9% of their cases [12]. Karakoç *et al.* [24] evaluated the S/Co value as 8.1

when using PCR as confirmatory test for the samples screened with the Ortho test, and found the sensitivity as 100% and the specificity as 95%. When the RIBA test was used for confirmation, they found the S/Co value as 7.5 and determined the sensitivity and specificity as 95% and 81%, respectively [24]. Pan *et al.* [25] used Elecsys Anti-HCV II (Roche Diagnostics) screening test and confirmed the results with RIBA and found the S/Co ratio as 12.27 with 97.8% sensitivity and 86% specificity. Kao *et al.* [26] examined the S/Co ratio for AxSYM Microparticle Enzyme Immunoassay (MEIA) (Abbott Laboratories) using PCR for confirmation and found the S/Co ration optimal at 24 and 44. Using a cutoff S/Co ratio of 24, they could confirm HCV viremia with a sensitivity and positive predictive value (PPV) of 91.7%, specificity and negative predictive value (NPV) of 82.4%. The sensitivity, specificity, PPV, and NPV were found to be 86.1%, 94.1%, 96.9%, 76.2% respectively when S/Co ratio was set 44 as cutoff [26].

In this study, anti-HCV EIA results confirmed with LIA were evaluated with the ROC Analysis, the Area Under the Curve was 0.987 (SE:0.003), and the optimal S/Co ratio was found to be 15.85 (Fig. 2). According to these results, the accuracy was found to be 94.9% when the S/Co ratio was set 15.85 in anti-HCV EIA screening.

Recombinant immunoblot analysis is a complementary serological confirmation test preferred with its robust specificity [10]. However, indeterminate results can also be detected in this system. In our study, 80 (5.6%) of 1.419 reactive samples that were confirmed with LIA were found to be indeterminate. LIA indeterminate results were previously considered to be false anti-HCV positive. However, in a study Makuria *et al.* [27] showed that indeterminate results represent decreased antibody responses in individuals who have recovered from HCV infection. Mazzarella *et al.* [7] has associated indeterminate LIA results with declining antibodies in old age patients. After viral clearance, HCV antibodies persist for several years, and can be detected in laboratory tests during this period. HCV clearance is associated with the appearance of antibodies and reversal of HCV-specific T cell depletion. In the event of spontaneous or treatment-induced HCV clearance, antibodies gradually decrease and disappear in the absence of HCV RNA [7]. Researchers have discovered that individuals who spontaneously

recover from HCV infection had much stronger Cell-Mediated Immune (CMI) responses compared to controls that had never been infected with HCV before [27]. Hitzinger *et al.* [28] retested the individuals tested five and two years ago, found a decrease in positivity, similar to the study of Makuria *et al.* [7]. Also, the researchers showed a gradual decrease in antibody level by using the quantitative Luciferase Immuno-Precipitation System (LIPS), as a patient moves from being chronic carrier (highest antibody level) to spontaneously recover (mid-level) and RIBA indeterminate (low level) [27]. Seeff *et al.* [29], who supported this concept, showed that there was complete antibody loss in some patients who were followed up as anti-HCV positive for 20 years. In another study, anti-HCV prevalence rates tended to decrease in a 12-year follow-up, and positivity declined from 43.6% to 29.2% during the study period [30].

Another approach is that perhaps the initial viral inoculum or exposure may be very low in individuals losing their serological response to HCV [27]. These studies show that anti-HCV positive, LIA-indeterminate results are not false positive, and there might be a declining antibody response. In addition, Pereira *et al.* [31] stated that false positive results may occur in populations with low HCV prevalence or in cases with cross-reactivity due to other viral factors in immunocompromised individuals.

In our research, 44 (55%) of the 80 LIA tests that resulted indeterminate were found to be positive for NS3 band, 22 (27.5%) for C1 band and 8 (10%) for C2 band. Consistent with our research, Pereira *et al.* [31], found that NS3 was the most detected band with 86% (12/14) in indeterminate samples. When interpreting the LIA test, if one HCV antigen band has a reactivity rating of 1+ or higher or if the NS3 band reacts with a reactivity of \pm or higher and all other antigen bands are negative, the sample is considered indeterminate. For this reason, higher positivity rate of NS3 band can be considered as an expected result. Most patients who are infected with HCV give a humoral and cellular response to core antigens. Persistent HCV infection is induced with the suppression of early host immune response by core antigens released during the acute phase in HCV infection. High levels of core antigens disrupt the function of T-lymphocytes by interacting with the complement receptor gC1qR, and lead to a decrease in immune response against

HCV. It is considered that HCV persistence occurs with immune destruction mechanism [32]. Rafik *et al.* [10] found reactivity of 91.2% in C1 band, 76.5% in C2 band, 97.3% in NS3 band. Pereira *et al.* [31], on the other hand, found 96% reactivity in C1 band and 100% in NS3 band. In our research, LIA test yielded 93.2% reactivity in NS3 band, 96.3% and 90.4% reactivity in core proteins C1 and C2, respectively for EIA reactive samples. Strong antibody response against NS3 antigen have been associated with viral persistence. Beld *et al.* [33] reported that individuals with viral persistence had higher antibody response to NS3 than individuals with significant viral clearance. Viral clearance was associated with significant decrease in antibodies against NS3, independent of HCV genotype, compared to individuals with persistent viremia [33]. In individuals with spontaneous recovery of infection, anti-HCV may persist and remain detectable for a lifetime while it may decrease slightly or gradually disappear after a few years. Anti-HCV continues indefinitely in patients who develop chronic infection, but antibodies may become undetectable in immunocompromised or hemodialysis patients [20].

It has been suggested that high anti-HCV EIA index values may reflect the actual state of infection or viremia. Since anti-HCV is produced by antigen stimulation secondary to viral replication, anti-HCV antibody levels appear to increase with strong viral stimulation. For this reason, the anti-HCV-S/Co ratio is likely to be higher in patients with HCV viremia, who have strong and continuous viral stimulation compared to patients with spontaneous recovery [19, 34]. The conclusion of a study conducted by Seo *et al.* [19] is that the anti-HCV S/Co ratio is significantly dependent on the presence of HCV viremia and contributes significantly to predicting the presence of HCV viremia. Pereira *et al.* [31] established a statistically significant relationship between high anti-HCV index values and the presence of viremia in 92% of RIBA positive samples with an HCV index value > 5.0 . Studies have shown that in cases where the anti-HCV antibody titer is higher in the patient's sera, the chances of the test result being real positive are higher than the false positivity [20]. In our study, PPV was found to be 96.6% when S/Co ratio was set 15.85.

In a study conducted by Rafik *et al.* [10] 3-band-and-above positivity was found as 90.9% in individuals with chronic HCV infection, and 86.2% in HCV in-

Table 5. LIA positive band groups, number of level 3 + bands within the group and S/Co mean values

Positive Band Counts	Level 3+ Bands	n	%	Mean S/Co
2 bands	1	27	32.5	52.7
	2	22	26.5	73.8
3 bands	1	28	21.7	60
	2	34	26.4	73
	3	21	16.3	82
4 bands	1	24	11.3	85
	2	39	18.3	84
	3	70	32.9	74
	4	60	28.1	46
5 bands	1	10	3.8	81
	2	18	6.9	80
	3	69	26.5	62
	4	98	37.8	50
	5	62	23.9	46.7
6 bands	1	2	1.5	90
	2	5	3.7	74
	3	9	6.7	67
	4	42	31.1	51
	5	50	37	35
	6	26	19.3	38

LIA = Line Immunoassay, quartile range, S/co = signal to cut-off

fectured healthcare workers via LIA confirmatory test. In another study using RIBA, authors found 4-band positivity as 60%, 3-band positivity as 28%, and total of 3-band-and-above positivity as 88% [31]. In this study, positivity rate of 3-band-and-above was found as 89.9% in all cases (Table 4).

In our confirmation with LIA, we grouped the antigen positivity as 2, 3, 4, 5 and 6-band positivity. While mean S/Co values increased from two band positivity and reached the highest level as 68 in four band positivity, it was noteworthy that individuals

with five and six band positivity showed a decrease in mean S/Co values (Table 4). When the positive band groups were examined, it was observed that the mean S/Co values increased in individuals with level 3 positivity in two and three bands within each group, and a decrease was observed if the number of level 3 positive bands was four and above (Table 5). The reason for the decrease in the mean value when level 3 positive band number increased to four and above was investigated. Among the samples newly confirmed with the LIA test, those with a level 3 positive band number

over 3 or 4 were retested in serial dilutions. The index values of these samples were between 26-50 with EIA, and when retested with serial dilution, it was observed that the index values increased, reaching up to 3000s. However, there was no change in index values for the samples with an index value of 119, three level 3 positive bands, and indeterminate samples with an index value of 20 when tested with serial dilution. These results show that when the number of level 3 positive bands is four and above, the actual index value can be reached with dilution study, since the absorbance value of the sample may be above linearity due to excess antibody, which suggests that there may be a correlation between strong band positivity and high index value. We believe that further researches in concordance with the HCV clinical course and treatment response are needed on this issue.

The NAAT or Western Blot modifications are confirmatory tests for HCV infection. Elaborate procedures, the need for equipment and qualified personnel limit the widespread use of molecular techniques [14]. RIBA is an alternative to NAAT which needs hardware and infrastructure for countries with limited resources [13, 35]. A previous study recommends the RIBA test to confirm HCV exposure after anti-HCV reactive results, and if the RIBA test is positive, additional PCR test is recommended to evaluate the status of HCV viremia [36]. In another study, it is stated that RIBA is needed for patients with EIA reactive, NAAT negative results, thus a better evaluation could be made by following these patients who recovered from HCV infection. Nevertheless, it has been stated that neglecting RIBA has a minimal effect on HCV diagnosis, provided that the anti-HCV S / Co ratio is included in the diagnostic algorithm [37]. Despite the decision of CDC to remove RIBA from the diagnostic algorithm for HCV, some authors reported that their results indicate the RIBA should continue to be used [10]. Similarly, there are some studies arguing that EIA reactive results are not indicative of HCV infection without a complementary RIBA test [8]. The CDC stated that future studies are needed for good practices [9].

Limitations

One of the limitations of our study is that the population we screened for anti-HCV includes not only possible hepatitis cases, but also individuals with rou-

tine medical examinations. Besides, just as there were patients who had been treated in different hospitals, there were individuals who were followed up in different hospitals. Therefore, we were not able to include HCV-RNA and alanine aminotransferase (ALT) results. The strengths of our study are that it contains a high number samples screened for anti-HCV and the antibody bands, the level of positivity and S/Co mean values are determined and analyzed for all the samples tested positive or indeterminate by LIA confirmatory test.

CONCLUSION

EIA tests are indispensable tools for laboratories as anti-HCV screening tests due to its low cost, easy and time-saving procedure, ease of working with automated devices. However, the number of false-positive results is high in anti-HCV EIA screening test, but the use of the S/Co value will make a significant contribution to reducing both false-positive results and the LIA confirmatory test consumption. In our study, the S/Co value was found to be 15,85 with an accuracy of 94.9%. In addition, it has been observed that there is a correlation between the increase in index value and the number of level 3 positive bands in the LIA confirmatory test. We are of the opinion that this relationship, which does not have much data in the literature, should be examined together with the clinic course of HCV infection, and further researches are needed on this subject.

Authors' Contribution

Study Conception: MEB, MO; Study Design: MEB, MO; Supervision: MEB; Funding: N/A; Materials: MEB; Data Collection and/or Processing: MO, MEB; Statistical Analysis and/or Data Interpretation: MO, MEB; Literature Review: MEB; Manuscript Preparation: MO, MEB and Critical Review: MO, MEB.

Conflict of interest

The authors disclosed no conflict of interest during the preparation or publication of this manuscript.

Financing

The authors disclosed that they did not receive any grant during conduction or writing of this study.

Acknowledgments

Statistical analyses were performed by Arat Statistics.

Ethical approval

This study has been approved by the University of Health Sciences, Şişli Hamidiye Etfal Training and Research Hospital Ethics Committee, Resolution 2832.

REFERENCES

- Selek MB, Baylan O, Karagöz E, Özyurt M. Changes in hepatitis C virus genotype distribution in chronic hepatitis C infection patients. *Indian J Med Microbiol* 2018;36:416-21.
- Ergünay K, Abacıoğlu H. [Clinical impact of hepatitis C virus genomic variations]. *Mikrobiyol Bul* 2015; 49(4): 625-635. [Article in Turkish]
- Arora S, Doda V. Role of signal-to-cut-off ratios of anti-hepatitis C virus antibody by enzyme immunoassays along with ID-NAT for screening of whole blood donors in India. *Asian J Transfus Sci* 2016;10:75-8.
- Tabak F. *Enfeksiyon Hastalıkları*, 4th.ed., İstanbul Tıp Kitapevi: İstanbul, 2019.
- Tiryaki Y, Duran AC, Ozcolpan OO. Distribution of hepatitis c virus genotypes in Aydın province. *Viral Hepat J* 2018;24:70-4.
- Petruzzello A, Marigliano S, Loquercio G, Cozzolino A, Cacciapuoti C. Global epidemiology of hepatitis C virus infection: an up-date of the distribution and circulation of hepatitis C virus genotypes. *World J Gastroenterol* 2016;22:7824.
- Mazzarella C, Rocco C, Vallefuoco L, Sorrentino R, Braschi U, Lauritano G, et al. Differential reactivity of anti-hepatitis C virus screening assays in patients with waning antibodies. *Future Virol* 2019;14:303-9.
- Choi MS, Lee K, Hong YJ, Song EY, Kim DS, Song J. The role of the signal-to-cutoff ratio in automated Anti-HCV chemiluminescent immunoassays by referring to the nucleic acid amplification test and the recombinant immunoblot assay. *Ann Lab Med* 2018;38:466-72.
- Getchell JP, Wroblewski KE, DeMaria Jr A, Bean C L, Parker MM, Pandori M, et al. Testing for HCV infection: an update of guidance for clinicians and laboratorians. *MMWR. Morb Mortal Wkly Rep* 2013;62: 362-5.
- Rafik M, Bakr S, Soliman D, Mohammed N, Ragab D, Abd ElHady W, Samir N. Characterization of differential antibody production against hepatitis C virus in different HCV infection status. *Virol J* 2016;13:116.
- Tsukiyama-Kohara K, Kohara M. Hepatitis C virus: viral quasispecies and genotypes. *Int J Mol Sci* 2018;19:23.
- Altuğlu I, Gürsel D, Aksoy A, Orman M, Erensoy S. The importance and role of anti-HCV signal/cutoff ratio in diagnosis of hepatitis C virus infection. *Ege J Med* 2011;50:223-8.
- Warkad SD, Song KS, Pal D, Nimse S. B. Developments in the HCV screening technologies based on the detection of antigens and antibodies. *Sensors (Basel)* 2019;19:4257.
- Sirin MC, Aridogan BC, Cetin ES, Sirin FB. Evaluation of biochemical, hematological, RIBA and PCR assays in predicting viremia in anti-HCV positive patients. *J Infect Dev Ctries* 2019;13:736-43.
- Erensoy S. Diagnosis of hepatitis C virus (HCV) infection and laboratory monitoring of its therapy. *J Clin Virol* 2001;21:271-81.
- Alter MJ, Kuhnert WL, Finelli L. Centers for Disease Control and Prevention. Guidelines for laboratory testing and result reporting of antibody to hepatitis C virus. Centers for Disease Control and Prevention. *MMWR Recomm Rep* 2003;52:1-13, 5; quiz CE1-4.
- Zhang K, Wang L, Lin G, Li J. Is anti-hepatitis C virus antibody level an appropriate marker to preclude the need for supplemental testing? *Intervirol* 2015;58:310-7.
- Kodani M, Martin M, de Castro VL, Drobeniuc J, Kamili S. An automated immunoblot method for detection of IgG antibodies to hepatitis C virus: a potential supplemental antibody confirmatory assay. *J Clin Microbiol* 2019;57:e1567-18.
- Seo YS, Jung ES, Kim JH, Jung YK, Kim JH, An H, et al. Significance of anti-HCV signal-to-cutoff ratio in predicting hepatitis C viremia. *Korean J Intern Med* 2009;24:302-8.
- Gupta E, Bajpai M, Choudhary A. Hepatitis C virus: screening, diagnosis, and interpretation of laboratory assays. *Asian J Transfus Sci* 2014;8:19-25.
- Kalem F, Yüksekaya Ş, Türk Dagi H, Ertuğrul Ö, Doğan M. Comparative evaluation of automated chemiluminescence tests and RIBA assay used in HCV diagnosis. *Biomed Res J* 2016;27:1261-4.
- Centers for Disease Control and Prevention. Hepatitis C. Available at: <https://www.cdc.gov/hepatitis/hcv/labtesting.htm> (12.12.2017).
- Aydin G, Adaleti R, Boz ES, Yücel FM, Özhan HK, Aksaray S. [Investigation of anti-HCV S/CO value in detecting viremia in patients with hepatitis C virus infection]. *Mikrobiyol Bul* 2020; 54:110-9. [Article in Turkish]
- Karakoc AE, Berkem R, Irmak H, Demiroz AP, Yenicesu I, Ertugrul N, et al. Investigation of an algorithm for anti HCV EIA reactivity in blood donor screening in Turkey in the absence of nucleic acid amplification screening. *Transfus Apher Sci* 2017;56:732-7.
- Pan J, Li X, He G, Yuan S, Feng P, Zhang X. Reflex threshold of signal-to-cut-off ratios of the Elecsys anti-HCV II assay for hepatitis C virus infection. *J Infect Dev Ctries* 2016;10:1031-4.
- Kao HH, Chen KS, Lin CL, Chang JJ, Lee CH. Utilization of signal-to-cutoff ratio of hepatitis C virus antibody assay in predicting HCV viremia among hemodialysis patients. *Nephron* 2015;130:127-33.
- Makuria AT, Raghuraman S, Burbelo PD, Cantilena CC, Allison RD, Gobble J, et al. The clinical relevance of persistent recombinant immunoblot assay–indeterminate reactions: insights into the natural history of hepatitis C virus infection and implications for donor counseling. *Transfusion* 2012;52:1940-8.
- Hitziger T, Schmidt M, Schottstedt V, Hennig H, Schumann A, Ross S, et al. Cellular immune response to hepatitis C virus

- (HCV) in nonviremic blood donors with indeterminate anti-HCV reactivity. *Transfusion* 2009;49:1306-13.
29. Seeff LB, Hollinger FB, Alter HJ, Wright EC, Cain CM, Buskell Z, et al. Long-term mortality and morbidity of transfusion-associated non-A, non-B, and type C hepatitis: a National Heart, Lung, and Blood Institute collaborative study. *Hepatology* 2001;33:455-63.
30. Kondili LA, Chionne P, Costantino A, Villano U, Noce CL, Panno F, et al. Infection rate and spontaneous seroreversion of anti-hepatitis C virus during the natural course of hepatitis C virus infection in the general population. *Gut* 2002;50:693-6.
31. Pereira FM, Zarife MAS, Reis EAG, Reis MG. Indeterminate RIBA results were associated with the absence of hepatitis C virus RNA (HCV-RNA) in blood donors. *Rev Soc Bras Med Trop* 2014;47:12-7.
32. Kittleson DJ, Chianese-Bullock KA, Yao ZQ, Braciale TJ, Hahn YS. Interaction between complement receptor gC1qR and hepatitis C virus core protein inhibits T-lymphocyte proliferation. *J Clin Invest* 2000;106:1239-49.
33. Beld M, Penning M, van Putten M, Lukashov V, van den Hoek A, McMorro M, et al. Quantitative antibody responses to structural (Core) and nonstructural (NS3, NS4, and NS5) hepatitis C virus proteins among seroconverting injecting drug users: impact of epitope variation and relationship to detection of HCV RNA in blood. *Hepatology* 1999;29:1288-98.
34. Contreras AM, Ochoa-Jiménez RJ, Celis A, Méndez C, Olivares L, Rebolledo CE, et al. High antibody level: an accurate serologic marker of viremia in asymptomatic people with hepatitis C infection. *Transfusion* 2010;50:1335-43.
35. Sekongo YM, Kabore S, Dembele B, Yao KD, Bogui-Siransy L, Adjoumani JL, et al. Interest of confirmation tests in the diagnosis of viral hepatitis C to blood donors in Abidjan-Côte d'Ivoire. *J Hematol Oncol Res* 2020;3:32-7.
36. Lai KK, Jin M, Yuan S, Larson MF, Dominitz JA, Bankson DD. Improved reflexive testing algorithm for hepatitis C infection using signal-to-cutoff ratios of a hepatitis C virus antibody assay. *Clin Chem* 2011;57:1050-6.
37. Gong S, Schmotzer CL, Zhou L. Evaluation of quantitative real-time PCR as a Hepatitis C virus supplementary test after RIBA discontinuation. *J Clin Lab Anal* 2016;30:418-23.



This is an open access article distributed under the terms of Creative Commons Attribution-NonCommercial-NoDerivatives 4.0 International License.

Is primary dysmenorrhea affected by gray matter volumetric changes in the brain?

Ela Kaplan¹, Selçuk Kaplan²

¹Department of Radiology, Adiyaman University Training and Research Hospital, Adiyaman, Turkey; ²Department of Gynecology and Obstetrics, Adiyaman University School of Medicine, Adiyaman, Turkey

ABSTRACT

Objectives: We aimed this study to investigate the relationship between gray matter volume differences women who suffer from primary dysmenorrhea (PD) and asymptomatic women.

Methods: Brain magnetic resonance (MRI) imaging of 113 PD patients and 113 healthy women were performed. The volume of gray matter structures was calculated with the VolBrain automatic calculation system.

Results: Cut-off values were found by ROC analysis for right, left and total volumes in both groups. A caudate lobe volume above 6.33 cm³ is 99.1% sensitive and 77.9% specific for a diagnosis of PD. In addition, the volumes of other pain-related gray matter regions were decreased in PD patients ($p < 0.001$).

Conclusions: Atrophic changes in the medial GM structures in the brain in women with PD may cause hyperalgesia and the quantitative determination of these morphological changes may play an important role in the diagnosis of PD.

Keywords: Primary dysmenorrhea, gray matter volumetry, magnetic resonance imaging, thalamus, hippocampus, caudate nucleus

Primary dysmenorrhea (PD) is characterized by pain in the lower abdomen during the menstrual cycle without an underlying organic disease. It is more common especially in the adolescent age [1]. In PD pathophysiology is held responsible myometrial hypercontractility, especially due to increased release of prostaglandins [2]. Myometrial hypercontractility causes menstrual pain. In addition, it has been stated that the neurohypophyseal hormones vasopressin and oxytocin also contribute to the process. Women with PD suffer from both lower abdominal pain and symptoms such as headache, nausea, and vomiting [3]. PD is an important factor in decreasing the quality of life

and the ability to perform daily activities due to all these symptoms [4]. Although endocrine evaluations have been made for the etiology of PD in some previous studies, the central mechanisms underlying PD remain largely uncertain. PD should also be seen as one of the central sensitivity syndromes due to systemic symptoms such as headache, nausea and vomiting. Since there is a cyclical nature of pain and painless periods in PD, it has been suggested in previous publications that neuroimaging can explain the brain mechanisms in determining the pathophysiology of PD [5]. In previous studies, normal and abnormal brain changes that occur in PD are examined [6, 7]. In



e-ISSN: 2149-3189

Received: September 11, 2021; Accepted: November 26, 2022; Published Online: June 21, 2022

How to cite this article: Kaplan E, Kaplan S. Is primary dysmenorrhea affected by gray matter volumetric changes in the brain? Eur Res J 2023;9(3):495-501. DOI: 10.18621/eurj.994103

Address for correspondence: Ela Kaplan, MD., Adiyaman University Training and Research Hospital, Department of Radiology, Adiyaman, Turkey
E-mail: elakaplan15@gmail.com, Phone: +90 416 223 38 00



©Copyright © 2023 by Prusa Medical Publishing
Available at <http://dergipark.org.tr/eurj>
info@prusamp.com

addition, in a previous study, it was stated that voxel changes in gray matter (GM) volume on magnetic resonance imaging (MRI) may be associated with PD [8].

Determining brain structure and brain volume in MRI images is used to understand the etiology of diseases associated with atrophy [9]. Manual segmentation volume measurement in MRI was used to determine neuroanatomical structures, but its application is limited because it takes time [10]. Automated brain volume analysis from MRI images is a modern and fast computer-aided diagnosis (CAD) management. There are many software packages available that provide quick and easy brain segment volume measurements.

VolBrain (VB) is a software package that automatically measures brain volume. The volume measurement is presented in centimeter cube (cm³) and as a percentage by measuring the brain volume from both the main brain parenchyma structures and small structures. It also specifies the normal volume and percentage ranges according to the gender and age of the patient. Presents the volume measurements obtained from the brain parenchyma as a result file [9].

The purpose of this study is to investigate the relationship between GM volume differences women who suffer from PD and asymptomatic women.

METHODS

This study is a case-control study conducted by examining brain MRI images of 113 female patients diagnosed with primary dysmenorrhea between January 2019 and October 2020 at the gynecology outpatient clinic of Adiyaman Training and Research Hospital.

Brain MRI images of 113 female patients who were not diagnosed with PD and whose brain MRI images were recorded in our system were included in the study as the control group.

The diagnosis of primary dysmenorrhea was made by a gynecologist with 10 years of experience. The Gracey box scale, which is used to evaluate pelvic pain, was used for pain assessment in patients. Patients with a pelvic pain intensity score of 9 or more and an unpleasantness score of 7 or more were included in the study [11].

For patients with PD diagnosis, being in the reproductive age between 18-45 years of age, having no known pelvic pathology (adenomyosis, endometriosis, previous pelvic inflammatory disease, etc.), having brain MRI images in the hospital database, and not having a history of minor and / or major surgery in the last two years are the criteria for inclusion.

Patients under 18 years of age, having additional pathologies that may cause chronic pelvic pain, being diagnosed with / receiving migraine even if suffering from PD, being a tension headache, being diagnosed with known intracranial hypo / hypertension, intracranial mass, cerebrovascular disease, previous cerebral venous thrombosis or a history of neurological disease such as demyelinating pathologies (such as multiple sclerosis, acute disseminated encephalomyelitis) were exclusion criteria. In addition, patients with complaints of menstrual irregularity, menorrhagia and menometrorrhagia and using oral contraceptives due to these complaints were excluded from the study.

Imaging Parameters

MRI imaging was carried out in the periovulatory phase of the menstrual cycle 12-16 days. T1-weighted,

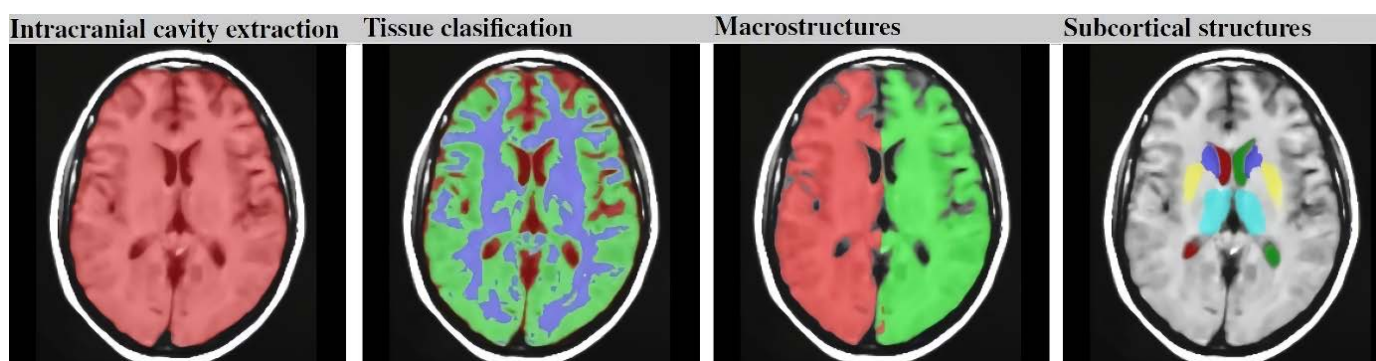


Fig. 1. Images presenting highlighted subcortical structures, as occurred from the processing of VolBrain.

3-dimensional gradient-echo anatomic MRI scans using a 3-dimensional fast spoiled gradient recall sequence (TR = 8.548 ms, TI = 400 ms, flip angle = 15°, matrix = 256 × 256 × 124, in-plane field of view = 260 × 260 × 1.5 mm³) on a 1.5-T MRI scanner (Gyrosan Intera, Philips Medical Systems, Best, The Netherlands).

Volume Measurement with VB

Evaluation of MRI images was done by a 5-year-experienced radiologist. Analysis was done with VB software from VB internet platform. DICOM images were converted to NIFTI format using ITK Snap software before being transmitted to VB. The relevant volumes of the brain structures of patients with PD were measured using NQ software, and a "multiple structure report" and a "general report" were created about the data (Fig. 1).

The hippocampus is part of the limbic system and plays a role in learning, decision making and memory formation. It also contributes to the processing of pain and the formation of attention and anxiety associated with pain [12, 13]. The amygdala plays a role in pain anticipation and emotional processing of pain [14, 15]. It has also been reported to be associated with lower back pain [15]. The thalamus has many roles, from transmitting sensory and motor signals to regulating consciousness and wakefulness [17]. Studies on patients suffering from chronic pain have noted a decrease in GM volume in areas such as the thalamus. These pain processing regions have also been reported in chronic pain conditions such as migraine and cluster headache [18-21, 22-25]). Right, left and total volumes were measured and noted for each patient from each of these regions.

Statistical Analysis

SPSS 22 program was used to analyze the data. Kolmogorov Smirnov test was used as normal distribution test. Mann Whitney U test and ROC analysis were used in the analyzes. A value of $p < 0.05$ was considered significant.

RESULTS

Demographic characteristics and clinical symptoms of the PD group and control group in this study are shown in Table 1.

When the volumetric measurements made for the PD patient group and the healthy female group (HG) were compared, the caudate nucleus, globus pallidus, thalamus and hippocampus volumes decreased in women with PD ($p < 0.001$), and the amygdala volume increased in women with PD ($p = 0.005$). When the GM total volume was compared, there was no significant difference between the groups ($p = 0.060$) (Table 2).

The effect of GM volumes on diagnostic decision making for PD distinction was evaluated by ROC analysis and the cut off values are given in Table 3. It was found that the caudate nucleus volume was a very good diagnostic test for PD, while the putamen and globus pallidus volumes were good diagnostic tests ($p < 0.001$). A caudate nucleus volume above 6.33 cm³ is 99.1% sensitive and 77.9% specific for the diagnosis of PD. Putamen volume above 8.06 cm³ is 81.4% sensitive and 46% specific for the diagnosis of PD. If the thalamus volume is above 5.21 cm³, it is 81.4% sensitive and 67.3% specific for the diagnosis of PD. Globus pallidus volume above 1.85 cm³ is 86.7% sen-

Table 1. Demographics and clinical characteristics of the participants

	PD	HG
Age (years)	24.9 ± 4.21	27 ± 3.26
Menstrual cycle (Days)	27.8 ± 1.9	28.9 ± 2.2
Menstrual phase (Days)	3-7	3-9
Disease duration(years)	5.3 ± 2.7	0
Average pain intensity GBS	15.7 ± 3.2	2.4 ± 1.1
Average pain unpleasantness GBS	13.1 ± 2.1	3.8 ± 1.7

Data are shown as mean±standard deviation or minimum-maximum. HG = Healthy Group, PD = Primary dismenorrea, GBS = Gracey Box Scale

Table 2. Gray matter volume comparisons according to the presence of primary dysmenorrhea

	Groups										p value
	HG					PD					
	X	SD	Median	Min	Max	X	SD	Median	Min	Max	
Caudate R	3.40	0.35	3.54	2.79	3.76	2.78	0.27	2.75	2.40	3.29	< 0.001
Caudate L	3.43	0.26	3.52	3.00	4.02	3.02	0.27	2.97	2.65	3.54	< 0.001
Caudate T	6.84	0.59	7.23	5.79	7.44	5.81	0.38	5.82	5.11	6.36	< 0.001
Putamen R	4.04	0.38	4.12	3.09	4.97	3.19	0.86	3.71	1.75	4.22	< 0.001
Putamen L	3.86	0.22	3.91	3.45	4.35	3.29	0.50	3.37	2.52	4.02	< 0.001
Putamen T	7.91	0.53	7.98	7.00	9.32	6.49	1.33	7.08	4.27	8.12	< 0.001
Thalamus R	5.22	0.84	5.36	3.76	7.12	4.31	0.49	4.14	3.69	5.19	< 0.001
Thalamus L	5.19	1.04	5.60	3.71	7.45	4.67	0.55	5.13	3.84	5.23	< 0.001
Thalamus T	10.41	1.86	10.95	7.48	14.57	8.99	0.92	9.18	7.53	10.42	< 0.001
Globus Pallidus R	1.02	0.23	1.00	0.65	1.48	0.75	0.15	0.72	0.28	1.00	< 0.001
Globus Pallidus L	0.99	0.25	1.01	0.70	1.39	0.71	0.14	0.65	0.48	0.92	< 0.001
Globus Pallidus T	2.01	0.43	1.98	1.39	2.68	1.46	0.29	1.37	0.75	1.92	0.468
Hippocampus R	3.97	0.57	3.94	3.08	4.90	3.86	0.49	3.75	3.32	5.22	0.001
Hippocampus L	3.57	0.70	3.65	2.61	5.70	3.78	0.46	3.79	3.21	4.61	0.016
Hippocampus T	7.53	1.20	7.20	5.70	10.56	7.65	0.82	7.37	6.55	9.72	0.921
Amygdala R	0.62	0.12	0.60	0.47	0.82	0.61	0.09	0.62	0.44	0.75	< 0.001
Amygdala L	0.72	0.08	0.74	0.42	0.79	0.65	0.11	0.68	0.46	0.80	0.038
Amygdala T	1.34	0.15	1.28	0.92	1.56	1.27	0.18	1.33	0.97	1.47	< 0.001
Accumbens T	0.18	0.05	0.19	0.11	0.28	0.27	0.09	0.26	0.16	0.55	0.005
Accumbens R	0.30	0.11	0.24	0.06	0.46	0.26	0.10	0.27	0.08	0.41	0.556
Accumbens L	0.48	0.14	0.47	0.17	0.65	0.46	0.20	0.51	0.09	0.78	0.468
GMR	608.40	137.74	546.85	497.25	1057.35	563.94	66.32	552.16	471.60	669.91	0.985
GMT	303.18	67.52	274.48	248.69	525.20	279.40	34.24	275.62	232.49	334.10	0.060
GML	305.1	70.23	272.52	248.56	532.15	284.85	32.39	279.78	239.22	336.12	0.867

R = Right, L = Left, T = Total, HG = Healthy Group, PD = Primary dismenorrea, GM = Gray matter, SD = standard deviation, Min = minimum, Max = maximum

sitive and 59.3% specific for the diagnosis of PD. On the other hand, if the nucleus acumbens volume is below 0.23 cm³, the diagnosis of PD is 76.1% sensitive and 80.5% specific (Fig. 2).

DISCUSSION

This study reveals brain morphological changes such as GM volumes in women suffering from PD in com-

parison with healthy female patients. There are significant changes in GM volumes in patients with PD, and it has decreased compared to healthy women. Especially the caudat nucleus volume being above 6.33 cm³ has a high specificity and sensitivity for the diagnosis of PD. These findings show that spontaneous cyclic recurrent pain such as PD can be explained by quantitative measurements of macroscopic brain structures.

The relationship between the hippocampus and

Table 3. Gray matter volumes validity results

	AUC	p value	Cut-off	Sensitivity	Specificity
Caudate R	0.883	< 0.001	3.16	90.3	77.9
Caudate L	0.872	< 0.001	3.26	85.8	77.9
Caudate T	0.890	< 0.001	6.33	99.1	77.9
Putamen R	0.794	< 0.001	4.11	86.7	61.9
Putamen L	0.807	< 0.001	3.85	81.4	67.3
Putamen T	0.741	< 0.001	8.06	81.4	46.0
Thalamus R	0.817	< 0.001	4.65	80.5	83.2
Thalamus L	0.688	< 0.001	5.21	81.4	67.3
Thalamus T	0.747	< 0.001	10.08	81.4	67.3
Globus Pallidus R	0.819	< 0.001	0.95	86.7	68.1
Globus Pallidus L	0.833	< 0.001	0.89	86.7	59.3
Globus Pallidus T	0.852	< 0.001	1.85	86.7	59.3
Accumbens T	0.770	< 0.001	0.23	76.1	80.5

R = Right, L = Left, T = Total, AUC = Area Under the ROC Curve

chronic processes such as depression, post-traumatic stress disorder, and chronic back pain has been investigated and it has been reported that the hippocampus plays a role in the underlying mechanisms [12]. MRI has been used to evaluate the correlation of hippocam-

pal structural volume in pathologies characterized by chronic headache that previously occurred with cyclical triggers such as migraine [22]. In addition, in the studies conducted by Liu and Chen [12] in patients suffering from episodic migraine, it was reported that

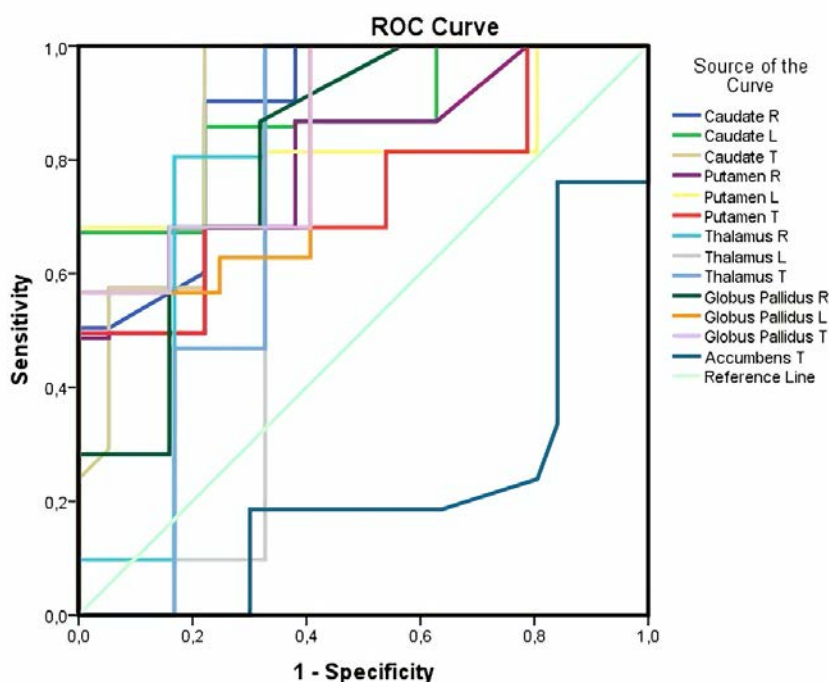


Fig. 2. ROC analysis chart and AUC values by regions. ROC = Receiver Operating Characteristic, AUC = Area Under the ROC Curve

the hippocampal volume was higher than in healthy groups. It is known that the thalamus transmits peripheral nociceptive stimulation to the necessary areas in the brain for sensory separation [23]. Macroscopic GM changes may also be associated with changes in spinal synapse density, changes in cell size, and changes in interstitial fluid and blood flow [24]. Considering this, it can be thought that the peripheral cyclic nociceptive stimulation in the thalamus tries to reduce the effect due to the menstrual cycle by rearranging and therefore, it undergoes volumetric changes adaptively. In this study, supporting these data in female patients suffering from cyclically occurring chronic pelvic pain, the hippocampus, bilateral putamen and caudate nucleus volumes of women suffering from cyclic pain have changed and their removal has decreased, unlike the studies. This may be a result of constant exposure to hormonal cyclic changes. Consistent with these studies, thalamus and hippocampus volumes were decreased in patients suffering from chronic pain such as primary dysmenorrhea. This data supports that volume changes in these regions in patients with PD also play a role in the patient clinic. In addition, the determination of volume cut-off values that can be evaluated in predicting the diagnosis of PD in the described areas with increased volume is also very important. Measuring the volume of these structures in female patients of reproductive age who admitted to neurology outpatient clinics with headache complaints without knowing the diagnosis and clinic of PD can also be a guide for diagnosis and may allow women to be directed for correct treatment and diagnosis. Moreover these study results helps to distinguish between PD and other gynecological and non-gynecological syndromes that cause chronic pelvic pain accompanied by underlying pathologies.

In female patients suffering from episodic migraine, connections were discovered in the hippocampus, bilateral insula, right amygdala, bilateral putamen and caudate nucleus pain-related regions in the healthy female group compared to the patient female group [25]. PD, just like migraine, can be considered as a chronic disease with episodic features but limited to the menstrual phase [26].

Strengths of this study; the study was planned as a case control and the volume of all GM area which were thought to contribute to the formation and trans-

mission of pain was measured for both the right and left brain lobes, and the necessary analyzes were made to determine the diagnostic value and the volume values with high sensitivity and specificity were determined. In addition, it was calculated using an easily accessible automatic software program for volume analysis. In many previous studies, it has been shown that the VB program performs volume measurement accurately and quickly [27].

Limitations

Our study has some limitations. First of all, the study was conducted in a single center and volumetric brain parenchymal changes that may be due to factors such as race and origin were not taken into consideration. In addition, in patients with PD who participated in the study, MRI scans were performed only in the periovulatory phase. Further studies including the menstrual phase can be performed for morphological evaluations related to this cyclic pain.

CONCLUSION

The results of this study show that atrophic changes in the medial GM structures in the brain in women with PD may cause hyperalgesia and the quantitative determination of these morphological changes may play an important role in the diagnosis of PD. In order to generalize the results of the study to the population, studies with larger patient populations are needed.

Authors' Contribution

Study Conception: EK; Study Design: EK; Supervision: N/A; Funding: SK; Materials: SK; Data Collection and/or Processing: EK, SK; Statistical Analysis and/or Data Interpretation: EK, SK; Literature Review: SK; Manuscript Preparation: EK and Critical Review: EK, SK.

Conflict of interest

The authors disclosed no conflict of interest during the preparation or publication of this manuscript.

Financing

The authors disclosed that they did not receive any grant during conduction or writing of this study.

REFERENCES

- Iacovides S, Avidon I, Baker FC. What we know about primary dysmenorrhea today: a critical review. *Hum Reprod Update* 2015;21:762-78.
- Dawood MY. Dysmenorrhea and prostaglandins. In: Gold JJ, Josimovich JB, editors. *Gynecologic endocrinology*. New York, USA: Plenum Press, 1987: pp. 405-21.
- Younesy S, Amiraliakbari S, Esmaili S, Alavimajd H, Nouraei S. Effects of fenugreek seed on the severity and systemic symptoms of dysmenorrhea. *J Reprod Infertil* 2014;15:41-8.
- Dolatian M, Jafari HNV, Afrakhteh M, Taleban FA, Gachkar L. [Effects of fish oil on primary dysmenorrhea]. *J Adv Med Biomed Res* 2004;12:7-15. [Article in Persian.]
- Yunus MB. Fibromyalgia and overlapping disorders: the unifying concept of central sensitivity syndromes. *Semin Arthritis Rheum* 2007;36:339-56.
- Tu CH, Niddam DM, Chao HT, Chen LF, Chen YS, Wu YT, et al. Brain morphological changes associated with cyclic menstrual pain. *Pain* 2010;150:462-8.
- Tu CH, Niddam DM, Chao HT, Liu RS, Hwang RJ, Yeh TC, et al. Abnormal cerebral metabolism during menstrual pain in primary dysmenorrhea. *Neuroimage* 2009;47:28-35.
- Tu CH, Niddam DM, Yeh TC, Lirng JF, Cheng CM, Chou CC, et al. Menstrual pain is associated with rapid structural alterations in the brain. *Pain* 2013;154:1718-24.
- Manjón JV, Coupé P. volBrain: an online MRI brain volumetry system. *Front Neuroinform* 2016;10:30.
- Keller SS, Roberts N. Measurement of brain volume using MRI: software, techniques, choices and prerequisites. *J Anthropol Sci* 2009;87:127-51.
- As-Sanie S, Harris RE, Napadow V, Kim J, Neshewat G, Kairys A, et al. Changes in regional gray matter volume in women with chronic pelvic pain: a voxel-based morphometry study. *Pain* 2012;153:1006-14.
- Liu MG, Chen J. Roles of the hippocampal formation in pain information processing. *Neurosci Bull* 2009;25:237-66.
- Chattarji S, Tomar A, Suvrathan A, Ghosh S, Rahman MM. Neighborhood matters: divergent patterns of stress-induced plasticity across the brain. *Nat Neurosci* 2015;18:1364-75.
- Ziv M, Tomer R, Defrin R, Hendler T. Individual sensitivity to pain expectancy is related to differential activation of the hippocampus and amygdala. *Hum Brain Mapp* 2010;31:326-38.
- Bingel U, Quante M, Knab R, Bromm B, Weiller C, Buchel C. Subcortical structures involved in pain processing: Evidence from single-trial fMRI. *Pain*. 2002;99:313-21.
- Mao C, Wei L, Zhang Q, Liao X, Yang X, Zhang M. Differences in brain structure in patients with distinct sites of chronic pain: A voxel-based morphometric analysis. *Neural Regen Res* 2013;8:2981-90.
- Torrice TJ, Munakomi S. *Neuroanatomy, Thalamus*. Treasure Island (FL): StatPearls Publishing, 2020.
- Maleki N, Becerra L, Nutile L, Pendse G, Brawn J, Bigal M, et al. Migraine attacks the basal ganglia. *Mol Pain*. 2011;7:71
- Naegel S, Holle D, Obermann M. Structural imaging in cluster headache. *Curr Pain Headache Rep* 2014;18:415.
- Luchtman M, Steinecke Y, Baecke S, Lützkendorf R, Bernarding J, Kohl J, et al. Structural brain alterations in patients with lumbar disc herniation: a preliminary study. *PLoS One* 2014;9:e90816.
- Smallwood RF, Laird AR, Ramage AE, Parkinson AL, Lewis J, Clauw DJ, et al. Structural brain anomalies and chronic pain: a quantitative meta-analysis of gray matter volume. *J Pain* 2013;14:663-75.
- Lucassen PJ, Pruessner J, Sousa N, Almeida OF, Van Dam AM, Rajkowska G, et al. Neuropathology of stress. *Acta Neuropathol* 2014;127:109-35.
- Craig AD. How do you feel? Interoception: the sense of the physiological condition of the body. *Nat Rev Neurosci* 2002;3:655-66.
- May A. Experience-dependent structural plasticity in the adult human brain. *Trends Cogn Sci* 2011;15:475-82.
- Gao Q, Xu F, Jiang C, Chen Z, Chen H, Liao H, et al. Decreased functional connectivity density in pain-related brain regions of female migraine patients without aura. *Brain Res* 2016;1632:73-81.
- Bigal ME, Lipton RB. Clinical course in migraine: conceptualizing migraine transformation. *Neurology* 2008;71:848-55.
- Koussis P, Glotsos D, Lamprou E, Toulas P, Gyftopoulos A, Kehagias D, et al. Comparing NeuroQuant and volBrain software for automated brain analysis. *Research Square* 2021. doi: 10.21203/rs.3.rs-289753/v1.



This is an open access article distributed under the terms of Creative Commons Attribution-NonCommercial-NoDerivatives 4.0 International License.

Importance of paravertebral muscle quality in the etiology of degenerative lumbar spinal stenosis

İsmail Kaya 

Department of Neurosurgery, Niğde Ömer Halisdemir University, Faculty of Medicine, Niğde, Turkey

ABSTRACT

Objectives: Degenerative lumbar spinal stenosis (DLSS) is the leading cause of pain, disability, and loss of independence in older adults. In this study, the relationship between DLSS and paravertebral muscle thickness and density was investigated using computed tomography (CT) and magnetic resonance imaging (MRI) methods. Thus, the importance of muscles has been examined to take precautions in the name of preventive medicine.

Methods: This study was planned as a cross-sectional study. The patient group (n = 77) who had surgery for DLSS and the control group (n = 77) were examined. A total of 154 participants (55 females and 22 males in each group) were evaluated retrospectively in terms of cross-sectional area (CSA) and density in the psoas, erector spina and multifidus muscles. In both groups age, gender and body mass index values equalized. Measurements was averaged from the mid-lumbar 3 level from both sides and multi-points.

Results: There was no significant difference between muscle thicknesses ($p > 0.05$). When evaluated in terms of muscle densities, a significant difference was found between the patient and the control group in terms of psoas muscle ($p < 0.05$). Likewise, there is the same relationship between erector spinae muscle density and multifidus muscle density ($p < 0.05$).

Conclusions: Roughly no difference was found between the patient and control groups in terms of CSA of the psoas, erector spinae and multifidus muscles, but it was observed that the muscle density, especially in the multifidus, decreased significantly in the patients. Our results suggest that paravertebral muscle density assessment is an important criterion in disease prediction and can inform preventive treatment.

Keywords: Paravertebral muscle quality, degenerative lumbar spinal stenosis, preventive medicine, literature review

Paraspinal muscles are the most important structure in maintaining stability and function of the lumbar vertebra [1]. The lumbar spine is inherently unstable, and its stability depends on the integrated function of active, passive, and neural subsystems [1]. Degenerative lumbar spinal stenosis (DLSS) is an age-related

chronic disease [2, 3]. It progresses with the degradation of 3 joint complexes and ligamentum flavum hypertrophy [2, 4]. Spinal instability plays an important role in DLSS [5].

The density and cross-sectional area (CSA) of the paraspinal muscle are known to vary with age, sex,

Received: September 19, 2021; Accepted: January 6, 2022; Published Online: May 19, 2022



e-ISSN: 2149-3189

How to cite this article: Kaya İ. Importance of paravertebral muscle quality in the etiology of degenerative lumbar spinal stenosis. Eur Res J 2023;9(3):502-510. DOI: 10.18621/eurj.997335

Address for correspondence: İsmail Kaya, MD., Assistant Professor, Niğde Ömer Halisdemir University, Faculty of Medicine, Department of Neurosurgery, Niğde, Turkey. E-mail: hekimikaya@gmail.com, Tel: +90 546 925 73 40



©Copyright © 2023 by Prusa Medical Publishing
Available at <http://dergipark.org.tr/eurj>
info@prusamp.com

and weight [6]. Literature suggests that these muscles have smaller CSA in patients with chronic back pain than in similarly aged healthy individuals [7]. Muscle CSA and density are believed to reflect the performance of individuals. Muscle status information such as density and CSA can be obtained using non-invasive medical imaging techniques that offer high reproducibility [8]. Magnetic resonance imaging (MRI) and computed tomography (CT) have been used to measure CSA and the rate of muscle degeneration in patients with muscular diseases [9].

Although several studies have been published on the importance of paravertebral muscle quality, consensus on the subject does not exist; furthermore, most studies have several inadequacies [7, 10-18]. Analyzing the shortcomings of these studies, we took the subject again with a new model.

In this study, the association between DLSS and paravertebral muscle thickness and density was investigated using CT and MRI methods. Thus, the importance of muscles has been examined to take precautions. We believe that the results of our study will help design medical strategies to prevent DLSS onset and progression.

METHODS

This study recruited participants into 2 groups. For the first (DLSS) group, patients visiting the Cumhuriyet

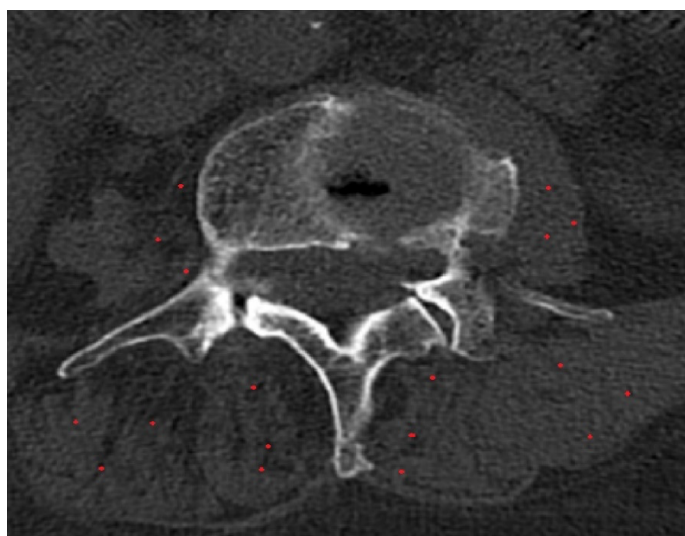


Fig. 1. Density measurement with Hounsfield units from computed tomography using 3 random points from each muscle.

University Medical Faculty Hospital who were evaluated for spinal stenosis between January 1, 2015, and December 30, 2019, were included. These patients were referred to lumbar MR imaging and CT scans given their symptoms of spinal stenosis, and they received surgical treatment after imaging. Inclusion criteria were reduction in the CSA of the lumbar spinal canal ($< 100 \text{ mm}^2$) in at least 1 level with concurrent symptoms associated with spinal stenosis (intermittent claudication, and radicular pain) [19]. In addition, images of the patients in the first group were taken at least at 6 months and at most at 5 years after surgery. For the second (control) group, the same number of asymptomatic male and female of similar body mass indices (BMI) (± 5) and age who had undergone lumbar MR and CT scans for other reasons and did not have lumbar stenosis, were enrolled at the same time frame and same institution. Exclusion criteria included congenital stenosis, traumatic fractures, spondylolysis, spinal tumors, Paget disease, long-term steroid therapy, renal colic, and scoliosis of > 10 degrees [20]. Lumbar MR and CT images of the patients archived on Picture Archiving and Communication Systems (PACS) were screened. Measurements were made by author using the Sisoft imaging program used at our hospital. Random and blind consistency control was performed by 2 separate neurosurgeons.

The density and CSA of the psoas, erector spinae, and multifidus muscles were measured at the mid-lumbar (L) 3 level [20, 21]. The muscles to be inves-

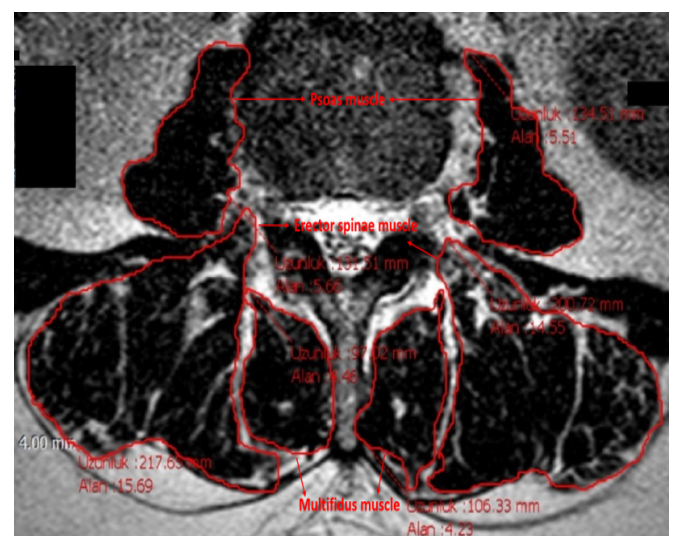


Fig. 2. The cross-sectional area measurement of the psoas, multifidus, and erector spinae muscles.

tigated at this level are at their widest and the most appropriate level in terms of separating the erector spinae from the multifidus [20, 21]. In addition, all the images were obtained with the patient in the supine position and feet stretched out. No contrast was used.

The density of the psoas, multifidus and erector spinae muscles were measured in Hounsfield units (HU) using CT combined with MRI to obtain clearer separation. The density value for each side was calculated as the average density from 3 random regions. Then, the final muscle density was calculated as the mean of the densities of the right and left muscles (Fig. 1).

The CSA of the psoas, multifidus and erector spinae muscles were measured from the fascia border using MRI on both sides separately. Then average values were calculated for the right and left muscles (Fig. 2).

An informed consent form for lumbar spine surgery was obtained from each of the patients in the current National Brain and Nerve Surgery Association consent form list, and written consents were obtained from outpatient clinic applications which clearly stated that the data could be used within ethical limits. The signed consents are in the file archive of Cumhuriyet University Faculty of Medicine. Ethical approval for the study was obtained with the decision numbered 2020-08/18 of the non-interventional ethics committee of Cumhuriyet University, where I worked on the specified dates.

Statistical Analysis

The sample size of this study was based on the statistical power analysis. Descriptive statistics (arithmetic mean, standard deviation, minimum-maximum and median values) and frequency distributions of the study data were obtained. Statistical analyses were performed using SPSS program (version 22.0). If the data provided parametric test assumptions for evaluation (data obtained by interval, ratio scale, normal distribution), a t-test for two groups (independent, conjugate); when not fulfilled (Kolmogorov-Smirnov) a Mann-Whitney U test and a chi-squared test used. Chi-squared exact test was used to determine the chi-squared value of Fisher's exact test Monte Carlo model. A *p* - value of < 0.05 was considered statistically significant.

RESULTS

The study included 154 participants (77 patients, 77 controls). Of total, 110 (71.42%) were females and 44 (28.58%) were males. Both the patient and control groups had 22 males and 55 females. In order to rule out the effect of age on the muscles, control group patients were selected as the same ages as the DLSS patients. The mean age of the females was 58.6 years (range: 27-80 years; median: 59 years) and that of the males was 63 years (range: 34-80 years; median: 64 years), respectively. The mean age across both the patient and control groups was 59.8 years. We did not match the number of females and males to avoid further reducing the sample size. Furthermore, the statistical analyses were conducted separately for the males and females to eliminate the effect of the differences in age and sex (Table 1).

Weight also affects muscle properties. To eliminate the effect of weight on the study results, we selected patients with similar (± 5 units) BMI in both groups. In this respect the mean BMI among the female patients with stenosis was 31.45 kg/m² (median: 31 kg/m²; range: 24-43 kg/m²; standard deviation: 4.68

Table 1. Patient and control group age descriptive statistics

Variables		Value
Age*	Female	Mean 58.6
		Median 59
		Minimum 27
		Maximum 80
		Standard deviation 12.7
Male	Mean 63	
	Median 64	
	Minimum 34	
	Maximum 80	
	Standard deviation 10.9	
Total	Mean 59.8	
	Median 63	
	Minimum 27	
	Maximum 80	
	Standard deviation 12.3	

*Patient and control group ages were equal, and 55 females 22 males were found in both groups

Table 2. Patient and control group body mass index descriptive statistics

Variables			Female	Male	Total
*Weight	Patient group	Mean	31.45	29	30
		Median	31	29	30
		Minimum	24	22	22
		Maximum	43	35	43
		Standarddeviation	4.68	3.39	4.46
Controlgroup		Mean	31.3	29	30
		Median	31	30	31
		Minimum	20	21	20
		Maximum	44	38	44
		Standarddeviation	5.79	5.36	5.72

*Body mass index, There is no statistical difference in weight between the patient and control groups ($p > 0.05$)

years). Among the female controls, the mean BMI was 31.3 kg/m² (median: 31 kg/m²; range: 20–44 kg/m²; standard deviation: 5.79 kg/m²). Among the men with stenosis, the mean BMI was 29 kg/m² (median: 29 kg/m²; range: 22–35 kg/m²; standard deviation: 3.39 kg/m²). Among the male controls, the mean BMI was 29 kg/m² (median: 30 kg/m²; range: 21–38 kg/m², standard deviation: 5.36 kg/m²). The mean BMI of all patients with stenosis was 30 kg/m² (median: 30 kg/m²; range: 22–43 kg/m²; standard deviation: 4.46 kg/m²); the mean BMI of the entire control group was 30 kg/m² (median: 31 kg/m²; range: 20–44; standard deviation: 5.72 kg/m²). No significant difference in BMI was found between the stenosis and control groups (males, females, and total participants; $p > 0.05$). Thus, the variables that could affect muscle thickness and density were eliminated (Table 2).

When we made statistical analysis between psoas muscle thicknesses, there was no significant difference between the males and females and the all participants between the patient and control groups ($p > 0.05$). A significant difference was found between the thickness of the erector spinae in females ($p < 0.05$). No difference was found in males ($p > 0.05$). When evaluated as the all participants, a significant difference was found due to excess number of females ($p < 0.05$). On the other hand, when the number is ignored, the relationship gets weaker. There was no difference between the thickness of the multifidus muscle amongst the patient and control groups in both females, males, and

the total participants ($p > 0.05$) (Table 3) (see Table 5).

On comparing muscle densities, a significant difference was found between the patient and the control group in terms of psoas muscle in females, males, and in the total participants ($p < 0.05$). Likewise, there is the same relationship between erector spinae muscle density and multifidus muscle density ($p < 0.05$) (Table 4) (see Table 5). All values of the patients and control groups are reported in the table with the statistical results (Table 5).

DISCUSSION

DLSS is a common disease of the lumbar spine among the elderly [22]. Degenerative changes in the intervertebral disc ligamentum flavum and facet joints cause stenosis in the spinal canal and neural foramen [3]. Clinical manifestations of DLSS are low back and leg pain [3]. Neurogenic claudication is characteristic of DLSS [3]. DLSS is the leading cause of pain, disability, and loss of independence in elderly patients [23]. Given the aging population, the prevalence, and economic burden of DLSS is increasing exponentially [23]. Hence, understanding its etiology is important. Preventive medicine inhibits all treatment and job loss related costs as well as increases the life quality of the population.

There are limited number of studies with low sam-

Table 3. Paravertebral muscle cross-sectional area descriptive statistics.

Variables			Female	Male	Total
Psoas cross-sectional area*	Patient group	Mean	587.4	957.2	693
		Median	583	941	640
		Minimum	299	264	264
		Maximum	935	1841	1841
		Standard deviation	22.1	341.8	282.5
	Control group	Mean	651.6	947	710.3
		Median	628	892	657
		Minimum	283	605	283
		Maximum	1052	1613	1613
		Standard deviation	22.8	268.2	251.1
Erector spinae cross-sectional area	Patient group	Mean	1391.5	1719.5	1485.2
		Median	1396	1641.5	1419
		Minimum	646	479	479
		Maximum	2667	2769	2769
		Standard deviation	59.5	539.1	490.4
	Control group	Average	1643.9	1777.9	1682.2
		Mean	1651	1743	1660
		Minimum	109	854	109
		Maximum	2478	2881	2881
		Standard deviation	55.3	482.2	433.2
Multifidus cross-sectional area	Patient group	Mean	435.6	538,9	465.1
		Median	389	439,5	420
		Minimum	123	197	123
		Maximum	1014	1709	1709
		Standard deviation	26.2	320.9	239.8
	Control group	Mean	471	509.9	482.6
		Median	446	492,5	469
		Minimum	176	320	176
		Maximum	943	891	943
		Standard deviation	18.1	149.9	139.2

*mm²

ple size about the effect of muscles on the etiology of DLSS [7, 10-18]. Results of these studies are inconsistent [7, 10-18]. In comparison, our study is one of the few studies with the highest sample. In addition, variables that affect muscle quality, such as age, weight, gender, and socioeconomic characteristics, which were not present in other studies, were analyzed

by equalizing on the base parameters of patients, not by regression analysis. Furthermore, to eliminate patient, position and device related artefacts, bilateral and multi-point measurements were made, and the average values used for analyses, and all analyses were performed with the same software. These measures lend robustness to our results (Figs. 1 and 2).

Table 4. Paravertebral muscle density descriptive statistics

Variables			Female	Male	Total
Psoas density*	Patient group	Mean	46	51.2	47.5
		Median	45	52	48
		Minimum	22	35	22
		Maximum	87	60	87
		Standard deviation	1.4	5.4	9.5
	Control group	Mean	85	97,3	89
		Median	90	101	95
		Minimum	41	69	41
		Maximum	109	120	120
		Standard deviation	2.5	14.6	18.4
Erector spinae density	Patient group	Mean	40.7	46.6	42.4
		Median	42	47	43
		Minimum	19	32	19
		Maximum	62	57	62
		Standard deviation	1.1	7	8.6
	Control group	Mean	63	74.8	66.4
		Median	63	80	65
		Minimum	22	31	22
		Maximum	101	118	118
		Standard deviation	2.5	26.7	22
Multifidus density	Patient group	Mean	30.2	43	33.9
		Median	31	44,5	35
		Minimum	10	22	10
		Maximum	54	55	55
		Standard deviation	1.4	8.4	11.8
	Control group	Mean	47.8	55.6	50.1
		Median	41	52,5	45
		Minimum	20	33	20
		Maximum	103	94	103
		Standard deviation	2.7	19.3	20

*Hounsfield units

As far as we understand from the data, there is no gender-related change among CSA of muscles between the groups, except for erector spinae thickness. This could be attributed to the larger number of female participants in the study. However, statistical significance is maintained when considering the averages even if the difference is reduced. Higher density of this muscle in men, in addition to its being the thickest

muscle among the muscle groups, could be the likely reason for this observation. However, no effect of muscle thickness on DLSS was seen in the general population. Spinal instability has been described by Pope and Panjabi [24] as a mechanical phenomenon associated with a loss of rigidity. Paraspinal muscles play an important role in lumbar spine dynamics [25]. The multifidus muscles are the deep muscle group re-

Table 5. Final results between patient and control groups

Variables	Psoas cross-sectional area*	Erector spinae cross-sectional area*	Multifidus cross-sectional area*	Psoas density**	Erector spinae density**	Multifidus density**
Female	$p > 0.05$	$p < 0.05$	$p > 0.05$	$p < 0.05$	$p < 0.05$	$p < 0.05$
Male	$p > 0.05$	$p > 0.05$	$p > 0.05$	$p < 0.05$	$p < 0.05$	$p < 0.05$
Total	$p > 0.05$	$p < 0.05$	$p > 0.05$	$p < 0.05$	$p < 0.05$	$p < 0.05$

*mm², **Hounsfield units

sponsible for spinal extension, rotation, and stabilization [25]. It spreads over three joint segments and works to stabilize the spine [25]. Thus, it enables each vertebra to work more effectively and reduces the degeneration of joint structures [25]. The erector spinae muscle group is responsible for spinal hyperextension, rotation, and lateral flexion [25]. The psoas muscle is main flexor relative to the hip joint. While this muscle acts as the spine extensor in the lumbar area, it functions as an active postural muscle for the body [25]. These three muscles have different functions in stabilizing the lumbar spine. Although some studies have reported results that are in line with our findings, some have presented differing results, particularly with regard to erector spinae and multifidus thickness [7, 10-18]. This could primarily be attributed to factors affecting muscles not being well identified; however, basis our study results, muscle volume is not important to DLSS development. Regarding muscle density, however, significant differences were seen between patients with DLSS and healthy controls in each muscle group in both women and men. Although the multifidus muscle volume does not change after surgery, the muscle fibers lose their density and show fatty changes and fibrosis becomes highly evident. This result was thought to be since the multifidus muscle is the main muscle that controls spinal movement and contributes to most of the spinal stability [26]. Erector spinae is less affected by surgery. Although the psoas muscle was essentially untouched by the surgeon, the density change highlights the importance of muscle quality change in degenerative processes. This difference in density after surgery signifies the importance of muscle quality in degenerative processes more objectively than other muscles even if the psoas muscle

is the least affected. Most previous studies attributed the decrease in density to denervation and muscle disuse in patients with a degenerative spine [27, 28]. Abbas *et al.* [20] suggested that muscle hypertrophy seen at higher levels is a response to degeneration at lower levels, which is more common. Although the same level was examined in our study, the opposite result was observed. Similar to the study by Abbas *et al.* [20], our study had more patients with DLSS at lower levels; however, we only examined patients who received surgical treatment. Although some of our patients had degeneration at the L3 level, most of them had degeneration at lower levels. However, no significant effect of surgery on muscle volume underlines the importance of muscle density. In addition, our follow-up of the patients within 6 months to 5 years after surgery suggests that we may have ruled out reflex hypertrophy that could occur in the first stage and that we examined patients in the late stage of the disease. It was thought that the results of some studies contrary to our article were because of examinations were conducted according to either radiological or clinical criteria as well as low back pain rather than as a stenosis patient who had undergone surgery [7, 10-18]. In the end, it was the factors that could affect muscle quality were not ruled out properly in the selection of patients. Our data firmly supports this.

DLSS is an important health problem today and, given the aging population, increasing exponentially. As can be understood from all these data, the quality of paravertebral muscles plays a key role in the etiology of DLSS. We think the results in this study will shed light on preventing the occurrence of DLSS. It is a known fact that long-term problems such as adjacent segment disease and the need for reoperation after nar-

row canal surgery are common and do not definitively cure DLSS [29]. It is observed that although the surgery provides short-term decompression of the spinal nerves the decrease in the quality of the erector spinae and psoas muscle that is not intervened, especially in the multifidus muscle that is intervened by surgery, does not affect the progression of the DLSS in the long term. It has also been proven by our data that post-surgical compensation mechanisms are not sufficient. Being alert about the low paravertebral muscle density we see in our patients followed up with stenosis and taking early precautions is the best treatment option in DLSS. Early awareness and rehabilitation maintain muscle quality as well as provide preventive medicine. There is also a need for studies related to the long-term rehabilitation follow-up of patients with DLSS.

Limitations

To mention the limitations, we saw in our study, although no patients in our study engaged in sport, daily activities differed among patients. Different races have not been studied. In order to make a more ideal evaluation, it would be appropriate if the number of men and women were equal, but in terms of not limiting the number of cases, the case and control group gender equality were provided, and situation was taken into consideration in the evaluation and statistical analysis. Lastly, although our study had one of the largest sample sizes compared to studies on this topic, further research with larger groups and multi-center designs are needed.

CONCLUSION

In this study, the relationship between DLSS and paravertebral muscle thickness and density was investigated using CT and MR imaging methods. No significant difference was found between the patient and control groups regarding CSA of the psoas, erector spinae, and multifidus muscles; however, the patients with DLSS had significantly lower muscle density, particularly in the multifidus muscle. Considering the prevalence and economic burden of DLSS and given their exponential increase owing to population aging, preventive treatment is critical. Our results suggest that paravertebral muscle density assessment is an im-

portant criterion in disease prediction and can inform preventive treatment. The importance of the study was explained by making an appropriate literature comparison.

Authors' Contribution

Study Conception: İK; Study Design: İK; Supervision: İK; Funding: İK; Materials: İK; Data Collection and/or Processing: İK; Statistical Analysis and/or Data Interpretation: İK; Literature Review: İK; Manuscript Preparation: İK and Critical Review: İK.

Conflict of interest

The authors disclosed no conflict of interest during the preparation or publication of this manuscript.

Financing

The authors disclosed that they did not receive any grant during conduction or writing of this study.

Acknowledgments

Preparation (English language redaction) for publication of this article is partly supported by the Turkish Neurosurgical Society. I am grateful to Prof. Dr. Ünal ÖZÜM and my apprentice Giray Güneş for their support for the article.

REFERENCES

1. Panjabi M, Abumi K, Duranceau J, Oxland T. Spinal stability and intersegmental muscle forces. A biomechanical model. *Spine (Phila Pa 1976)* 1989;14:194-200.
2. Bozkurt H, Kaya İ, Oztoprak B. The role of triangular vertebral canal shape in surgical management of patients with lumbar spinal stenosis: a cross-sectional study. *Turk Neurosurg* 2018;28:792-8.
3. Kirkaldy-Willis WH, McIvor GW. Editorial: Lumbar spinal stenosis. *Clin Orthop Relat Res* 1976;(115):2-3.
4. Abbas J, Hamoud K, Masharawi YM, May H, Hay O, Medlej B, et al. Ligamentum flavum thickness in normal and stenotic lumbar spines. *Spine (Phila Pa 1976)* 2010;35:1225-30.
5. Kirkaldy-Willis WH, Farfan HF. Instability of the lumbar spine. *Clin Orthop Relat Res* 1982;(165):110-23.
6. Lexell J. Human aging, muscle mass, and fiber type composition. *J Gerontol A Biol Sci Med Sci* 1995;50 Spec No:11-16.
7. Danneels LA, Vanderstraeten GG, Cambier DC, Witvrouw EE, De Cuyper HJ. CT imaging of trunk muscles in chronic low back pain patients and healthy control subjects. *Eur Spine J* 2000;9:266-72.

8. Keller A, Gunderson R, Reikerås O, Brox JI. Reliability of computed tomography measurements of paraspinal muscle cross-sectional area and density in patients with chronic low back pain. *Spine (Phila Pa 1976)* 2003;28:1455-60.
9. Sollmann N, Dieckmeyer M, Schlaeger S, Rohrmeier A, Syvaeri J, Diefenbach MN, et al. Associations between lumbar vertebral bone marrow and paraspinal muscle fat compositions-An investigation by chemical shift encoding-based water-fat MRI. *Front Endocrinol (Lausanne)* 2018;9:563.
10. Battié MC, Niemelainen R, Gibbons LE, Dhillon S. Is level- and side-specific multifidus asymmetry a marker for lumbar disc pathology? *Spine J* 2012;12:932-9.
11. Bouche KG, Vanovermeire O, Stevens VK, Coorevits PL, Caemaert JJ, Cambier DC, et al. Computed tomographic analysis of the quality of trunk muscles in asymptomatic and symptomatic lumbar discectomy patients. *BMC Musculoskelet Disord* 2011;12:65.
12. Chan ST, Fung PK, Ng NY, Ngan TL, Chong MY, Tang CN, et al. Dynamic changes of elasticity, cross-sectional area, and fat infiltration of multifidus at different postures in men with chronic low back pain. *Spine J* 2012;12:381-8.
13. Hicks GE, Simonsick EM, Harris TB, Newman AB, Weiner DK, Nevitt MA, et al. Cross-sectional associations between trunk muscle composition, back pain, and physical function in the health, aging and body composition study. *J Gerontol A Biol Sci Med Sci* 2005;60:882-7.
14. Kader DF, Wardlaw D, Smith FW. Correlation between the MRI changes in the lumbar multifidus muscles and leg pain. *Clin Radiol* 2000;55:145-9.
15. Kalichman L, Hodges P, Li L, Guermazi A, Hunter DJ. Changes in paraspinal muscles and their association with low back pain and spinal degeneration: CT study. *Eur Spine J* 2010;19:1136-44.
16. Laasonen EM. Atrophy of sacrospinal muscle groups in patients with chronic, diffusely radiating lumbar back pain. *Neuroradiology* 1984;26:9-13.
17. Paalanne N, Niinimäki J, Karppinen J, Taimela S, Mutanen P, Takatalo J, et al. Assessment of association between low back pain and paraspinal muscle atrophy using opposed-phase magnetic resonance imaging: a population-based study among young adults. *Spine (Phila Pa 1976)* 2011;36:1961-8.
18. Parkkola R, Rytökoski U, Kormanen M. Magnetic resonance imaging of the discs and trunk muscles in patients with chronic low back pain and healthy control subjects. *Spine (Phila Pa 1976)* 1993;18:830-6.
19. Steurer J, Roner S, Gnannt R, Hodler J; LumbSten Research Collaboration. Quantitative radiologic criteria for the diagnosis of lumbar spinal stenosis: a systematic literature review. *BMC Musculoskelet Disord* 2011;12:175.
20. Abbas J, Slon V, May H, Peled N, Hershkovitz I, Hamoud K. Paraspinal muscles density: a marker for degenerative lumbar spinal stenosis? *BMC Musculoskelet Disord* 2016;17:422.
21. Han JS, Ahn JY, Goel VK, Takeuchi R, McGowan D. CT-based geometric data of human spine musculature. Part I. Japanese patients with chronic low back pain. *J Spinal Disord* 1992;5:448-58.
22. Fanuele JC, Birkmeyer NJ, Abdu WA, Tosteson TD, Weinstein JN. The impact of spinal problems on the health status of patients: have we underestimated the effect? *Spine (Phila Pa 1976)* 2000;25:1509-14.
23. Machado GC, Maher CG, Ferreira PH, Harris IA, Deyo RA, McKay D, et al. Trends, complications, and costs for hospital admission and surgery for lumbar spinal stenosis. *Spine (Phila Pa 1976)* 2017;42:1737-43.
24. Pope MH, Panjabi M. Biomechanical definitions of spinal instability. *Spine (Phila Pa 1976)* 1985;10:255-6.
25. Hansen L, de Zee M, Rasmussen J, Andersen TB, Wong C, Simonsen EB. Anatomy and biomechanics of the back muscles in the lumbar spine with reference to biomechanical modeling. *Spine (Phila Pa 1976)* 2006;31:1888-99.
26. Wilke HJ, Wolf S, Claes LE, Arand M, Wiesend A. Stability increase of the lumbar spine with different muscle groups. A biomechanical in vitro study. *Spine (Phila Pa 1976)* 1995;20:192-8.
27. Haig AJ. Paraspinal denervation and the spinal degenerative cascade. *Spine J* 2002;2:372-80.
28. Leinonen V, Määttä S, Taimela S, Herno A, Kankaanpää M, Partanen J, et al. Paraspinal muscle denervation, paradoxically good lumbar endurance, and an abnormal flexion-extension cycle in lumbar spinal stenosis. *Spine (Phila Pa 1976)* 2003;28:324-31.
29. Patel CK, Truumees E. Spinal stenosis: pathophysiology, clinical diagnosis, and differential diagnosis. In: Rothman-Simeone the Spine: Expert Consult. Herkowitz HN, Garfin SR, Eismont FJ, Bell GR, Balderston RA, eds., vol. 2, 6th ed., Philadelphia: Elsevier Saunders, 2011: pp.1064-77.



Percutaneous nephrostomy experience in pediatric patients: comparison of fine and thick needle techniques

Ömer Fatih Nas¹, Muhammed Firat Öztepe¹, Selman Candan¹, Sedat Giray Kandemirli², Cem Bilgin³, Mehmet Fatih İncikli¹, Güven Özkaya⁴, Gökhan Öngen¹, Cüneyt Erdoğan⁵

¹Department of Radiology, Bursa Uludag University School of Medicine, Bursa, Turkey; ²Department of Radiology, University of Iowa Hospital and Clinics, Iowa, IA, USA; ³Department of Radiology, University of Health Sciences, Bursa Yüksek İhtisas Training and Research Hospital, Bursa, Turkey; ⁴Department of Statistics, Bursa Uludag University School of Medicine, Bursa, Turkey; ⁵Department of Radiology, Bursa Medicana Hospital, Bursa, Turkey

ABSTRACT

Objectives: The aim of this study is to assess the effect of needle size in pediatric percutaneous nephrostomy (PN) placement in terms of complications and success rates.

Methods: Seventy one percutaneous nephrostomies were performed in 51 patients aged 1 month to 18 years (mean 6.03 ± 5.88 years) between May 2012 and March 2020. Demographic data, indication for PN placement, puncture technique (calyceal entry level: upper, middle, lower pole or pelvis) and needle size, anesthesia type (general or local anesthesia), duration of catheter use and complications were retrospectively retrieved from the hospital electronic recording system.

Results: Thirty procedures were performed using a 21 gauge needle and 41 procedures using a 18 gauge needle. There was no statistically significant difference between the two groups in terms of age, gender, degree of hydronephrosis, and calyceal entry level. Technical success and complication rates were similar in two groups ($p = 0.423$).

Conclusions: In the pediatric age group, both 18 and 21 gauge needle techniques can be used safely based on the preference of the interventionalist.

Keywords: Pediatric patient, percutaneous nephrostomy, 18 gauge needle, 21 gauge needle

Percutaneous nephrostomy (PN) is a widely used method for urinary diversion. It has been widely performed in adults after its initial description by Goodwin *et al.* in 1955 [1]. In the pediatric population, it has been started to be performed in the 1980s and continues to be widely used today [1].

In pediatric patients, PN is most often performed

in urinary obstruction due to congenital causes or compression by mass lesions. PN can be applied temporarily to preserve kidney function until definitive treatment [2-5]. PN can also be used for functional assessment in hydronephrotic kidneys, temporary urinary diversion in obstructive uropathies or as a bridge to more complex interventions [5, 6].

Received: July 24, 2021; Accepted: September 5, 2021; Published Online: March 24, 2022



e-ISSN: 2149-3189

How to cite this article: Nas OF, Oztepe MF, Candan S, Kandemirli SG, Bilgin C, İncikli MF, et al. Percutaneous nephrostomy experience in pediatric patients: comparison of fine and thick needle techniques. *Eur Res J* 2023;9(3):511-516. DOI: 10.18621/eurj.959652

Address for correspondence: Ömer Fatih Nas, MD., Associate Professor, Bursa Uludag University School of Medicine, Department of Radiology, Görükle, 16059 Bursa, Turkey. E-mail: omerfatihnas@gmail.com, Tel: +90 224 295 33 41



©Copyright © 2023 by Prusa Medical Publishing
Available at <http://dergipark.org.tr/eurj>
info@prusamp.com

PN has a certain different aspects in pediatric patients compared to adults. The procedure is mostly performed under general anesthesia in pediatric patients due to limited cooperation. The close proximity of the kidney to the skin in children makes it easier to access the pelvicalyceal system, however, in newborns, mobility of kidney hinders tract dilatation over small wires [7].

PN in both adult and pediatric patients is usually performed under ultrasonography (US) and fluoroscopy guidance. US-guided thick (18 Gauge) or fine (21 Gauge) needles can be used to access the pelvicalyceal system. The use of a larger gauge size is the easiest approach in large collector systems [7]. Increased renal parenchyma stiffness in non-dilated collecting systems makes the fine needle method easier [5].

Our aim in this study is to assess the effect of needle size in pediatric PN placement in terms of complications and success rates.

METHODS

The Institutional Review Board approved the study protocol. Due to the retrospective and anonymous nature of this study, informed consent was waived. Between May 2012 and March 2020, 51 patients underwent PN in our interventional radiology department. Patient data were evaluated retrospectively. Demographic data, indications for PN, puncture technique (calyceal entry level: upper, middle, lower pole or pelvis) and needle size, size of catheter placed, anesthesia type (general or local anesthesia), duration of catheter use and complications were recorded. Placement of an appropriately sized catheter to ensure adequate drainage was considered as technical success [6].

The degree of hydronephrosis was assessed based on the US examinations obtained prior to the procedure. Hydronephrosis grading was performed according to the Society for Fetal Urology guidelines: Grade 0, no expansion; grade 1, slight enlargement of the pelvis without enlargement in calyces; grade 2, enlargement of the pelvis and major calyces; grade 3, grade 2 without parenchymal changes and enlargement of minor calyces; grade 4, grade 3 and thinning in the parenchyma [8].

All patients' parents were informed in detail about

the procedure and consent was obtained for each procedure. Complete blood count and coagulation parameters (International normalized ratio [INR] < 1.5 and Platelet count > 50,000/ μ L) were checked prior to procedures. All patients received 25 mg/kg ampicillin one hour before the procedure as prophylaxis. PN procedure was performed under local or general anesthesia. The 18 and 21 gauge needle selection was made based on the preference of interventionalists.

Fine Needle Technique (21 Gauge)

A 21 gauge fine needle was used to access the kidney collecting system under US guidance and usually preferred lower pole calyx. The collecting system was opacified by injecting contrast material through the needle. If calyceal access was achieved, 0.018" microwire was sent through the needle, and a 6F coaxial access was advanced over the wire. In the second stage, a 0.035" or 0.038" thicker guidewire with a stiff body was placed. Gradually the entry tract was dilated over this wire with dilators of appropriate diameter for nephrostomy catheter placement.

Thick Needle Technique (18 Gauge)

An 18 gauge needle was inserted under US guidance into the collecting system usually from a lower point by targeting the lower pole of the kidney. The collecting system was opacified by injecting contrast material from the needle. The needle was removed after inserting a guidewire with a diameter of 0.035" or 0.038". The nephrostomy catheter was placed through the wire by dilating the entrance tract according to the diameter of the catheter.

Statistical Analysis

Shapiro-Wilk test was used to check the normal distribution of the data. Descriptive statistics were expressed as mean \pm standard deviation or median (minimum-maximum) for continuous variables and frequency for categorical data. For non-normally distributed data, Mann Whitney U test was used for two-group comparisons. Pearson Chi-square test and Fisher's exact Chi-square test were used for the analysis of categorical data. Duration of catheter use without complications was estimated by considering the time until a complication occurs based on Kaplan Meier analysis. The significance level was determined to be $\alpha = 0.05$. Statistical analysis was performed

using IBM SPSS 23.0 (IBM Corp. Released 2015. IBM SPSS Statistics for Windows, Version 23.0. Armonk, NY: IBM Corp.)

RESULTS

A total of 71 PN procedures were performed in 51 patients (32 boys, 19 girls). Mean age was 1 month-18 years (mean 6.03 ± 5.88 years). Fine needle technique was used in 30 procedures, and thick needle technique was used in 41 procedures. Fifty-nine procedures were performed under general anesthesia and 12 procedures were performed under local anesthesia. Seventy procedures (70/71; 98.6%) were technically successful. The most common indication for catheter placement was ureteropelvic junction (UPJ) stenosis (13/71; 18.3%). Other PN placement indications are given in Tables 1 and 2.

Table 1. Patient demographic data and PN indications

Patient characteristics	N = 51
Age	6.03 ± 5.88
Gender	
Male	32
Female	19
Indications	
UPJ stenosis	11
Postoperative anastomotic strictures	8
UVJ stenosis	8
Obstruction due to urinary stone	7
Obstruction due to mass compression	5
Neurogenic bladder	3
Vesicoureteral reflux	3
PUV	2
Ureteral injury	2
Urinary fistula to the skin	1
Urinary trauma	1

Descriptive statistics are specified as mean, standard deviation, minimum and maximum for quantitative data; frequency for qualitative data.

UPJ = Ureteropelvic junction, UVJ = Ureterovesical junction, PUV = Posterior urethral valve, PN = Percutaneous nephrostomy

The mean duration of catheter dwell time was 34.3 ± 32.9 (1-148) days. Other data related to the procedures are given in detail in Table 2.

There was no statistically significant difference be-

Table 2. Procedural data

Procedure data	n = 71
Anesthesia type	
Local	12
General	59
Technical success	
Successful	70
Failure	1
Indication	
UPJ stenosis	13
Postoperative anastomotic strictures	11
UVJ stenosis	9
Obstruction due to urinary stone	8
Obstruction due to mass compression	8
Neurogenic bladder	5
Vesicoureteral reflux	5
PUV	5
Ureteral injury	5
Urinary fistula to the skin	1
Urinary trauma	1
Hydronephrosis	
Absent	5
Grade 1	0
Grade 2	16
Grade 3	37
Grade 4	13
Level of entry	
Upper pole	4
Middle pole	22
Lower pole	30
Pelvis	15
Duration of catheter use	34.3 ± 32.9 (1-148)

Descriptive statistics are specified as mean, standard deviation, minimum and maximum for quantitative data; frequency for qualitative data.

UPJ = Ureteropelvic junction, UVJ = Ureterovesical junction, PUV = Posterior urethral valve

Table 3. Statistical comparisons of procedures with fine and thick needle methods

Procedure Data	Fine Needle (n = 30)	Thick Needle (n = 41)	p value
Age(years)	4.5(0.1-18.0)	6.0(0.1-17.0)	0.766 ¹
Gender			
Male	22	21	0.060 ²
Female	8	20	
Type of anesthesia			
Local anesthesia	8	4	0.060 ²
General anesthesia	22	37	
Technical success			
Successful	29	41	0.423 ³
Unsuccessful	1	0	
Hydronephrosis			
Absent	5	0	0.063 ³
Grade 1	0	0	
Grade 2	6	10	
Grade 3	14	23	
Grade 4	5	8	
Level of entry			
Upper pole	2	2	0.098 ³
Middle pole	8	14	
Lower pole	17	13	
Pelvis	3	12	
Indication			
UPJ stenosis	7	6	0.141 ³
Postoperative anastomotic strictures	5	6	
UVJ stenosis	3	6	
Obstruction due to urinary stone	2	6	
Obstruction due to mass compression	3	5	
Neurogenic bladder	2	3	
Vesicoureteral reflux	0	5	
PUV	5	0	
Ureteral injury	2	3	
Urinary fistula to the skin	1	0	
Urinary trauma	0	1	

Descriptive statistics are specified as mean, standard deviation, minimum and maximum for quantitative data; frequency for qualitative data.

¹Mann Whitney U test

²Pearson Chi-Square test

³Fisher's exact chi-square test

UPJ = Ureteropelvic junction, UVJ = Ureterovesical junction, PUV = Posterior urethral valve

tween the two groups in terms of age, gender, degree of hydronephrosis, and calyceal entry levels (Table 3). There was no statistically significant difference in technical success rate between the two techniques ($p = 0.423$).

No major complications were encountered. Minor complications were seen in 13 procedures: Dislocation (7 procedures), leakage (4 procedures), infection (1 procedure), and obstruction (1 procedure). Apart from these, 6 patients had temporary hematuria, and these patients recovered without additional treatment or intervention.

Based on Kaplan Meier analysis, the mean duration of the catheter use without complications was 95 ± 15.9 days. No complications occurred in 82.7% of patients at the end of the first month, and 51.4% of patients at the end of 3 months (Fig. 1).

DISCUSSION

PN is a frequently performed procedure since it can be applied easily, quickly, and safely. However, in the pediatric age group, especially in newborns and infants, the procedure can be technically challenging when compared to adults or the rest of pediatric patients [5]. The kidney is mobile in newborns and infants, making it difficult to perform tract dilation [7]. In addition, smaller kidney sizes compared to adults and older children poses technical difficulties. Generally, two methods are used to access the renal calyx in interventions performed with a combination of US and fluoroscopy guidance. The fine needle method, is generally more widely preferred by physicians [7]. Espe-

cially in non-dilated systems, this method is more preferable as there is less damage to the kidney. The thick needle method is more widely adopted in patients with significant hydronephrosis and has the advantage of decreased procedure times [5].

Koral *et al.* [5] reported that the fine needle technique is advantageous in non-dilated systems and the thick needle technique in patients with ureteropelvic stenosis in their study on newborns and infants. They also reported that the procedure time of thick needle technique was statistically significantly shorter than the fine needle method [5]. In our study, fine and thick needle techniques were compared among groups that had similar variables like age, indication, degree of hydronephrosis, and calyceal entry level that may affect the final technical. Statistically, both methods were not different from each other in terms of technical success. We think that both methods can be adapted in pediatric patients with different indications.

Temporary minor hematuria occurs in approximately 95% of cases and is not considered a complication [9]. Serious bleeding requiring transfusion has been reported in 1-4% of patients [6]. In this study, we did not encounter any patient with hematuria requiring transfusion. Six patients had mild hematuria after the procedure, and these patients recovered without need for additional treatment.

Catheter dislocation poses a problem in young children and infants because providing adequate care in this age group can be challenging [10, 11]. In previous studies, the dislocation rate in the pediatric population has been reported between 1 and 14% [10-12]. In our study, the dislocation rate was (7/71; 10%). Providing adequate fixation and educating parents about catheter care can help to prevent this complication.

In this study, urinary tract infection was encountered only in one patient. Procedure-related sepsis rates have been reported as 0-5% in previous studies [3, 4, 10, 13]. In this study, we did not have any patients progressing to sepsis.

A multicenter study by Shellikeri *et al.* [14] done in 441 pediatric patient groups reported that 75% of patients in 37 days and 50% of patients in 89 days did not develop any complications. In this study, no complications developed in 82.7% of patients in the first month and 51.4% of patients at the end of 3 months. In both our study and the study by Shellikeri *et al.* [14], approximately half of the patients developed

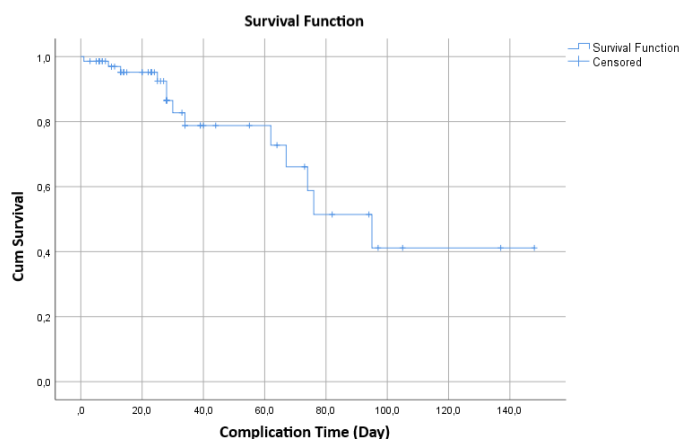


Fig. 1. The mean duration of the catheter use

complications after 3 months. Therefore, catheter replacement can be scheduled every 3 months.

Limitations

This study had some limitations including, a limited number of patients, heterogeneous distribution of indications, and retrospective nature. Future studies can be planned to compare the success rates of both techniques in wider and more homogeneous patient groups.

CONCLUSION

Percutaneous nephrostomy can be performed in the pediatric population with low complication and high success rate. Regardless of age, indication, degree of hydronephrosis and entry level, fine and thick needle techniques can be performed successfully based on the preference of the interventionalist.

Authors' Contribution

Study Conception: ÖFN, MFÖ, SC, SGK, CB, MFİ, GÖ, CE; Study Design: ÖFN, MFÖ, SC, SGK, CB, MFİ, GÖ, CE; Supervision: ÖFN; Funding: ÖFN, MFİ, CE; Materials: ÖFN, MFİ, CE; Data Collection and/or Processing: ÖFN, SC; Statistical Analysis and/or Data Interpretation: GÖ; Literature Review: MFÖ; Manuscript Preparation: ÖFN, MFÖ and Critical Review: ÖFN.

Conflict of interest

The authors disclosed no conflict of interest during the preparation or publication of this manuscript.

Financing

The authors disclosed that they did not receive any grant during conduction or writing of this study.

REFERENCES

1. Goodwin WE, Casey WC, Woolf W. Percutaneous trocar (needle) nephrostomy in hydronephrosis. *J Am Med Assoc* 1955;157:891-4.
2. Winfield AC, Kirchner SG, Brun ME, Mazer MJ, Braren HV, Kirchner FK Jr. Percutaneous nephrostomy in neonates, infants, and children. *Radiology* 1984;151:617-9.
3. Stanley P, Bear JW, Reid BS. Percutaneous nephrostomy in infants and children. *Am J Roentgenol* 1983;141:473-7.
4. Irving HC, Arthur RJ, Thomas DFM. Percutaneous nephrostomy in paediatrics. *Clin Radiol* 1987;38:245-8.
5. Koral K, Saker MC, Morello FP, Rigsby CK, Donaldson JS. Conventional versus modified technique for percutaneous nephrostomy in newborns and young infants. *J Vasc Interv Radiol* 2003;14:113-6.
6. Ramchandani P, Cardella JF, Grassi CJ, Roberts AC, Sacks D, Schwartzberg MS, et al. Quality improvement guidelines for percutaneous nephrostomy. *J Vasc Interv Radiol* 2001;12:1247-51.
7. Barnacle AM, Wilkinson AG, Roebuck DJ. Paediatric interventional urology. *Cardiovasc Interv Radiol* 2011;34:227-40.
8. Nguyen HT, Herndon CA, Cooper C, Gatti J, Kirsch A, Kokorowski P, et al. The Society for Fetal Urology consensus statement on the evaluation and management of antenatal hydronephrosis. *J Pediatr Urol* 2010;6:212-31.
9. Dagli M, Ramchandani P. Percutaneous nephrostomy: technical aspects and indications. *Semin Interv Radiol* 2011;28:424-37.
10. Hogan MJ, Coley BD, Jayanthi VR, Shiels WE, Koff SA. Percutaneous nephrostomy in children and adolescents: outpatient management. *Radiology* 2001;218:207-10.
11. Yavascan O, Aksu N, Erdogan H, Aydin Y, Kara OD, Kangin M, et al. Percutaneous nephrostomy in children: diagnostic and therapeutic importance. *Pediatr Nephrol* 2005;20:768-72.
12. Sancaktutar AA, Bozkurt Y, Tüfek A, Söylemez H, Önder H, Atar M, et al. Radiation-free percutaneous nephrostomy performed on neonates, infants, and preschool-age children. *J Pediatr Urol* 2013;9:464-71.
13. Ball WS Jr, Towbin R, Strife JL, Spencer R. Interventional genitourinary radiology in children: a review of 61 procedures. *Am J Roentgenol* 1986;147:791-6.
14. Shellikeri S, Daulton R, Sertic M, Connolly B, Hogan M, Marshalleck F, et al. Pediatric percutaneous nephrostomy: a multicenter experience. *J Vasc Interv Radiol* 2018;29:328-34.



This is an open access article distributed under the terms of Creative Commons Attribution-NonCommercial-NoDerivatives 4.0 International License.

Expression and prognostic value of *ING3* in advanced laryngeal squamous cell carcinoma

Neslisah Barlak^{1,2}, Gulnur Kusdemir^{1,2}, Rasim Gumus^{1,2}, Abdulkadir Sahin³, Betul Gundogdu⁴, Omer Faruk Karatas^{1,2}, Arzu Tatar³

¹Department of Molecular Biology and Genetics, Erzurum Technical University, Erzurum, Turkey; ²High Technology Application and Research Center, Erzurum Technical University, Erzurum, Turkey; ³Department of Otorhinolaryngology Diseases, Ataturk University, Faculty of Medicine, Erzurum, Turkey; ⁴Department of Medical Pathology, Ataturk University, Faculty of Medicine, Erzurum, Turkey

ABSTRACT

Objectives: Laryngeal squamous cell carcinomas (LSCC) is one of the most common aggressive neoplasms of the head and neck region. There is a significant need for identification of successful and accurate prognostic markers to better estimate the clinical outcomes for LSCC patients. In this study, we aimed at analyzing the differential expressions of inhibitor growth (*ING*) family members and to evaluate the prognostic values of deregulated *ING* genes in LSCC.

Methods: We investigated the relative expressions of *ING* genes in laryngeal tumor-normal tissue pairs at mRNA level using quantitative real-time polymerase chain reaction and relative expression of *ING3* in the protein level using Western Blot analysis.

Results: The rate of genetic alterations of *ING3* was relatively higher in head and neck cancers including LSCC. *ING3* expression was significantly upregulated in LSCC tissue samples at both mRNA and protein level. Higher expression of *ING3* was also correlated with poor disease-free survival of patients with head and neck cancer.

Conclusions: Our findings assigned an oncogenic feature for *ING3* in laryngeal cancer with a significant upregulation detected in advanced cases and suggested a vital prognostic potential for *ING3*.

Keywords: Larynx cancer, *ING* gene family, oncogene, prognosis

Laryngeal squamous cell carcinomas (LSCC) is one of the most common aggressive neoplasms of the head and neck region, accounting for approximately 85 to 90% of all malignant laryngeal tumors [1]. Multiple factors including smoking, alcohol consumption, air pollution, diet, HPV infection, and radiation are related to the occurrence of LSCC, which is a complex process where the imbalance between the

expressions of multiple tumor suppressor genes and oncogenes, deregulation of vital signaling pathways and defects of immune system are observed [2, 3]. Despite considerable advances have been achieved in radiotherapy, chemotherapy, adjuvant chemotherapies, surgical treatment, and diagnosis techniques, approximately 60% of patients with LSCC progress to advanced stages, who experience dyspnea, dysphagia,

Received: May 11, 2022; Accepted: September 15, 2022; Published Online: January 14, 2023



e-ISSN: 2149-3189

How to cite this article: Barlak N, Kusdemir G, Gumus R, Sahin A, Gundogdu B, Karatas OF, et al. Expression and prognostic value of *ING3* in advanced laryngeal squamous cell carcinoma. *Eur Res J* 2023;9(3):517-528. DOI: 10.18621/eurj.1108404

Address for correspondence: Omer Faruk Karatas, PhD., Erzurum Technical University, Department of Molecular Biology and Genetics, Omer Nasuhi Bilmen Mah. Havaalani Yolu Cad. No: 53 Yakutiye, Erzurum, Turkey. E-mail: faruk.karatas@erzurum.edu.tr, Phone: +90 444 5 388 ext. 2390, Fax: +90 442 230 00 39



©Copyright © 2023 by Prusa Medical Publishing
Available at <http://dergipark.org.tr/eurj>
info@prusamp.com

and dysphonia leading to significant reduction in the quality of life [4, 5]. Invasion, lymphatic metastasis, and tumor recurrence, which are observed along with late diagnosis, are the main factors that contribute to poor prognosis and high mortality rates in advanced LSCC [6]. In addition, due to late diagnosis at advanced stages, the 5-year survival rates of LSCC patients remain poor that did not change over the last 30 years [7]. Therefore, there is a significant need for identification of successful and accurate prognostic markers to better estimate the clinical outcomes for LSCC patients.

The human Inhibitor of Growth (*ING*) family comprised of five conserved genes, *ING1*, *ING2*, *ING3*, *ING4* and *ING5*, which share between 32% and 76% DNA sequence homology [8, 9]. Their encoded proteins contain a highly conserved plant homeodomain (PHD) in the C-terminal region, a Cys4-His-Cys3 form of zinc finger that interacts directly with histone H3, a nuclear localization signal (NLS) in the middle region, and a novel conserved region (NCR) with unknown function [10-12]. Previous studies showed that *ING* proteins are involved in a wide variety of cellular processes including DNA repair, histone methylation and acetylation, senescence, cell growth, colony formation, apoptosis, cell cycle control, chromatin remodeling, and angiogenesis [9, 13, 14]. Mutations and altered expressions of *INGs* have been reported in different types of cancers including lung cancer, osteosarcoma, oral squamous cell carcinoma, breast cancer, prostate cancer, gastric cancer, colorectal cancer, and laryngeal squamous cell carcinoma [15-17].

ING3 gene, located on chromosome 7q31.3, is a member of the *ING* family, which consists of 12 exons encoding a 46.8 kDa protein with 418 amino acids [14, 15, 18-20]. *ING3* is a part of the NuA4-Tip60 MYST-HAT multi-subunit complex core unit, which also contains EPC1, EAF6, and TIP60 as main participants, that are responsible for the acetylation of histones H2A and H4 [13, 21, 22]. So far, studies showed that *ING3* acts as a type II tumor suppressor as downregulated in many types of cancer and play significant roles in modulating transcription, cell cycle control, and apoptosis [23-25]. However, recent studies have reported that *ING3* is highly expressed in rapidly proliferating human tissues [22, 26]. In addition, in contrast to tumor suppressor role, various studies have reported

that upregulation of *ING3* stimulate cell proliferation, tumor growth, and androgen receptor activation. High *ING3* levels also correlated with poor prognosis in prostate cancer suggesting an oncogenic potential for *ING3* [26, 27]. Although *ING3* has been reported to be abnormally expressed in a number of cancer types, the roles of *ING3* in laryngeal carcinogenesis are largely unknown. Therefore, we aimed at analyzing the differential expressions of *ING* family members and to evaluate the prognostic value of deregulated *ING3* in LSCC.

In this study, we assigned an oncogenic potential for *ING3* in laryngeal cancer with a significant upregulation detected in advanced cases. We also demonstrated that *ING3* expression significantly correlates with its physical interactor EPC1 with oncogenic potential in head and neck cancer. Our results suggest a vital prognostic potential for *ING3* in laryngeal cancer although further functional studies are required to strengthen its potential as a prognostic marker.

METHODS

In Silico Analysis

cBioPortal web tool was used to analyze the differential expression and copy number changes of *ING* gene family members and *ING3* interactors using the RNA sequencing expression data of tumor and normal samples of head and neck origin collected from the Cancer Genome Atlas Program (TCGA) [28]. Co-occurrence analysis of *ING3* and its interactors was carried out using cBioPortal as well. The mean differential expression of *ING* gene family members, the relative expression of *ING3* in tumor tissue samples considering their stage and T classification, and *ING3/EPC1* correlation were presented using the data obtained from UALCAN, which is a comprehensive web resource for analyzing cancer OMICS data [29]. Differential expression of *ING3* in 11 datasets deposited at Oncomine was evaluated and Sengupta (26 nasopharyngeal tumor and 12 normal specimens) and Ginos (41 head and neck squamous cell carcinoma and 13 normal specimens) data with profound alterations in *ING3* expression were plotted [30]. The interactors of *ING3* was identified using String web tool [31]. Overrepresentation analysis of *ING3* and its interactors was performed using WEB-based GENE SeT

AnaLysis Toolkit.

Patients and Tissue Samples

This study was reviewed and approved by the Institutional Ethics Committee of Ataturk University, Faculty of Medicine (IRB No: B.30.2.ATA.0.01.00/555). Participants were included into the study after receiving their written informed consents. 28 laryngeal tumor tissue specimens with at least 70% tumor cell content and 28 corresponding adjacent laryngeal normal tissue samples were obtained from Department of Otorhinolaryngology, Faculty of Medicine, Atatürk University. The tumor cell content of the laryngeal tumor tissue specimens and the absence of any cancerous or dysplastic content in the corresponding adjacent laryngeal normal tissue samples was histopathologically confirmed at Department of Medical Pathology, Faculty of Medicine, Ataturk University. All tumors and matched non-tumor tissue samples were histologically analyzed by a pathologist. Histological analysis was reviewed by two independent pathologists after H&E staining. Clinical stages were categorized according to the seventh edition of the UICC-TNM classification. Fresh tissue materials were collected immediately after surgery to prevent degradation of RNA and protein contents, snap frozen, and stored at -80 °C. Patients didn't receive radiotherapy, chemotherapy, or immunotherapy prior to the surgery. The clinico-pathological data of patients were summarized in Table 1.

RNA Isolation

Total RNA samples from equal amounts of tumor and normal laryngeal tissue specimens grounded within liquid nitrogen were extracted using TRIzol reagent (Invitrogen, San Diego, CA, United States) following the manufacturer's protocol. Total RNA concentrations and purities were measured spectrophotometrically with Epoch 2 Microplate Spectrophotometer (BioTek, Winooski, VT, United States).

cDNA Synthesis and Quantitative Real-Time PCR

A total of 1µg RNA for each sample was reverse-transcribed into complementary DNA (cDNA) using "High Capacity cDNA Reverse Transcription Kit" (Thermo Fisher Scientific, Waltham, MA, United States) according to manufacturer's instructions. Relative expression levels of *ING* family members were

analyzed with quantitative real time polymerase chain reactions (qRT-PCR) with 5 × HOT FIREPol Eva-Green qPCR Mix Plus (Solis Bio-Dyne, Tartu, Estonia) using Rotor-Gene qRT-PCR (Qiagen, Düsseldorf, Germany) device with standard parameters. Data were normalized to Glyceraldehyde 3-phosphate dehydrogenase (GAPDH) expressions. Primers used in qRT-PCR were listed in Supplementary Table 1. All reactions were carried out in duplicates. Relative expression levels were calculated using the $2^{-\Delta\Delta CT}$ method.

Table 1. The clinico-pathological data of the patients

LSCC Subjects	
Age	
≤ 60	15
> 60	13
Gender	
Male	27
Female	1
Tumor Location	
Supraglottic	16
Subglottic	12
Size (cm)	
≤ 2	13
>2	15
T Classification	
T1 and T2	12
T3 and T4	16
Histological Grade	
I and II	10
III and IV	17
Lymphatic metastasis	
N0	17
N+	11
Neck Dissection	
No	15
Yes	13
Adjuvant Therapy	
No	8
Yes	20

Western Blot Analysis

Proteins were extracted using modified RIPA Lysis Buffer (EcoTech Biotechnology, Erzurum, Turkey) containing phenylmethanesulfonyl fluoride (Roche, Basel, Switzerland) and phosphatase inhibitor cocktail (Santa Cruz Biotechnology, Dallas, TX, United States). Equal amounts of each protein sample mixed with $10 \times$ Laemmli Sample Buffer (EcoTech Biotechnology, Erzurum, Turkey) in 9/1 ratio was loaded and separated in 10% sodium dodecyl sulfate-polyacrylamide gel electrophoresis (SDS-PAGE) and transferred to nitrocellulose membrane (EcoTech Biotechnology, Erzurum, Turkey) using semi-dry electrophoretic transfer cell (Bio-Rad, Hercules, CA, United States). Membranes were blocked in 5% non-fat milk powder dissolved in $1 \times$ PBST buffer (EcoTech Biotechnology, Erzurum, Turkey) for 1 hour at room temperature, and then incubated with primary antibodies against ING3 (diluted in 1:1000; Santa Cruz Biotechnology, Cat No: sc-101245, Dallas, TX, United States), β -actin (diluted in 1:200; Santa Cruz Biotechnology, Cat No: sc-47778, Dallas, TX, United States) diluted in PBST buffer on a shaker overnight at 4°C. After washing with PBST, membranes were incubated with appropriate HRP-conjugated secondary antibodies (1/3,000; Santa Cruz Biotechnology, Dallas, TX, United States) for 1 hour at room temper-

ature. The Clarity Max ECL Western Blotting Substrate (BioRad, United States, Hercules, CA, Dallas, TX, United States) or *ClearBand* Western Blotting Substrate (EcoTech Biotechnology, Erzurum, Turkey) were used to visualize protein signals and quantification of bands was performed using Image J program.

Statistical Analysis

Correlation of *ING3/EPC1* expressions was measured using Pearson's Correlation test. Association of histologic grade with the presence of genomic alteration in at least one of the *ING3* and *EPC1* in the tumor specimens was tested using Chi-squared test. $P < 0.05$ was considered as statistically significant.

RESULTS

Expressions of *ING* family genes are upregulated and these genes have genetic alterations in LSCC patients

We initially analyzed mutation characteristics and genetic alteration of *ING* family members in head and neck squamous cell carcinoma samples deposited at TCGA database (TCGA-HNSCC) using cBioPortal. As shown in Figure 1A, high mutation frequencies of *ING* family members were observed in head and neck

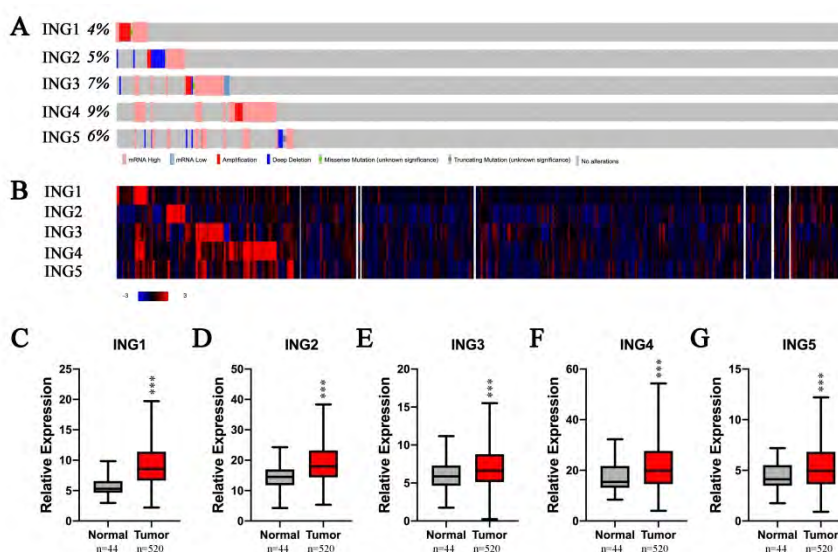


Fig. 1. *ING* family members have genetic alterations and are upregulated in head neck cancer patients. (A) Frequent genetic alterations observed in *ING* family members in head and neck cancer tissues. (B) Expression profile of *ING* family members in head and neck cancer tissues. Relative mean expression levels of (C) *ING1*, (D) *ING2*, (E) *ING3*, (F) *ING4* and (G) *ING5*. Gene expressions were normalized to *GAPDH*. *** $p < 0.001$.

squamous cell carcinoma patients. *ING3*, *ING4*, and *ING5* were the three genes with the highest rate of sequence alterations, and their mutation rates were 7%, 9%, and 6%, respectively (Fig. 1A). Similar pattern was observed when their expressions in tumor samples were analyzed in the mRNA level using RNA sequencing data of TCGA-HNSCC (Fig. 1B). Next, the mRNA expression patterns of *ING* family members were investigated between head and neck squamous cell carcinoma and normal tissues using UALCAN web portal. The result showed that all of *ING* family members were significantly upregulated in primary head and neck squamous cell carcinoma tissues compared to normal samples (Figs. 1C-G, all $p < 0.05$).

Expression of *ING3* is upregulated in LSCC tissues and significantly related to clinicopathological parameters

To explore levels of *ING* family members, we ini-

tially examined the mRNA expression of *ING1a*, *ING1b*, *ING2*, *ING3*, *ING4*, and *ING5* in LSCC patients using qRT-PCR. The results revealed that the expression of *ING3* was significantly increased in laryngeal cancer tissues compared with adjacent non-cancerous tissues, while no significant statistical difference was observed in the expressions of *ING1a*, *ING1b*, *ING2*, *ING4*, and *ING5* between cancer tissues and adjacent non-cancerous tissues (Fig. 2A). We then used Oncomine online portal further to verify the mRNA levels of *ING3*. Sengupta (26 nasopharyngeal tumor and 12 normal specimens) and Ginos (41 head and neck squamous cell carcinoma and 13 normal specimens) data showed that *ING3* was profoundly upregulated in the cancer tissues compared with adjacent non-cancerous tissues (Figs. 2B and 2C). Interestingly, *ING3* expression was not significantly altered in other datasets deposited in Oncomine, which were mostly comprised of specimens with oral cavity ori-

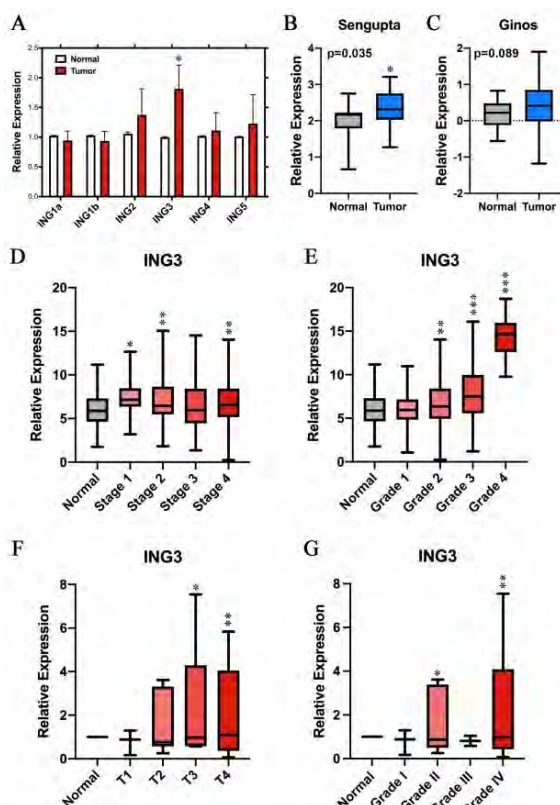


Fig. 2. Expression of *ING3* is upregulated in LSCC tissues and its expression is significantly related to clinicopathological parameters. (A) Relative mean expression levels of *ING* family members in LSCC tissues and adjacent non-tumor tissues. (B) Relative mRNA level of *ING3* in Sengupta dataset obtained from Oncomine. (C) Relative mRNA level of *ING3* in Ginos dataset obtained from Oncomine. (D) Relative *ING3* level in different stage head and neck tumor tissue samples deposited in TCGA. (E) Relative *ING3* expression level in different grade head and neck tumor tissue samples deposited in TCGA. (F) Relative *ING3* expression level in different T stage LSCC tissue samples. (G) Relative *ING3* expression level in different grade LSCC tissue samples. * $p < 0.05$, ** $p < 0.01$, *** $p < 0.001$.

gin.

After mRNA expression of *ING3* found to be up-regulated in LSCC patients, we then focused on the relationship of *ING3* mRNA expressions with clinicopathological parameters in individual head and neck squamous cell carcinoma patients using UALCAN. The results show that patients with advanced stage head and neck cancer had relatively higher *ING3* mRNA expression compared with normal tissue samples (Fig. 2D). In addition, *ING3* mRNA expression was also significantly upregulated in tumor tissue samples of head and neck cancer patients with higher grades compared with normal specimens (Fig. 2E). In line with these findings, we also observed overexpression of *ING3* in patients with advanced LSCC (Figs. 2F and 2G). Taken together, these results suggested that transcriptional levels of *ING3* is significantly correlated with different clinicopathological parameters in LSCC patients and LSCC patients with advanced stages tended to have higher levels of *ING3*.

ING3 has increased protein level in LSCC patients

ING3 mRNA level was significantly higher in LSCC tissues compared with matched non-cancerous LSCC tissues. To further confirm these results, we performed western blot analysis using 10 tumor-normal tissue pairs collected from LSCC patients (Fig. 3A). Our data revealed that, *ING3* expression in protein level was significantly increased in cancer tissues compared with adjacent non-cancerous tissues (Fig.

3B), which is consistent with our qRT-PCR and *in silico* analysis. These results provided strong evidence that *ING3* is upregulated in LSCC.

ING3 interacts with a hub of genes mostly related to DNA damage

After analysis of *ING3* genetic alterations, expression pattern, and its prognostic value in LSCC patients, we performed protein-protein interaction analysis using the STRING database to explore the possible functional protein network of *ING3*. The top 10 hub genes with the highest protein-protein interaction confident scores were located in the core shell of the network including *KAT5*, *BRD8*, *MEAF6*, *MRGBP*, *EPC1*, *MORF4L2*, *DMAP1*, *YEATS4*, *MORF4L1*, and *RUVBL2* (Fig. 4A). Further molecular gene set enrichment analysis revealed that these proteins were involved in chromatin modification, chromatin organization, HATs acetylate histones, sensing of DNA double strand breaks, telomere extension by telomerase, regulation of TP53 activity, activation of the TFAP2 (AP-2) family of transcription factors, and resolution of D-loop structures through synthesis-dependent strand annealing (Table 2). Subsequently, the genetic information and function of these 10 genes in association with *ING3* in HNSCC patients were explored using the cBioPortal web tool. We investigated the cancer genomic alteration characteristics of these genes in HNSCC and found a significant rate of genetic alterations across a set of HNSCC samples based

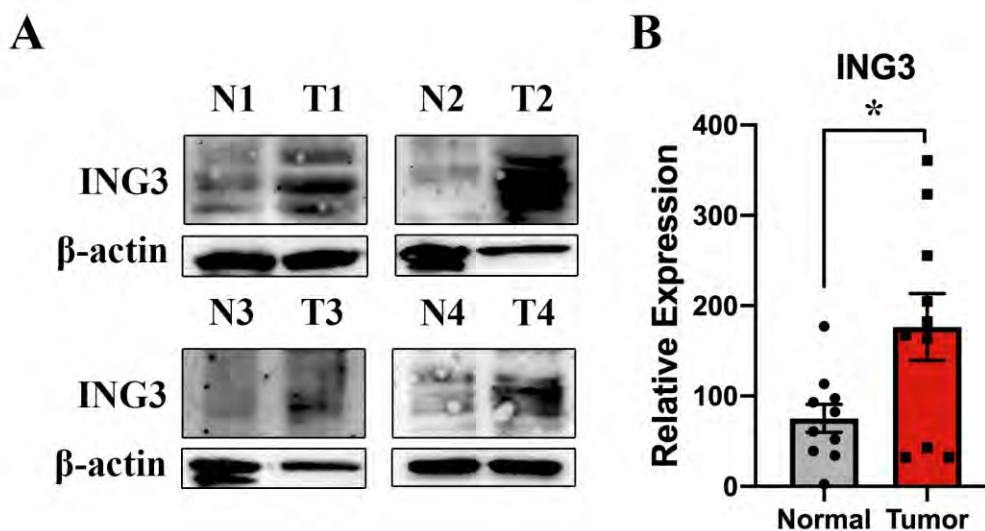


Fig. 3. *ING3* have increased protein level in LSCC patients. (A) Representative images of *ING3* expression in laryngeal normal and tumor tissue samples. (B) Relative mean *ING3* expression in protein level in LSCC tissue samples. Protein levels were normalized to β -Actin. * $p < 0.05$; t-test.

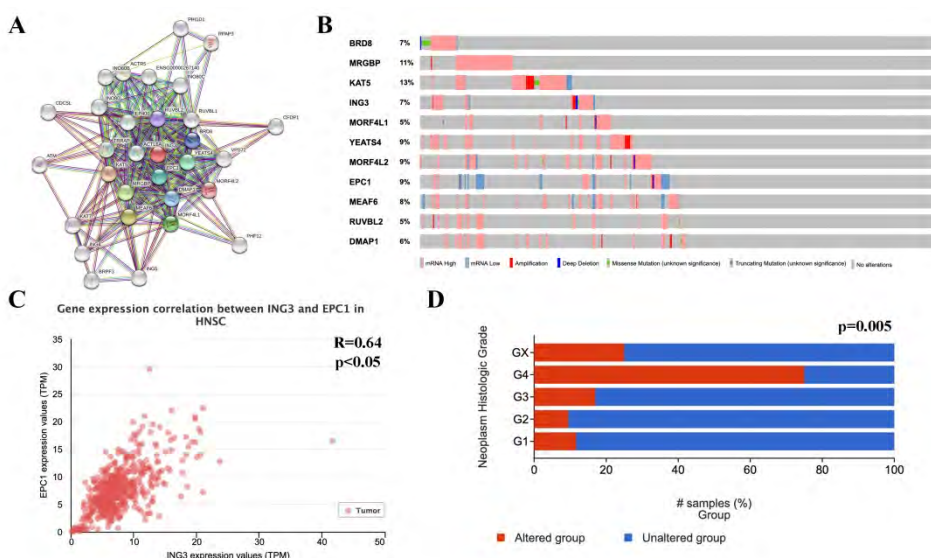


Fig. 4. Functional protein interaction network analysis of *ING3* and predicted mutations and functions of hub genes. (A) Protein interaction network of *ING3* depicted using STRING database. (B) Genetic alterations of *ING3* related genes (C) The correlation of *ING3* and *EPC1* expressions. (D) Association of alterations of these two genes with advanced histological grade of head and neck cancer.

on a query of these 10 genes associated with *ING3*. As shown in Fig. 4B, they were altered in five types of genetic alterations including amplification and high mRNA expression, in the queried HNSCC samples. Among these alterations, the deep deletion and high mRNA expression accounted for the most changes in HNSCC. Then, we investigated co-occurrence of

ING3 interactors in tumor HNSCC sample. The results showed that *ING3* was associated with both *EPC1* and *MEAF6*, where only the relationship of *ING3* with *EPC1* was statistically significant (Table 3). Therefore, *EPC1* was selected for further analysis. The correlation of *ING3* and *EPC1* expression was assessed using UALCAN web portal. The statistical scatter plots

Table 2. Over-representation analysis of *ING3* interactors

Enriched Gene Set	Size	Expect	Ratio	p value
Chromatin modifying enzymes	275	0.28665	38.375	> 0.001
Chromatin organization	275	0.28665	38.375	> 0.001
HATs acetylate histones	142	0.148	74.317	> 0.001
Sensing of DNA Double Strand Breaks	6	0.0062536	159.91	0.0062388
Telomere Extension By Telomerase	6	0.0062536	159.91	0.0062388
Regulation of TP53 Activity	160	0.16676	11.993	0.011483
Activation of the TFAP2 (AP-2) family of transcription factors	12	0.012507	79.955	0.012442
Generic Transcription Pathway	1169	1.2184	3.283	0.026095
Resolution of D-loop Structures through Synthesis-Dependent Strand Annealing (SDSA)	26	0.027099	36.902	0.02678
Regulation of TP53 Activity through Acetylation	30	0.031268	31.982	0.030842

Table 3. Co-occurrence of ING3 interactors in HNSCC tumor samples

Gene A	Gene B	Neither	A Not B	B Not A	Both	Log2 Odds Ratio	p value	Tendency
MEAF6	DMAP1	194	6	0	3	> 3	< 0.001	Co-occurrence
MORF4L2	MEAF6	182	12	5	4	> 3	0.003	Co-occurrence
ING3	MEAF6	187	7	6	3	> 3	0.006	Co-occurrence
MRGBP	MORF4L2	176	11	12	4	2.415	0.021	Co-occurrence
ING3	EPC1	188	8	5	2	> 3	0.04	Co-occurrence

showed that *ING3* expression had a strong positive association with the expression of *EPC1* in HNSCC patients (Fig. 4C). In addition, we investigated the relationship between the alteration status of these two genes and the histological grade of neoplasm in HNSCC samples using cBioPortal web tool. Most notably, we found that the patients possessing any kind of alterations of these two genes tended to have advanced histological grade HNSCC (Fig. 4D).

DISCUSSION

LSCC is a frequent aggressive tumor type occurring in the head and neck region with a quite unsatisfactory overall 5-year survival rate for patients (50-70%) [32]. Of the cancers with head and neck origin, LSCC along with pharyngeal cancers display significant divergence from oral cavity cancers in terms of clinical outcome characteristics that might be partly due to distinct tumor biology including discrete mutation profiles [33]. Another recent study pointed a considerable dissimilarity in the methylation patterns of genes and allelic imbalances present in oral cancers and cancer of the larynx and pharynx, pointing potential differences during the carcinogenesis processes of tumors originated from distinct parts of the head and neck region [34]. These differences might be speculated to be responsible for altered chemoradiotherapy response, depicting the significance of the investigation of molecular features of each type on their own and also together to be able to figure out the underlying mechanisms more clearly.

Although there have been constant evolution in the surgical and oncological techniques, long term survival of LSCC patients still remains unfavorable [35].

The main factors leading to poor clinical outcome are considered to be frequent locoregional recurrence and metastasis [36] and the lack of reliable prognostic markers make current treatment modalities less effective, which necessitates the urgent identification of vital predictive biomarkers and the related underlying molecular mechanisms associated with acquisition of aggressive phenotype of LSCC. Unraveling those markers will help determination of patients with higher recurrence and metastasis risk after surgery and will give the opportunity to treat them with appropriate adjuvant postoperative treatment strategies.

In this study, we investigated the differential expression of *ING* family members and found *ING3* as a potential biomarker for advanced LSCC. We showed its overexpression in tumor tissues compared to corresponding adjacent normal specimens, pointing its oncogenic potential in laryngeal cancer. Our *in silico* analysis also demonstrated the significant overexpression of *ING3* in late stage and high grade head and neck tumor tissues, which is in parallel with our findings.

The members of *ING* family, comprised of five genes with varying number of isoforms, function as important transducers of cell signaling associated with DNA repair, apoptosis, senescence, cell cycle regulation, histone modifications, and transcriptional regulation through interactions with proteins or DNA [14]. Considering their frequent inactivation in cancer cells, they are mostly recognized as tumor suppressor genes [37] and reduced expression of *ING3* was reported in various cancers including head neck squamous cell carcinoma [38]. However, a recent study reported overexpression of *ING3* in rapidly proliferating tissues with high self-renewal capacity like small intestine and bone marrow, suggesting a potential role for *ING3*

in cellular growth [39]. Similarly, overexpression of *ING3* was found in hypertrophic cardiomyocytes, which lead to an abnormal enlargement of the heart muscle as a result of inactivation of the AMPK and activation of the p38 MAPK signaling pathways [40].

More interestingly, mice models deficient for *ING1* and *ING2* were found to develop spontaneous cancers, whereas, *ING4* deficient mice were reported to be free of spontaneous tumor formation, however, a recent study investigated *ING3* deficiency in mouse models and described homozygous *ING3* deficient mice as embryonic lethal and associated loss of *ING3* expression with growth retardation [22]. This condition was reported to be related to inhibited proliferation and induced apoptosis, which were associated with DNA damage and distortion of PI3K/AKT signaling pathway [41]. Another study demonstrated that *ING3* is overexpressed in prostate cancer cells compared to benign prostate tissues that is correlated with therapeutic resistance and poor clinical outcome [42]. Same study reported that ectopic *ING3* overexpression is sufficient on its own to transform the non-tumorigenic normal human dermal fibroblasts to cancerous state and sets up a gene expression profile that is necessary for cell proliferation [42]. In addition, suppression of *ING3* expression in DU145 prostate cancer cells resulted in inhibition of cellular migration and invasion *in vitro*, ascribing a possible oncogenic potential for *ING3* [15]. Interestingly, increased *ING3* expression was associated with poor prognosis in erythroblast transformation-specific-related gene (ERG) negative prostate cancer patients [15]. Besides, ERG-like 10-gene signature, which includes *ING3* with higher expression in castration-resistant prostate cancer tissues compared to benign or localized prostate cancer specimens, was demonstrated to better estimate patients' clinical outcome than ERG status alone [43]. Another study proposed *ING3* as an androgen receptor (AR) coactivator with the function of AR nuclear translocation that lead to increased proliferation and migration of prostate cancer cells [26].

As to the head and neck squamous cell carcinoma, allelic loss and low *ING3* expression was reported in 2002 in human head and neck cancers including laryngeal cancer. However, considering the low number of laryngeal samples and lack of detection in the protein level, this study does not provide strong clues

about the function of *ING3* [44]. Additional analysis of *ING3* expression in head and neck cancer tissue samples in the mRNA level conducted by the same group demonstrated downregulation of *ING3* expression in cancerous samples compared to normal head and neck tissues. However, of the 71 tissue pairs collected from head and neck cancer patients, only 13 pairs were from laryngeal cancer patients and 7 tumor samples of them were either with high or normal *ING3* expression compared to normal tissues [24]. These findings point the need for further analysis for characterization of *ING3* functions in head and neck cancers with a specific attention on laryngeal cancer. Our results demonstrated that the mean expression of *ING3* is higher in laryngeal tumor tissue samples in both mRNA and protein level compared to normal tissue specimens. On the other hand, it is of importance to mention that the cytoplasmic vs. nuclear localization of *ING3* is also important for its potential to contribute to the carcinogenesis [45]. A recent study reported that cytoplasmic expression of *ING3* was significantly up-regulated in head and neck tumor samples compared to normal tissues, although a decreased nuclear expression of *ING3* was detected [46]. Additionally, high cytoplasmic *ING3* expression was significantly correlated with lymph node metastasis [46]. These findings suggest further detailed analysis of laryngeal tumor samples using immunohistochemistry to delineate into the potential involvement of differential subcellular localization of *ING3* protein during laryngeal carcinogenesis.

Although named as inhibitor of growth, *ING2* was also suggested as an oncoprotein in colon cancer, where its overexpression was detected in cancerous lesions although not supported by further functional tests [47]. Standing as a potential oncogene in laryngeal cancer, *ING3* is the most distinguished member of the *ING* family with the features of less similarity in amino acid sequence to *ING1/2* and *ING4/5* and not localization within the close proximity to telomeric regions in contrast to other members of the family [13]. *ING3* is involved in a histone acetyl transferase complex called NuA4-Tip60 MYST as a core member, which is responsible for H2A and H4 acetylation that is generally linked to transcriptional activation. In contrast to transcriptional repressor properties of *ING1* and *ING2*, *ING3* functions as a transcriptional activa-

tor that might be important for its putative oncogenic function during laryngeal carcinogenesis [13]. Interestingly, we found strong correlation between *ING3* and another component of the NuA4-Tip60 MYST histone acetyl transferase complex, *EPC1*, assigning a potential role for *EPC1* in laryngeal cancer. Suppression of *EPC1* was reported to promote E2F1 mediated apoptotic signaling as a result of DNA damage leading to inhibition of tumor cell motility. On the other hand, *EPC1* in cooperation with *E2F1* induces a metastasis related gene expression fingerprint in especially advanced cancers [48]. Interestingly, in a study where a cancer-relevant subset of more than 500 mutant ESC lines were investigated, a gene signature involving *EPC1* was reported to be associated with response to radiotherapy [49]. In line with these findings, *Epc2* knock down in murine MLL-AF9 AML cells led to induction of apoptosis and loss of stem cell potency of leukemia cells [50]. In addition, side population of human myeloma cell lines with high tumorigenic and self-renewal potential were demonstrated to be enriched with a gene set including *EPC1* [51].

Lastly, as we found overexpression of *ING3* in advanced LSCC cases, many researches reported detection of genomic and transcriptional alterations of *ING* gene family members in advanced cancers. Borkosky *et al.* demonstrated statistically significant relation of frequent deletion of *ING2* locus at 4q35.1 with advanced T stage, proposing the occurrence of *ING2* loss of heterozygosity in advanced stages during HNSCC progression [52]. Similarly, low expression of *ING1* was found in high malignancy grades of astrocytoma [53] and its reduced expression was related to poor prognosis in advanced neuroblastomas [54]. More interestingly, decreased expression of *ING4* in colorectal cancer was reported to contribute to metastasis and poor prognosis via promoting angiogenesis and its expression was negatively correlated with lymph node metastasis, advanced TNM stage and poor overall survival [55]. In line with this report, reduced *ING4* expression was found to be associated with increased stage and histological grade of ovarian cancers and was in negative correlation with micro vessel density [56]. Low *ING4* expression was also correlated with advanced Dukes' stages of colorectal cancer, where *ING4* expression levels were lower in tumor samples of patients with lymphatic metastasis [57].

Here, we reported oncogenic potential of *ING3* in

laryngeal cancer with the significant deregulation observed in advanced cases. We also found that *ING3* expression significantly correlates with its physical interactor *EPC1* with oncogenic potential as well in head and neck cancer. Our results assign a crucial prognostic potential for *ING3* in laryngeal cancer although further clinical studies that are going to be performed in larger cohorts and further *in vitro* and *in vivo* functional tests are required to strengthen its potential as a prognostic marker.

CONCLUSION

Here, we reported oncogenic potential of *ING3* in laryngeal cancer with the significant deregulation observed in advanced cases. We also found that *ING3* expression significantly correlates with its physical interactor *EPC1* with oncogenic potential in head and neck cancer. Our results assign a prognostic potential for *ING3* in laryngeal cancer although further clinical studies that are going to be performed in larger cohorts and further *in vitro* and *in vivo* functional tests are required to strengthen its potential as a prognostic marker.

Authors' Contribution

Study Conception: GK, NB, OFK, AT, AS; Study Design: OFT, AT; Supervision: OFK; Funding: AT; Materials: N/A; Data Collection and/or Processing: NB, GK, RG, AS; Statistical Analysis and/or Data Interpretation: BG, AT, OFK; Literature Review: N/A; Manuscript Preparation: NB, GK, OFK and Critical Review: AT, AS, BG, OFK.

Conflict of interest

Neslisah Barlak, Gulnur Kusdemir, Rasim Gumus, Betul Gundogdu, Abdulkadir Sahin, and Arzu Tatar, declare that they have no conflict of interests. Omer Faruk Karatas holds stocks in EcoTech Biotechnology. The terms of this arrangement have been reviewed and approved by Erzurum Technical University in accordance with its policy on objectivity in research.

Funding

This study was funded by The Scientific Research Projects of Ataturk University under Grant TCD-2020-7724.

REFERENCES

- Genden EM, Ferlito A, Silver CE, Jacobson AS, Werner JA, Suarez C, et al. Evolution of the management of laryngeal cancer. *Oral Oncol* 2007;43:431-9.
- Yang C, Gao S, Zhang H, Xu L, Liu J, Wang M, et al. CD47 is a potential target for the treatment of laryngeal squamous cell carcinoma. *Cell Physiol Biochem* 2016;40:126-36.
- Vassileiou A, Vlastarakos PV, Kandiloros D, Delicha E, Ferikidis E, Tzagaroulakis A, et al. Laryngeal cancer: smoking is not the only risk factor. *B-ENT* 2012;8:273-8.
- Groome PA, O'Sullivan B, Irish JC, Rothwell DM, Schulze K, Warde PR, et al. Management and outcome differences in supraglottic cancer between Ontario, Canada, and the Surveillance, Epidemiology, and End Results areas of the United States. *J Clin Oncol* 2003;21:496-505.
- Luo J, Wu J, Lv K, Li K, Wu J, Wen Y, et al. Analysis of post-surgical health-related quality of life and quality of voice of patients with laryngeal carcinoma. *Medicine (Baltimore)* 2016;95:e2363.
- Liu Y, Su Z, Li G, Yu C, Ren S, Huang D, et al. Increased expression of metadherin protein predicts worse disease-free and overall survival in laryngeal squamous cell carcinoma. *Int J Cancer* 2013;133:671-9.
- Almadori G, Bussu F, Paludetti G. Predictive factors of neck metastases in laryngeal squamous cell carcinoma. Towards an integrated clinico-molecular classification. *Acta Otorhinolaryngol Ital* 2006;26:326-34.
- Zhang X, Xu LS, Wang ZQ, Wang KS, Li N, Cheng ZH, et al. ING4 induces G2/M cell cycle arrest and enhances the chemosensitivity to DNA-damage agents in HepG2 cells. *FEBS Lett* 2004;570:7-12.
- He GH, Helbing CC, Wagner MJ, Sensen CW, Riabowol K. Phylogenetic analysis of the ING family of PHD finger proteins. *Mol Biol Evol* 2005;22:104-16.
- Coles AH, Jones SN. The ING gene family in the regulation of cell growth and tumorigenesis. *J Cell Physiol* 2009;218:45-57.
- Soliman MA, Riabowol K. After a decade of study-ING, a PHD for a versatile family of proteins. *Trends Biochem Sci* 2007;32:509-19.
- Campos EI, Chin MY, Kuo WH, Li G. Biological functions of the ING family tumor suppressors. *Cell Mol Life Sci* 2004;61:2597-613.
- Dantas A, Al Shueili B, Yang Y, Nabbi A, Fink D, Riabowol K. Biological Functions of the ING Proteins. *Cancers (Basel)* 2019;11:1817.
- Gou WF, Yang XF, Shen DF, Zhao S, Sun HZ, Luo JS, et al. Immunohistochemical profile of ING3 protein in normal and cancerous tissues. *Oncol Lett* 2017;13:1631-6.
- Almami A, Hegazy SA, Nabbi A, Alshalalfa M, Salman A, Abou-Ouf H, et al. ING3 is associated with increased cell invasion and lethal outcome in ERG-negative prostate cancer patients. *Tumour Biol* 2016;37:9731-8.
- Smolle E, Fink-Neuboeck N, Lindenmann J, Smolle-Juettner F, Pichler M. The biological and clinical relevance of inhibitor of growth (ING) genes in non-small cell lung cancer. *Cancers (Basel)* 2019;11:1118.
- Du Y, Cheng Y, Su G. The essential role of tumor suppressor gene ING4 in various human cancers and non-neoplastic disorders. *Biosci Rep* 2019;39:BCR20180773.
- Gournay M, Paineau M, Archambeau J, Pedoux R. REGULATINGs in tumors and diseases: Focus on ncRNAs. *Cancer Lett* 2019;447:66-74.
- Li X, Kikuchi K, Takano Y. ING genes work as tumor suppressor genes in the carcinogenesis of head and neck squamous cell carcinoma. *J Oncol* 2011;2011:963614.
- Yang C, Gao J, Yan N, Wu B, Ren Y, Li H, et al. Propofol inhibits the growth and survival of gastric cancer cells in vitro through the upregulation of ING3. *Oncol Rep* 2017;37:587-93.
- Gou WF, Sun HZ, Zhao S, Niu ZF, Mao XY, Takano Y, et al. Downregulated inhibitor of growth 3 (ING3) expression during colorectal carcinogenesis. *Indian J Med Res* 2014;139:561-7.
- Fink D, Yau T, Nabbi A, Wagner B, Wagner C, Hu SM, et al. Loss of Ing3 expression results in growth retardation and embryonic death. *Cancers (Basel)* 2019;12:180.
- Nagashima M, Shiseki M, Pedoux RM, Okamura S, Kitahama-Shiseki M, Miura K, et al. A novel PHD-finger motif protein, p47ING3, modulates p53-mediated transcription, cell cycle control, and apoptosis. *Oncogene* 2003;22:343-50.
- Gunduz M, Beder LB, Gunduz E, Nagatsuka H, Fukushima K, Pehlivan D, et al. Downregulation of ING3 mRNA expression predicts poor prognosis in head and neck cancer. *Cancer Sci* 2008;99:531-8.
- Lu M, Chen F, Wang Q, Wang K, Pan Q, Zhang X. Downregulation of inhibitor of growth 3 is correlated with tumorigenesis and progression of hepatocellular carcinoma. *Oncol Lett* 2012;4:47-52.
- Nabbi A, McClurg UL, Thalappilly S, Almami A, Mobahat M, Bismar TA, et al. ING3 promotes prostate cancer growth by activating the androgen receptor. *BMC Med* 2017;15:103.
- Ngollo M, Lebert A, Daures M, Judes G, Rifai K, Dubois L, et al. Global analysis of H3K27me3 as an epigenetic marker in prostate cancer progression. *BMC Cancer* 2017;17:261.
- Cerami E, Gao J, Dogrusoz U, Gross BE, Sumer SO, Aksoy BA, et al. The cBio cancer genomics portal: an open platform for exploring multidimensional cancer genomics data. *Cancer Discov* 2012;2:401-4.
- Chandrashekar DS, Bashel B, Balasubramanya SAH, Creighton C, Ponce-Rodriguez I, Chakravarthi BVSK, et al. UALCAN: a portal for facilitating tumor subgroup gene expression and survival analyses. *Neoplasia* 2017;19:649-58.
- Rhodes DR, Yu J, Shanker K, Deshpande N, Varambally R, Ghosh D, et al. ONCOMINE: a cancer microarray database and integrated data-mining platform. *Neoplasia* 2004;6:1-6.
- Jensen LJ, Kuhn M, Stark M, Chaffron S, Creevey C, Muller J, et al. STRING 8--a global view on proteins and their functional interactions in 630 organisms. *Nucleic Acids Res.* 2009;37(Database issue):D412-6.
- Obid R, Redlich M, Tomeh C. The Treatment of Laryngeal Cancer. *Oral Maxillofac Surg Clin North Am* 2019;31:1-11.
- Vossen DM, Verhagen CVM, Verheij M, Wessels LFA, Vens

- C, van den Brekel MWM. Comparative genomic analysis of oral versus laryngeal and pharyngeal cancer. *Oral Oncol* 2018;81:35-44.
34. Shiga K, Ogawa T, Katagiri K, Yoshida F, Tateda M, Matsuura K, et al. Differences between oral cancer and cancers of the pharynx and larynx on a molecular level. *Oncol Lett* 2012;3:238-43.
35. Yuan H, Jiang H, Wang Y, Dong Y. Increased expression of lncRNA FTH1P3 predicts a poor prognosis and promotes aggressive phenotypes of laryngeal squamous cell carcinoma. *Biosci Rep* 2019;39:BSR20181644.
36. Prabhu RS, Hanasoge S, Magliocca KR, Hall WA, Chen SA, Higgins KA, et al. Lymph node ratio influence on risk of head and neck cancer locoregional recurrence after initial surgical resection: implications for adjuvant therapy. *Head Neck* 2015;37:777-82.
37. Ludwig S, Klitzsch A, Baniahmad A. The ING tumor suppressors in cellular senescence and chromatin. *Cell Biosci* 2011;1:25.
38. Zhang R, Jin J, Shi J, Hou Y. INGs are potential drug targets for cancer. *J Cancer Res Clin Oncol* 2017;143:189-97.
39. Nabbi A, Almami A, Thakur S, Suzuki K, Boland D, Bismar TA, et al. ING3 protein expression profiling in normal human tissues suggest its role in cellular growth and self-renewal. *Eur J Cell Biol* 2015;94:214-22.
40. Wang J, Liu Z, Feng X, Gao S, Xu S, Liu P. Tumor suppressor gene ING3 induces cardiomyocyte hypertrophy via inhibition of AMPK and activation of p38 MAPK signaling. *Arch Biochem Biophys* 2014;562:22-30.
41. Mouche A, Archambeau J, Ricordel C, Chaillot L, Bigot N, Guillaudeux T, et al. ING3 is required for ATM signaling and DNA repair in response to DNA double strand breaks. *Cell Death Differ* 2019;26:2344-57.
42. McClurg UL, Nabbi A, Ricordel C, Korolchuk S, McCracken S, Heer R, et al. Human ex vivo prostate tissue model system identifies ING3 as an oncoprotein. *Br J Cancer* 2018;118:713-26.
43. Bismar TA, Alshalalfa M, Petersen LF, Teng LH, Gerke T, Bakkar A, et al. Interrogation of ERG gene rearrangements in prostate cancer identifies a prognostic 10-gene signature with relevant implication to patients' clinical outcome. *BJU Int* 2014;113:309-19.
44. Gunduz M, Ouchida M, Fukushima K, Ito S, Jitsumori Y, Nakashima T, et al. Allelic loss and reduced expression of the ING3, a candidate tumor suppressor gene at 7q31, in human head and neck cancers. *Oncogene* 2002;21:4462-70.
45. Zhou R, Rotte A, Li G, Chen X, Chen G, Bhandaru M. Nuclear localization of ING3 is required to suppress melanoma cell migration, invasion and angiogenesis. *Biochem Biophys Res Commun* 2020;527:418-24.
46. Li X, Zhang Q, Zhang M, Luo Y, Fu Y. Downregulation of nuclear ING3 expression and translocation to cytoplasm promotes tumorigenesis and progression in head and neck squamous cell carcinoma (HNSCC). *Histol Histopathol* 2020;35:681-90.
47. Kumamoto K, Fujita K, Kurotani R, Saito M, Unoki M, Hagiwara N, et al. ING2 is upregulated in colon cancer and increases invasion by enhanced MMP13 expression. *Int J Cancer* 2009;125:1306-15.
48. Wang Y, Alla V, Goody D, Gupta SK, Spitschak A, Wolkenhauer O, et al. Epigenetic factor EPC1 is a master regulator of DNA damage response by interacting with E2F1 to silence death and activate metastasis-related gene signatures. *Nucleic Acids Res* 2016;44:117-33.
49. Loesch K, Galaviz S, Hamoui Z, Clanton R, Akabani G, Deveau M, et al. Functional genomics screening utilizing mutant mouse embryonic stem cells identifies novel radiation-response genes. *PLoS One* 2015;10:e0120534.
50. Huang X, Spencer GJ, Lynch JT, Ciceri F, Somerville TD, Somerville TC. Enhancers of Polycomb EPC1 and EPC2 sustain the oncogenic potential of MLL leukemia stem cells. *Leukemia* 2014;28:1081-91.
51. Nara M, Teshima K, Watanabe A, Ito M, Iwamoto K, Kitabayashi A, et al. Bortezomib reduces the tumorigenicity of multiple myeloma via downregulation of upregulated targets in clonogenic side population cells. *PLoS One* 2013;8:e56954.
52. Borkosky SS, Gunduz M, Nagatsuka H, Beder LB, Gunduz E, Sheikh Ali MAL, et al. Frequent deletion of ING2 locus at 4q35.1 associates with advanced tumor stage in head and neck squamous cell carcinoma. *J Cancer Res Clin Oncol* 2009;135:703-13.
53. Tallen G, Kaiser I, Krabbe S, Lass U, Hartmann C, Henze G, et al. No ING1 mutations in human brain tumours but reduced expression in high malignancy grades of astrocytoma. *Int J Cancer* 2004;109:476-9.
54. Takahashi M, Ozaki T, Todo S, Nakagawara A. Decreased expression of the candidate tumor suppressor gene ING1 is associated with poor prognosis in advanced neuroblastomas. *Oncol Rep* 2004;12:811-6.
55. Chen Y, Huang Y, Hou P, Zhang Z, Zhang Y, Wang W, et al. ING4 suppresses tumor angiogenesis and functions as a prognostic marker in human colorectal cancer. *Oncotarget* 2016;7:79017-31.
56. Liu Y, Yu L, Wang Y, Zhang Y, Zhang G. Expression of tumor suppressor gene ING4 in ovarian carcinoma is correlated with microvessel density. *J Cancer Res Clin Oncol* 2012;138:647-55.
57. You Q, Wang XS, Fu SB, Jin XM. Downregulated expression of inhibitor of growth 4 (ING4) in advanced colorectal cancers: a non-randomized experimental study. *Pathol Oncol Res* 2011;17:473-7.



This is an open access article distributed under the terms of [Creative Commons Attribution-NonCommercial-NoDerivatives 4.0 International License](https://creativecommons.org/licenses/by-nc-nd/4.0/).

Evaluation of hematopoietic - and neurologic-expressed sequence 1-like (HN1L) protein levels in tissue and plasma of breast cancer patients

Elif Erturk¹, Mehmet Sarimahmut², Mustafa Sehsuvar Gokgoz³, Sahsine Tolunay⁴

¹Vocational School of Health Services, Bursa Uludag University, Bursa, Turkey; ²Department of Biology, Bursa Uludag University, Faculty of Science and Arts, Bursa, Turkey; ³Department of General Surgery, Bursa Uludag University, Faculty of Medicine, Bursa, Turkey; ⁴Department of Medical Pathology, Bursa Uludag University, Faculty of Medicine, Bursa, Turkey

ABSTRACT

Objectives: Breast cancer is the second leading cause of cancer deaths among women. Therefore, there is a need for new approaches that increase the success of treatment in breast cancer. Cancer stem cells (CSCs) are associated with treatment resistance and metastasis, which are important problems in cancer treatment including breast tumors. In this study, the Hematopoietic- and neurologic-expressed sequence 1-like (HN1L), also known as Jupiter microtubule associated homolog 2 (JPT2) protein levels which is involved in the self-renewal of CSCs were evaluated in common and rare breast tumor types.

Methods: In this context, HN1L protein levels were measured from plasma of 17 patients and from tumor and normal tissues of 9 patients by enzyme linked immunosorbent assay method.

Results: Mean HN1L levels were measured as 1.63 ± 0.88 ng/mL in plasma samples, 2.18 ± 0.75 ng/mL in tumor tissue samples and 2.71 ± 0.88 ng/mL in normal tissue samples. A significant difference was observed between mean HN1L levels in plasma and normal tissue ($p < 0.05$). Correlation of HN1L protein levels with clinicopathological characteristics were analyzed. Accordingly, HN1L levels were positively correlated with tumor size and invasion status ($r = 0.425$; $p < 0.05$ and $r = 0.449$; $p < 0.05$, respectively).

Conclusions: We believe that the importance of HN1L in management of breast cancers will be demonstrated more thoroughly when further studies are conducted with increased number of patients.

Keywords: HN1L, JPT2, breast cancer, cancer stem cell

Cancer is one of the leading causes of mortality and morbidity all over the world and is accepted as one of the most common diseases in the world after cardiovascular diseases [1]. According to the GLOBOCAN database, part of the International Agency for Research on Cancer (IARC), there were 19.3 million new cancer cases and 10.0 million cancer deaths in 2020. In the same year, the most frequently diagnosed

cancer in men were lung (25.8%), followed by prostate (14.6%) and colorectal cancer (9%). In women, breast cancer (23.9%) is the leading cause of death, followed by thyroid (10.9%) and colorectal cancer (9.1%). Breast cancer is the most frequently diagnosed cancer type in the world and is estimated to be the leading cause of cancer death in women worldwide. The latest data show that there were 2.26 million



e-ISSN: 2149-3189



Received: July 27, 2022; Accepted: October 19, 2022 Published Online: March 10, 2023

How to cite this article: Erturk E, Sarimahmut M, Gokgoz MS, Tolunay S. Evaluation of hematopoietic- and neurologic-expressed sequence 1-like (HN1L) protein levels in tissue and plasma of breast cancer patients. *Eur Res J* 2023;9(3):529-535. DOI: 10.18621/eurj.1149697

Address for correspondence: Mehmet Sarimahmut, PhD., Bursa Uludag University, Faculty of Science and Arts, Department of Biology, 16059, Bursa, Turkey. E-mail: msarimahmut@uludag.edu.tr; Phone: +90 224 294 17 53

©Copyright © 2023 by Prusa Medical Publishing
Available at <http://dergipark.org.tr/eurj>
info@prusamp.com

cases of breast cancer in 2020 [2]. With the increase in targeted treatment options in recent years, the need for more effective management of breast cancer treatment has also increased. Research and clinical use of new molecular biomarker candidates will make significant contributions to the treatment of the disease.

Hematopoietic - and neurologic-expressed sequence 1-like (HN1L), also known as Jupiter microtubule associated homolog 2 (JPT2), is a protein with very limited information and is thought to play a role in embryo development [3]. HN1L gene is located on chromosome 16p13.3 that encodes a 20-kDa protein [3]. HN1L protein, which is localized in the nucleus and cytoplasm of the cell, has been found in liver, kidney, uterus, testis and prostate tissues [3]. There are a limited number of studies revealing the role of HN1L protein in various types of cancer. It has been reported that the HN1L gene is altered in a quarter of breast cancer cases and is correlated with low overall survival in triple negative breast cancer (TNBC) cases [4]. On the other hand, it was revealed that the number of breast cancer stem cells has decreased and sensitivity to chemotherapy was improved by silencing HN1L [4]. HN1L plays a role in the self-renewal processes of cancer stem cells (CSCs). Due to the high frequency of mutations in this gene, it has been determined that measuring mutant HN1L gene fragments in the bloodstream can exhibit tumor burden and be effective in tracking progression [5]. In another study, it was shown that HN1L is highly expressed in breast cancer tissues, positively correlated with metastasis in breast cancer patients, and significantly inhibited invasion and metastasis when silenced [6]. In terms of its molecular interactions, the HN1L protein has been associated with the signal transducer and activator of transcription (STAT) pathway and has been reported to upregulate the expression of high-mobility group protein 1 (HMGB1) protein, which plays a key role in breast cancer invasion and metastasis [4, 6].

In the current study, it is aimed to investigate the potential of HN1L as a promising biomarker candidate in breast cancer.

METHODS

Patients and Clinical Characteristics

Nine fresh tissue (tumor and normal) samples and 17

plasma samples were collected from breast cancer patients who were admitted to Breast Surgery Department. The study was approved by the local Clinical Research Ethics Committee (2021-10/44) and conducted in accordance with Helsinki Declaration. Informed consent was obtained from all patients. Clinicopathological characteristics of the patients were obtained from Breast Surgery and Medical Pathology Departments. Histological and molecular subtypes of breast cancer were defined by respective clinical departments.

HN1L Enzyme Linked Immunosorbent Assay

HN1L protein levels were measured from plasma of 17 patients and from tumor and normal tissues of 9 patients by Enzyme linked immunosorbent assay (ELISA) method. Whole blood samples collected into EDTA-coated tubes from patients were centrifuged at $2000 \times g$ for 10 min (Nüve NF800R, Turkey). Then, 1 mL aliquots of the supernatant were transferred into cryovials for long term storage. Tissue samples were cut into thin pieces with a scalpel and subsequently incubated with RIPA lysis buffer supplemented with protease inhibitors and sodium vanadate in a microcentrifuge tube for 20 min. Tumor and normal tissues were homogenized on ice for 1 min at 900 rpm (Schuett Homgenplus, Germany). The homogenized samples were centrifuged at $10,000 \times g$ for 10 min at 4°C (Nüve NF800R, Turkey). Clean supernatants were transferred to a new 1.5 ml microcentrifuge tube and stored at 4°C to determine protein concentration and perform ELISA. Bicinchoninic acid assay was utilized to evaluate total protein concentration as described by Smith *et al.* [7]. All accumulated plasma and tissue samples were stored at -80°C until further use.

For ELISA, HN1L protein levels were evaluated according to the manufacturer's instructions (Abxexa, Cambridge, United Kingdom). Briefly, standard solutions, reagents and samples were prepared. Equal amounts of protein at 100 μL volume were loaded into each well of a 96-well plate. Also, 100 μL of standard solutions were pipetted in order to generate a calibration curve. After different incubation times and washing steps, 100 μL of biotin conjugated detection antibody, 100 μL of HRP (horseradish peroxidase) conjugated detection antibody, 90 μL of TMB (3,3',5,5'-Tetramethylbenzidine) substrate solution and

Table 1. Clinicopathological characteristics of patients from plasma and tumor tissue group

Characteristics	Plasma (n = 17)	Tumor tissue (n = 9)	p value
Gender, n (%)			
Female	17 (100.0)	8 (88.9)	0.346 ^a
Male	-	1 (11.1)	
Age (years), mean ± SD	57.47 ± 12.28	55.44 ± 15.74	0.742 ^b
Histological subtype, n (%)			
Invasive ductal	16 (94.1)	1 (11.1)	0.001^c
Invasive lobular	-	2 (22.2)	
Mucinous	-	1 (11.1)	
Tubular	-	1 (11.1)	
Malignant phyllodes tumor	-	1 (11.1)	
Mixed type	1 (5.9)	3 (33.3)	
Molecular subtype, n (%)			
Luminal A	7 (41.2)	8 (88.9)	0.024^a
Luminal B	10 (58.8)	1 (11.1)	
ER positive, n (%)	17 (100.0)	8 (88.9)	0.346 ^a
PR positive, n (%)	13 (76.5)	7 (77.8)	0.668 ^a
HER2 positive, n (%)	2 (11.8)	-	0.453 ^a
Tumor localization, n (%)			
Right	9 (52.9)	5 (55.6)	0.613 ^a
Left	8 (47.1)	4 (44.4)	
Tumor stage, n (%)			
I	1 (5.9)	5 (55.6)	
II	13 (76.5)	3 (33.3)	0.017^c
III	3 (17.6)	1 (11.1)	
BRCA negative, n (%)	1 (7.1)	-	0.609 ^a
P53 positive, n (%)	3 (17.6)	-	0.262 ^a
P63 positive, n (%)	8 (47.1)	3 (33.3)	0.402 ^a
Calponin positive, n (%)	8 (47.1)	3 (33.3)	0.402 ^a
E-Cadherin positive, n (%)	17 (100.0)	3 (33.3)	0.000 ^a
CK5/6 positive, n (%)	10 (66.7)	3 (33.3)	0.122 ^a
In situ component, n (%)			
No	6 (35.3)	4 (44.4)	
Under 25%	11 (64.7)	4 (44.4)	0.261 ^c
Over 25%	-	1 (11.1)	
Necrosis, n (%)	2 (11.8)	1 (11.1)	0.732 ^a
Lymphatic invasion, n (%)	3 (17.6)	-	0.262 ^a
Perineural invasion, n (%)	6 (35.3)	-	0.054 ^a
Vascular invasion, n (%)	1 (5.9)	-	0.654 ^a
Microcalcification, n (%)	7 (41.2)	3 (33.3)	0.517 ^a
HN1L (ng/mL), mean ± SD	1.63 ± 0.88	2.18 ± 0.75	0.124 ^b
Tumor size, mean ± SD	2.05 ± 1.26	2.66 ± 1.57	0.302 ^b
Metastasis status	0.65 ± 0.79	0.67 ± 1.41	0.450 ^b
BRH, mean ± SD	1.35 ± 1.46	1.11 ± 0.78	0.587 ^b
Ki-67, mean ± SD	155.06 ± 140.31	105.56 ± 124.13	0.383 ^b

ER = estrogen receptor, PR = progesterone receptor, HER2 = human epidermal growth factor receptor 2, BRCA = breast cancer susceptibility protein, CK = cytokeratin, BRH = benign reactive hyperplasia, SD = Standard Deviation

^aFischer's Exact Test, ^bIndependent Samples T-Test, ^cLikelihood Ratio

50 μ L of stop solution were added, respectively. Finally, absorbance was measured in a spectrophotometer (EL \times 800, BioTek Instruments, Inc., Winooski, VT, USA) at 450 nm. HN1L protein concentration was expressed as ng/mL.

Statistical Analysis

Nominal and ordinal parameters were described as frequencies; whereas, scale parameters were described as mean and standard deviations. Fischer's Exact Test, Chi-Square and Likelihood ratio tests were used to indicate differences between categorical variables. Kolmogorov Smirnov test was used to analyze normality of scale parameters. Independent Samples t-test and One Way ANOVA were used to detect differences of normally distributed scale parameters. Spearman's rho correlation and ROC analysis were implemented for relational analysis. SPSS 17.0 for Windows was used, and 95% Confidence Interval was mentioned at 0.05 significance level.

RESULTS

Management of breast cancer should be improved in order to accomplish better outcomes in clinical practice. CSC hypothesis posits that cells with stem cell like properties take part in processes such as therapy resistance and recurrence; which in turn, lowers the effectiveness of treatment and hinders therapy success [8, 9]. A better understanding of proteins associated with CSCs could shed light on how to overcome the important obstacles in breast cancer treatment. Thus, we have investigated a CSC associated protein, HN1L, to evaluate its levels in plasma and tumor tissue of breast cancer patients and its correlation with clinical parameters. To our knowledge, this is the first study that aims to determine the levels of HN1L protein

from the circulation with any type of cancer including breast carcinomas.

The present study included 35 samples from 26 breast cancer patients. The samples were divided into two groups; namely plasma and tumor tissue, to describe the origin of sample. Clinicopathological characteristics of patients is shown in Table 1. Histological subtype distribution in plasma samples was invasive ductal (n = 16) and mixed carcinoma (n = 1); whereas the histological subtype distribution of tissue samples was invasive ductal (n = 1), invasive lobular (n = 2), mucinous (n = 1), tubular (n = 1), mixed (n = 3) carcinoma, and malignant phyllodes tumor (n = 1). Mucinous, tubular and mixed carcinomas and malignant phyllodes tumors are among rare type of tumors that are represented with a frequency of less than 5% within breast carcinomas [10]. There is also a tumor sample collected from a male breast cancer patient which is a rare case as well, with less than 1% frequency of all breast cancer cases [11]. Considering the molecular subtype distribution, plasma and tissue samples of luminal subtypes were selected and included in the study, which in turn contributed to the homogeneity of the study groups.

Circulating HN1L protein levels detected from plasma and levels of HN1L protein measured from homogenized tumor and normal tissue of breast cancer patients are shown in Table 2. Mean HN1L concentration values were ranked from lowest to highest as plasma, tumor tissue and normal tissue. Comparison of HN1L protein levels between plasma, tumor and normal tissue groups demonstrated that HN1L protein levels differ significantly between normal tissue and plasma groups ($p < 0.05$). However, difference in mean HN1L protein levels was statistically insignificant both between tumor and normal tissue groups as well as between tumor tissue and plasma groups ($p > 0.05$). Therefore, the absence of significant difference

Table 2. Comparison of HN1L protein levels between plasma, normal and tumor tissue groups

	Plasma (n = 17)	Tumor tissue (n = 9)	Normal tissue (n = 9)	Total	<i>p</i> value
HN1L (ng/mL) mean \pm SD	1.63 \pm 0.88 ^a	2.18 \pm 0.75	2.71 \pm 0.88 ^a	2.05 \pm 0.94	0.014^b

^aTukey's Post hoc, plasma and normal tissue (mean difference: -1.08; $p = 0.011$)

^bOne Way ANOVA

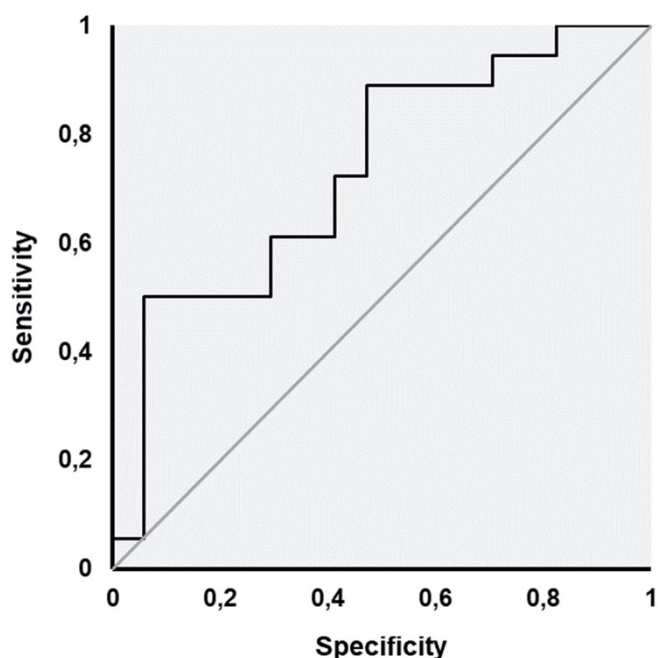


Fig. 1. ROC analysis results for predictive value of HN1L for plasma. According to the results of the ROC analysis AUC was 73.2% and was found to be statistically significant ($p < 0.05$).

between plasma and tumor tissue HN1L protein levels suggests that evaluation of plasma HN1L protein levels may prove to be useful as a surrogate of tumor HN1L protein levels. We have further examined the difference between plasma and normal tissue HN1L levels in detail by analyzing receiver operating characteristic (ROC) curve to determine the discriminatory accuracy (Fig. 1). Predictive value of HN1L for plasma was 73.2% with statistically significant area under curve ($p < 0.05$). Sensitivity for 1.55 cut off level was 52.9% and specificity was 88.9%. For 2.08 cut off level of HN1L, sensitivity was 70.6% and specificity was 61.1%. Overall, this model indicates a good discriminatory ability for the prediction of HN1L concentration from plasma and normal tissue. Then, the correlation between HN1L protein levels and clinical parameters were explored. Spearman’s correlation analysis revealed that tumor size ($r = 0.449$; $p < 0.05$) and lymphatic invasion ($r = 0.425$; $p < 0.05$) had significant positive correlation with HN1L protein levels (Table 3). However, there was no significant correlation with age, presence of metastasis or any of the assessed pathological parameters. This finding suggests that HN1L protein levels might accurately reflect the tumor size and lymphatic invasion in breast cancer.

Table 3. Spearman’s rho correlation analysis results between HN1L protein levels and clinicopathological characteristics

Characteristics	r	p value
Sample type	0.286	0.157
Age	0.162	0.430
Histological subtype	0.134	0.514
Molecular subtype	0.057	0.782
ER status	-0.280	0.166
PR status	-0.073	0.723
HER2 status	0.184	0.379
Tumor localization	0.010	0.960
Tumor stage	-0.027	0.897
BRCA status	-0.354	0.098
P53 status	0.120	0.558
P63 status	-0.151	0.463
Calponin status	-0.151	0.463
E-Cadherin status	-0.280	0.166
CK5/6 status	-0.151	0.481
In situ component	-0.106	0.606
Necrosis	-0.088	0.668
Lymphatic invasion	0.425*	0.030
Perineural invasion	0.110	0.594
Vascular invasion	0.200	0.327
Microcalcification	-0.179	0.381
Tumor size	0.449*	0.024
Metastasis status	-0.093	0.652
BRH	-0.119	0.563
Ki-67	0.200	0.326

ER = estrogen receptor, PR = progesterone receptor, HER2 = human epidermal growth factor receptor 2, BRCA = breast cancer susceptibility protein, CK = cytokeratin, BRH = benign reactive hyperplasia

DISCUSSION

The importance of guiding therapeutic strategy and the management of patients has increased dramatically in recent years with the expansion of available treatment options such as targeted therapies and immunotherapy [12]. In this respect, especially the utilization of circulating tumor DNA analyses into the routine clinical practice has the potential to be an extremely effective

tool in the management of cancer therapy [13-15]. Furthermore, the analysis circulating proteins as a minimally invasive and an inexpensive tool in determination of disease risk, treatment adjustment, prognostication and disease progression monitoring has been a trending research area [16]. In fact, new breakthroughs in early detection of cancer has been achieved with the adoption of both circulating nucleic acids and proteins as new instruments in this field [16-18]. In this regard, investigation of circulating levels of CSC associated proteins might contribute to the improvement of clinical outcome in breast cancer.

There is a limited number of studies regarding the analysis of circulating levels of CSC associated cellular proteins in many types of malignancies including breast cancer. Mirzaei *et al.* [19] has assessed the levels of double cortin like kinase 1 (DCLK1) extracted from peripheral blood mononuclear cells of patients diagnosed with colorectal cancer and healthy individuals who displayed significantly different levels of the protein by ELISA method. Later, Christman *et al.* [20] utilized the same protein and showed that DCLK1 may have potential as a circulating biomarker for therapy response in esophageal adenocarcinoma. Another example is Glutaredoxin3 (GLRX3), a secretory protein that is upregulated in pancreatic ductal adenocarcinoma CSC enriched spheres. GLRX3 protein levels were measured by ELISA from the plasma of both healthy individuals and pancreatic cancer patients which revealed that there was a significant difference between the two groups, a finding that may have implications in diagnosis of pancreatic cancer. Majority of the previous studies on the role of HN1L in different types of cancer demonstrate that overexpression of this protein promotes cell migration, invasion and metastasis in in vitro and in vivo models and is an indication of worse disease free survival in non-small cell lung cancer patients and poor prognosis in hepatocellular carcinoma patients [21, 22]. Furthermore, silencing HN1L expression lowered the capability of breast CSCs to initiate tumor and inhibited tumor formation in vivo in mice injected with prostate cancer cells [4, 21]. According to immunohistochemistry analysis with tumor and non-tumor tissue samples from breast cancer and esophagogastric junction adenocarcinoma patients, an overexpression of HN1L was reported in tumor tissues compared to adjacent normal tissue of

the patients [6, 23]. Our findings however did not confirm this data, most probably due to low number of tumor samples and partly because of diverse histopathological background of the collected tumor samples.

To the best of our knowledge, there is only a couple of studies investigating the plasma levels of HN1L in cancer patients which were conducted by our research group. In these studies, the mean HN1L plasma levels were measured as 1.05, 1.70, 0.95 and 1.03 ng/mL from 29 luminal A, luminal B, triple negative and HER2+ subtypes, respectively [24, 25]. These mean values are comparable with our current findings. Moreover, in the previous study, HN1L levels in luminal subtype samples were in positive correlation with lymphatic invasion and tumor size which is in agreement with our findings considering that sample group was selected from luminal subtype of breast cancer cases as well [25]. The fact that the results obtained are mutually supportive strengthens our study. The significance of correlation between lymphatic invasion and tumor size with HN1L levels may be associated with the aggressiveness of the tumor. Therefore, this result might gain importance in the future for the follow-up of the disease.

CONCLUSION

To conclude, we have determined the HN1L protein levels in plasma, tumor and normal tissues in breast cancer patients and shown that these levels did not differ significantly between plasma and tumor tissue. We have found out that HN1L protein levels were positively correlated with tumor size and lymphatic invasion. Our analyses also included cases of rare breast cancers with different histological background. Future studies with a higher number of cases would ensure a more comprehensive investigation of the relationship between the change in HN1L protein levels and clinical parameters.

Authors' Contribution

Study Conception: EE, MS, MSG; Study Design: EE, MS, ST; Supervision: EE, MS, MSG, ST; Funding: MS; Materials: MSG, EE, MS; Data Collection and/or Processing: ST, EE, MS; Statistical Analysis

and/or Data Interpretation: EE, MS; Literature Review: EE, MS; Manuscript Preparation: EE, MS and Critical Review: EE, MS.

Conflict of interest

The authors disclosed no conflict of interest during the preparation or publication of this manuscript.

Financing

This work was financially supported by Bursa Uludag University Scientific Research Coordination Unit (Project No: FHIZ-2021-602).

Acknowledgments

The authors would like to thank Prof. Ferda Ari for her support and Ahmet Sari Mahmout for English editing and proofreading of the manuscript.

REFERENCES

- Ames BN, Gold LS, Willett WC. The causes and prevention of cancer. *Proc Natl Acad Sci U S A* 1995;92:5258-65.
- Wilkinson L, Gathani T. Understanding breast cancer as a global health concern. *Br J Radiol* 2022;95:20211033.
- Zhou G, Wang J, Zhang Y, Zhong C, Ni J, Wang L, et al. Cloning, expression and subcellular localization of HN1 and HN1L genes, as well as characterization of their orthologs, defining an evolutionarily conserved gene family. *Gene* 2004;331:115-23.
- Liu Y, Choi DS, Sheng J, Ensor JE, Liang DH, Rodriguez-Aguayo C, et al. HN1L promotes triple-negative breast cancer stem cells through LEPR-STAT3 pathway. *Stem Cell Rep* 2018;10: 212-27.
- Liu ZB, Ezzedine NE, Eterovic AK, Ensor JE, Huang HJ, Albanell J, et al. Detection of breast cancer stem cell gene mutations in circulating free DNA during the evolution of metastases. *Breast Cancer Res Treat* 2019;178:251-61.
- Jiao D, Zhang J, Chen P, Guo X, Qiao J, Zhu J, et al. HN1L promotes migration and invasion of breast cancer by up-regulating the expression of HMGB1. *J Cell Mol Med* 2021;25:397-410.
- Smith PE, Krohn RI, Hermanson GT, Mallia AK, Gartner FH, Provenzano M, et al. Measurement of protein using bicinchoninic acid. *Anal Biochem* 1985;150:76-85.
- Kakarala M, Wicha MS. Implications of the cancer stem-cell hypothesis for breast cancer prevention and therapy. *J Clin Oncol* 2008;26:2813-20.
- Bai X, Ni J, Beretov J, Graham P, Li Y. Cancer stem cell in breast cancer therapeutic resistance. *Cancer Treat Rev* 2018;69:152-63.
- İlvan Ş. Meme Karsinomu Patolojisi. *İÜ Cerrahpaşa Tıp Fakültesi Sürekli Tıp Eğitimi Etkinlikleri* 2006;54:65-71.
- Yousef AJA. Male breast cancer: epidemiology and risk factors. *Semin Oncol* 2017;44:267-72.
- Markou A, Tzanikou E, Lianidou E. The potential of liquid biopsy in the management of cancer patients. *Semin Cancer Biol* 2022;84:69-79.
- Thomas ML, Marcato P. Epigenetic modifications as biomarkers of tumor development, therapy response, and recurrence across the Cancer Care Continuum. *Cancers (Basel)* 2018;10:101.
- Asante DB, Calapre L, Ziman M, Meniawy TM, Gray ES. Liquid biopsy in ovarian cancer using circulating tumor DNA and cells: ready for prime time? *Cancer Lett* 2020;468:59-71.
- Cescon DW, Bratman SV, Chan SM, Siu LL. Circulating tumor DNA and liquid biopsy in oncology. *Nat Cancer* 2020;1:276-90.
- Veysière H, Bidet Y, Penault-Llorca F, Radosevic-Robin N, Durando X. Circulating proteins as predictive and prognostic biomarkers in breast cancer. *Clin Proteomics* 2022;19:25.
- Aravanis AM, Lee M, Klausner RD. Next-generation sequencing of circulating tumor DNA for early cancer detection. *Cell* 2017;168:571-4.
- Campos-Carrillo A, Weitzel JN, Sahoo P, Rockne R, Mokhnatkin JV, Murtaza M, et al. Circulating tumor DNA as an early cancer detection tool. *Pharmacol Ther* 2020;207:107458.
- Mirzaei A, Madjd Z, Kadijani AA, Tavakoli-Yaraki M, Modarresi MH, Verdi J, et al. Evaluation of circulating cellular DCLK1 protein, as the most promising colorectal cancer stem cell marker, using immunoassay based methods. *Cancer Biomark* 2016;17:301-11.
- Christman EM, Chandrakesan P, Weygant N, Maple JT, Tierney WM, Vega KJ, et al. Elevated doublecortin-like kinase 1 serum levels revert to baseline after therapy in early stage esophageal adenocarcinoma. *Biomark Res* 2019;7:5.
- Nong S, Wang Z, Wei Z, Ma L, Guan Y, Ni J. HN1L promotes stem cell-like properties by regulating TGF- β signaling pathway through targeting FOXP2 in prostate cancer. *Cell Biol Int* 2022;46:83-95.
- Li L, Zheng YL, Jiang C, Fang S, Zeng TT, Zhu YH, et al. HN1L-mediated transcriptional axis AP-2 γ /METTL13/TCF3-ZEB1 drives tumor growth and metastasis in hepatocellular carcinoma. *Cell Death Differ* 2019;26:2268-83.
- Wang ZY, Xiao W, Jiang YZ, Dong W, Zhang XW, Zhang L. HN1L promotes invasion and metastasis of the esophagogastric junction adenocarcinoma. *Thorac Cancer* 2021;12:650-8.
- Ertürk E, Sarımahmut M, Gökgöz MŞ. [Evaluation of the effectiveness of HN1L as a novel biomarker candidate in aggressive breast tumors]. *Proceedings of the 7th International Medicine and Health Sciences Researches Congress (UTSAK) 2021*;216-7. [Oral Presentation in Turkish]
- Sarımahmut M, Ertürk E, Gökgöz MŞ. Determination of the Potential of HN1L as a Biomarker in Luminal Type Breast Cancers. *Proceedings of the VII. International Hippocrates Congress On Medical and Health Sciences 2021*;16. [Oral Presentation in Turkish]



This is an open access article distributed under the terms of [Creative Commons Attribution-NonCommercial-NoDerivatives 4.0 International License](https://creativecommons.org/licenses/by-nc-nd/4.0/).

Information, attitudes and behaviors of mothers about breastfeeding behavior during the COVID-19 pandemic process

Mehmet Emin Parlak¹, Osman Küçükkeleşçe², Dilek Ener³, Erdoğan Öz², Volkan Bayar⁴

¹Department of Child Health and Diseases, Kahta State Hospital, Adıyaman, Turkey; ²Adıyaman Province Health Directorate, Adıyaman, Turkey; ³Kahta District Health Directorate, Adıyaman, Turkey; ⁴Department of Child Health and Diseases, Besni State Hospital, Adıyaman, Turkey

ABSTRACT

Objectives: In this study, besides the factors affecting breastfeeding, such as the tendency to breastfeed, the number of children, educational status, maternal age, working style, it was investigated how the breastfeeding behavior was affected during the epidemic.

Methods: At least 384 mothers were included in the study with a 95% confidence level, 0.05 margin of error, and 403 mothers were included in the study. A questionnaire form prepared by the researchers was used as a data collection tool and consent form was obtained from the participants.

Results: The mean age of the mothers participating in the study was 29.2 ± 5.9 years (range:18 to 52 years). Two hundred and one (49.8%) mothers participating in the study do not find it safe for mothers with COVID-19 to breastfeed their baby. However, only 20.2% of mothers think that COVID-19 can be transmitted to the baby through breast milk. Ninety-eight (24.4%) mothers stated that they could breastfeed their babies even if they had COVID-19, and 15.5% stated that mothers with COVID-19 around them could breastfeed their babies.

Conclusions: Although the COVID-19 epidemic had a negative impact on all aspects of life globally, it did not generally change the breastfeeding decisions of breastfeeding mothers. In fact, due to the closures and extended maternity leave, mothers spent more time with their babies and enabled them to breastfeed more frequently. However, it should not be neglected that misinformation is at a substantial level. In the studies conducted, wrong or incomplete information was observed in a significant part of the mothers who did not consider breastfeeding due to the epidemic, although the rates were low. For this reason, besides health professionals, media organs should be actively used for information.

Keywords: COVID-19, breastfeeding, pandemic

Effective breastfeeding is defined as the continuation of breast milk with only breast milk in the first month of the baby, and then with supportive foods until the age of two [1]. Breastfeeding can be considered the baby's first vaccine as it strengthens the baby's

immune system with antibodies passed from the mother. Effective breastfeeding is the most effective global intervention for promoting health and development in infants. It reduces the risk of disease development and disease severity in childhood and has a high

Received: December 24, 2022; Accepted: March 6, 2023; Published Online: March 16, 2023



e-ISSN: 2149-3189

How to cite this article: Parlak ME, Küçükkeleşçe O, Ener D, Öz E, Bayar V. Information, attitudes and behaviors of mothers about breastfeeding behavior during the COVID-19 pandemic process. Eur Res J 2023;9(3):536-542. DOI: 10.18621/eurj.1223949

Address for correspondence: Mehmet Emin Parlak, MD., Kahta State Hospital, Department of Child Health and Diseases, 02200, Adıyaman, Turkey. E-mail: meparlak02@gmail.com, Phone: +90 416 216 10 15



©Copyright © 2023 by Prusa Medical Publishing
Available at <http://dergipark.org.tr/eurj>
info@prusamp.com

life-saving potential by preventing half a million infant deaths and 13% of child deaths worldwide [2].

While breastfeeding is the most cost-effective and recommended nutritional practice, its implementation globally is still not optimal. Effective breastfeeding practice is high in low- and middle-income countries, while formula is more commonly used in Western Europe, Australia, and North America. In effective breastfeeding practices, besides cultural and sociodemographic characteristics, physiological, health policies, encouraging (excessive maternity leave, assistance from spouse or family, etc.) or restrictive (inability of mothers working in the private sector to take maternity leave, insufficient maternity leave, etc.) factors are known to be important. The physiological burden of pregnancy and breastfeeding on mothers (nipple infections, postpartum problems) should not be forgotten [3].

The COVID-19 virus, which affected more than 600 million people globally and caused the death of 6.5 million people, also affected 17 million people in our country and caused the death of more than 100 thousand people [4]. The virus has deeply affected socioeconomic status and health practices. Throughout the epidemic, breastfeeding behaviors were also affected positively or negatively. Examples of positive effects are that mothers spend more time with their babies due to the prolonged maternity leave, and spouses stay at home longer, and mothers find more support through this. While the World Health Organization does not recommend stopping breastfeeding even when infected, mothers' interruption of breastfeeding when infected and difficulties in accessing the health care they need due to closures can be given as examples of negative effects [3].

In this study, besides the factors affecting breastfeeding, such as the tendency to breastfeed, the number of children, educational status, maternal age, and the way of working, it was investigated how the breastfeeding behavior was affected during the epidemic.

METHODS

Study Design

The study was carried out in accordance with the 1975 Declaration of Helsinki, after obtaining approval from

the Turkish Republic Ministry of Health, ethics committee approval (No:2021/09-01) from local ethics committee. The research is a cross-sectional and descriptive study. The research was carried out in Adiyaman-Kahta district between January 2022 and May 2022. The population of the study consisted of breastfeeding mothers who applied to the Kahta State Hospital Pediatrics Polyclinic. At least 384 mothers were planned to be included in the study with a 95% confidence level and a 0.05 margin of error and 403 mothers were included. A questionnaire form prepared by the researchers was used as a data collection tool and consent form was obtained from the participants.

Statistical Analysis

Qualitative data were given as number and % frequency, and Chi-Square test was used for comparisons between groups. A p value of < 0.05 was accepted as statistically significant.

RESULTS

The mean age of the mothers participating in the study was 29.2 ± 5.9 years (range 18 to 52 years). The descriptive characteristics of the mothers are presented in Table 1. Two hundred and one (49.8%) mothers participating in the study do not find it safe for mothers with COVID-19 to breastfeed their baby. However, only 20.2% of mothers think that the COVID-19 virus can be transmitted to the baby through breast milk. Ninety-eight (24.4%) mothers stated that they could breastfeed their babies even if they had COVID-19, and 15.5% stated that mothers with COVID-19 around them could breastfeed their babies.

The rate of mothers who did not wash their hands before breastfeeding was 42.8% and the rate of cleaning their breasts was 34.6%. The rate of mothers wearing masks while breastfeeding their babies is 35.8%, the rate of removing items such as rings and wristbands is 32.6%, the rate of using gloves is 35.6%, the rate of using visors is 28.7%, the rate of using caps is 30.7% and the rate of using protective clothing is 29.4%.

When the mothers participating in the study were examined according to age, there was no significant difference between finding breastfeeding safe during COVID-19. The proportion of those who are unde-

Table 1. Descriptive characteristics of the mothers participating in the study

Characteristics	n	%
Age		
18-24 age	83	20,6
25-34 age	253	62,8
35 and above	67	16,6
Mother's educational status		
Illiterate	20	5,0
Literate/primary/secondary school graduate	276	68,5
High school graduate	63	15,6
College/university or higher	44	10,9
Perception of the economic situation		
Very good	30	7,4
Good	149	37
Moderate	168	41,7
Bad	43	10,7
Very bad	13	3,2
Number of children		
Not parent	13	3,2
1	115	28,5
2	157	39,0
3	60	14,9
4	38	9,4
5 and above	20	4,9
Breastfeeding status		
Yes	294	73,5
No	106	26,5
Age of the child breastfed		
0 age	80	21,2
1 age	158	41,9
2 age	88	23,3
3 age	45	11,9
4 age	6	1,6
COVID-19 infected		
Yes	288	71,5
No	115	28,5
COVID-19 infected relatives		
Yes	350	86,8
No	53	13,1

Table 2. Breastfeeding knowledge and attitudes of the mothers participating in the study about breastfeeding during the COVID-19 pandemic process

	Agreed %	Not-agreed %	Hesitant %
It is safe for a mother with COVID-19 to breastfeed her baby.	36.8	49.8	13.4
COVID-19 can be passed to an infant through breast milk.	20.2	45.6	34.2
I would breastfeed my baby even if I had COVID-19.	24.4	47.9	27.7
Mothers with COVID-19 around me should breastfeed their babies.	15.5	52.1	32.4
It wouldn't upset me if I couldn't breastfeed my baby due to COVID-19.	22.7	55.9	21.4
COVID-19 should use the method of expressing rather than breastfeeding directly.	25.1	43.5	31.3

cided on this issue increases with age. There was no significant difference between finding breastfeeding safe while having COVID-19, according to the educational status of the mothers and the status of having COVID-19 in their relatives. Compared to mothers with moderate and poor economic status, the rate of finding breastfeeding safe during COVID-19 is significantly lower. The rate of finding breastfeeding safe during COVID-19 is significantly lower in mothers with one child compared to mothers with two or more children. The rate of finding breastfeeding safe during COVID-19 is significantly lower in lactating mothers compared to non-breastfeeding mothers. The rate of finding breastfeeding safe while having COVID-19 is

significantly higher in mothers whose children are 0 and 1 years old compared to mothers who are 2 years and older. The rate of finding breastfeeding safe while suffering from COVID-19 is significantly lower in mothers who have had COVID-19 compared to mothers who have not.

DISCUSSION

Although breastfeeding is a feeding method as old as human history, effective breastfeeding is not practiced sufficiently in many countries [2]. The COVID-19 pandemic has emerged as a new problem in the lives

Table 3. Breastfeeding behaviors of the mothers participating in the study about breastfeeding during the COVID-19 pandemic process

	Always or very often %	Sometime %	Never %
I wash my hands before breastfeeding my baby.	42,8	24,3	33,0
I wear a mask while breastfeeding my baby.	35,8	31,5	32,7
I take off items such as rings and bracelets while breastfeeding my baby.	32,6	35,7	31,6
I use gloves while breastfeeding my baby.	35,6	27,9	36,4
I clean my breast before breastfeeding my baby.	34,9	33,6	31,6
I use a visor while breastfeeding my baby.	28,7	33,4	38,0
I use a bonnet while breastfeeding my baby.	30,7	37,0	32,2
I use protective clothing while breastfeeding my baby.	29,4	37,7	32,9

Table 4. According to the descriptive characteristics of the mothers participating in the study, the rates of those who found breastfeeding safe while they had COVID-19

Characteristics	n	Those who think breastfeeding is safe while suffering from COVID-19		X ²	p value
		Number	%		
Age					
18-24 age	83	36	43.4	3.90	0.143
25-34 age	252	87	34.5		
35 and above	67	25	37.3		
Mother's educational status					
Under high school	295	107	36.3	7.01	0.136
High school graduate	63	25	39.7		
College/university or higher	44	16	36.4		
Perception of the economic situation					
Very good/good	178	48	27.0	26.71	0.001
Moderate	168	76	45.2		
Bad/very bad	56	24	42.9		
Number of children					
1	115	30	26.1	8.08	0.018
2 and above	274	108	39.4		
Breastfeeding status					
Yes	393	98	33.4	48.14	0.001
No	106	48	45.3		
Age of the child breastfed					
0 - 1 age	238	94	39.5	16.92	0.001
2 age and above	139	39	28.1		
COVID-19 infected					
Yes	288	94	32.6	12.13	0.002
No	114	54	47.4		
COVID-19 infected relatives					
Yes	350	122	39.4	4.52	0.104
No	52	26	50.0		

of breastfeeding mothers. However, it was determined that vertical virus transmission from pregnant to baby was not possible during the process [5]. Later, WHO recommended that the mother continue to breastfeed her baby with standard precautions as long as the mother's health permits [6].

Although 36.8% of the mothers who participated in our study found it safe for a mother with COVID-

19 to breastfeed her baby, the rate of mothers who would breastfeed their baby when they have covid increases to 47.9%. In a study conducted with 114 women in Sedwick, Kansas, it was observed that 68.5% of the participants did not change their breastfeeding plans/tendencies [7]. Likewise, in a study conducted in Belgium with 6470 women, 3823 of whom were breastfeeding, 91% of the participants stated that

their breastfeeding behaviors would not change, and 82% of them stated that the duration of breastfeeding became longer because the duration of stay at home was prolonged [8]. An online study by Brown and Shenker [9] also showed that breastfeeding behaviors were positively affected by 41.8%. Although breastfeeding behaviors are affected positively during the epidemic in general, it is a problem frequently expressed by pregnant/breastfeeding women in the surveys; It is stated that it is difficult to reach professional health support when needed [3].

In a study conducted with 390 mothers in Thailand, breastfeeding behaviors of mothers were questioned during the epidemic, while the duration of breastfeeding increased as the education level and economic status increased, while in our study there was no significant difference according to education level, it was observed that mothers who defined their economic status as poor had a longer breastfeeding period [10]. It has been interpreted that this may be due to the fact that breastfeeding is an economical feeding method and the food costs cannot be met. In the study conducted with 104 mothers in Egypt, knowledge and behaviors about breastfeeding were found to be strongly positive as the education level increased. was observed to be affected [11].

Studies have shown that multiparous pregnant women have significantly higher breastfeeding knowledge and tendencies than nulliparous pregnant women [2]. In our study, mothers with two or more children breastfeed their children longer than mothers with one child. In addition, in our study, it was observed that if the child breastfed by the mother is younger than one year old, there is a tendency to breastfeed for a longer period of time. In a study conducted in China in 2019, it was found that multiparous pregnant women approached breastfeeding more positively than nulliparous pregnant women [12].

In our study, the mothers answered the question "Can the COVID-19 virus be transmitted to the baby through breast milk?" 20.2% of the participants answered that it could pass, while 45.6% could not exceed it. In a study conducted in India with 1636 participants, 28% of the participants answered that the virus can be transmitted to the baby through breast milk, and this rate increased significantly when the women of productive age were examined [13]. In a study conducted with 623 pregnant participants in

Hong Kong, 11.6% of the participants stated that they decided not to breastfeed their babies due to the COVID-19 outbreak, and 77.8% of them stated that they believed that the virus could be transmitted to their babies through breast milk [14].

In a study conducted with 104 mothers in Egypt, it was observed that mothers who had previously had COVID-19 breastfed their babies for a longer period of time, and their knowledge and behavior regarding breastfeeding was significantly higher than that of mothers who had not had COVID-19 before [11]. In our study, it was seen that mothers who have had COVID-19 before have less knowledge about breastfeeding their babies and they tend to breastfeed their babies less.

In our study, 25.1% of the participants stated that the method of expressing should be used instead of breastfeeding while they have COVID-19. In a study conducted on 125 COVID-19 positive mothers in Turkey, it was observed that 71.5% of the mothers fed their babies with formula, and 36% fed their babies with the milking method [15]. In a study conducted with 200 pregnant participants in India, 47% of the participants who were asked about the breastfeeding method of COVID-19 positive mothers preferred formula, 25% answered the milking method and 17% answered breastfeeding [16].

It was determined in our survey study that the rate of mothers who confidently look after the breastfeeding of COVID-19 positive mothers decreases as the maternal age increases. In a study conducted in Thailand, it was observed that the duration of breastfeeding shortened with increasing maternal age [10].

CONCLUSION

Although the COVID-19 epidemic has had a negative impact on all aspects of life globally, it has not generally changed the breastfeeding decisions of breastfeeding mothers. In fact, due to the closures and extended maternity leave, mothers spent more time with their babies and enabled them to breastfeed more frequently. However, it should not be neglected that misinformation is at a substantial level. In the studies conducted, wrong or incomplete information was observed in a significant part of the mothers who did not consider breastfeeding due to the epidemic, although

the rates were low. For this reason, besides health professionals, media organs should be actively used for information.

Authors' Contribution

Study Conception: MEP, DE, VB; Study Design: MEP, EÖ, OK; Supervision: DE, EÖ, VB; Funding: N/A; Materials: N/A; Data Collection and/or Processing: MEP, DE; Statistical Analysis and/or Data Interpretation: EÖ, DE, VB; Literature Review: MEP, DE, OK; Manuscript Preparation: MEP, EÖ, OK, VB and Critical Review: DE, OK, VB.

Conflict of interest

The authors disclosed no conflict of interest during the preparation or publication of this manuscript.

Financing

The authors disclosed that they did not receive any grant during conduction or writing of this study.

REFERENCES

1. World Health Organization. Indicators for Assessing Infant and Young Child Feeding Practices. Part 1: Definitions. Conclusions of a consensus meeting held 6-8 November 2007 in Washington DC, USA. World Health Organization, 2008.
2. Chekol Abebe E, Ayalew Tiruneh G, Asmare Adela G, Mengie Ayele T, Tilahun Muche Z, Behaile T/Mariam A, et al. Levels and determinants of prenatal breastfeeding knowledge, attitude, and intention among pregnant women: a cross-sectional study in Northwest Ethiopia. *Front Public Health* 2022;10:920355.
3. Pacheco F, Sobral M, Guiomar R, de la Torre-Luque A, Caparrós-González RA, Ganho-Ávila A. Breastfeeding during COVID-19: a narrative review of the psychological impact on mothers. *Behav Sci (Basel)* 2021;11:34.
4. World Health Organization. <https://covid19.who.int/> last access date: 11.11.2022
5. Giuliani C, Li Volsi P, Brun E, Chiambretti A, Giandalia A, Tonutti L, et al. Breastfeeding during the COVID-19 pandemic: suggestions on behalf of woman study group of AMD. *Diabetes Res Clin Pract* 2020;165:108239.
6. WHO. Update 65 – Breastfeeding and newborn care in the context of COVID-19. 2021.
7. Ahlers-Schmidt CR, Hervey AM, Neil T, Kuhlmann S, Kuhlmann Z. Concerns of women regarding pregnancy and childbirth during the COVID-19 pandemic. *Patient Educ Couns* 2020;103:2578-82.
8. Ceulemans M, Verbakel JY, Van Calsteren K, Eerdeken A, Allegaert K, Foulon V. SARS-CoV-2 infections and impact of the COVID-19 pandemic in pregnancy and breastfeeding: results from an observational study in primary care in Belgium. *Int J Environ Res Public Health* 2020;17:6766.
9. Brown A, Shenker N. Experiences of breastfeeding during COVID-19: lessons for future practical and emotional support. *Matern Child Nutr* 2021;17:e13088.
10. Nuampa S, Ratinthorn A, Patil CL, Kuesakul K, Prasong S, Sudphet M. Impact of personal and environmental factors affecting exclusive breastfeeding practices in the first six months during the COVID-19 pandemic in Thailand: a mixed-methods approach. *Int Breastfeed J* 2022;17:73.
11. Amer ST, Al-Rafay SSE, Sadek BN, Mohamed HR. Knowledge and practices of breastfeeding mothers regarding protective measures for their neonates against COVID-19. *Egypt J Health Care* 2022;13:964-81.
12. Hamze L, Mao J, Reifsnider E. Knowledge and attitudes towards breastfeeding practices: a cross-sectional survey of post-natal mothers in China. *Midwifery* 2019;74:68-75.
13. Sahoo S, Pattnaik JI, Mehra A, Nehra R, Padhy SK, Grover S. Beliefs related to sexual intimacy, pregnancy and breastfeeding in the public during COVID-19 era: a web-based survey from India. *J Psychosom Obstet Gynaecol* 2021;42:100-7.
14. Lok WY, Chow CY, Kong CW, To WWK. Knowledge, attitudes, and behaviours of pregnant women towards COVID-19: a cross-sectional survey. *Hong Kong Med J* 2022;28:124-32.
15. Oncel MY, Akın IM, Kanburoglu MK, Tayman C, Coskun S, Narter F, et al. A multicenter study on epidemiological and clinical characteristics of 125 newborns born to women infected with COVID-19 by Turkish Neonatal Society. *Eur J Pediatr* 2021;180:733-742.
16. Kaur TP, Rana A, Perumal V, Sharma A, Dadhwal V, Kulshrestha V, et al. A cross-sectional analysis to evaluate knowledge, attitude and practices among pregnant women during COVID-19 pandemic. *J Obstet Gynaecol India* 2021;71:18-27.



This is an open access article distributed under the terms of [Creative Commons Attribution-NonCommercial-NoDerivatives 4.0 International License](https://creativecommons.org/licenses/by-nc-nd/4.0/).

Immunohistochemical approach to obesity disease in terms of expression levels of glutathione s-transferase (sigma, zeta, theta) isozymes

Mahammad Davudov¹, Hakan Buluş¹, Onur Dirican², Pınar Kaygın³, Gülçin Güler Şimşek⁴, Sezen Yılmaz Sarıaltın⁵, Fatıma Nurdan Gürbüz³, Serpil Oğuztüzün³

¹Department of General Surgery, University of Health Sciences, Keçiören Training and Research Hospital, Ankara, Turkey; ²Department of Pathology Laboratory Techniques, Istanbul Gelişim University, Vocational School of Health Services, Istanbul, Turkey; ³Department of Biology, Kırıkkale University, Faculty of Science, Kırıkkale, Turkey; ⁴Department of Pathology, University of Health Sciences, Gulhane Training and Research Hospital, Ankara, Turkey; ⁵Department of Pharmaceutical Toxicology, Ankara University, Faculty of Pharmacy, Ankara, Turkey

ABSTRACT

Objectives: Obesity is a complex multifactorial disease with recently increasing prevalence and incidence. Several studies have been conducted to explain the ethiology, pathophysiology, epidemiology, molecular and genetic mechanisms, and effective treatments of obesity. Glutathione S-transferase (GST) S1, GSTZ1, and GSTT1 are essential enzymes for oxidative stress and metabolism-related disorders. For this purpose, we aimed to reveal the role of GSTS1, GSTZ1, and GSTT1 in obesity.

Methods: The gastric tissue samples were taken from the patients diagnosed with obesity who underwent bariatric surgery in Ankara Keçiören Training and Research Hospital General Surgery Clinic between 2017 and 2019. Immunostaining was performed on paraffin-embedded tissues to evaluate GSTS1, GSTZ1, and GSTT1 expressions. Laboratory data of the patients were recorded. All the results were analyzed statistically.

Results: Weak GSTS1 expression was observed in 38.1% of tissues and moderate in 6.3%. 37.3% of the tissues presented weak GSTZ1 expression, and 11 (8.7%) displayed moderate. There were weak GSTT1 expressions in 7.1% of the tissues and moderate 0.8% of them. A positive and statistically significant correlation was observed between GSTS1 and GSTT1 expression levels ($r = 0.028$, $p = 0.010$; $p < 0.05$). There were no significant differences between expression levels and gender, age, comorbidities, and medication usage ($p > 0.05$).

Conclusions: GSTs, in particular GSTS1, GSTT1, and GSTZ1, might contribute to molecular mechanisms and the progression of obesity. In our study, GSTS1, GSTT1, and GSTZ1 were found to be moderately expressed in gastric tissues taken from obese patients. However, new studies using more samples and advanced techniques are needed to elucidate the relationship.

Keywords: Obesity, xenobiotics, phase II enzymes, GSTS1, GSTZ1, GSTT1, immunohistochemistry

Received: May 25, 2022; Accepted: August 10, 2022; Published Online: March 18, 2023



e-ISSN: 2149-3189

How to cite this article: Davudov M, Buluş H, Dirican O, Kaygın P, Şimşek GG, Yılmaz Sarıaltın S, et al. Immunohistochemical approach to obesity disease in terms of expression levels of glutathione s-transferase (sigma, zeta, theta) isozymes. Eur Res J 2023;9(3):543-554. DOI: 10.18621/eurj.1121110

Address for correspondence: : Onur Dirican, Assist. Prof., Department of Pathology Laboratory Techniques, Istanbul Gelişim University, Vocational School of Health Services, Istanbul, Turkey . E-mail: odirican@gelisim.edu.tr, Phone: +90 212 422 70 00/512



©Copyright © 2023 by Prusa Medical Publishing
Available at <http://dergipark.org.tr/eurj>
info@prusamp.com

In addition to genetic predisposition, it is accepted that external factors such as lifestyle and cultural environment are the determining parameters in terms of obesity formation and susceptibility [1]. It is one of the most important steps towards the treatment of the disease to reveal the formation mechanism of this disease in a clearer and more understandable way. Due to these reasons, current research has gained importance in terms of revealing the functioning or anomaly of the genes responsible for these hormones, which are known to have hormonal and regulating effects on these hormones, together with habits such as human life style, nutrition and diet. In particular, studies related to the elimination of diseases such as type 2 diabetes and hypertension after surgical interventions related to obesity are seen in the literature. [2]. Adipose tissue constitutes 15-20% of the body weight of adult men and 25-30% of women. If this rate rises above 25% in men and 30% in women, obesity can be mentioned [3]. Following obesity; It has been determined that diseases such as hypertension, cardiovascular diseases, diabetes, degenerative arthritis, thrombophlebitis are seen directly or indirectly, and this is valid in all age groups [4]. Neuroendocrine system diseases such as Cushing's Syndrome, Hypothyroidism, Polycystic Ovary Disease are known to be factors in the formation of obesity [5, 6]. Along with parameters such as nutrition, lifestyle, genetic predisposition, and physical activity, drug use such as psychotropic drugs, steroids, and contraceptives has also been reported as another factor that can cause obesity [7, 8]. It has consequences in the form of various diseases on many systems such as the endocrine system, cardiovascular system, respiratory system, gastrointestinal system, nervous system. These diseases; hypertension, type 2 diabetes, coronary heart disease, acute myocardial infarction, cerebrovascular diseases, respiratory distress, obstructive sleep apnea, gallbladder disease, fatty liver, dyslipidemia, hyperuricemia, insulin resistance, breast cancer, osteoarthritis, nerve entrapment, proteinuria, lymphedema and in a psychological form [9]. In morbidly obese people, no results can be obtained with any non-surgical method. When morbidly obese people lose weight with non-surgical treatment methods, the frequency of weight regain is approximately 95%. Morbid obesity; The only treatment option that is effective, proven and can provide long-term results is surgical techniques [10]. In reac-

tions catalyzed by metals, reactive oxygen compounds can be produced in two different ways. The first of these; It is produced endogenously in the cell by the catalytic effect of various enzymes such as peroxisomal oxidation, electron transport reactions catalyzed in mitochondria, microsomal cytochrome P450 metabolism, xanthine oxidase and aldehyde oxidase as a result of immune system activation. The second is; It can be produced exogenously as a result of radiation caused by X, gamma and UV rays. It can also be found in the atmosphere as pollution. Environmental pollutants, barbiturates, xenobiotics such as chlorinated compounds, some metal ions and smoking are other exogenous sources [11-13]. Beneficial and harmful effects of free radicals on the organism can be seen. It is known that they play a bidirectional role in biological systems. Examples of the beneficial effects of free radicals are the active roles they play in the immune system defense against infectious agents and in intracellular communication pathways. However, it also induces mitogenic response at low concentrations. Considering its negative effects, it causes damage to cell structures such as fats, proteins and nucleic acids at high concentrations [14, 15]. The harmful effects of Reactive Oxygen Compounds are kept under control by enzymatic and non-enzymatic antioxidants. Despite the antioxidant defense system, the excessive increase in the production of ROB or the decrease in the capacity of the antioxidant defense system and the accumulation of ROB in the body cause oxidative damage known as oxidative stress. Oxidative stress plays an important role in the emergence of cancer, atherosclerosis, arthritis, neurodegenerative disorders and many other diseases [16, 17]. Obesity-induced oxidative stress is thought to be the main cause of diseases that play a role in the pathogenesis of long-term complications such as cardiovascular diseases and Type 2 diabetes. Although body mass index, body fat percentage, low density lipoprotein oxidation and triglyceride levels are important indicators of oxidative stress, they are associated with obesity as well as parameters. A diet rich in fat and carbohydrates has been found to induce significant oxidative stress and inflammation in obesity [18]. It has been determined that reactive oxygen compounds may cause insulin resistance by negatively affecting the balance of insulin secretion in the pancreas and glucose transport system in skeletal tissue and adipose tissue [19, 20]. De-

creased insulin sensitivity is thought to be one of the main factors of the metabolic syndrome [21, 22]. Therefore, it can be said that there is a direct relationship between oxidative stress, obesity and metabolic syndrome [23]. Cardiovascular disease risk increases with metabolic syndrome [24]. There are many studies on the presence of obesity-induced oxidative stress [25-27].

Genetic variation can affect both toxic and xenobiotic pharmacokinetics and pharmacodynamics, and these consequences appear as phenotypes in pharmacogenomics. Pharmacokinetics refers to the body's actions on a drug, including the absorption, distribution, metabolism, and excretion (ADME) of an administered drug, performed by proteins such as metabolizing enzymes and membrane transporters involving the cytochrome P450 (CYP) system [28]. Through xenobiotic biotransformation, lipophilic (fat-soluble) chemicals are converted to hydrophobic (water-soluble) chemicals and excreted in urine or bile. As a result of xenobiotic biotransformation, it can change biological effects such as increase, decrease or loss in the pharmacological activity of the xenobiotic [29]. Examples of Phase I drug metabolizing enzymes localized in the endoplasmic reticulum are heme-containing CYP, flavin-containing monooxygenase, monoamine oxidase, and xanthine oxidase/aldehyde oxidases. CYP enzymes play the most prominent role in Phase I metabolism [30]. In cases where the polarity of the molecule formed as a result of Phase I reactions is not sufficient, Phase II reactions are carried out by attaching glucuronic acid, acetic acid, sulfuric acid, or an amino acid to the drug. Glucuronide in glucuronic acid conjugation; can be attached to oxygen, nitrogen and sulfur groups. Conjugation with glutathione is important for electrophilic compounds. Glutathione (GSH) is a tripeptide (γ -glutamylcysteinylglycine). Forms glutathione S-conjugates, which are excreted in the urine or bile. The reaction is catalyzed by glutathione S-transferases (GST). Acetyl-CoA is used as the acetyl donor in acetylation and the reaction is catalyzed by acetyltransferases. Xenobiotics are methylated by methyltransferases. S-adenosyl-methionine (SAM) is used as methyl donor [31]. GSH is an atypical tripeptide with gamma-L-glutamyl-L-cysteinyl glycine structure. It is atypical because of the gamma bond between the amine group of cysteine and the carboxyl

group in the side chain of glutamate. GSH is synthesized in the body from L-cysteine, L-glutamic acid and glycine. It is a thiol that has a fundamental role in maintaining redox balance in the cell and responding to oxidative stress [32, 33]. GSH is found in high concentrations, especially in liver cells [34, 35]. GSH can reduce unstable molecules such as reactive oxygen compounds. GSH constitutes more than 90% of the GSH pool in healthy cells and tissues. GSH acts as a substrate in numerous conjugation and reduction reactions catalyzed by GST in the cytosol, microsomes, and mitochondria [36]. The aim of our study is contribute to the determination of the relationship of the detoxification mechanism with obesity in terms of GST- Sigma (S) 1, GST Zeta (Z) 1, and GST Theta (T) 1. The determination of the expressions of these isoenzymes in obesity patients was carried out in order to contribute to research on the prognostic, diagnosis and treatment of obesity.

Complete blood count, the most commonly used blood test in the whole world, is a blood test used to evaluate people's general health and detect a wide variety of disorders, as it provides information about the life cycle and physiology of the various cell components [37]. Especially the levels of white blood cell (WBC), hemoglobin (HGB), and platelet (PLT) give essential information to medical professionals about inflammatory conditions, metabolic diseases and obesity. There are several ways in which obesity increases cardiovascular and diabetes risk, including high low-density lipoprotein (LDL), total cholesterol, and triglyceride, low high-density lipoprotein (HDL), excessive fasting, postprandial blood glucose and hemoglobin A1c (HbA1c) and unsteady insulin levels [38, 39]. Several studies reported that there may be a relationship between obesity and hormone levels including free T3, and T4, thyroid-stimulating hormone (TSH), estradiol, follicle-stimulating hormone (FSH), luteinizing hormone (LH), C-peptide, cortisol, adrenocorticotropic hormone (ACTH) and sex hormone-binding globulin (SHBG) [40-43]. Therefore, this study also aimed to investigate the association of GSTS1, GSTZ1, and GSTT1 expressions and complete blood count, cardiovascular and diabetes and hormone parameters. To the best of our knowledge our study is the first to evaluate all these parameters simultaneously.

METHODS

In this study, 126 gastric tissues of obese patients who underwent bariatric surgery were received from the General Surgery Clinic of Keçiören Training and Research Hospital between 2017 and 2019. The gastric tissues were stained by the immunohistochemistry method to evaluate GSTS1, GSTZ1, and GSTT1 expressions.

Ethics committee approval of this study was provided by the decision of the Ethics Committee of Keçiören Training and Research Hospital with the decision number 2012-KAEK-15/2218.

Immunohistochemical (IHC) Staining

The tissue sections were peroxidase-incubated for 10 minutes using 3% hydrogen peroxide in methanol (v/v). After that, the sections were performed for 3 min using a 0.01M citrate buffer, pH 6.0 in a domestic pressure cooker. Sections were incubated at room temperature for 10 min with superblock (SHP125; Scy Tek laboratories, West Logan, UT). The sections were then covered with the primary antibodies diluted (1:250 for GSTS1; 1:250 for GSTZ1; 1:250 for GSTT1) in TBS at 4°C. AntiGST-Theta1 (PAA622Hu01) was obtained from Cloud Clone Corp. TX,USA; anti-GSTS1 (Sc-30,067) was obtained from Santa Cruz Biotechnology, Inc; anti-GSTZ1 (bs-13442R) was obtained from Bioss Antibodies Inc. Woburn, Massachusetts, USA. After washing for 15 minutes in TBS, the sections were incubated at room temperature with a biotinylated link antibody (SHP125; ScyTek Laboratories) followed by streptavidin/HRP complex (SHP125; ScyTek laboratories). The sections were incubated at room temperature with biotinylated link antibody (SHP125; ScyTek Laboratories) then diaminobenzidine was used to visualize peroxidase activity in tissues and they were counterstained with hematoxylin. Scoring of immunohistochemically stained sections were performed for each parameter was: 0 negative (no staining); 1 weak staining, 2, moderate staining.

Laboratory Findings

The blood test results of the cases were obtained from the patients' documentation. The patients' WBC, HGB, and platelet PLT levels were recorded as complete blood count parameters. Cholesterol parameters

were noted, including HDL, LDL, total cholesterol, and triglyceride. Diabetes parameters included fasting glucose, postprandial glucose, and HbA1c. The hormone parameters were assessed, including free T3, free T4, TSH, estradiol, FSH, LH, C-peptide, insulin, cortisol, ACTH, and SHBG.

Statistical Analysis

Statistical analysis was performed using IBM SPSS Version 25.0 (Armonk, NY: IBM Corp). The data were presented as mean \pm standard deviation (SD) and standard error of the mean (SEM). The categorized data were expressed as numbers of patients (n) and percentages (%). The Shapiro-Wilk test was used to evaluate the normality. The Levene test was performed to test the homogeneity of variances. The data was not normally distributed. Therefore, the Mann-Whitney U test was performed to compare differences between two independent groups, and The Kruskal-Wallis test was conducted to analyze three or more independent groups. Bonferroni correction was then applied. Spearman's rank correlation test was used to determine correlations. A p-value lower than 0.05 was considered statistically significant.

RESULTS

Our study group included 126 obese patients with a body mass index (BMI) equal to or greater than 40 kg/m². The mean weight was 125.10 kg, and the mean BMI was 46.77 kg/m². 111 female (88.1%) and 15 male (11.9%) patients were in our study group. Almost half of the patients (47.6%) were between the ages of 31 and 45. The mean age of the patients was 37.91 years. Obesity was the only disease in 75 patients, while 50 had an additional disease. 58.7% of the patients did not use medications, while 40.5% used.

The patients' whole blood parameters such as WBC, HGB, and PLT; glucose parameters such as fasting glucose, postprandial glucose, and HbA1c; cholesterol parameters such as HDL, LDL, total cholesterol, and triglyceride; hormone parameters such as free T3, and T4, TSH, estradiol, FSH, LH, C-peptide, insulin, cortisol, ACTH, and SHBG were recorded. The clinical and demographic characteristics of the patients are detailed in Table 1.

IHC staining levels for GSTS1, GSTZ1, and

Table 1. Clinical and demographic characteristics of the patients

Characteristics	Data
	Mean \pm SD (Range)
Age (years) (n = 126)	37.91 \pm 11.01 (16-63)
Height (cm) (n = 126)	163.48 \pm 8.21 (148-189)
Weight (kg) (n = 126)	125.10 \pm 19.26 (91-182)
BMI (kg/m ²) (n = 126)	46.77 \pm 6.18 (40-70.31)
WBC ($\times 10^9/L$) (n = 126)	8.96 \pm 2.00 (5.27-14.90)
HGB (g/dL) (n = 126)	13.68 \pm 1.55 (9.87-18.40)
PLT ($\times 10^3/\mu L$) (n = 126)	290.39 \pm 80.71 (34.30-53.500)
Glucose (fasting) (mg/dL) (n = 126)	111.16 \pm 54.50 (69.00-498.00)
Glucose (postprandial) (mg/dL) (n = 88)	139.35 \pm 62.43 (71.00-394.00)
HbA1c (%) (n = 117)	6.06 \pm 1.36 (4.10-13.10)
HDL (mg/dL) (n = 21)	43.19 \pm 7.77 (32.00-60.00)
LDL (mg/dL) (n = 15)	124.60 \pm 34.55 (55.00-168.00)
Triglyceride(mg/dL) (n = 118)	173.03 \pm 85.86 (42.00-545.00)
Total cholesterol (mg/dL) (n = 118)	215.62 \pm 170.75 (108.00-2016.00)
Total T3 (ng/dL) (n = 124)	3.01 \pm 0.41 (1.84-4.08)
Free T4 (ng/dL) (n = 125)	1.03 \pm 0.14 (0.61-1.55)
TSH (mIU/L) (n = 125)	2.58 \pm 2.17 (0.05-16.28)
Estradiol (pg/mL) (n = 56)	78.45 \pm 62.99 (9.00-247.00)
FSH (mIU/mL) (n = 75)	11.38 \pm 15.91 (0.96-75.98)
LH (IU/mL) (n = 75)	10.54 \pm 10.58 (1.07-45.09)
C peptide (ng/mL) (n = 117)	3.33 \pm 1.09 (1.28-6.23)
Insulin (mIU/L) (n = 122)	19.60 \pm 25.31 (1.70-275.60)
Cortisol ($\mu g/dL$) (n = 122)	10.17 \pm 4.10 (0.8-20.00)
ACTH (pg/mL) (n = 87)	29.14 \pm 19.10 (5.00-126.00)
SHBG (nmol/L) (n = 55)	37.80 \pm 31.30 (7.51-226.00)

The data were presented as mean \pm SD (minimum-maximum values). BMI = body-mass index, WBC = white blood cell, HGB = hemoglobin, PLT = platelet, HbA1c = hemoglobin A1c, HDL = high-density lipoprotein, LDL = low-density lipoprotein, TSH = thyroid-stimulating hormone, FSH = follicle stimulating hormone, LH = luteinizing hormone, ACTH = adrenocorticotropic hormone, SHBG = sex hormone-binding globulin

GSTT1 were determined in the tissues of the patients. The expression levels were evaluated as shown in Table 2. Weak GSTS1 expression was observed in 48 (38.1%) tissues and moderate in 8 (6.3%) ones. 47 (37.3%) of the tissues presented weak GSTZ1 expression, and 11 (8.7%) displayed moderate. Weak GSTT1 expression was noted in 9 (7.1%) tissues and moderate in 1 (0.8%).

Mean GSTS1, GSTZ1, and GSTT1 IHC scores of

the tissues are presented in Fig. 1. The highest expression was observed in GSTZ1, followed by GSTS1 and GSTT1. IHC expression patterns of GSTS1, GSTZ1, and GSTT1 in gastric tissues of patients are shown in Figs. 2, 3, and 4, respectively.

IHC expression levels of GSTS1, GSTZ1, and GSTT1 were determined regarding the patients' clinical and demographic characteristics, including gender, age, comorbidities, medication, and operation status

Table 2. GSTS1, GSTZ1, and GSTT1 IHC staining profile

IHC Staining Scores	GSTS1	GSTZ1	GSTT1
0	70/126 ^a (55.6%)	68/126 ^a (54.0%)	116/126 ^a (92.1%)
1	48/126 ^a (38.1%)	47/126 ^a (37.3%)	9/126 ^a (7.1%)
2	8/126 ^a (6.3%)	11/126 ^a (8.7%)	1/126 ^a (0.8%)
Mean	0.51 ± 0.05 ^b (0-2) ^c	0.55 ± 0.06 ^b (0-2) ^c	0.09 ± 0.03 ^b (0-2) ^c

Staining scores were determined based on the staining intensity of the tissues. 0 = negative staining, 1 = weak staining, 2 = moderate staining. IHC = immunohistochemical, GST = glutathione S-transferases, GSTS1 = GST-Sigma 1, GSTZ1 = GST Zeta 1, GSTT1 = GST Theta 1

^aNumber of samples stained at specified level / Total number of samples (percent:%),

^bMean ± SEM,

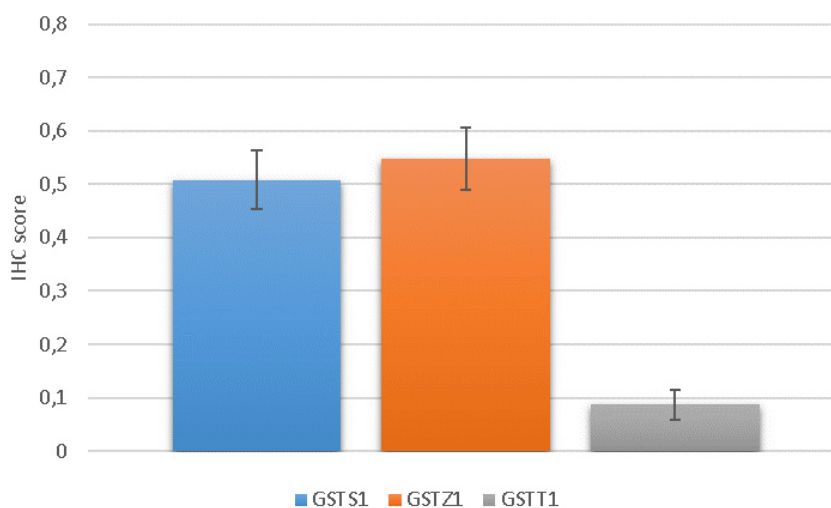
^cMinimum-maximum

(Table 3). There were no significant differences between expression levels and these parameters ($p > 0.05$).

Correlation analysis was performed between the GSTS1, GSTZ1, and GSTT1 expressions, and the results are explained in Table 4. A positive and statistically significant correlation was observed between GSTS1 and GSTT1 expression levels ($r = 0.028$, $p = 0.010$; $p < 0.05$).

Correlation analyses were also carried out between the clinical and demographic characteristics of the patients and the expression levels. Table 5 is dis-

played the results of these analysis. There was no statistically significant correlation between the GSTS1 expression levels and the clinical and demographic characteristics examined ($p > 0.05$). GSTZ expression and PLT levels were positively correlated ($p < 0.05$). There was a positive and significant correlation between GSTZ1 expression and total cholesterol levels ($p < 0.05$). Free T4 levels of the patients were also significantly correlated with GSTZ1 expression ($p < 0.05$). A positive and significant correlation was noted between the GSTT1 expression and cortisol levels ($p < 0.05$).

**Fig. 1. Mean GSTS1, GSTZ1, and GSTT1 IHC scores of the tissues.**

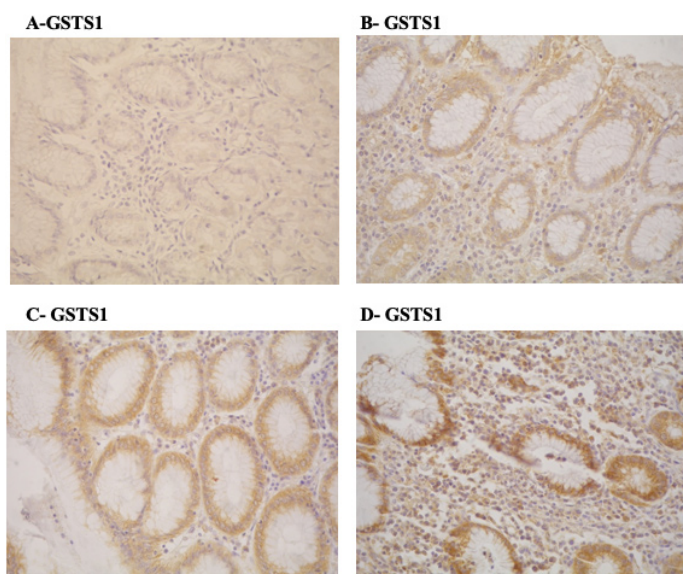


Fig. 2. Immunohistochemical expression of GSTS1 protein in stomach tissues (A: Expression of negative protein in stomach tissue, 40×; B: Weak (+1) protein expression in stomach tissue 20×; C: Weak (+2) protein expression in stomach tissue 20×; D: Weak expression in stomach tissue intense nuclear (+2) protein expression 40×).

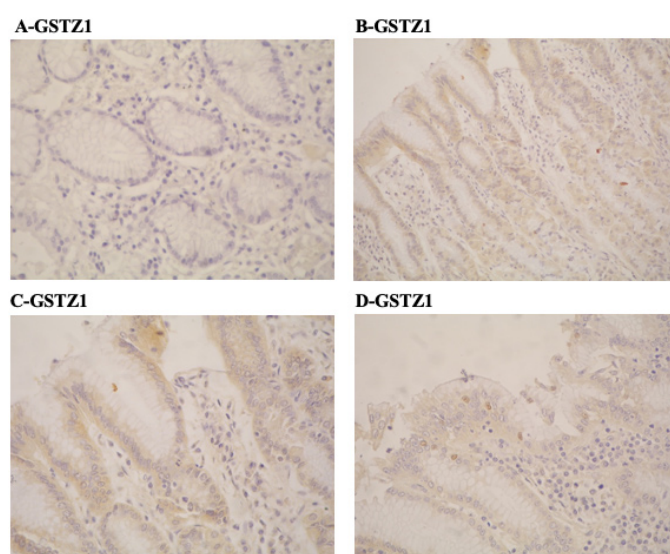


Fig. 3. Immunohistochemical expression of GSTZ1 protein in stomach tissues (A: Expression of negative protein in stomach tissue, 40×; B: Weak (+1) protein expression in stomach tissue 20×; C: Weak (+2) protein expression in stomach tissue 20×; D: Weak expression in stomach tissue intense nuclear (+2) protein expression 40×).

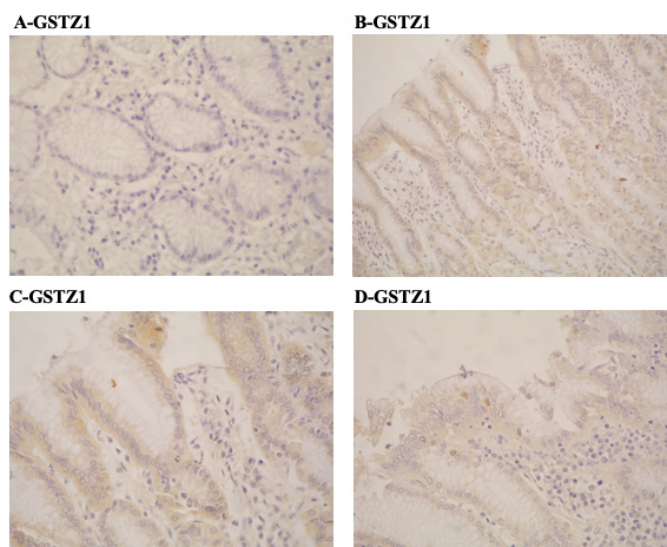


Fig. 4. Immunohistochemical expression of GSTT1 protein in stomach tissues (A: Expression of negative protein in stomach tissue, 40×; B: Weak (+1) protein expression in stomach tissue 20×; C: Weak (+2) protein expression in stomach tissue 40×; D: Weak expression in stomach tissue intense nuclear (+2) protein expression 40×).

DISCUSSION

Reactive oxygen species cause direct or indirect damage to different organs under many diseases and psychological conditions. Oxidative stress; includes

pathological processes such as obesity, diabetes, cardiovascular disease. It has been reported that obesity can be stimulated by the oxidative stress system. Oxidative stress, on the other hand, is related to the irregular production of adipokines secreted from adipose

Table 3. IHC GSTS1, GSTZ1, and GSTT1 expressions regarding the clinical and demographic characteristics of the patients

Variable	GSTS1	GSTZ1	GSTT1
Gender			
Female	0.51 ± 0.06 ^a (0-2) ^b	0.56±0.06 ^a (0-2) ^b	0.07 ± 0.02 ^a (0-1) ^b
Male	0.47 ± 0.13 ^a (0-1) ^b	0.47 ± 0.17 ^a (0-2) ^b	0.20 ± 0.14 ^a (0-2) ^b
<i>p value</i>	0.952	0,605	0,376
Age			
≤ 30	0.49 ± 0.10 ^a (0-2) ^b	0.57 ± 0.12 ^a (0-2) ^b	0.09 ± 0.05 ^a (0-1) ^b
31-45	0.55 ± 0.09 ^a (0-2) ^b	0.50 ± 0.08 ^a (0-2) ^b	0.08 ± 0.04 ^a (0-1) ^b
> 45	0.45 ± 0.09 ^a (0-1) ^b	0.61 ± 0.11 ^a (0-2) ^b	0.10 ± 0.07 ^a (0-2) ^b
<i>p value</i>	0.903	0.614	0.955
Comorbidities			
Yes	0.50 ± 0.08 ^a (0-2) ^b	0.56 ± 0.09 ^a (0-2) ^b	0.08 ± 0.05 ^a (0-2) ^b
No	0.52 ± 0.07 ^a (0-2) ^b	0.55 ± 0.07 ^a (0-2) ^b	0.09 ± 0.03 ^a (0-1) ^b
<i>p value</i>	0.993	0.973	0.527
Medication			
Yes	0.53 ± 0.08 ^a (0-2) ^b	0.57 ± 0.09 ^a (0-2) ^b	0.08 ± 0.05 ^a (0-2) ^b
No	0.50 ± 0.08 ^a (0-2) ^b	0.54 ± 0.08 ^a (0-2) ^b	0.09 ± 0.03 ^a (0-1) ^b
<i>p value</i>	0.606	0.726	0.494
Surgery			
Yes	0.54 ± 0.07 ^a (0-2) ^b	0.49 ± 0.07 ^a (0-2) ^b	0.11 ± 0.04 ^a (0-2) ^b
No	0.46 ± 0.09 ^a (0-2) ^b	0.63 ± 0.09 ^a (0-2) ^b	0.06 ± 0.03 ^a (0-1) ^b
<i>p value</i>	0.367	0,227	0.385

GST = glutathione S-transferases, GSTS1 =GST-Sigma 1, GSTZ1 = GST Zeta 1, GSTT1= GST Theta 1

^aMean ± SEM,

^bMinimum-maximum

Table 4. Correlation analyzes of GSTS1, GSTZ1, and GSTT1 expressions

	GSTS1		GSTZ1		GSTT1	
	correlation coefficient	<i>p value</i>	correlation coefficient	<i>p value</i>	correlation coefficient	<i>p value</i>
GSTS1	1.000	-	0,020	0.822	0.228	0.010
GSTZ1	0.020	0.822	1.000	-	-0.056	0.532
GSTT1	0.228	0.010	-0.056	0.532	1.000	-

GST = glutathione S-transferases, GSTS1 =GST-Sigma 1, GSTZ1 = GST Zeta 1, GSTT1= GST Theta 1

tissue, which contributes to the development of metabolic syndrome [44]. C-reactive protein and other oxidative damage biomarkers are high in obese individuals and are directly correlated with BMI and body lipid percentage, LDL oxidation and triglyceride level [45]. Antioxidant defense markers are lower than the amount of body fat in them [46]. Hartwich *et al.* determined that vitamin E, vitamin C, beta carotene and glutathione decreased in obesity [47]. Some research; showed that a high-fat and carbohydrate diet significantly stimulated the increase of oxidative stress and inflammation in obese individuals [48]. In literature studies on the detoxification mechanism, it has been shown that as a result of long-term obesity, a decrease in antioxidant sources and a decrease in the activities of super oxide dismutase and catalase enzymes [49]. In another study, it was shown that SOT and glutathione peroxidase activities were decreased in obese individuals compared to healthy individuals [50]. In a study, it was shown that oxidative stress in the cell increases as a result of the increase in CYP2E1 in mitochondria and has a role in liver diseases, obesity and type-2 diabetes [51].

In this study, it is known that oxidative stress is associated with the development of obesity, a multifactorial disease that is very common in all countries. II, which plays an important role in the xenobiotic mechanism. In this study, the relationship between the expressions of GSTT1, GSTS1 and GSTZ1 isozymes, which are members of the GST enzyme system that catalyzes the phase reactions, with obesity was investigated. In our findings, weak GSTS1 expression was observed 38.1% of the tissues and moderate in 6.3%. The GSTZ1 expression was weak in 37.3% of the tissues and moderate in 8.7%. Weak GSTT1 expression was noted in 7.1% of the tissues and moderate in 0.8%. Positive and statistically significant correlations

were found between GSTZ1 expression and PLT, total cholesterol, and free T4 levels of the patients ($p < 0.05$). A positive and significant correlation was also found between GSTT1 expression and the cortisol levels of the patients ($p < 0.05$).

It is seen that other studies in the literature indicate the relationship between obesity and oxidative stress. Apart from these studies, which also show their relationship with the concepts of obesity and oxidative stress separately, in this study, which we aim to contribute to revealing the relationship between obesity and Glutathione enzymes, which directly play a role in the xenobiotic mechanism, findings that overlap with other studies in the literature were obtained.

All these results indicate that GSTS1, GSTZ1, and GSTT1 enzyme amounts and oxidative stress increase in obesity. Significant changes occur in the amount GSTS1, GSTZ1, and GSTT1 enzymes in obese individuals. While these changes may occur as an adaptive response, the findings suggest that oxidative stress observed in obesity may be one of the possible mechanisms underlying this change. Findings that contribute to the definition of the physiopathology of obesity are important in the prevention of complications such as cardiovascular diseases that may develop due to obesity and in the development of preventive approaches.

CONCLUSION

In obese people, metabolic load due to overnutrition and, as a result, free radical formation due to overloading of metabolic pathways increase. Increased ROS in obese individuals cause oxidative stress. The negativities caused by free radicals are eliminated by the antioxidant defense system of the cell and the antioxidants taken through food. However, in the case

Table 5. Correlation analyses of IHC GSTS1, GSTZ1, and GSTT1 expression levels and the clinical and demographic characteristics

Data	GSTS1		GSTZ1		GSTT1	
	correlation coefficient	p value	correlation coefficient	p value	correlation coefficient	p value
Age	-0.002	0.979	0,042	0.640	-0.041	0.649
Height	-0.085	0.341	-0.017	0.852	0.177	0.047
Weight	-0.020	0.821	-0,063	0.481	0.171	0.056
BMI	0.122	0.172	-0.034	0.707	0.070	0.439
WBC	0.030	0.741	-0.023	0.797	-0.104	0.247
HGB	0.010	0.909	-0.081	0.365	-0.117	0.190
PLT	0.046	0.608	0.188	0.035	-0.058	0.520
Glucose (fasting)	0.052	0.566	0.115	0.201	0.071	0.431
Glucose (postprandial)	-0.002	0.988	0.007	0.952	0.105	0.330
HbA1c	0.052	0.578	0.180	0.052	-0.057	0.544
HDL	0.346	0.124	0.123	0.596	-	-
LDL	0.309	0.262	0.209	0.454	-	-
Triglyceride	0.067	0.469	0.022	0.816	0.088	0.345
Total cholesterol	-0.017	0.859	0.188	0.041	0.078	0.403
Free T3	-0.060	0.507	-0.017	0.855	0.162	0.072
Free T4	0.174	0.053	0.178	0.046	0.047	0.600
TSH	-0.118	0.188	0.090	0.318	0.029	0.746
Estradiol	0.053	0.699	0.212	0.117	-0.164	0.226
FSH	-0.016	0.891	0.042	0.718	-0.143	0.222
LH	0.024	0.840	0.009	0.940	-0.117	0.317
Insulin	-0.015	0.867	-0.043	0.636	-0.001	0.988
C Peptide	-0.011	0.910	-0.010	0.914	0.013	0.889
Cortisol	0.071	0.437	0.047	0.611	0.223	0.014
ACTH	0.058	0.592	0.069	0.524	-0.001	0.991
SHBG	0.037	0.789	0.112	0.415	0.062	0.655

IHC = immunohistochemical, GST = glutathione S-transferases, GSTS1 =GST-Sigma 1, GSTZ1 = GST Zeta 1, GSTT1= GST Theta 1, BMI = body-mass index, WBC = white blood cell, HGB = hemoglobin, PLT = platelet, HbA1c = hemoglobin A1c, HDL = high-density lipoprotein, LDL = low-density lipoprotein, TSH = thyroid-stimulating hormone, FSH = follicle stimulating hormone, LH = luteinizing hormone, ACTH = adrenocorticotropic hormone, SHBG =: sex hormone-binding globulin

of long-term obesity, antioxidant system enzymes are lower. Obesity causes cell damage and various diseases such as type 2 diabetes, cardiovascular diseases and cancer. GSTs, in particular GSTS1, GSTT1, and GSTZ1, might contribute to molecular mechanisms and the progression of obesity. GSTS1, GSTT1, and GSTZ1 were moderately expressed in gastric tissues

taken from obese patients regarding to the results of study. However, new studies using more samples and advanced techniques are needed to elucidate the relationship.

Authors' Contribution

Study Conception: MD, HB; Study Design: HB,

OD, SO; Supervision: HB; Funding: SO; Materials: MD, HB, PK, SYS, SO; Data Collection and/or Processing: GGS, OD, PK, SYS, FNG, SO; Statistical Analysis and/or Data Interpretation: SYS, SO; Literature Review: OD, SYS, SO; Manuscript Preparation: OD and Critical Review: GGS, SO, HB.

Conflict of interest

The authors disclosed no conflict of interest during the preparation or publication of this manuscript.

Financing

The authors disclosed that they did not receive any grant during conduction or writing of this study.

REFERENCES

- Hedley AA, Ogden CL, Johnson CL, Carroll MD, Curtin LR, Flegal KM. Prevalence of overweight and obesity among US children, adolescents, and adults, 1999-2002. *JAMA* 2004;291:2847-50.
- Buchwald H, Estok R, Fahrenbach K, Banel D, Jensen MD, Pories WJ, et al. Weight and type 2 diabetes after bariatric surgery: systematic review and meta-analysis. *Am J Med* 2009;122:248-56.
- Campfield LA, Smith FJ. The pathogenesis of obesity. *Baillieres Best Pract Res Clin Endocrinol Metab* 1999;13:13-30.
- Toshima S, Hasegawa A, Kurabayashi M, Itabe H, Takano T, Sugano J, et al. Circulating oxidized low density lipoprotein levels. A biochemical risk marker for coronary heart disease. *Arterioscler Thromb Vasc Biol* 2000;20:2243-7.
- Björntorp P. *International Textbook of Obesity*. John Wiley and Sons Ltd, 2001: pp. 305-14.
- Goran MI. Energy Metabolism and obesity. *Med Clin North Am* 2000;84:333-45.
- Hill JO, Peters JC. Environmental contributions to the obesity epidemic. *Science* 1998;280:1371-4.
- Schrauwen P and Westerterp KR. The role of high-fat diets and physical activity in the regulation of body weight. *BJ Nutr* 2000;84:417-27.
- Fletcher GF, Grundy SM, Hayman LL. Obesity: Impact on cardiovascular disease. American Heart Association. Futura Publishing Company, Armonk NY, 1999: pp. 3-46.
- Steinbrook R. Surgery for severe obesity. *N Eng J Med* 2004;350:1075-9.
- Seaver LC, Imlay JA. Are respiratory enzymes the primary sources of intracellular hydrogen peroxide? *J Biol Chem* 2004;279:48742-50.
- Messner KR, Imlay A. Mechanism of superoxide and hydrogen peroxide formation by fumarate reductase, succinate dehydrogenase, and aspartate oxidase. *J Biol Chem* 2002;277:42563-71.
- Imlay JA. Pathways of oxidative damage. *Ann Rev Microbiol* 2003;57:395-418.
- Martemucci G, Costagliola C, Mariano M, D'andrea L, Napolitano P, D'Alessandro AG. Free radical properties, source and targets, antioxidant consumption and health. *Oxygen* 2022;2: 48-78.
- Valko M, Rhodes CJ, Moncol J, Izakovic M, Mazur M. Free radicals, metals and antioxidants in oxidative stress-induced cancer. *Chem Biol Interact* 2006;160:1-40.
- Valko M, Leibfritz D, Moncol J, Cronin MT, Mazur M, Telser J. Free radicals and antioxidants in normal physiological functions and human disease. *Int J Biochem Cell Biol* 2007;39:44-84.
- Djordjevic VB. Free radicals in cell biology. *Int Rev Cytol* 2004;237:57-89.
- Wellman NS, Friedberg B. Causes and consequences of adult obesity: health, social and economic impacts in the United States. *Asia Pac J Clin Nutr* 2002;11:S705-S709.
- Furukawa S, Fujita T, Shimabukuro M, Iwaki M, Yamada Y, Nakajima Y, et al. Increased oxidative stress in obesity and its impact on metabolic syndrome. *J Clin Invest* 2004;114:1752-61.
- Maddux BA, See W, Lawrence JC Jr, Goldfine AL, Goldfine ID, Evans JL. Protection against oxidative stress-induced insulin resistance in rat L6 muscle cells by micromolar concentrations of alpha-lipoic acid. *Diabetes* 2001;50:404-10.
- Isomaa B, Almgren P, Tuomi T, Forsén B, Lahti K, Nissén M, et al. Cardiovascular morbidity and mortality associated with the metabolic syndrome. *Diabetes Care* 2001;24:683-9.
- Grundy SM. Atherosclerosis imaging and the future of lipid management. *Circulation* 2004;110:3509-11.
- Hansel B, Giral P, Nobecourt E, Chantepie S, Bruckert E, Chapman MJ, et al. Metabolic syndrome is associated with elevated oxidative stress and dysfunctional dense high-density lipoprotein particles displaying impaired antioxidative activity. *J Clin Endocrinol Metab* 2004;89:4963-71.
- Lakka HM, Laaksonen DE, Lakka TA, Niskanen LK, Kumpusalo E, Tuomilehto J, et al. The metabolic syndrome and total and cardiovascular disease mortality in middle-aged men. *JAMA* 2002;288:2709-16.
- Vincent HK, Taylor AG. Biomarkers and potential mechanisms of obesity-induced oxidant stress in humans. *Int J Obes (Lond)* 2006;30:400-18.
- Myara I, Alamowitch C, Michel O, Heudes D, Bariety J, Guy-Grand B, et al. Lipoprotein oxidation and plasma vitamin E in nondiabetic normotensive obese patients. *Obes Res* 2003;11:112-20.
- Russell AP, Gastaldi G, Bobbioni-Harsch E, Arboit P, Gobelet C, Dériaz O, et al. Lipid peroxidation in skeletal muscle of obese as compared to endurance-trained humans: a case of good vs. bad lipids? *FEBS Lett* 2003;11:104-6.
- Birdwell K. Role of pharmacogenomics in dialysis and transplantation. *Curr Opin Nephrol Hypertens* 2014;23:570-7.
- Parkinson A, Ogilvie BW, Buckley DB, Kazmi F, Czerwinski M, Parkinson O. Biotransformation of Xenobiotics. In: Klaassen CD, Watkins III JB, eds. *Casarett & Doull's Essentials of Toxicology*. 3rd ed. United States, 2015: pp. 79-108.
- Prakash C, Zuniga B, Song CS, Jiang S, Cropper J, Park S, et al. Nuclear receptors in drug metabolism, drug response and

drug interactions. *Nucl Receptor Res* 2015;2101178.

31. Haddad JJ, Land SC. O(2)-evoked regulation of HIF-1alpha and NF-kappaB in perinatal lung epithelium requires glutathione biosynthesis. *Am J Physiol Lung Cell Mol Physiol* 2000;278:L492-L503.

32. May JM. Ascorbate function and metabolism in the human erythrocyte. *Front Biosci* 1998;3:d1-10.

33. Powis G, Gasdaska JR, Gasdaska PY, Berggren M, Kirkpatrick DL, Engman L, et al. Selenium and the thioredoxin redox system: effects on cell growth and death. *Oncol Res* 1997;9:303-12.

34. Haddad JJ, Harb HL. L-gama-Glutamyl-L-cysteinyl-glycine (glutathione; GSH) and GSH-related enzymes in the regulation of pro- and antiinflammatory cytokines: a signaling transcriptional scenario for redox(y) immunologic sensor(s)? *Mol Immunol* 2005;42:987-1014.

35. Croom E. Metabolism of xenobiotics of human environments. *Prog Mol BiolTransl Sci* 2012;112:31-88.

36. Hoffmann MF, Preissner SC, Nickel J, Dunkel M, Preissner R, Preissner S. The transformer database: biotransformation of xenobiotics. *Nucleic Acids Res* 2014;42:1113-7.

37. Worku M, Aynalem M, Biset S, Woldu B, Adane T, Tigabu A. Role of complete blood cell count parameters in the diagnosis of neonatal sepsis. *BMC Pediatr* 2022;22:411.

38. Alston MC, Redman LM, Sones JL. An overview of obesity, cholesterol, and systemic inflammation in preeclampsia. *Nutrients* 2022;14:2087.

39. Klein S, Gastaldelli A, Yki-Järvinen H, Scherer PE. Why does obesity cause diabetes? *Cell Metab* 2022;34:11-20.

40. Lu D, Yuan Z, Gao Y, Liu W, Zhang J. Central obesity is associated with variations in TSH and ACTH levels among euthyroid obese individuals. *Int J Endocrinol* 2022;2022:3830380.

41. El-Zawawy HT, El-Aghoury AA, Katri KM, El-Sharkawy EM, Gad SMS. Cortisol/DHEA ratio in morbidly obese patients before and after bariatric surgery: relation to metabolic parameters and cardiovascular performance. *Int J Obes* 2022;46:381-92.

42. Sun Y, Teng D, Zhao L, Shi X, Li Y, Shan Z et al. Thyroid Disorders, Iodine Status and Diabetes Epidemiological Survey Group (TIDE) . Impaired Sensitivity to Thyroid Hormones Is

Associated with Hyperuricemia, Obesity, and Cardiovascular Disease Risk in Subjects with Subclinical Hypothyroidism. *Thyroid* 2022 32(4), 376-384.

43. Genchi VA, Rossi E, Lauriola C, D'Oria R, Palma G, Borrelli Aetal. Adipose tissue dysfunction and obesity-related male hypogonadism. *Int J Mol Sci* 2022;23:8194.

44. Esposito K, Ciotola M, Schisano B, Misso L, Giannetti G, Ceriello A, et al. Oxidative stress in the metabolic syndrome. *J Endocrinol Invest* 2006;29:791-5.

45. Pihl E, Zilmer K, Kullisaar T, Kairane C, Magi A, Zilmer M. Atherogenic inflammatory and oxidative stress markers in relation to overweight values in male former athletes. *Int J Obes (Lond)* 2006;30:141-6.

46. Chrysohoou C, Panagiotakos DB, Pitsavos C, Skoumas I, Papademetriou L, Economou M, et al. The implication of obesity on total antioxidant capacity apparently healthy men and women: The ATTICA study. *Nutr Metab Cardiovasc Dis* 2007;17:590-7.

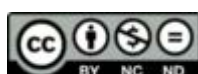
47. Hartwich J, Goralska J, Siedlecka D, Gruca A, Trzos M, Dembinska-Kiec A. Effect of supplementation with vitamin E and C on plasma hsCPR level and cobalt-albumin binding score as markers of plasma oxidative stress in obesity. *Genes Nutr* 2007;2:151-4.

48. Vincent H, Vincent K, Vourguignon C, Braith R. Obesity and postexercise oxidative stress in older women. *Med Sci Sports Exer* 2005;37:213-9.

49. Raunio H, Pasanen M, Maenpaa J, Hakkola J, Pelkonen O. Expression of extrahepatic cytochrome P450 in humans. In: Pacifici GM and Fracchia GN (eds) *Advances in Drug Metabolism in Man*: 234-287. European Commission, Office for Official Publications of the European Communities, Luxembourg, 1995.

50. Imaoka S, Yamada T, Hiroi T, Hayashi K, Sakaki T, Yabusaki Y, et al. Multiple forms of human P450 expressed in *Saccharomyces cerevisiae*, systematic characterization and comparison with those of the rat. *Biochem Pharmacol* 1996;51:1041-50.

51. Butura A, Nilsson K, Morgan K, Morgan TR, French SW, Johansson I, et al. The impact of CYP2E1 on the development of alcoholic liver disease as studied in a transgenic mouse model. *J Hepatol* 2009;50:572-83.



This is an open access article distributed under the terms of [Creative Commons Attribution-NonCommercial-NoDerivatives 4.0 International License](https://creativecommons.org/licenses/by-nc-nd/4.0/).

Investigation of general surgery consultations in COVID-19 patients treated in a tertiary hospital

Mehmet Eşref Ulutaş¹, Kemal Arslan²

¹Department of General Surgery, Derecik State Hospital, Hakkari, Turkey; ²Department of General Surgery, University of Health Sciences, Konya City Hospital, Konya, Turkey

ABSTRACT

Objectives: The aim of the study is to reveal the most common general surgery problems during the pandemic period in our center, where all departments only deal with COVID-19 patients.

Methods: In our study, general surgery consultations made between 1st November 2020 and 1st February 2021, when our center only served pandemic patients, were retrospectively examined. Demographic data of the patients, distribution of the departments where consultation was requested, reasons for consultation, pathology detection rate, treatment modalities, mortality rates and surgical procedures were included.

Results: A total of 70 patients, 33 female, and 37 male, were included in this study. The most common problems of the patients were gastrointestinal system (GIS) problems (46/70, 65.7%). The second most common problem was hepatopancreaticobiliary problems (12/70, 17.1%). This was followed by soft tissue disorders, hernia problems, and trauma cases, respectively. These were mostly treated medically, but surgical treatment was sometimes required (77.1% vs 22.9%).

Conclusions: As reported in the literature, the most common surgical pathologies in patients diagnosed with COVID-19 are usually related to the GIS. These pathologies can mostly be treated medically (73.9%). However, surgical treatment was more rarely required (26.1%). The highest rate of surgical treatment was for hernia patients (100%). In general, medical treatment was successful.

Keywords: General surgery, COVID-19, consultation, pandemic

With the COVID-19 pandemic, various medical associations published new guidelines on the management of diseases other than COVID-19 [1]. Based upon this, elective procedures were delayed in many health facilities, but emergency surgery and cancer cases have continued their routine process. In some centers, however, cancer and emergency surgical procedures were subject to various alterations. Uncomplicated appendicitis cases were treated medically in

some centers. In some centers, neoadjuvant therapy was preferred more frequently and primarily, especially in colorectal cancer cases [2-4].

In Turkey, a total of 2,470,901 COVID-19 cases have been detected from 11th March 2020, when the first COVID-19 case was detected, up to 4th March 2021. 12.2% of the cases were detected in Western Anatolian Region, in which our city is located. A study from Turkey reported that the number of emergency

Received: June 7, 2022; Accepted: January 7, 2023; Published Online: March 9, 2023



e-ISSN: 2149-3189

How to cite this article: Ulutaş ME, Arslan K. Investigation of general surgery consultations in COVID-19 patients treated in a tertiary hospital. Eur Res J 2023;9(3):555-560. DOI: 10.18621/eurj.1126832

Address for correspondence: Mehmet Eşref Ulutaş, MD., Derecik State Hospital, Department of General Surgery, Derecik 30802, Hakkari, Turkey. E-mail: esref_ulutas@hotmail.com, Phone: +90 332 221 00 00, Fax: +90 332 324 18 54



©Copyright © 2023 by Prusa Medical Publishing
Available at <http://dergipark.org.tr/eurj>
info@prusamp.com

surgery patients, inpatient treatment, and surgical interventions decreased by half in 2020 compared to the last 2 years [5].

The main purpose of this study is to explain which surgical diseases and problems may be encountered in patients with a diagnosis of COVID-19. However, detailed diagnoses and treatments were not elaborated on. Therefore, in our center, where all departments care only for COVID-19 patients, the distribution of general surgery consultations by departments, the rate of those with detected pathology from these consultations, treatments given, and the most common pathologies was investigated.

METHODS

This retrospective study was carried out between 1st November 2020 and 1st February 2021, during which the General Surgery Department at the University of Health Sciences, Konya Meram Training and Research Hospital cared only for pandemic patients. The ethics committee of the University of Health Sciences approved the study (Number: 21-170, Date: 12/02/21). The data were retrospectively obtained via the hospital's electronic file system and clinical notes. Investigated parameters included patients' demographic data, the distribution of the departments requesting a consultation, reasons for consultations, the rate of those with detected pathology, the rate of patients taken over by our department, ways of treatment given, mortality rates, and performed surgical procedures. Rates were calculated according to the per number of patients consulted.

Because the patients were COVID-19 positive, patients' physical examinations, work-ups, anesthesiology procedures, surgery, and postoperative follow-ups, and all other procedures were performed using protective equipment by taking all necessary protective measures.

Statistical Analysis

Descriptive statistics, including means, standard deviations, medians, minimums, maximums, frequencies, and rates, were calculated. For analyses, Statistical Package for the Social Sciences (SPSS), version 22.0 (SPSS Inc., Chicago, IL, ABD) program was used.

Table 1. Patient characteristics and reasons for consultation

Characteristics	n	%
Gender		
Male	37	52.9
Female	33	47.1
Reasons		
Gastrointestinal system		
Acute appendicitis	11	15.7
Constipation	9	12.9
Nonspecific abdominal pain	6	8.6
Malnutrition	5	7.1
Lower gastrointestinal bleeding	4	5.7
Ileus	3	4.3
Peptic ulcer and complications	1	1.4
Foreign body ingestion	2	2.9
Sigmoid volvulus	1	1.4
Perianal abscess	1	1.4
Diarrhea	1	1.4
Hemorrhoids	1	1.4
Inflammatory bowel	1	1.4
Hepatopancreaticobiliary system		
Cholecystitis	6	8.6
Mechanical jaundice	3	4.3
Pancreatitis	2	2.8
Portal vein thrombosis	1	1.4
Soft tissue disorders		
Surgical site infection		
Decubitus ulcer		
2. degree burn		
Hernia		
Incarcerated inguinal hernia	3	4.3
Incarcerated umbilical hernia	1	1.4
Trauma		
Firearm injury	1	1.4
Sharps injury	1	1.4

RESULTS

A total of 70 patients, 33 females and 37 males, were included in this study. In Table 1, patients' general features, the type of follow-up, and the reason for consultation are given in detail.

In Table 2, the distribution of the departments requesting consultation is given. Among the departments, the one that requested consultation most frequently was the Emergency Department (46/70, 65.7%). The second most common problem was hepatopancreaticobiliary problems (12/70, 17.1%). This was followed by soft tissue disorders, hernia problems, and trauma cases, respectively. Fourteen patients were consulted while being followed up in secondary and tertiary intensive care units (14/70, 20%).

Of the consulted patients, 16 were given surgical treatment (16/70, 22.9%), and 37 were given medical treatment (37/70, 52.9%). No surgical pathology was detected in the remaining 17 patients (17/70, 24.3%). Mortality was developed in only 1 of these patients (1/70, 1.4%).

In Table 3, a classification of the diseases and treatment approaches is given. The most common problems of the patients were gastrointestinal system problems (46/70, 65.7%). These include, in descending order, acute appendicitis (11/70, 15.7%), constipation (9/70, 12.9%), nonspecific abdominal pain (6/70, 8.6%), feeding problems (PEG and NG placement) (5/70, 7.1%), lower GI bleeding (4/70, 5.7%), ileus (3/70, 4.3%), peptic ulcer and its complications (1/70, 1.4%), foreign body ingestion (2/70, 2.9%), sigmoid volvulus (1/70, 1.4%), perianal abscess (1/70, 1.4%), gastroenteritis (1/70, 1.4%), thrombosed hemorrhoid

(1/70, 1.4%), and inflammatory bowel disease (1/70, 1.4%).

At the second rank were hepatopancreatic biliary system problems (12/70, 17.1%). These included cases of acute cholecystitis (6/70, 8.6%), mechanical jaundice (3/70, 4.3%), acute pancreatitis (2/70, 2.9%), and portal vein thrombosis (1/70, 1.4%).

At the third rank was soft tissue disorders (6/70, 8.6%). These included postoperative wound site infections (4/70, 5.7%), decubitus ulcers (1/70, 1.4%), and burn wounds (1/70, 1.4%).

Hernia problems were the fourth most common reason for admission (4/70, 5.7%). Of these, three patients were operated on for incarcerated inguinal hernia (3/70, 4.3%), and one patient was operated on urgently for incarcerated umbilical hernia (1/70, 1.4%).

Among the last causes of admission were trauma cases (2/70, 2.9%). One was a gunshot, and the other was a sharp injury. In the case of gunshot injury involving the lower extremities and anal region, the patient was followed up, as no surgical pathology was detected (1/70, 1.4%). The other case was followed up due to liver injury and did not require surgery (1/70, 1.4%).

DISCUSSION

In this study, general surgery-related problems of patients diagnosed with COVID-19 were hospitalized in the largest pandemic hospital in the city during the COVID-19 pandemic. Even though the disease disappears during these days of vaccination, the late-term

Table 2. The distribution of treatment types according to the services requested for consultation

Departments	Treatment types			Total n (%)
	Medical	Surgical	Conservative	
Emergency service	11 (15.7)	16 (22.9)	13 (18.6)	40 (57.1)
Others	12 (17.1)	0 (0)	4 (5.7)	16 (22.9)
Intensive care unit	14 (20)	0 (0)	0 (0)	14 (20)
Total	37 (56.5)	16 (18.8)	17 (24.6)	70 (100)

Table 3. The distribution of treatment types according to systems

	Surgical treatment n (%)	Medical and conservative treatment n (%)	Total
Gastrointestinal system	12 (26.1)	34 (73.9)	46
Hepatopancreaticobiliary system	0 (0)	12 (100)	12
Soft tissue disorders	0 (0)	6 (100)	6
Hernia	4 (100)	0 (0)	4
Trauma	0 (0)	2 (100)	2
Total	16 (22.9)	54 (77.1)	70

effects of COVID-19 will continue. In addition to respiratory problems, pathologies related to other systems will arise. This also includes the department of general surgery.

It will be beneficial to know surgical diseases that develop in patients being followed up with the diagnosis of COVID-19 and to take measures in arranging treatment of these diseases. Therefore, our study is important to be the first one in reporting general surgery pathologies that develop in patients diagnosed with COVID-19.

In previous studies conducted with COVID-19 patients, gastrointestinal system problems have been reported to be common. It has been revealed that the tropism of the SARS coronavirus (SARS-CoV) to the gastrointestinal system (bowel) has been verified by the detection of the virus in biopsy specimens and stools of even discharged patients, and this, thusly, may provide partial explanations for gastrointestinal symptoms [6, 7]. The frequency of gastrointestinal symptoms, including nausea and/or diarrhea, was reported as under 5% by some authors and as high as 50% by others [8]. Apart from these problems, ileus, constipation, mesenteric ischemia, and feeding problems are also observed. Although these GIS complications are thought to be associated with pharmacological adverse events and metabolic and electrolyte disorders, vascular thromboses or viral enteroneuropathies, which are induced by severe COVID-19 respiratory problems, may also lead to this [9]. In a previous study, it was reported that the presence of gastrointestinal symptoms might be associated with a longer duration of hospital stay, a lower rate of

ICU admission, and lower mortality among COVID-19-positive patients. This, in turn, has led to the comment that COVID-19 may have a slower progression in those with GIS symptoms [10].

In our study, the patients consulted our department most commonly for GIS pathologies (65.7%). Among these, the most common surgical pathology was acute appendicitis, and the most common pathology treated medically was constipation (15.7%-12.9%). This was followed by, in descending order, nonspecific abdominal pain, feeding problems, and diarrhea. We are in thought of impaired mobilization of patients due to low oxygen saturation and increased constipation. Furthermore, the necessity of uninterrupted use of noninvasive and invasive ventilators raises feeding problems for patients. This, in turn, leads to a consultation with the department of general surgery for the resolution of enteral feeding problems. In some studies, enterally-fed patients had higher respiratory complication rates, and longer duration of noninvasive ventilation (NIV) compared to that unfed enterally [11]. Preference for parenteral nutrition is more appropriate for these patients, as enteral feeding methods may cause nasogastric air leaks and endanger the effectiveness of NIV or CPAP [12]. Therefore, the preference for enteral routes for patients without these mentioned risks is recommended [13]. Also, in our clinic, interventions for enteral feeding of these patients were performed, and enteral feeding was provided by placing nasogastric or orogastric tubes.

Another important GIS pathology is GIS bleeding. COVID-19 cases presenting with GIS bleeding have been reported in the literature [14]. However, since an-

tiaggregant therapy is usually routinely used in these patients, these bleeding conditions may arise. We think that antiaggregant therapy may have affected bleeding in our patients. Predisposition to embolism in these patients has been reported in several studies. If there is no abundant bleeding that may impair the stability of the patient, these patients may continue their antiaggregant therapy with appropriate blood transfusions and monitoring. In the patients we followed up on, this bleeding stopped with medical treatment, and blood transfusions and antiaggregant therapies were not discontinued.

The second most common pathologies are hepatopancreatobiliary system pathologies (17.1%). These include acute cholecystitis, obstructive jaundice, acute pancreatitis, and portal vein thrombosis. In some studies in the literature, an increase in the incidence of acute acalculous cholecystitis in patients with a long hospital stay due to COVID-19 was reported [15]. However, our patients more commonly had calculous cholecystitis. Antibiotherapy of these patients was arranged, and the patients were cured with medical treatment and then discharged with the recommendation of elective cholecystectomy. Some authors determined an association between acute pancreatitis and COVID-19 that causes patients to have a higher risk of multiorgan insufficiency, morbidity, and mortality [16]. In our clinic, the cases that developed pancreatitis were successfully treated with medical treatment. In the literature, the development of portal vein thrombosis was reported in patients with SARS-CoV-2 infection. This, in turn, was reported to be associated with a hypercoagulability state in these patients and COVID-19-related increased risk of venous thrombosis [17, 18]. Portal vein thrombosis observed in one of our patients was evaluated in this manner, the medical treatment was arranged in the clinic, the patient was hospitalized, and the patient was then discharged with a cure.

It is possible to carry on the treatment of the patients consulted to the department of general surgery in the department that hospitalized the patient. In our study, this seems to be succeeded with a rate of 67.1%.

Limitations

Limitations of this study include a limited number of patients, being a single-center study, lack of randomization, and retrospective design of the study.

CONCLUSION

In conclusion, considering all departments and diseases, the patients consulted by the department of general surgery were treated medically to a great extent (77.1%). All of the operated patients were those consulted from the emergency department. The mortality rate was low (1.45%). Follow-up and treatment of all diseases can be successfully conducted when the measures were taken with the appropriate types of equipment. This study addresses the diseases and conditions that may be encountered in patients diagnosed with COVID-19. In this manuscript, diagnoses and treatments of these diseases were not elaborated. Addressing these diseases' diagnoses and treatments elaborately is another study's subject. Addressing Patients' diagnoses and treatments were not elaborated on, as addressing diagnoses and treatments of consulted patients in detail is another study's subject. Explaining the situations which surgeons in hospitals caring for patients diagnosed with COVID-19 may encounter is the objective of this study.

Authors' Contribution

Study Conception: MEU; Study Design: MEU; Supervision: KA; Funding: MEU; Materials: MEU; Data Collection and/or Processing: MEU; Statistical Analysis and/or Data Interpretation: MEU; Literature Review: MEU; Manuscript Preparation: KA and Critical Review: KA.

Conflict of interest

The authors disclosed no conflict of interest during the preparation or publication of this manuscript.

Financing

The authors disclosed that they did not receive any grant during conduction or writing of this study.

REFERENCES

1. American College of Surgeon COVID-19: Elective case triage guidelines for surgical care. <https://www.facs.org/covid-19/clinical-guidance/elective-case>.
2. COVIDSurg Collaborative. Global guidance for surgical care during the COVID-19 pandemic. *Br J Surg* 2020;107:1097-103.
3. Søreide K, Hallet J, Matthews JB, Schnitzbauer AA, Line PD, Lai PBS, et al. Immediate and long-term impact of the COVID-

- 19 pandemic on delivery of surgical services. *Br J Surg* 2020;107:1250-61.
4. Di Saverio S, Pata F, Khan M, Ietto G, Zani E, Carcano G. Convert to open: the new paradigm for surgery during COVID-19? *Br J Surg* 2020;107:e194.
5. Alimoglu O, Erol CI, Kayali A, Acar M, Colapkulu N, Leblebici M, et al. Emergency surgery during COVID-19 pandemic; What has changed in practice? *Br J Surg* 2020;107:e581-2.
6. Gu J, Han B, Wang J. COVID-19: gastrointestinal manifestations and potential fecal-oral transmission. *Gastroenterology* 2020;158:1518-9.
7. Zhou Z, Zhao N, Shu Y, Han S, Chen B, Shu X. Effect of gastrointestinal symptoms in patients with COVID-19. *Gastroenterology* 2020;158:2294-7.
8. Huang C, Wang Y, Li X, Ren L, Zhao J, Hu Y, et al. Clinical features of patients infected with 2019 novel coronavirus in Wuhan, China. *Lancet* 2020;395:497-506.
9. Kaafarani HM, El Moheb M, Hwabejire JO, Naar L, Christensen MA, Breen K, et al. Gastrointestinal complications in critically ill patients with COVID-19. *Ann Surg* 2020;272:e61-2.
10. Nobel YR, Phipps M, Zucker J, Lebwohl B, Wang TC, Sobieszczyk ME, et al. Gastrointestinal symptoms and coronavirus disease 2019: a case-control study from the United States. *Gastroenterology* 2020;159:373-5.
11. Caccialanza R, Laviano A, Lobascio F, Montagna E, Bruno R, Ludovisi S, et al. Early nutritional supplementation in non-critically ill patients hospitalized for the 2019 novel coronavirus disease (COVID-19): rationale and feasibility of a shared pragmatic protocol. *Nutrition* 2020;74:110835.
12. Singer P, Rattanachaiwong S. To eat or to breathe? The answer is both! Nutritional management during noninvasive ventilation. *Crit Care* 2018;22:27.
13. Barazzoni R, Bischoff SC, Breda J, Wickramasinghe K, Krznaric Z, Nitzan D, et al. ESPEN expert statements and practical guidance for nutritional management of individuals with SARS-CoV-2 infection. *Clin Nutr* 2020;39:1631-8.
14. Gulen M, Satar S. Uncommon presentation of COVID-19: gastrointestinal bleeding. *Clin Res Hepatol Gastroenterol* 2020;44:e72-6.
15. Wahid N, Bhardwaj T, Borinsky C, Tavakkoli M, Wan D, Wong T, et al. Acute acalculous cholecystitis during severe COVID-19 hospitalizations. *Am J Gastroenterol* 2020;115:S794.
16. Dirweesh A, Li Y, Trikudanathan G, Mallery JS, Freeman ML, Amateau SK, et al. Clinical outcomes of acute pancreatitis in patients with coronavirus disease 2019. *Gastroenterology* 2020;159:1972-4.
17. Franco-Moreno A, Piniella-Ruiz E, Montoya-Adarraga J, Balzano-Franco C, Alvarez-Miguel F, Peinado-Martinez C, et al. Portal vein thrombosis in a patient with COVID-19. *Thromb Res* 2020;194:150-2.
18. Borazjani R, Seraj SR, Fallahi MJ, Rahmanian Z. Acute portal vein thrombosis secondary to COVID-19: a case report. *BMC Gastroenterol* 2020;20:386.



This is an open access article distributed under the terms of [Creative Commons Attribution-NonCommercial-NoDerivatives 4.0 International License](https://creativecommons.org/licenses/by-nc-nd/4.0/).

Evaluation of the uric acid and hematological parameters in patients with nodal hand osteoarthritis

Ayşe Ünal Enginar 

Department of Rheumatology, Konya City Hospital, Konya, Turkey

ABSTRACT

Objectives: To compare patients with symptomatic nodal hand osteoarthritis (OA) with a control group in respect of inflammation parameters, uric acid, and hematological parameters.

Methods: The study included 50 post-menopausal female patients, aged 40-80 years, diagnosed with symptomatic nodal hand OA, and a control group of 50 post-menopausal females in the same age range with no hand OA. Patient data including age, monocyte, neutrophil, lymphocyte, and thrombocyte counts, erythrocyte sedimentation rate (ESR), C-reactive protein (CRP) level, uric acid level, and the Kellgren-Lawrence (KL) score obtained from evaluations of hand radiographs, were recorded retrospectively from the hospital information system. The neutrophil-lymphocyte ratio (NLR), platelet-lymphocyte ratio (PLR), and monocyte-lymphocyte ratio (MLR) were calculated. The data were compared between the two groups.

Results: The data of 100 females were compared, comprising a patient group of 50 patients with symptomatic nodal OA, and a control group of 50 females. Age, monocyte, neutrophil, lymphocyte, and thrombocyte counts, NLR, PLR, MLR, ESR, CRP, and uric acid level were compared. With the exception of MLR and ESR, no statistically significant difference was determined between the two groups. The MLR was determined to be statistically significantly higher in the control group than in the patient group ($p = 0.024$). The ESR was determined to be statistically significantly higher in the patient group than in the control group ($p < 0.001$). When patients with a KL score of 2 and 3 were compared, with the exception of age, no other difference was determined. Patients with a KL score of 3 were seen to be significantly older ($p = 0.032$).

Conclusions: ESR was determined to be significantly higher in patients with symptomatic nodal OA. Clarification of the relationship between inflammation, uric acid, and hand OA, which is a heterogeneous disease, will be useful in the follow-up and treatment of patients.

Keywords: Hand osteoarthritis, monocyte-lymphocyte ratio, neutrophil-lymphocyte ratio, uric acid, erythrocyte sedimentation rate, C-reactive protein

Osteoarthritis (OA) is the most commonly seen joint disease worldwide. The frequency of OA is increased together with an increase in obesity and ageing [1]. The hand is one of the most frequently involved areas, and hand OA is seen more often in

females [2]. In the Framingham study, the incidence of radiographic hand OA was determined to be 34%, and the incidence of symptomatic hand OA was 7% [3]. Symptoms may be in the form of pain, stiffness, restricted movement, and decreased grip strength.

Received: December 3, 2022; Accepted: March 13, 2023; Published Online: March 30, 2023



©-ISSN: 2149-3189

How to cite this article: Ünal Enginar A. Evaluation of the uric acid and hematological parameters in patients with nodal hand osteoarthritis. Eur Res J 2023;9(3):561-556. DOI: 10.18621/eurj.1214186

Address for correspondence: Ayşe Ünal Enginar, MD., Konya City Hospital, Department of Rheumatology, Akabe Mah., Adana Çevre Yolu Cad., No:135, 42020, Konya, Turkey. E-mail: ftrdayseenginar@gmail.com, Phone: +90 332 310 50 00



©Copyright © 2023 by Prusa Medical Publishing
Available at <http://dergipark.org.tr/eurj>
info@prusamp.com

Hand OA is a heterogenous disease [4]. Obesity and genetic factors are significant risk factors for hand OA [5]. Hand OA can be separated into subgroups of first carpometacarpophalangeal joint OA, erosive joint OA, and nodal hand OA. In the subgroup of nodal OA, there may be nodules in the distal interphalangeal and proximal interphalangeal joints. These nodules are named Heberden and Bouchard nodules, respectively [2]. Mechanical, inflammatory, and metabolic factors are involved in the pathogenesis of OA. In the light of new information about the pathogenesis in the last 10 years, OA is now defined as a multifactorial diseases characterised by low-grade chronic inflammation, rather than as a degenerative disease which progresses with wear and destruction.

Unlike rheumatoid arthritis, there is chronic, low-grade inflammation mediated by the immune system from birth [6, 7]. There is no specific laboratory test for OA, although the erythrocyte sedimentation rate (ESR), and C-reactive protein (CRP) level may be slightly increased in OA patients. This is more evident in patients with erosive hand OA [8]. There are few studies related to the parameters of uric acid [9, 10], neutrophil-lymphocyte ratio (NLR) and platelet-lymphocyte ratio (PLR) in OA, and these studies have been conducted more on patients with knee OA [11-13].

The aim of this study was to evaluate these parameters, which are often used in daily practice, in patients with symptomatic nodal hand OA.

METHODS

The study included 50 post-menopausal females in the age range of 40-80 years, who presented at the Rheumatology Clinic between January and May 2022, and were diagnosed with symptomatic nodal hand OA according to the American College of Rheumatology (ACR) hand OA classification criteria. A control group was formed of 50 post-menopausal females in the age range of 40-80 years, with no hand OA. Patient data including age, monocyte, neutrophil, lymphocyte, and thrombocyte counts, ESR, CRP level, uric acid level, and the Kellgren-Lawrence (KL) score obtained from evaluations of hand radiographs, were recorded retrospectively from the hospital information system. The NLR, PLR, and monocyte-lymphocyte ratio (MLR)

were calculated.

Patients and control subjects were excluded from the study if they were pregnant, had any malignant disease, active infection, erosive hand OA, rheumatoid arthritis, psoriasis, psoriatic arthritis, gout, chondrocalcinosis, chronic liver or kidney disease, were using diuretics, or had any trauma-related deformity or contracture in the hand joints.

The study protocol was approved by the Ethics Committee of Necmettin Erbakan University Faculty of Medicine (Decision number 2022/3849).

Statistical Analysis

The SAS version 9.4 was used for statistical analysis. While evaluating the study data, descriptive statistics, including the mean, standard deviation, median, frequency, ratio, minimum and maximum values were obtained. The Kolmogorov-Smirnov test was conducted to check the normality distribution of independent data. Since the data were found to be non-normally distributed, the independent mann Whitney U test was used for the comparative analysis. The chisquare test was used for the analysis of qualitative independent data. Pearson correlation coefficient (rs) was used for correlations between parametric data. Statistical significance was accepted as $p < 0.05$.

RESULTS

The findings of 100 females were compared, comprising a patient group of 50 patients with symptomatic nodal OA, and a control group of 50 females. Age, monocyte, neutrophil, lymphocyte, and thrombocyte counts, NLR, PLR, MLR, ESR, CRP, and uric acid level were compared. With the exception of MLR and ESR, no statistically significant difference was determined between the two groups. The MLR was determined to be statistically significantly higher in the control group than in the patient group ($p = 0.024$). The ESR was determined to be statistically significantly higher in the patient group than in the control group ($p < 0.001$) (Table 1). When patients with a KL score of 2 and 3 were compared, with the exception of age, no other difference was determined. Patients with a KL score of 3 were seen to be significantly older ($p = 0.032$) (Table 2).

Table 1. Relationship of blood parameters between osteoarthritis patients and the control group

	Groups		p value
	Patient (n = 50) Median (IQR) n (%)	Control (n = 50) Median (IQR) n (%)	
Age (years)	65.0 (60.0-68.0)	61.5 (59.0-65.0)	0.13
Neutrophil (× 10 ⁹ /L)	3.5 (3.0-5.1)	3.9 (3.2-4.8)	0.64
Lymphocyte (× 10 ⁹ /L)	2.3 (2.1-3.0)	2.4 (1.9-2.9)	0.59
Monocyte (× 10 ⁹ /L)	0.6 (0.5-0.7)	0.6 (0.6-0.8)	0.13
Platelet (× 10 ⁹ /L)	241.5 (202.0-293.0)	275.0 (225.0-323.0)	0.06
NLR	1.5 (1.3-2.0)	1.7 (1.4-2.0)	0.24
PLR	100.9 (85.5-120.9)	109.6 (91.5-140.5)	0.05
MLR	0.2 (0.2-0.3)	0.3 (0.2-0.3)	0.024
Uric acid (mg/dL)	4.6 (3.7-5.9)	4.4 (3.1-5.5)	0.12
ESR (mm/h)	20.5 (16.0-26.0)	7.5 (3.0-18.0)	< 0.001
CRP (mg/dL)	2.0 (1.3-3.0)	2.4 (1.5-3.6)	0.45
KL score			
Grade 2	43 (86.00)	00 (0.00)	
Grade 3	07 (14.00)	00 (0.00)	

NLR = neutrophil-lymphocyte ratio, PLR = platelet-lymphocyte ratio, MLR = monocyte-lymphocyte ratio, ESR = erythrocyte sedimentation rate, CRP = C-reactive protein, KL = Kellgren-Lawrence

Table 2. Comparison of KL score

	KL score		p value
	Grade 2 (n = 43) Median (IQR)	Grade 3 (n = 7) Median (IQR)	
Age (years)	64.0 (58.0-67.0)	68.0 (66.0-73.0)	0.032
Neutrophil (× 10 ⁹ /L)	3.5 (3.0-5.1)	3.9 (3.5-5.2)	0.20
Lymphocyte (× 10 ⁹ /L)	2.3 (2.1-3.0)	2.3 (2.1-3.0)	1.00
Monocyte (× 10 ⁹ /L)	0.6 (0.5-0.7)	0.7 (0.5-0.8)	0.39
Platelet (× 10 ⁹ /L)	235.0 (200.0-292.0)	284.0 (234.0-333.0)	0.14
NLR	1.5 (1.3-2.0)	1.8 (1.0-2.2)	0.62
PLR	100.9 (85.4-118.6)	104.0 (94.2-149.3)	0.29
MLR	0.2 (0.2-0.3)	0.3 (0.2-0.3)	0.39
Uric acid (mg/dL)	4.7 (3.7-5.9)	4.5 (3.7-5.8)	0.98
ESR (mm/h)	20.0 (15.0-25.0)	22.0 (18.0-29.0)	0.17
CRP (mg/dL)	2.1 (1.3-3.0)	1.9 (1.2-4.5)	0.82

KL = Kellgren-Lawrence, NLR = neutrophil-lymphocyte ratio, PLR = platelet-lymphocyte ratio, MLR = monocyte-lymphocyte ratio, ESR = erythrocyte sedimentation rate, CRP = C-reactive protein

DISCUSSION

The results of this study demonstrated that ESR was higher and the MLR was lower in females with nodal hand OA. In a study by Gao *et al.*, it was reported that the MLR could be diagnostic in patients with knee OA. Patients with a KL score of grade 3 and 4 were included and the MLR was determined to be statistically significantly higher in patients at KL grade 4 compared to those at grade 3 [11]. The current study examined patients with hand OA and KL score of grade 2 and 3, but the greater number of patients with grade 2 could have affected the results. Shi *et al.* [12] reported that PLR could show inflammation in knee OA. In another study, no relationship was determined between NLR and symptomatic knee OA [13]. In the current study, no difference was determined between the patients and the control group in respect of NLR and PLR.

In a previous meta-analysis, high-sensitive CRP (hsCRP) levels were determined to be at a moderately high level in patients with OA. A relationship was determined between hsCRP and clinical symptoms such as pain and function loss, but no correlation was determined between hsCRP and the KL score [15].

In another study that included 694 patients with hand OA, no relationship was determined between radiographic OA and inflammatory biomarkers [16]. Levels of hsCRP have been determined to be significantly higher in patients with erosive OA compared to patients with non-erosive OA [17]. A correlation has been shown between pain and higher body mass index (BMI) in patients with hand OA, and it has been reported that low-grade inflammation measured with hsCRP could be associated with pain in obese patients [18]. In a study of patients with advanced stage knee and /or hip OA, the CRP level was reported to be higher in females and elevated CRP was found to be correlated with joint pain [19]. Another study reported that ESR and the hsCRP level in patients with knee OA were higher than in patients without knee OA [20]. Erosive OA patients were compared with non-erosive OA patients in another study, and ESR and CRP levels were found to be higher in the non-erosive group [21]. In the current study, although ESR was found to be higher in the patients than in the control group, no sig-

nificant difference was determined in respect of CRP. However, most previous studies have used hsCRP, and this difference could be related to that.

There are studies in literature which have aimed to understand the relationship between OA, uric acid, and gout, but this relationship has not yet been clearly explained. The combination of gout and OA is known. It is thought that hyperuricemia could lead to the progression of OA, or there could be a two-way relationship between a predisposition to the development of gout in a joint with OA [22, 23].

Ding *et al.* [9] reported that there was a relationship between hyperuricemia and osteophytes in females with knee OA. In another study of 71 patients with knee OA, more abnormalities were observed on MRI in those with high levels of serum uric acid [10]. From a study in which patients with knee OA and no gout were followed up for 24 months, there was observed to be greater narrowing of the joint space in those with a high level of uric acid [24]. In another cohort study, no significant relationship was determined between tibiofemoral cartilage loss seen on MRI and serum uric acid level [25]. Uric acid can activate NLRP3 (Nucleotide-binding domain, leucine-rich repeat and pyrin domain containing protein 3) and as a result, IL-18 and IL-1 β levels increase. In a study that analyzed the synovial fluid of patients with knee OA and no gout, increased IL-18 and IL-1 β levels were found to be correlated with the serum uric acid level. This was determined radiographically and scintigraphically to be related to the severity of knee OA [26]. It has been reported that while uric acid at low concentrations is chondroprotective and anti-inflammatory [27], at high levels it can trigger OA. Therefore, it may play an antioxidant or pro-oxidant role [28]. In the current study, uric acid was determined at a higher level in the OA patients than in the control group, but the difference was not determined to be statistically significant, and no difference was determined between patients with KL score of 2 and 3.

Limitations

Limitations of this study can be said to be that it was conducted in a single centre, the number of patients was relatively low, and comorbidities were not reported.

CONCLUSION

In conclusion, the results of this study demonstrated that the ESR was significantly higher in patients with symptomatic nodal hand OA compared to the control group. However, as hand OA is a heterogenous disease, there is a need for further studies related to uric acid and inflammation parameters.

Authors' Contribution

Study Conception: AUE; Study Design: AUE; Supervision: AUE; Funding: AUE; Materials: AUE; Data Collection and/or Processing: AUE; Statistical Analysis and/or Data Interpretation: AUE; Literature Review: AUE; Manuscript Preparation: AUE and Critical Review: AUE.

Conflict of interest

The authors disclosed no conflict of interest during the preparation or publication of this manuscript.

Financing

The authors disclosed that they did not receive any grant during conduction or writing of this study.

REFERENCES

- Hunter DJ, Bierma-Zeinstra S. Osteoarthritis. *Lancet* 2019;393:1745-59.
- Marshal M, Watt FE, Vincent TL, Dziedzic K. Hand osteoarthritis: clinical phenotypes, molecular mechanisms and disease management. *Nat Rev Rheumatol* 2018;14:641-56.
- Zhang Y, Niu J, Kelly-Hayes M, Chaisson CE, Aliabadi P, Felson DT. Prevalence of symptomatic hand osteoarthritis and its impact on functional status among the elderly: the Framingham study. *Am J Epidemiol* 2002;156:1021-7.
- Kloppenburg M, Kwok W-Y. Hand osteoarthritis -a heterogeneous disorder. *Nat Rev Rheumatol* 2012;8:22-31.
- Plotz B, Bomfim F, Sohail MA, Samuels J. Current epidemiology and risk factors for the development of hand osteoarthritis. *Curr Rheumatol Rep* 2021;23:61.
- Robinson WH, Lepus CM, Wang Q, Raghu H, Mao R, Lindstrom TM, et al. Low-grade inflammation as a key mediator of the pathogenesis of osteoarthritis. *Nat Rev Rheumatol* 2016;12:580-92.
- Berenbaum F. Osteoarthritis as an inflammatory disease (osteoarthritis is not osteoarthrosis!). *Osteoarthritis Cartilage* 2013;21:16-21.
- Favero M, Belluzzi E, Ortolan A, Lorenzin M, Oliviero F, Doria A, et al. Erosive hand osteoarthritis: Latest findings and outlook. *Nat Rev Rheumatol* 2022;18:171-83.
- Ding X, Zeng C, Wei J, Li H, Yang T, Zhang Y, et al. The associations of serum uric acid level and hyperuricemia with knee osteoarthritis. *Rheumatol Int* 2016;36:567-73.
- Xiao L, Lin S, Zhan F. The association between serum uric acid level and changes of MRI findings in knee osteoarthritis: a retrospective study (A STROBE-compliant article). *Medicine (Baltimore)* 2019;98:e1581.
- Gao K, Zhu W, Liu W, Ma D, Li H, Yu W, et al. Diagnostic value of the blood monocyte-lymphocyte ratio in knee osteoarthritis. *J Int Med Res* 2019;47:4413-21.
- Shi J, Zhao W, Ying H, Du J, Chen J, Chen S, et al. The relationship of platelet to lymphocyte ratio and neutrophil to monocyte ratio to radiographic grades of knee osteoarthritis. *Z Rheumatol* 2017;77:533-7.
- Ionitescu M, Vermeşan D, Haraguş H, Sucui O, Todor A, Dumitraşcu CV, et al. Association of neutrophil to lymphocyte ratio with patient reported outcomes in knee osteoarthritis. *Appl Sci* 2020;10:8173.
- Altman R, Alarcon G, Appelrouth D, Bloch D, Borenstein D, Brandt K, et al. The American College of Rheumatology criteria for the classification and reporting of osteoarthritis of the hand. *Arthritis Rheum* 1990;33:1601-10.
- Jin X, Beguerie JR, Zhang W, Blizzard L, Otahal P, Jones G, et al. Circulating C reactive protein in osteoarthritis: a systematic review and meta-analysis. *Ann Rheum Dis* 2015;74:703-10.
- Vlad SC, Neogi T, Aliabadi P, Fontes JDT, Felson DT. No association between markers of inflammation and osteoarthritis of the hands and knees. *J Rheumatol* 2011;38:1665-70.
- Punzi L, Ramonda R, Oliviero F, Sfriso P, Mussap M, Plebani M, et al. Value of C reactive protein in the assessment of erosive osteoarthritis of the hand. *Ann Rheum Dis* 2005;64:955-7.
- Gløersen M, Steen Pettersen P, Neogi T, Jafarzadeh SR, Vistnes M, Thudium CS, et al. Associations of body mass index with pain and the mediating role of inflammatory biomarkers in people with hand osteoarthritis. *Arthritis Rheumatol* 2022;74:810-7.
- Perruccio AV, Chandran V, Power JD, Kapoor M, Mahomed NN, Gandhi R. Systemic inflammation and painful joint burden in osteoarthritis: a matter of sex? *Osteoarthritis Cartilage* 2017;25:53-9.
- Hanada M, Takahashi M, Furuhashi H, Koyama H, Matsuyama Y. Elevated erythrocyte sedimentation rate and high-sensitivity C-reactive protein in osteoarthritis of the knee: relationship with clinical findings and radiographic severity. *Ann Clin Biochem* 2016;53(Pt 5):548-53.
- Olejárová M, Kupka K, Pavelka K, Gatterova J, Sholfa J. Comparison of clinical, laboratory, radiographic, and scintigraphic findings in erosive and nonerosive hand osteoarthritis. Results of a two-year study. *Joint Bone Spine* 2000;67:107-12.
- Ma CA, Leung YY. Exploring the link between uric acid and osteoarthritis. *Front Med (Lausanne)* 2017;4:225.
- Neogi T, Krasnokutsky S, Pillinger MH. Urate and osteoarthritis: evidence for a reciprocal relationship. *Joint Bone Spine* 2019;86:576-82.
- Krasnokutsky S, Oshinsky C, Attur M, Ma S, Zhou H, Zheng F, et al. Serum urate levels predict joint space narrowing in non-gout patients with medial knee osteoarthritis. *Arthritis Rheumatol*

2017;69:1213-20.

25. Go DJ, Kim DH, Kim JY, Guermazi A, Crema MD, Hunter DJ, et al. Serum uric acid and knee osteoarthritis in community residents without gout: a longitudinal study. *Rheumatology (Oxford)* 2021;60:4581-90.

26. Denoble AE, Huffman KM, Stabler TV, Kelly SJ, Hershfield MS, McDaniel GE, et al. Uric acid is a danger signal of increasing risk for osteoarthritis through inflammasome activation. *Proc*

Natl Acad Sci U S A 2011;108:2088-93.

27. Lai JH, Luo SF, Hung LF, Huang CY, Lien SB, Lin LC, et al. Physiological concentrations of soluble uric acid are chondroprotective and anti-inflammatory. *Sci Rep* 2017;7:2359.

28. Neogi T, George J, Rekhraj S, Choi H, Terkeltaub RE. Are either or both hyperuricemia and xanthine oxidase directly toxic to the vasculature? A critical appraisal. *Arthritis Rheum* 2012;64:327-38.



This is an open access article distributed under the terms of [Creative Commons Attribution-NonCommercial-NoDerivatives 4.0 International License](https://creativecommons.org/licenses/by-nc-nd/4.0/).

Protective effects of methylprednisolone in kidney: aortic occlusion-reperfusion model in rats

Serkan Seçici¹, Kadir Kaan Özsin², M. Özgür Özyiğit³, Ömer Arda³, Yasemin Üstündağ⁴

¹Department of Pediatric Cardiovascular Surgery, Medicana Bursa Hospital, Bursa, Turkey; ²Department of Cardiovascular Surgery, Bursa Yüksek İhtisas Training and Research Hospital, Bursa, Turkey; ³Department of Pathology, Uludag University, Faculty of Veterinary Medicine, Bursa, Turkey; ⁴Department of Clinical Biochemistry, Bursa Yüksek İhtisas Training and Research Hospital, Bursa, Turkey

ABSTRACT

Objectives: Ischemia/reperfusion (I/R) injury is commonly seen in cardiovascular surgery, activates inflammation and causes renal damage. In this experimental study, we aimed to assess the effects of different doses (5 and 30 mg/kg) of methylprednisolone (MP), which has anti-inflammatory effect, on renal ischemia/reperfusion (I/R) injury.

Methods: Thirty-two male Wistar albino rats were randomly divided into four groups (n = 8). The sham group underwent midline laparotomy and dissection of the abdominal aorta without occlusion while the I/R group underwent suprarenal aortic ischemia for 45 minutes followed by 180 minutes of reperfusion. In the 5 mg/kg MP and 30 mg/kg MP groups, MP was administered intraperitoneally. At the end of the experiment, blood samples were obtained, and kidneys were extracted.

Results: Pretreatment with methylprednisolone did not influence serum BUN and creatinine levels. Serum TNF- α levels and ischemia-modified albumin levels were significantly lower in the MP groups compared to the I/R group ($p < 0.05$). Histological examination demonstrated severe injury in the I/R group and treatment with MP attenuated the severity. The difference was significant in doses of 30 mg/kg MP.

Conclusions: This results of the model of renal I/R injury presented in this work reveal the anti-inflammatory and the protective effects of MP in cases of renal I/R.

Keywords: Ischemia-reperfusion injury, kidney, methylprednisolone, inflammation

Ischemia-reperfusion (I/R)-induced acute renal injury is a significant complication and one of the most important causes of morbidity and mortality in cardiovascular surgery [1]. Lack of oxygen caused by ischemia leads to a shift to anaerobic glycolysis, depletion of ATP, increased intracellular calcium, and formation of reactive oxygen species (ROS), resulting in cell apoptosis and necrosis [2]. While restoring the blood flow can save the affected tissue, it also acti-

vates inflammatory mediators, leading to leukocyte activation and leukocyte endothelial adhesion, which may in turn cause multi-organ dysfunction and death [3, 4].

Glucocorticoids have been used for their anti-inflammatory and immunosuppressive effects [5]. Methylprednisolone (MP) is a synthetic glucocorticoid with many systemic effects, the most important of which include anti-inflammatory, immunosuppressive,

Received: September 29, 2022; Accepted: December 1, 2022; Published Online: April 2, 2023



e-ISSN: 2149-3189

How to cite this article: Seçici S, Özsin KK, Özyiğit MÖ, Arda Ö, Üstündağ Y. Protective effects of methylprednisolone in kidney: aortic occlusion-reperfusion model in rats. Eur Res J 2023;9(3):567-573. DOI: 10.18621/eurj.1181742

Address for correspondence: Serkan Seçici, MD., Bursa Medicana Hospital, Department of Pediatric Cardiovascular Surgery, Odunluk Mah., İzmir Yolu Cad., No: 41, 16110 Nilüfer, Bursa, Turkey. E-mail: serkansecici@hotmail.com, Phone: +90 224 970 01 01



©Copyright © 2023 by Prusa Medical Publishing
Available at <http://dergipark.org.tr/eurj>
info@prusamp.com

and catabolic effects in protein metabolism. It was previously demonstrated that steroid administration in cases of renal I/R injury protected the morphology of tubular epithelium while reducing leukocyte infiltration and plasma interleukin-6 and serum creatinine concentrations in kidney tissues [6, 7].

Considering the data reported in the literature to date, we aimed to investigate the protective effects of different doses of MP against renal I/R injury in this experimental study.

METHODS

This study was approved by the Local Experimental Animal Ethics Committee of Uludag University with the number of 2018-04/07. Thirty-two male Wistar albino rats weighting 200-250 gr were employed for the study. All rats were permitted free access to standard chow and drinking water. They were maintained on a 12:12-hour light/dark cycle at a temperature of 22 ± 2°C. The included rats were randomly assigned to one of four groups with each group comprising eight animals. The rats were anesthetized intraperitoneal with 50 mg/kg ketamine hydrochloride (Ketalar, Eczacıbasi, Istanbul, Turkey) and 5 mg/kg xylazine hydrochloride (Rompun, Bayer, Istanbul, Turkey). Additional ketamine HCL was administered if needed. In Group 1 (Sham group), a midline laparotomy incision was made, and the intestines were wrapped in a warm wet sterile gauze. Blood samples were taken from the right ventricle, and the kidneys were extracted. In Group 2 (I/R group), the aorta was clamped at the level of the superior mesenteric artery for 45 minutes. After achieving reperfusion for 3 hours, blood samples were taken from the right ventricle, and kidneys were extracted. Before ischemia was induced in Group 3 (5 mg MP group) and Group 4 (30 mg MP group), 5 mg/kg MP and 30 mg/kg MP were injected intraperitoneally, respectively. Following 45 minutes of ischemia, 3 hours of reperfusion was achieved in both groups and then blood samples were taken from the right ventricle and kidneys were extracted.

Blood samples were centrifuged at 4000 rpm to separate the serum, and serum samples were stored at -80 °C. Levels of blood urine nitrogen (BUN; mg/dL) and creatinine (mg/dL) were determined by spectrophotometric analysis using commercially available

assay kits (Abbott Diagnostics, Abbott Park, IL, USA). Serum TNF- α concentrations were assayed using a commercial ELISA kit and measured at 540 nm using a Readwell Touch ELISA plate analyzer (Robonik Pvt. Ltd., Mumbai, India). Malondialdehyde (MDA) concentration was assayed using a spectrophotometric method [8]. Ischemia-modified albumin (IMA) was studied using the spectrophotometric method suggested by Bar-Or *et al.* [9], and results are reported in absorbance units (ABSU).

Histopathological Examinations

Paraffin sections from fixed kidneys (5 μ m in thickness) were cut and stained using a standard protocol for hematoxylin and eosin. Renal slides from each group were also scored. Severe tubular lysis, loss of brush border, and/or sloughed debris in the tubular lumen space were considered as damage of tubules. Tubular damage was graded as follows: 0 = no damage; 1 = 0-25% damaged tubules; 2 = 25-50% damaged tubules; 3 = 50-75% damaged tubules; 4 = > 75% damaged tubules.

Statistical Analysis

Statistical analysis was performed using IBM SPSS Statistics 20.0 for Windows (IBM Corp., Armonk, NY, USA). Results were given as mean \pm standard error of the mean (SEM). Multiple group comparisons were performed using ANOVA with Bonferroni post-tests. Values of $p < 0.05$ were considered significant.

RESULTS

Histopathological examination revealed severe injury in the I/R group (Fig 1). Treatment with 30 mg of MP significantly attenuated the severity of the injury ($p < 0.001$). Histological damage scores were lower in the 5 mg MP group than in the I/R group; however, this difference was not significant (Fig. 2).

Serum creatinine levels were significantly lower in the 5 mg MP ($p = 0.002$) and 30 mg MP ($p = 0.02$) groups compared to the I/R group ($p < 0.05$) (Fig. 3). Serum urea levels were significantly lower in the 30 mg MP group ($p < 0.001$) compared to the I/R group ($p < 0.05$) (Fig. 3). There was no significant difference between the I/R group and 5 mg MP group.

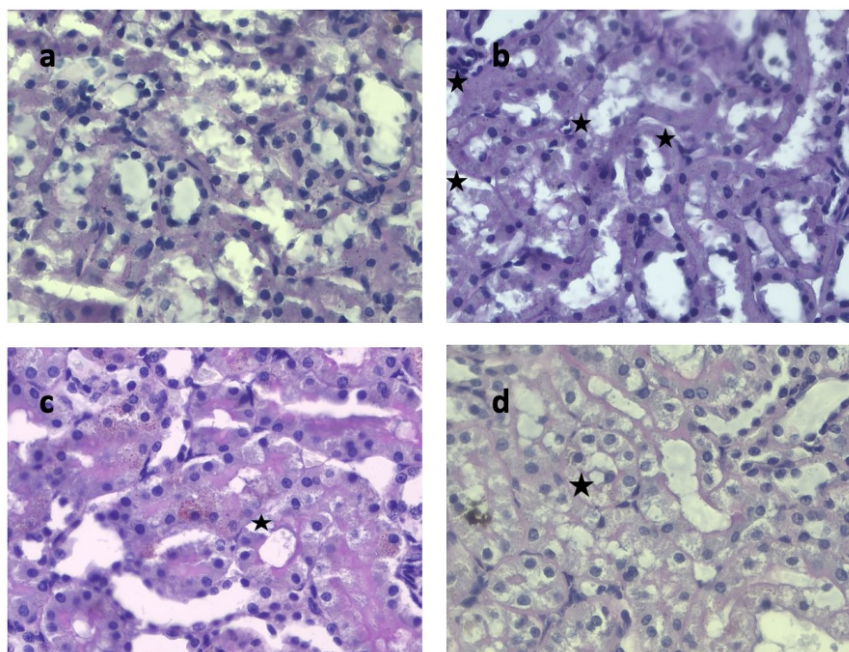


Fig. 1. Kidney sections prepared for hematoxylin and eosin staining to evaluate histological injury. (a) Sham Group, (b) I/R Group, (c) 5 mg/kg MP Group, (d) 30 mg/kg MP Group. Asterisk indicates vacuolar degenerations.

Serum TNF- α levels were significantly lower in the sham ($p < 0.001$), 5 mg MP ($p = 0.006$), and 30 mg MP ($p < 0.001$) groups compared to the I/R group ($p < 0.05$) (Table 1) (Fig. 4a). There was no significant difference between the sham group and 30 mg MP group ($p = 0.9$). However, serum TNF- α levels were significantly higher in the 5 mg MP group compared to the sham ($p < 0.001$) and 30 mg MP ($p = 0.02$) groups ($p < 0.05$). Although serum MDA levels were higher in the I/R group (Fig. 4b), there was no signif-

icant difference between the groups.

Serum troponin I (TnI) levels were higher in the I/R ($p < 0.001$), 5 mg MP ($p < 0.001$), and 30 mg MP ($p = 0.001$) groups compared to the sham group ($p < 0.05$) (Fig. 4c). Although there was no statistically significant difference, serum TnI levels were found to be lower in the 30 mg MP group compared to the I/R ($p = 1$) and 5 mg MP ($p = 0.62$) groups.

Serum IMA levels were higher in the I/R group compared to the sham ($p = 0.02$), 5 mg MP ($p =$

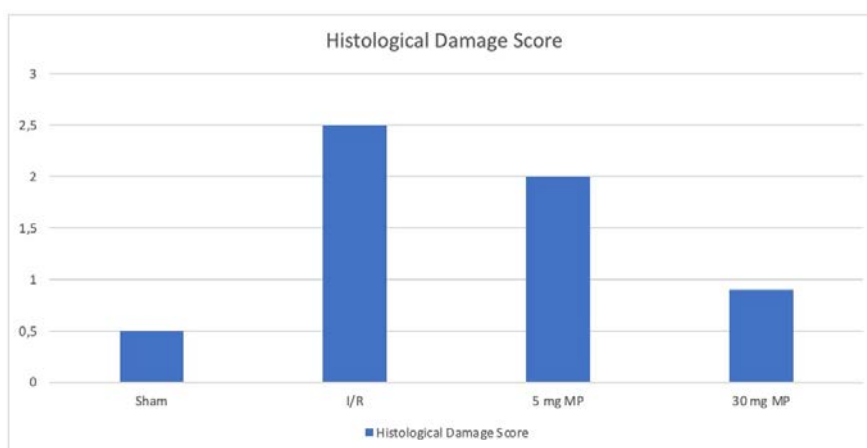


Fig. 2. Histological damage scores. All values are shown as mean \pm standard error of mean (n = 8).

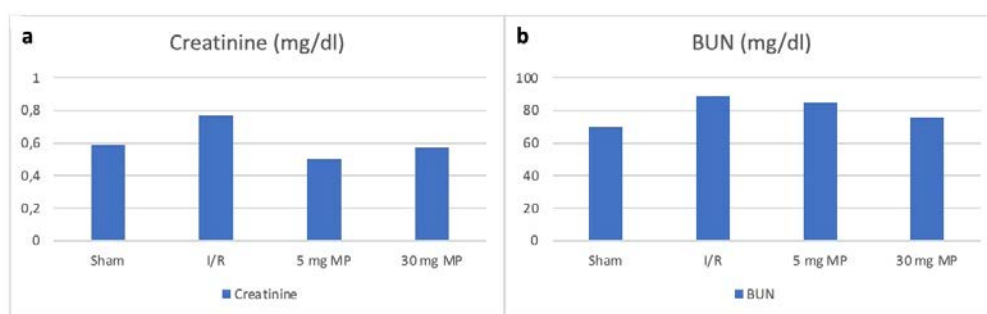


Fig. 3. Serum creatinine and BUN levels. All values are shown as mean ± standard error of mean (n = 8).

0.015), and 30 mg MP ($p = 0.011$) groups (Table 1) (Fig. 4d). Serum IMA levels were lower in the sham group than in the 5 mg MP and 30 mg MP groups, but this difference was not significant ($p = 1$ and $p = 1$, respectively).

DISCUSSION

The results of this study revealed that MP attenuated acute renal injury in a dose-dependent manner. Lower plasma TNF- α , MDA, and IMA levels were found in the MP groups. Moreover, MP administration attenuated the renal histological injury associated with I/R.

During abdominal aortic surgery, the clamping of the aorta and the subsequent restoration of blood flow causes I/R injury, which affects not only mesenteric tissues but also remote organs [10]. Tissue hypoxia, energy production through anaerobic metabolism, lactic acid accumulation, and ROS production are the main mechanisms of I/R injury processes [11]. An acute inflammatory response occurs with the activation of neutrophils due to I/R damage [12]. The excessive production of ROS and cytokine release cause

distant organ injury and apoptosis via lipid peroxidation in cell membranes with oxidative damage to DNA and proteins [1, 13].

TNF- α and IL-1 β induce chemokines that play an important role in the recruitment process of leukocytes. Therefore, they are important parts of the inflammatory reaction induced by acute kidney injury [14]. As a result of renal inflammation, endothelial cell activation, vascular disruption, and increased vascular permeability occur. This facilitates leukocyte recruitment in the renal parenchyma [15]. It has been demonstrated that steroid administration reduces I/R injury in many organs [16, 17]. In a study investigating the effect of steroids on renal damage, Kumar *et al.* [5] subjected rats to bilateral renal ischemia for 60 min, followed by reperfusion for 2 or 24 h. They found that a single dose of 3 mg/kg of dexamethasone 30 min before ischemia, or at the onset of reperfusion ameliorated biochemical and histological acute kidney injury [5]. In the present study, histopathological examination revealed that while vacuolar degenerations occurred in the renal tubules after ischemia-reperfusion, degeneration decreased in methylprednisolone administered groups. Moreover, it was observed that vacuo-

Table 1. Plasma TNF- α , MDA, TnI and IMA levels in groups

	TNF- α (pg/dl)	MDA (mmol/L)	TnI (ng/dl)	IMA (ABSU)
Sham	139.6 ± 22.53	0.49 ± 0.35	214.5 ± 142.4	0.255 ± 0.031
I/R	264.6 ± 36.69	1.03 ± 0.59	774 ± 221.3	0.464 ± 0.093
5 mg MP	209.9 ± 21.01*	0.90 ± 0.59	666.1 ± 188.5	0.297 ± 0.172*
30 mg MP	147.9 ± 35.17**	0.71 ± 0.52	615.9 ± 190.7	0.290 ± 0.041**

Values are expressed as the mean ± standard deviation. I/R = Ischemia/Reperfusion, MP = Methylprednisolone, TNF- α = Tumor necrosis factor-alpha, MDA = Malondialdehyde, TnI = Troponin I, IMA = Ischemia modified albumin.

* $p < 0.05$ (I/R vs 5 mg MP), ** $p < 0.05$ (I/R vs 30 mg MP).

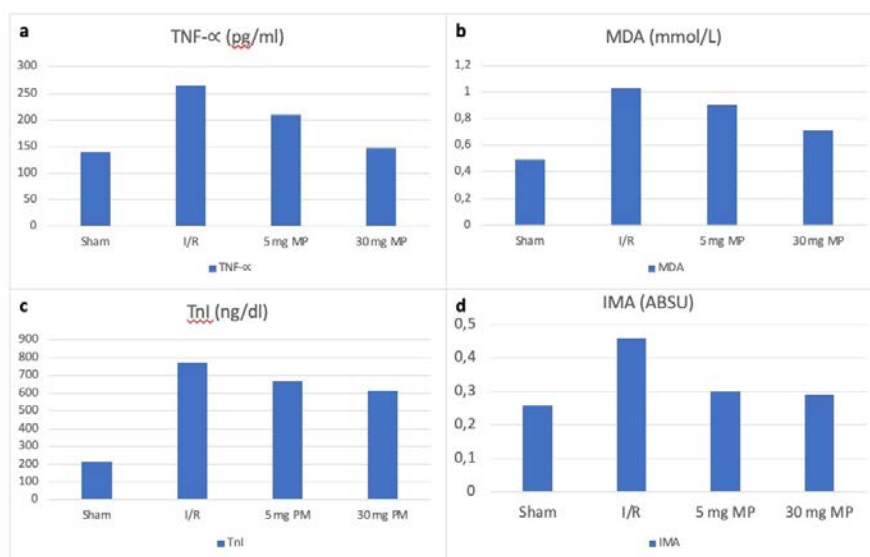


Fig. 4. Inflammatory markers in plasma: Effects of methylprednisolone plasma levels of (a) TNF- α , (b) MDA, (c) TnI, (d) IMA in rats. All values are shown as mean \pm standard error of mean (n = 8).

lar degenerations decreased with increasing dose. This was interpreted as methylprednisolone dose-dependently (30 vs. 5 mg/kg) reduced I/R injury (Figs. 1 and 2).

Baker *et al.* [18] also investigated the effects of steroids on renal damage in their study, in which clamped infrarenal abdominal aorta for 150 min followed by 180 min of reperfusion in a porcine model and showed that MP reduced the reperfusion injury of kidneys at a dose of 30 mg/kg. Fontana *et al.* [6] searched effects of 5 mg/kg s.c. daily prednisolone administration on ischemia-reperfusion injury. They demonstrated that continuous prednisolone application has protective effects and prednisolone treated group had significantly reduced TNF- α levels. Gozdzik *et al.* found that combination of inhaled NO and IV steroid diminished the systemic inflammatory response in I/R injury animal model and significantly lower TNF- α and IL-10 levels in treatment group [19]. In the present study, the TNF- α levels, one of the indicators of renal damage, were examined. Treatment with both 5 and 30 mg MP significantly reduced the serum TNF- α levels when compared to the I/R group ($p < 0.05$). However, this reduction was more evident in 30 mg/kg group, and the serum TNF- α levels were significantly lower when compared to the 5 mg MP group.

MDA, the end product of lipid peroxidation, is an important indicator of I/R injury. It has been demonstrated that MDA levels are sensitive markers of the

rate of lipid peroxidation [20]. Singh *et al.* [21] reported that MDA levels increased during renal I/R in rats. It was found herein that there were lower serum MDA levels in the MP-treated groups when compared to the I/R group. However, no statistically significant differences were detected. Gurer *et al.* [22] found that 30 mg/kg methylprednisolone treatment reduced MDA levels significantly. However, in this study groups were subjected to ischemia by aortic occlusion for 20 min which is shorter than our study.

In the event of I/R, structural changes occur in the albumin under the influence of acidosis and reactive oxygen radicals. Albumin has the ability to bind to some metal ions, particularly copper, nickel, and cobalt. However, this ability decreases, and the albumin cannot bind to those ions. This new form of albumin is known as ischemia-modified albumin (IMA) [23, 24]. IMA is accepted as a nonspecific biomarker in ischemic tissues [24]. Several studies showed increased IMA levels in cases of renal I/R injury parallel with the duration of ischemia [25, 26]. In the present study, the IMA levels of the groups receiving MP were significantly lower when compared to the I/R group ($p < 0.05$).

I/R injury may cause remote organ injury, including injury to the heart, liver, or intestines [27]. Yeginsu *et al.* [16] investigated the effects of different doses of MP on lung injury developing after extremity ischemia reperfusion in rats, and administered 15, 50, and 150

mg/kg MP. They found that MP reduced remote organ injury. However, the effect was in a dose dependent manner, and it was maximum at a dose of 150 mg/kg. Tai *et al.* [28] found that renal I/R injury was associated with cardiac dysfunction. TnI is a specific marker for myocardial damage. In the present study, no significant differences were detected between the I/R group and the MP treatment groups in this regard. Thus, it was not possible to demonstrate a protective effect of MP on remote cardiac injury.

In previous studies, protective effects of 5 and 30 mg/kg MP on I/R injury have been revealed [6, 18, 29]. In the current study, 5 and 30 mg/kg MP was administered. The results showed that the serum TNF- α levels, IMA levels, and histological damage score decreased in the 5 mg MP and 30 mg MP groups. Therefore, it can be concluded that MP treatment had protective effects on the suprarenal aortic I/R injury. However, the serum TNF- α levels and histological damage score were significantly lower in 30 mg/kg MP group, when compared to the 5 mg/kg MP group. These results indicated that treatment with 5 mg/kg MP may not be as beneficial as treatment with 30 mg/kg MP.

CONCLUSION

In conclusion, this experimental study has demonstrated that MP at doses of both 5 and 30 mg/kg attenuates I/R injury in the kidneys induced by suprarenal aortic I/R in rats. However, this benefit was dose dependent, and was more evident with the administration of 30 mg/kg MP.

Authors' Contribution

Study Conception: SÇ; Study Design: SÇ, KKÖ; Supervision SÇ, KKÖ, ÖA; Funding: SÇ, MÖÖ, ÖA, YÜ; Materials: SÇ, MÖÖ, ÖA, YÜ; Data Collection and/or Processing: SÇ, MÖÖ, ÖA, YÜ; Statistical Analysis and/or Data Interpretation: SÇ, MÖÖ, ÖA, YÜ; Literature Review: SÇ, KKÖ, MÖÖ; Manuscript Preparation: SÇ, KKÖ and Critical Review: SÇ, KKÖ, MÖÖ, ÖA, YÜ.

Conflict of interest

The authors disclosed no conflict of interest during the preparation or publication of this manuscript.

Financing

The authors disclosed that they did not receive any grant during conduction or writing of this study.

REFERENCES

1. Zou C, Hu H, Xi X, Shi Z, Wang G, Huang X. Pioglitazone protects against renal ischemia-reperfusion injury by enhancing antioxidant capacity. *J Surg Res* 2013;184:1092-5.
2. Erol B, Turker T, Tok A, Bektas S, Mungan G, Ozkanli S, et al. The protective effects of tadalafil on renal damage following ischemia reperfusion injury in rats. *Kaohsiung J Med Sci* 2015;31:454-62.
3. Youssef MI, Mahmoud AA, Abdelghany RH. A new combination of sitagliptin and furosemide protects against remote myocardial injury induced by renal ischemia/reperfusion in rats. *Biochem Pharmacol* 2015;96:20-9.
4. Bayrak S, Yurekli I, Gokalp O, Kiray M, Bademci MS, Ozcem B, et al. Assessment of protective effects of methylprednisolone and pheniramine maleate on reperfusion injury in kidney after distant organ ischemia: a rat model. *Ann Vasc Surg* 2012;26:559-65.
5. Kumar S, Allen DA, Kieswich JE, Patel NS, Harwood S, Mazzone E, et al. Dexamethasone ameliorates renal ischemia-reperfusion injury. *J Am Soc Nephrol* 2009;20:2412-25.
6. Fontana J, Vogt A, Hohenstein A, Vettermann U, Doroshenko E, Lammer E, et al. Impact of steroids on the inflammatory response after ischemic acute kidney injury in rats. *Indian J Nephrol* 2017;27:365-71.
7. Wystrychowski G, Wystrychowski W, Grzeszczak W, Wiecek A, Krol R, Wystrychowski A. Pentoxifylline and methylprednisolone additively alleviate kidney failure and prolong survival of rats after renal warm ischemia-reperfusion. *Int J Mol Sci* 2018;19:221.
8. De Leon JAD, Borges CR. Evaluation of oxidative stress in biological samples using the thiobarbituric acid reactive substances assay. *J Vis Exp* 2020;(159):e61122.
9. Bar-Or D, Lau E, Winkler JV. A novel assay for cobalt-albumin binding and its potential as a marker for myocardial ischemia - a preliminary report. *J Emerg Med* 2000;19:311-5.
10. Huang C, Huang C, Hestin D, Dent PC, Barclay P, Collis M, et al. The effect of endothelin antagonists on renal ischaemia-reperfusion injury and the development of acute renal failure in the rat. *Nephrol Dial Transplant* 2002;17:1578-85.
11. Tang PS, Mura M, Seth R, Liu M. Acute lung injury and cell death: how many ways can cells die? *Am J Physiol Lung Cell Mol Physiol* 2008;294:L632-L41.
12. Hearse DJ, Bolli R. Reperfusion induced injury: manifestations, mechanisms, and clinical relevance. *Cardiovasc Res* 1992;26:101-8.
13. Rodríguez-López JM, Sánchez-Conde P, Lozano FS, Nicolás JL, García-Criado FJ, Cascajo C, et al. Effects of propofol on the systemic inflammatory response during aortic surgery. *Can J Anesth* 2006;53:701-10.
14. Segerer S, Nelson PJ, Schlöndorff D. Chemokines,

chemokine receptors, and renal disease: from basic science to pathophysiologic and therapeutic studies. *J Am Soc Nephrol* 2000;11:152-76.

15. Akcay A, Nguyen Q, Edelstein CL. Mediators of inflammation in acute kidney injury. *Mediators Inflamm* 2009;2009:137072.

16. Yeginsu A. [The effects of methylprednisolone on the lung injury resulted from extremity ischemia reperfusion]. *Turk Gogus Kalp Damar Cerrahisi Derg* 2010;18:45-51. [Article in Turkish]

17. Chimalakonda AP, Mehvar R. Effects of methylprednisolone and its liver-targeted dextran prodrug on ischemia-reperfusion injury in a rat liver transplantation model. *Pharm Res* 2007;24:2231-8.

18. Baker RC, Armstrong MA, Young IS, McClean E, O'Rourke D, Campbell FC, et al. Methylprednisolone increases urinary nitrate concentrations and reduces subclinical renal injury during infrarenal aortic ischemia reperfusion. *Ann Surg* 2006;244:821-6.

19. Gozdzik W, Zielinski S, Zielinska M, Ratajczak K, Skrzypczak P, Rodziewicz S, et al. Beneficial effects of inhaled nitric oxide with intravenous steroid in an ischemia-reperfusion model involving aortic clamping. *Int J Immunopathol Pharmacol* 2018;32:394632017751486.

20. Ozcan AV, Sacar M, Aybek H, Bir F, Demir S, Onem G, et al. The effects of iloprost and vitamin C on kidney as a remote organ after ischemia/reperfusion of lower extremities. *J Surg Res* 2007;140:20-6.

21. Singh D, Chander V, Chopra K. The effect of Quercetin, a bioflavonoid on ischemia/reperfusion induced renal injury in rats. *Arch Med Res* 2004;35:484-94.

22. Gurer B, Karakoc A, Bektasoglu PK, Kertmen H, Kanat MA, Arikok AT, et al. Comparative effects of vitamin D and methylprednisolone against ischemia/reperfusion injury of rabbit spinal cords. *Eur J Pharmacol*. 2017;813:50-60.

23. Talwalkar SS, Bon-Homme M, Miller JJ, Elin RJ. Ischemia modified albumin, a marker of acute ischemic events: a pilot study. *Ann Clin Lab Sci* 2008;38:132-7.

24. Lippi G, Montagnana M, Guidi GC. Albumin cobalt binding and ischemia modified albumin generation: an endogenous response to ischemia? *Int J Cardiol* 2006;108:410-1.

25. Amasyali AS, Akkurt A, Kazan E, Yilmaz M, Erol B, Yildiz Y, et al. The protective effect of tadalafil on IMA (ischemia modified albumin) levels in experimental renal ischemia-reperfusion injury. *Int J Clin Exp Med* 2015;8:15766-72.

26. Kocan H, Citgez S, Yucetas U, Yucetas E, Yazici M, Amasyali A, et al. Can ischemia-modified albumin be used as an objective biomarker for renal ischemic damage? An experimental study with Wistar albino rats. *Transplant Proc* 2014;46:3326-9.

27. Fadillioglu E, Kurcer Z, Parlakpinar H, Iraz M, Gursul C. Melatonin treatment against remote organ injury induced by renal ischemia reperfusion injury in diabetes mellitus. *Arch Pharm Res* 2008;31:705-12.

28. Tai S, Fu Y, Yang Y, Wang J. Niacin ameliorates kidney warm ischemia and reperfusion injury-induced ventricular dysfunction and oxidative stress and disturbance in mitochondrial metabolism in rats. *Transplant Proc* 2015;47:1079-82.

29. Gill A, Wortham K, Costa D, Davis W, Ticho B, Whalley E. Protective effect of tonapofylline (BG9928), an adenosine A1 receptor antagonist, against cisplatin-induced acute kidney injury in rats. *Am J Nephrol* 2009;30:521-6.



This is an open access article distributed under the terms of [Creative Commons Attribution-NonCommercial-NoDerivatives 4.0 International License](https://creativecommons.org/licenses/by-nc-nd/4.0/).

Evaluation of organ donation process and affecting factors in COVID-19 pandemic

Gökhan Kılınc^{1,2}, Fuat Çöken²

¹Department of Anesthesiology and Reanimation, Atatürk City Hospital, Balıkesir, Turkey; ²Department of Organ and Tissue Transplantation, Atatürk City Hospital, Balıkesir, Turkey ;

ABSTRACT

Objectives: More than six million people worldwide are affected by end-stage organ failure and the COVID-19 pandemic has dramatically changed organ and tissue donation.

Methods: The data of patients diagnosed with brain death between July 2018-March 2020 (pre-pandemic period) and April 2020-December 2021 (pandemic period) were analyzed retrospectively. Donor characteristics, laboratory levels, time from intensive care admission to determination of brain death, time to family approval, family approval rates and organ types were analyzed.

Results: The mean age of 56 patients with pre-pandemic diagnosis of brain death was 61.82 ± 21.39 years, 37 (63%) patients were donors and 53 organs were obtained. Mean age of 39 patients diagnosed with brain death during the pandemic was 58.26 ± 18.02 years and 38 organs were obtained from 21 (52.5%) donors. Between the two periods, there was a decrease of 30.35% in the diagnosis of brain death, 43.24% in the number of donors and 26.41% in the number of organs supplied. The most common cause of brain death was intracranial hemorrhage during both periods. While the time elapsed between family interview and surgery was 9.33 ± 2.19 hours before the pandemic, it was 15.29 ± 4.28 hours during the pandemic period ($p = 0.01$). There was a significant difference between C-reactive protein levels at the time of diagnosis of brain death ($p < 0.05$). *Staphylococcus haemolyticus* was most frequently seen in blood culture.

Conclusions: Brain death and organ donation have decreased significantly during the pandemic period compared to previous years, similar to research conducted in different countries and regions. Due to COVID-19, prolonged stays in the intensive care unit (ICU) may pose a risk of infection in ICU donors, and care should be taken in terms of donor loss.

Keywords: Organ transplantation, organ donation, transplant surgery, infectious diseases, COVID-19, family consent, brain death

More than six million people worldwide are affected by end-stage organ failure. With the development of the transplantation field, the survival and quality of life of patients with end-stage organ failure has changed. It has changed the lives of these patients

as a life-saving treatment method in end-stage organ failure. With all these developments, cadaver donor pools are still insufficient. Accurate and timely detection of brain death is of critical importance in terms of dissemination of organ donations and ensuring the

Received: December 28, 2022; Accepted: January 26, 2023; Published Online: April 2, 2023



e-ISSN: 2149-3189

How to cite this article: Kılınc G, Çöken F. Evaluation of organ donation process and affecting factors in COVID-19 pandemic. Eur Res J 2023;9(3):574-581. DOI: 10.18621/eurj.1225842

Address for correspondence: Gökhan Kılınc, MD., Atatürk City Hospital, Department of Anesthesiology and Reanimation, Gaziosmanpaşa Mah., 209. Sok., No:26, 10100 Alteylül, Balıkesir Turkey. E-mail: gkilinc35@hotmail.com, Phone: +90 266 460 40 00, Fax: +90 266 460 40 45



©Copyright © 2023 by Prusa Medical Publishing
Available at <http://dergipark.org.tr/eurj>
info@prusamp.com

continuity of transplantation processes, especially heart and lung, which can be done through cadaver donors [1]. Organ procurement from living donors presents some difficulties. With the increasing importance of organ donation from cadavers, the importance of brain death diagnosis, organ donation and donor care has increased even more. It is characterized by the clinical condition that includes irreversible brain death with loss of cerebral function, apnea and absence of brainstem reflexes [2]. In many countries, the guidelines of the American Academy of Neurology are used as an example for brain death conditions, diagnosis and supportive tests [3].

There have been significant medical and technological advances in intensive care. Despite all these developments, the inability to diagnose brain death causes insufficient organ donation. This poses a serious problem for patients awaiting organ transplants. Early detection of potential donors, successful organ donation from families, and correct management of these donors are issues that need to be emphasized. Poor care of potential donors, prolonged family approval and donation process may lead to organ loss [4, 5].

Announced on March 11, 2020, the COVID-19 pandemic has dramatically changed organ and tissue donation. COVID-19 presents some difficulties in harvesting organs from living donors. With the increasing importance of cadaveric organ donation, the importance of brain death diagnosis, organ donation and donor care has increased even more. Recipients are at increased risk due to immunosuppressive drugs, prolonged hospital stay, and possible transmission from asymptomatic infected donors. In addition, there is a risk of contamination for health personnel working in organ transplantation. The risk of transmitting COVID-19 by organ transplant of an organ donor, who is infected with SARS-CoV-2, is still unknown. Transmission is affected by the incubation period of the virus, the degree of viremia, epidemiological risk factors, and viability in blood and organs. Also, real-time PCR, which is commonly used for laboratory confirmation of COVID-19, is not 100% sensitive. In this context, it is recommended to follow the guidelines published by the National Organ and Tissue Transplantation Organization [6]. We evaluated the COVID-19 pandemic process and tried to draw attention to the

differences with the pre-pandemic period so that it can be corrected.

METHODS

Patient Characteristics

The medical records of patients diagnosed with brain death in the Intensive Care Unit of Balıkesir Atatürk City Hospital between July 2018 - March 2020 (pre-pandemic period) and April 2020 - December 2021 (pandemic period) were retrospectively reviewed and donor characteristics (gender, age, cause of brain death), Glasgow Coma Scale scores at intensive care unit admission, time from intensive care unit admission to determination of brain death and time from family consent to procurement, family consent rates and organ types were analysed by anonymising details. The results of C-reactive protein (CRP), white blood cell count (WBC), blood sodium (Na), Creatinine levels and cultures (tracheal aspirate, urine and blood) were evaluated on the day of admission to the intensive care unit and the day of diagnosis of brain death.

COVID-19 Period Brain Death Diagnosis and Evaluation

During the pandemic process, potential donors were screened for COVID-19 according to the recommendations of the Scientific Committee of the Ministry of Health. Real-time polymerase chain reaction (RT-PCR) tests were required according to this instruction. SARS-CoV-2 RT-PCR tests were requested at least twice at 24-hour intervals from the patients' intratracheal aspirate samples. The patient's data was reported to the National Coordination Center by the transplant coordinators together with the SARS-CoV-2 RT-PCR results. All donors had at least one thorax computed tomography scan performed during hospitalization. All organ donors were consulted by Infectious Diseases and Clinical Microbiology doctors and Chest Diseases doctors for suspected COVID-19. Ethical approval was obtained for the study from the local ethics committee of Balıkesir University (Date: 07.09.2022, Decision no: 2022/100). This study was conducted in accordance with the tenets of the Declaration of Helsinki Principles.

Statistical Analysis

Statistical analysis was performed using Statistical Package for the Social Sciences 20.0 software (Statistical Package for the Social Sciences version 20, IBM Corp., Armonk, New York, IL, USA) software. Whether the variables fit the normal distribution or not was evaluated with the Kolmogorov - Smirnov test. Student -t test was used for the comparisons between groups of normally distributed continuous data. Parametric data with normal distribution were presented as mean \pm standard deviation (SD). Values with $p < 0.05$ were considered statistically significant. Categorical variables are presented as frequency and percentages.

RESULTS

The mean age of 56 patients diagnosed with brain death before the pandemic was 61.82 ± 21.39 years, 37 (63%) patients were donors and 53 organs were recovered. Mean age of 39 patients diagnosed with brain death during the pandemic was 58.26 ± 18.02 years and 38 organs were obtained from 21 (52.5%) donors. The procured organ details are shown in Table 1. Between the two periods, there was a decrease of 30.35% in the diagnosis of brain death, 43.24% in the number of donors and 26.41% in the number of organs procured. 51.6% of the patients were male and 48.4% were female. In the pre-pandemic period, one patient died while distribution was ongoing, and organ harvesting was not performed from 13 patients for medical reasons. During the pandemic period, three patients died while distribution was ongoing, and three families did not come to the meeting. Due to the suspicion of COVID-19 in two patients and COVID-19 positive in three patients during the donor preparation process, organ removal procedures were terminated. Organ removal was not performed in three patients for

medical reasons, and in one patient due to organ ischemia during surgery. In this process, 2663 of 10999 patients hospitalized in intensive care units were diagnosed with COVID-19.

The most common cause of brain death was intracranial haemorrhage both before and during the pandemic. While trauma patients were the 2nd in the pre-pandemic period, other intracranial events were in the second rank during the pandemic period (Table 2). While %33.9 of the patients with brain death had A Rh (+) blood group during the pandemic and %28.2 before the pandemic, %28.6 and %28.2 had O Rh (+) blood group and there was no significant difference between blood groups in terms of blood groups (Table 2).

CRP, WBC, Na and Creatinine levels of the patients were scanned and compared with each other at the time of hospitalization and at the time of brain death, both before and during the pandemic. A statistically significant difference was found between CRP levels at the time of diagnosis of brain death before and after the pandemic ($p < 0.05$). When the CRP, WBC, Na and creatinine levels of the patients before and during the pandemic were compared with the levels at the time of intensive care admission and brain death diagnosis, CRP, Na and creatinine levels were higher at the time of diagnosis of brain death, and there was a statistically significant difference. There was no significant difference between WBC levels (Table 3).

The time elapsed between admission to the intensive care unit and diagnosis of brain death was 115.37 ± 89.1 hours and 124.66 ± 152.68 hours before and during the pandemic, respectively. While the time from family interview to surgery was 9.33 ± 2.19 hours before the pandemic, it was found to be 15.29 ± 4.28 hours during the pandemic period, and there is a statistically significant difference ($p = 0.01$) (Table 2).

Blood, urine and tracheal aspirate cultures were sent from potential donors with brain death. In the pre-

Table 1. Organs procured from brain-dead patients

	Before COVID-19 (n = 56)	During COVID-19 (n = 39)
Kidney, n (%)	31 (55.35)	25 (64.10)
Liver, n (%)	19 (33.92)	10 (25.64)
Heart, n (%)	3 (5.35)	2 (5.12)

Table 2. Baseline characteristics of patients

	Before Pandemic (n = 56)	During Pandemic (n = 39)	p value
Age (years) (mean ± SD)	61.82 ± 21.39	58.26 ± 18.02	0.460
Gender, n (%)			
Male	30 (53.6)	19 (48.7)	
Female	26 (46.4)	20 (51.3)	
Primary hospital admission diagnosis, n (%)			
Intracranial hemorrhage	17 (30.35)	17 (43.58)	
Head trauma	11 (19.64)	2 (5.12)	
Postcardiorespiratory arrest	10 (17.85)	2 (5.12)	
Ischemic stroke	9 (16.07)	4 (10.25)	
Subarachnoid hemorrhage	5 (8.92)	4 (10.25)	
Blood group, n (%)			
A Rh (+)	19 (33.9)	11 (28.2)	
O Rh (+)	16 (28.6)	11 (28.2)	
B Rh (+)	14 (25)	5 (12.8)	
A Rh (-)	3 (5.4)	-	
AB Rh (+)	3 (5.4)	6 (15.4)	
O Rh (-)	1 (1.8)	3 (7.7)	
AB Rh (-)	-	2 (5.1)	
Time from Intensive care unit admission to diagnosis of death (mean ± SD)	115.37 ± 89.1	124.66 ± 152.68	0.310
Time from family interview to surgery (mean ± SD)	9.33 ± 2.19	15.29 ± 4.28	< 0.001

Table 3. Laboratory values of patients diagnosed with brain death

	Before Pandemic	p value	During Pandemic	p value
CRP (mg/dL) (ICU)	2.25 ± 4.01	< 0.05	4.44 ± 6.71	< 0.05
CRP (mg/dL) (BD)	13.81 ± 14.30		14.10 ± 8.48	
WBC (×10⁹/L) (ICU)	13.83 ± 6.27	0.293	16.83 ± 8.89	0.658
WBC (×10⁹/L) (BD)	15.07 ± 8.57		16.04 ± 7.24	
Na (mEq/L) (ICU)	138.73 ± 4.44	< 0.05	138.95 ± 4.01	< 0.05
Na (mEq/L) (BD)	153.75 ± 15.78		153.90 ± 18.95	
Creatinin (mg/dL) (ICU)	1.33 ± 1.43	< 0.05	1.31 ± 1.28	< 0.05
Creatinin (mg/dL) (BD)	1.96 ± 1.48		2.09 ± 1.46	

CRP = C-reactive protein, WBC = white blood cell, Na = Sodium, ICU = Intensive care unit, BD = Brain death

pandemic period, the most common microorganisms were *Staphylococcus haemolyticus* in blood culture, *Escherichia coli* in urine culture, and *Acinetobacter baumannii*, *Burkholderia cepacia*, *Staphylococcus aureus* in tracheal aspirate. During the pandemic period, *S. haemolyticus* was the most common in blood culture, no positivity was detected in urine culture, while *E. coli* and *Klebsiella oxytoca* were seen in tracheal aspirate culture.

DISCUSSION

During the COVID-19 pandemic, it was observed that there were serious decreases in the number of organ donations and family consent all over the world and in Turkey. Especially in the early stages of the pandemic, the number of organ donations and transplants has decreased worldwide, as in Turkey. In 2020, the diagnosis of brain death in our country decreased by 25% when evaluated according to the last 10 years, and 40% when evaluated compared to the previous year. Family consent rate decreased by 25% when evaluated according to the average of the last 10 years, and decreased by 50% when evaluated compared to the previous year [7].

According to the data of the Ministry of Health, 2309 patients were diagnosed with brain death in 2019 in Turkey. Six hundred nineteen family consents were obtained from 2309 patients. 2504 organs were harvested from these patients. When compared, the number of diagnosed brain death in 2020 and 2021 was 1391 and 1421, respectively, the number of family consents was 263 and 305, and the number of organs accepted for donation was 1059 and 1250, respectively [8].

In our study, 37 of our 56 patients diagnosed with brain death before the pandemic were donors, while 53 organs were recovered. During the pandemic, 21 of 39 patients became donors and 38 organs were provided. Between the two periods, there was a 30.35% decrease in the diagnosis of brain death, a 43.24% decrease in the number of donors and a 26.41% decrease in the number of organs supplied. Donations could not be received from 39 potential donors who were diagnosed with brain death during the pandemic period, because three families did not come to the meeting,

two patients had a suspicion of COVID-19 and three patients were SARS-CoV-2 RT-PCR positive. Causes directly related to COVID-19 resulted in a 20.51% reduction in donors.

During the pandemic, family interviews were generally conducted by telephone around the world [9]. In a study in Israel, the first family contact was made via telephone for 18% of potential donors, and it was suggested that this negatively affected the donation process [10]. Organ transplant coordinators at our center continued face-to-face meetings, observing preventive measures against infection. The decision to donate organs is often made in complex situations. The fact that families are in the acute period, which includes the bereaved period, may prevent emotional confusion and clarity about brain death. This negatively affects family decision-making and grieving, causing distress. There are many reasons that affect family approval in organ donation. Among the various reasons for not accepting donations, he cited variants of emotional exhaustion and inadequate staff responsiveness and coping with family pain [11]. The donor rate was 63% among 56 patients with pre-pandemic diagnosis of brain death. During the pandemic, there was a decrease in both the number of brain death ($n = 39$) and the rate of being a donor (52.5%). It is known that the family consent rate for organ donation in Europe is between 50% and 80%, consistent with our study. These rates are lower in Asian countries due to religious beliefs and the rate of practical consent is not well known [11-13]. It is clear that innovative technological solutions need to be worked on to increase virtual interactions with family members in times of crisis such as pandemics [10].

Viral RNA samples of SARS-CoV-2, which is primarily airborne and transmitted by droplet routes, have also been detected in hepatocytes, renal tubular cells and myocardium in critically ill patients. This raises concerns that infection may be transmitted from the donor [14]. Some authors argue that as the impact of the pandemic changes, existing recommendations should be reassessed. They suggested that for patients with life-threatening organ dysfunction who are unlikely to find a suitable and timely infected match, organ transplantation from SARS-CoV-2-infected but carefully selected donors could be lifesaving for these patients [15]. Our five patients, no organ removal was

performed due to the suspicion or positivity of COVID-19.

In a study, it was observed that the most common cause of brain death was intracerebral hemorrhage (42%), followed by traumatic brain injury (343/1844, 19%) [16]. Intracranial hemorrhage was the most common cause of brain death in different studies during the COVID-19 pandemic [17, 18]. Similarly, in our study, the most common cause of brain death was intracerebral hemorrhage both in the pre-pandemic period and during the pandemic period. In the pre-pandemic period, trauma patients were in the second rank, while other intracranial events were in the second rank during the pandemic period. The reason for this is thought to be the decrease in trauma cases due to pandemic bans. In the first wave of the pandemic, this was a 4.5% reduction in donors who died from trauma, and a 25% reduction in donors who died from traffic accidents [19].

Different results have been obtained in studies examining the effect of brain death diagnosis time on family donation rate. Kıraklı *et al.* [20] reported that the definitive diagnosis period of brain death was significantly shorter in those who accepted organ donation. Researchers have suggested that the shortening of the definitive diagnosis of brain death may increase the organ transplant acceptance rate of families. Lustbader *et al.* [21] in their study, they reported that the number of donors decreases as the duration of brain death diagnosis increases, and they recommended not to waste time for a second neurological examination. In a study, cases diagnosed with brain death were divided into “early diagnosed group (diagnosed with brain death before 48 hours following ICU admission)” and “delayed diagnosis group (diagnosed after 48 hours following ICU admission)”, donation rate was 73%, and 55% in those diagnosed late [11]. The time elapsed between admission to the intensive care unit and diagnosis of brain death was 115.37 ± 89.1 hours and 124.66 ± 152.68 hours before and during the pandemic, respectively. While the time between family interview and surgery was 9.33 ± 2.19 hours before the pandemic, it was found to be 15.29 ± 4.28 hours during the pandemic. We did not examine the relationship between diagnosis time and donation rate. In a study conducted in our country, the time between admission to the intensive care unit and diagnosis of

brain death was found to be 4 (IQR 5) days and 4 (IQR 12) days before and during the pandemic, respectively. In the same study, the duration of organ donation was found to be 8.5 ± 2.12 hours in the pre-pandemic period and 54 ± 11.53 hours in the pandemic period [17]. In another study, the median time from admission to the intensive care unit to the diagnosis of brain death was 4 (min-max, 1.0-36.0) days during the pandemic period [18]. Balkaya *et al.* [22] found similar results with our study as the time between admission to the ICU and diagnosis of BD was 114 ± 92.8 (11-360) hours.

Infection of the donor with any pathogen causes concern in organ transplantation. Many transplant centers are not willing to harvest organs from patients with bacteremia. In contrast, some centers are carefully examining documented cases of bacteremia from potential donors who have recently received adequate antibiotic therapy. Long-term ICU stays due to additional considerations on donors potentially increase the risk of ICU-derived infections. Patients under mechanical ventilation and invasive hemodynamic monitoring should be alert to complications such as ventilator-associated pneumonia and catheter-related infection. Infection control measures, rapid screening of blood cultures and, if necessary, appropriate antibiotic therapy can reduce donor loss [17, 18]. In this study, blood, urine and tracheal aspiration samples from potential donors with brain death were conducted. During the pandemic period, the most common microorganisms were *S. haemolyticus* in blood samples, *E. coli* in urine samples, and *A. baumannii*, *B. cepacia*, *S. aureus* in tracheal aspirate samples. During the pandemic period, *S. haemolyticus* was the most common in blood samples, no growth was detected in urine samples, *E. coli* and *K. oxytoca* were seen in tracheal aspirate samples. When the values of the patients before the pandemic and at the time of the diagnosis of brain death were compared, CRP values of the patients were higher than at the time of the diagnosis of brain death. In another study conducted in our country, CRP elevation was found in the diagnosis of brain death [17].

As the duration of brain death diagnosis increases, the survival expectancy of patients and the stress and sadness of families increase, especially in poorly informed families. The use of supportive diagnostic tests

other than neurological examination and apnea test in the brain death diagnosis process may be effective in shortening the diagnosis period. In addition, positive communication with the family from the moment the patient is taken to the intensive care unit and providing sufficient information about the treatment steps can eliminate the negative effects on donation rates.

Limitations

There are some limitations of our study, such as being single-centered and retrospective, not investigating the characteristics of families and what influences family decisions, and not including detailed information about family interview conditions.

CONCLUSION

In this study, the organ donation process during the COVID-19 period was examined. There was a decrease of 30.35% in the diagnosis of brain death, 43.24% in the number of donors and 26.41% in the number of organs supplied. The time between family interview and surgery was significantly longer during the pandemic period. Brain death procedures should be carried out quickly due to the increased risk of infection and deterioration of the general condition.

Authors' Contribution

Study Conception: GK; Study Design: GK; Supervision: GK, FÇ; Funding: GK, FÇ; Materials: GK, FÇ; Data Collection and/or Processing: GK, FÇ; Statistical Analysis and/or Data Interpretation: GK, FÇ; Literature Review: GK, FÇ; Manuscript Preparation: GK and Critical Review: GK, FÇ.

Conflict of interest

The authors disclosed no conflict of interest during the preparation or publication of this manuscript.

Financing

The authors disclosed that they did not receive any grant during conduction or writing of this study.

Acknowledgements

The authors thank all intensive care staff for their contribution to brain death and donor care.

REFERENCES

- Loupy A, Aubert O, Reese PP, Bastien O, Bayer F, Jacquelinet C. Organ procurement and transplantation during the COVID-19 pandemic. *Lancet* 2020;395:e95-6.
- Spears W, Mian A, Greer D. Brain death: a clinical overview. *J Intensive Care* 2022;10:16.
- Wijdicks EF, Varelas PN, Gronseth GS, Greer DM. Evidence-based guideline update: determining brain death in adults: report of the Quality Standards Subcommittee of the American Academy of Neurology. *Neurology* 2010;74:1911-8.
- Meyfroidt G, Gunst J, Martin-Loeches I, Smith M, Robba C, Taccone FS, et al. Management of the brain-dead donor in the ICU: general and specific therapy to improve transplantable organ quality. *Intensive Care Med* 2019;45:343-53.
- Park J, Yang NR, Lee YJ, Hong KS. A single-center experience with an intensivist-led brain-dead donor management program. *Ann Transplant* 2018;23:828-35.
- Chavali S, Rath GP, Sengupta D, Dube SK. Brain death diagnosis for potential organ donors during the Covid-19 pandemic. *Neurol India* 2021;69:995-6.
- Mengi T, Şirin H, Yaka E, Özdemir AÖ, Arsava EM, Topçuoğlu MA. Brain death diagnosis and management in the pandemic: expert opinion of the Turkish Neurological Society Neurological Intensive Care Scientific Working Group. *Turk J Neurol* 2021;27:1-4.
- Republic of Turkey Ministry of Health. Tissue OtaDSDaD-SRoTMOHT, Organ Transplantation and Dialysis Services. Donations and Donors. Available at: https://organkds.saglik.gov.tr/dss/PUBLIC/Brain_Death.aspx. Accessed November 13, 2022.
- Valdes E, Agarwal S, Carroll E, Kvermland A, Bondi S, Snyder T, et al. Special considerations in the assessment of catastrophic brain injury and determination of brain death in patients with SARS-CoV-2. *J Neurol Sci* 2020;417:117087.
- Katvan E, Cohen J, Ashkenazi T. Organ donation in the time of COVID-19: the Israeli experience one year into the pandemic-ethical and policy implications. *Isr J Health Policy Res* 2022;11:6.
- Han SY, Kim JI, Lee EW, Jang HY, Han KH, Oh SW, et al. Factors associated with a family's delay of decision for organ donation after brain death. *Ann Transplant* 2017;22:17-23.
- Gortmaker SL, Beasley CL, Sheehy E, Lucas BA, Brigham LE, Grenvik A, et al. Improving the request process to increase family consent for organ donation. *J Transpl Coord* 1998;8:210-7.
- Hulme W, Allen J, Manara AR, Murphy PG, Gardiner D, Pop-pitt E. Factors influencing the family consent rate for organ donation in the UK. *Anaesthesia* 2016;71:1053-63.
- Shah MB, Lynch RJ, El-Haddad H, Doby B, Brockmeier D, Goldberg DS. Utilization of deceased donors during a pandemic: argument against using SARS-CoV-2-positive donors. *Am J Transplant* 2020;20:1795-9.
- Kates OS, Fisher CE, Rakita RM, Reyes JD, Limaye AP. Use of SARS-CoV-2-infected deceased organ donors: Should we always "just say no?". *Am J Transplant* 2020;20:1787-94.

16. Escudero D, Valentín MO, Escalante JL, Sanmartín A, Perez-Basterrechea M, de Gea J, et al. Intensive care practices in brain death diagnosis and organ donation. *Anaesthesia* 2015;70:1130-9.
17. Çalışkan G, Sayan A, Kilic I, Haki C, Kelebek Girgin N. Has the COVID-19 pandemic affected brain death notifications and organ donation time? *Exp Clin Transplant* 2021 Aug 9. doi: . 10.6002/ect.2021.0090.
18. Dal HC. Brain death and organ donation during the COVID-19 pandemic: a retrospective observational study. *Çukurova Anestezi ve Cerrahi Bilimler Dergisi* 2022;5:33-42.
19. Ahmed O, Brockmeier D, Lee K, Chapman WC, Doyle MBM. Organ donation during the COVID-19 pandemic. *Am J Transplant* 2020;20:3081-8.
20. Kirakli C, Uçar Z, Anil A, Ozbek I. [The effect of shortening confirmed brain death diagnosis time on organ donation rates in the intensive care unit]. *Dahili ve Cerrahi Bilimler Yoğun Bakım Dergisi* 2011;2:8-11. [Article in Turkish]
21. Lustbader D, O'Hara D, Wijdicks E, MacLean L, Tajik W, Ying A, et al. Second brain death examination may negatively affect organ donation. *Neurology* 2011;76:119-24.
22. Balkaya AN, Demirel A, Korkmaz HA, Özyaprak B, Kılıçarslan N, Yılmaz C. Brain death diagnosis and management in the COVID-19 pandemic. *Cukurova Med J* 2022;47:942-9.



This is an open access article distributed under the terms of [Creative Commons Attribution-NonCommercial-NoDerivatives 4.0 International License](https://creativecommons.org/licenses/by-nc-nd/4.0/).

Evaluation of novel ventricular repolarization parameters in patients with acromegaly

Hayati Eren¹, Selin Genç², Bahri Evren², İbrahim Şahin²

¹Department of Cardiology, Elbistan State Hospital, Kahramanmaraş, Turkey; ²Department of Endocrinology and Metabolism, Inonu University, Faculty of Medicine, Malatya, Turkey.

ABSTRACT

Objectives: T wave's peak and end interval (Tp-e), Tp-e/QT ratio and Tp-e/QTc ratio are novel markers of ventricular repolarization and are associated with ventricular arrhythmias. Increased ventricular arrhythmia incidence is reported in patients with acromegaly. The purpose of this study is to evaluate ventricular repolarization using the Tp-e interval, Tp-e/QT ratio, and Tp-e/QTc ratio in patients with acromegaly.

Methods: Thirty-five patients with acromegaly were included in the study. The control group was consisted of forty-one subjects without acromegaly that having similar age, sex ratio and comorbidities. The Tp-e interval, Tp-e/QT ratio, Tp-e/QTc ratio, and other ventricular repolarization parameters of all patients were evaluated using electrocardiography.

Results: Tp-e interval, Tp-e/QT ratio and Tp-e/QTc ratio were significantly prolonged in patients with acromegaly compared to the control group. Furthermore, Tp-e interval, Tp-e/QT ratio, and Tp-e/QTc ratio showed a significant correlation with plasma GH levels and LVMI values.

Conclusions: Our study revealed that Tp-e interval, Tp-e/QT ratio, and Tp-e/QTc ratio are prolonged in patients with acromegaly. We believe that the Tp-e interval, Tp-e/QT ratio, and Tpe/QTc ratio can be used in the evaluation of increased cardiovascular risk in patients with acromegaly.

Keywords: Acromegaly, ventricular repolarization, novel electrocardiographic parameters

Acromegaly is a rare disease and the total prevalence ranges between 2.8 and 13.7 cases per 100,000 people and the annual incidence rates range between 0.2 and 1.1 cases/100,000 people [1, 2]. Acromegaly is a disorder that associated with increased cardiovascular morbidity and mortality, and around 60% of these patients die due to several cardiovascular complications, including cardiac arrhythmia [1, 2]. Especially, malign ventricular arrhythmias are the primary cause of sudden cardiac deaths [3, 4].

Increasing growth hormone (GH) and insulin-like growth factor 1 (IGF-1) in patients with acromegaly may cause the development of acromegalic cardiomyopathy (CMP) which in turn results in the development of myocardial hypertrophy and interstitial fibrosis [2, 5, 6]. The presence of acromegalic CMP becomes a source for the development of various arrhythmias and therefore, cardiac rhythm disorders occur more frequently and more severely in patients with acromegaly compared to the overall population

Received: June 11, 2022; Accepted: September 27, 2022; Published Online: March 21, 2023



e-ISSN: 2149-3189

How to cite this article: Eren H, Genç S, Evren B, Şahin İ. Evaluation of novel ventricular repolarization parameters in patients with acromegaly. Eur Res J 2023;9(3):582-590. DOI: 10.18621/eurj.1128668

Address for correspondence: Hayati Eren, MD., Elbistan State Hospital, Department of Cardiology, Kahramanmaraş, Turkey. E-mail: drhayatieren@hotmail.com, Phone: +90 344 413 80 01, Fax: +90 344 413 80 02



©Copyright © 2023 by Prusa Medical Publishing
Available at <http://dergipark.org.tr/eurj>
info@prusamp.com

[1, 7]. Therefore, knowing the predictors of arrhythmic events are crucial in the follow-ups of these patients [1, 6].

Traditionally, QT, dQT, QTc, dQTc QT, and transmural dispersion of repolarization are simple, non-invasive arrhythmogenic markers that are utilized to evaluate the homogeneity of cardiac repolarization. Recently, Tp-e interval, Tp-e/QT ratio, and Tp-e/QTc ratio have been used widely to evaluate the transmural dispersion of repolarization (TDR) [8-10]. Also, studies have shown that, in ECG, the Tp-e interval can be used as an index for total dispersion of repolarization, and furthermore, increased Tp-e interval can be a useful index to predict tachyarrhythmias and cardiovascular mortality [9-12]. In addition, the Tp-e interval, Tp-e/QT ratio, and Tp-e/QTc ratio are able to measure ventricular dispersion of repolarization better compared to QT and QTc, in that these methods are not affected by heart rate unlike QT and QTc [13-15]. As a result, membrane protein alterations and anatomical deterioration of cardiomyocytes that occur in patients with acromegaly can explain the impaired transmural dispersion of repolarization and prolonged ventricular repolarization [1, 2].

The purpose of this study is to evaluate the ventricular polarization using Tp-e interval, Tp-e/QT ratio, and Tp-e/QTc ratio in patients with acromegaly.

METHODS

Study Population

A total of 35 patients with acromegaly were included in the study. Afterward, 41 subjects with similar risk profiles were designated as the control group after they were evened out in terms of age and gender. 28 acromegaly patients had a previous transsphenoidal surgery history and 2 acromegaly patients had a previous transcranial surgery history. Furthermore, 5 acromegaly patients have radiotherapy or radiosurgery in their patient histories.

Acromegaly diagnoses have been made in line with the current guidelines [16]. The designated criteria for the diagnosis were the presence of clinical findings, high serum GH and IGF-1 confirmed with laboratory tests, serum GH value above 1 µg/L after 75 g oral glucose loading, and the presence of pituitary gland adenoma that is shown radiologically [16]. All

patients are evaluated in terms of concomitant diabetes mellitus (DM), hypertension (HT), panhypopituitarism, thyroid dysfunction, and all other systemic disorders, and the diagnosis of these diseases are determined in line with the current guidelines. All medicines used by patients were determined.

In our study, the follow-up period of acromegaly patients after the diagnosis were 96 (41-125) months (between minimum 12 months and maximum 296 months). In the evaluation after the follow-up, 23 patients were in remission, while 12 patients were on the active course of the disorder. Active disorder and remission conditions were defined in line with the latest acromegaly guidelines of the Endocrine Society [16].

Patients with coronary artery disease, moderate to severe valvular heart disease, chronic pulmonary disease, obstructive sleep apnea, chronic renal or hepatic impairment, thyroid dysfunction, persistent or uncontrolled HT, heart failure (Left ventricle ejection fraction of < 50%), hematologic disorders, electrolyte imbalance were not included in the study. Furthermore, all of the patients were within the sinus rhythm and patients with QT segments that cannot be analyzed in QT, any conduction problem, ST-T anomalies, pacemaker rhythm, atrial fibrillation, or arrhythmia or those who take any medicine that can affect Tp-e distance or QT interval (such as antiarrhythmics, tricyclic antidepressants, antihistamines, and antipsychotics) were not included in the study. The study protocol was approved by the local ethics committee in accordance with the Declaration of Helsinki and Good Clinical Practice Guidelines. All patients provided written informed consent.

Hormonal and Biochemical Evaluation

Serum GH and IGF-I levels of all patients were measured at the time of diagnosis and in follow-ups using chemiluminescence enzyme immunoassay commercial kits (IGF; Immulite 2000, Siemens healthcare, Diagnostic Products Ltd., Glyn Rhonwy, Llanberis, Gwynedd LL55 4EL United Kingdom and GH; Cobas e601, Roche Diagnostics GmbH, Sandhofer Strasse 116, D-68305 Mannheim, Germany). Furthermore, intra- and inter-test variation coefficients for IGF-1 were found to be 3.5% and 6.1% respectively, while intra- and inter-test variation coefficients for GH were 6.7% and 9.2% respectively. The reference interval for GH was 0.126-9.88 ng/mL. While IGF-I values are

given, these values were expressed as a percentage of the upper limit of the age-adjusted normal values and the age-specific reference intervals for IGF-1 were evaluated as recommended in the guidelines. The references were set as 80-330 ng/mL for patients aged 19 to 29, as 60-240 ng/mL for patients aged 30-39, as 50-220 ng/mL patients aged 40 to 49, as 40-210 ng/mL for patients aged 50 to 59, as 30-220 ng/mL for patients aged 60 to 130. Routine biochemical serum glucose, creatine, sodium, potassium, calcium, phosphorus, and magnesium levels of each patient were measured and all other hypophyseal hormones were routinely measured as well. All of these parameters were also measured for each person in the control group at least once. All other parameters were determined using routine methods. All serum samples were taken from the cubital venous vessel area in the early hours of the morning after 8 hours of fasting. None of the patients had pituitary insufficiencies or additional hormone secretion apart from GH and IGF-1.

Electrocardiography (ECG)

ECG with 12 leads was recorded in the supine position at 50 mm/s paper rate. To reduce erroneous measurements, all ECGs were scanned and transferred to a PC, zoomed in by $\times 400\%$ using Adobe Photoshop and the measurements were conducted using suitable programs. In ECG, the results with U waves were excluded. For each value, the mean of three different derivations was calculated. QT interval was determined as the distance between the start of the QRS complex to the end of the T wave, and the QTc value was calculated according to heart rate using the Bazett formula ($QTc = QT/RR^{1/2}$). The difference between the measured QT max and QT min was defined as QT dispersion. dQTc dispersion was defined as the difference between QTc max and QTc min. The interval between the peak point of the T wave to the end of the T wave was defined as the Tp-e interval. Tp-e was performed via precordial leads, as recommended [14]. From these measurements, the Tp-e/QT ratio and Tp-e/QTc ratio were calculated. The inter-observer variation coefficient was determined as 2.8%.

Echocardiography

All patients underwent transthoracic echocardiography (TTE) with a Phillips Affiniti 50C system (Philips Medical Systems, Netherlands). The exami-

nations were performed with the patient in the left decubitus position. Throughout the evaluation, patients were monitored using standard techniques. Echocardiographic evaluations included M-mode, two dimensional, and Doppler evaluation performed according to current guidelines [17]. Left atrial diameter (LAD) was measured using a parasternal long-axis view. Inter-ventricular septal (IVS) and posterior wall (PW) thicknesses and left ventricle end-diastolic (LVEDD) and end-systolic diameters (LVESD) were measured in parasternal long-axis view with M-mode. The left ventricular ejection fraction (LVEF) was calculated using Biplane Simpson's method [18]. The mean of three measurements was taken for all parameters. Left ventricle mass (LVM) was calculated using the equation previously recommended by Devereux et. al. [17]. Afterward, LVM was proportioned to the body surface area and left ventricle mass index (LVMI) was calculated [17].

Statistical Analysis

For all statistical analyses, SPSS 22.0 Statistical Package Program for Windows (SPSS Inc., Chicago, IL, USA) was used. Kolmogorov-Smirnov test was used to determine the normality of the dispersion. While the numerical data with normal dispersion is given as mean \pm standard deviation, numerical variables with non-normal dispersion were given as medians (interval between quarters). Categorical variables were presented as numbers and percentage values. The chi-square test was used when comparing categorical variables between the groups. Student t-test or Mann-Whitney U test was used to compare continuous variables between the groups. Pearson correlation analysis was performed to analyze the relation between repolarization parameters, and GH levels and LVMI. $P < 0.05$ value was considered to be statistically significant.

RESULTS

There was no significant difference between the acromegaly patients and the control group in terms of age, sex, body mass index (BMI), DM and HT frequencies, systolic and diastolic blood pressures, and smoking (Table 1). The basal, demographic, and laboratory parameters of both groups were given in Table

1. While the basal GH and IGF-1 levels of acromegaly patients were significantly higher compared to the control group, no other difference was detected in other blood parameters (Table 1).

ues of the acromegaly patients were significantly longer compared to the control group (Table 2). Also QT, QTc, dQT, dQTc, values of the acromegaly patients were significantly longer compared to the control group (Table 2). While there was no

Tp-e interval, Tp-e/QT ratio, Tp-e/QTc ratio val-

Table 1. The baseline characteristics and laboratory findings of study patients

	Control group (n = 41)	Acromegaly patients (n = 35)	p value
Demographic parameters			
Age, (years)	50.7 ± 9.8	51.5 ± 10.2	0.351
Female, n (%)	25 (60.9)	22 (62.8)	0.218
HT, n (%)	9 (21.9)	8 (22.8)	0.257
Smoking, n (%)	8 (19.5)	7 (20.0)	0.217
DM, n (%)	11 (26.8)	10 (28.5)	0.174
Body mass index (kg/m ²)	26.4 ± 4.5	26.8 ± 4.7	0.475
Family history of CAD, n (%)	6 (14.6)	5 (14.2)	0.237
Heart rate, (beat/minute)	78.4 (13.6)	80.5 (21.9)	0.817
Systolic blood pressure, (mm Hg)	127.8 (12.8)	129.3 (14.5)	0.345
Diastolic blood pressure, (mm Hg)	82.8 (7.9)	83.3 (9.2)	0.156
Follow-up duration, (months)	-	96 (41-125)	-
Laboratory parameters			
GH	0.6 ± 0.2	17.2 ± 10.2	< 0.001
IGF-1	123.2 ± 39.5	582.8 ± 125.1	< 0.001
Glucose (mg/dL)	120 ± 25	121 ± 31	0.325
HbA1c (%)	5.7 ± 1.3	5.7 ± 1.5	0.347
Hg (mg/dL)	13.5 ± 2.2	13.9 ± 2.4	0.152
Creatinine (mg/dL)	0.89 ± 0.16	0.91 ± 0.18	0.234
Total cholesterol (mg/dL)	159 ± 26	162 ± 31	0.123
Triglyceride (mg/dL)	149 ± 44	155 ± 53	0.239
Low-density lipoprotein (mg/dL)	129 ± 19	131 ± 21	0.329
High-density lipoprotein (mg/dL)	41 ± 10	39 ± 9	0.516
WBC Count, (×10 ³ /μL)	7.4 ± 2.9	7.3 ± 3.1	0.476
PLT Count, (×10 ³ /μL)	318 ± 42	321 ± 46	0.149
C-Reactive protein, (mg/dL)	0.65 ± 0.27	0.68 ± 0.29	0.521
Na (mmol/L)	141 ± 9	142 ± 7	0.236
K (mmol/L)	4.15 ± 0.23	4.12 ± 0.35	0.274
Ca (mg/dL)	8.9 ± 1.2	9.1 ± 1.4	0.574
TSH (μIU/mL)	2.35 ± 0.08	2.31 ± 0.09	0.138

Ca = calcium, CAD = coronary artery disease, DM = diabetes mellitus, GH = growth hormone, Hg = hemoglobin, HT = hypertension, IGF-1 = Insulin-like growth factor 1, K = potassium, Na = Sodium, PLT = Platelet count, TSH = thyroid-stimulating hormone, WBC = White blood cell

Table 2. The Electrocardiographic and echocardiographic findings of study patients

	Control group (n = 41)	Acromegaly patients (baseline) (n = 35)	p value
Electrocardiographic measurement (at baseline)			
Tp-e interval	67.6 ± 8.3	85.3 ± 12.7	< 0.001
Tp-e/QT ratio	0.192 ± 0.021	0.234 ± 0.030	< 0.001
Tp-e/QTc ratio	0.184 ± 0.023	0.223 ± 0.032	< 0.001
QT interval	361.6 ± 24.2	382.9 ± 35.4	< 0.001
cQT interval	382.3 ± 20.1	415.4 ± 41.6	< 0.001
QTd interval	62.5 ± 11.6	71.1 ± 10.4	< 0.001
cQTd interval	69.2 ± 14.1	78.1 ± 13.2	0.002
Echocardiographic parameters			
LV ejection fraction (%)	61.9 ± 4.8	63.5 ± 5.2	0.375
LV end-diastolic diameter (cm)	4.81 ± 0.83	4.92 ± 0.91	0.198
LV end-systolic diameter (cm)	2.81 ± 0.8	2.75 ± 0.7	0.321
Interventricular septal thickness (cm)	0.92 ± 0.10	1.19 ± 0.21	< 0.001
Posterior wall thickness (cm)	0.91 ± 0.09	1.17 ± 0.21	< 0.001
Left atrial diameter (cm)	36.9 ± 2.1	37.1 ± 2.3	0.102
LVMI	82.4 ± 21.7	117.3 ± 35.1	< 0.001
E/e'	6.37 ± 1.7	8.25 ± 3.1	< 0.001

LV = left ventricular, LVMI = left ventricular mass index

echocardiographic difference between the groups in terms of EF, LVEDD, LVEED, and LA diameter, the values for IVS, PW, LWMI, and E/e' were significantly higher in the acromegaly patients (Table 2). The basal electrocardiographic and echocardiographic findings of the acromegaly patients and the control

group are summarized in Table 2.

In addition, no significant difference was observed between the patients in remission (n = 23) and the patients in active phase (n = 12) in terms of QT interval, cQT interval, QTd interval, cQTd interval (for all parameters, p > 0.05). However Tp-e interval, Tp-e/QT

Table 3. Electrocardiographic findings after follow-up according to the active or remission status of the study patients

Variables	Acromegaly patients on remission (n = 23)	Acromegaly patients on active disease (n = 12)	p value
Tp-e interval	81.8 ± 11.5	91.4 ± 14.3	0.003
Tp-e/QT ratio	0.229 ± 0.021	0.242 ± 0.027	0.002
Tp-e/cQT ratio	0.219 ± 0.029	0.229 ± 0.033	0.007
QT interval	381.7 ± 31.2	383.9 ± 32.4	0.102
cQT interval	412.4 ± 36.6	415.9 ± 37.4	0.763
QTd interval	70.5 ± 6.2	72.8 ± 5.7	0.325
cQTd interval	79.2 ± 8.1	81.4 ± 7.7	0.271

Table 4. Correlation analysis showing the between new ventricular depolarizations parameters and GH levels, IGF-1 levels, LVMI and disease duration time

	Tp-e Interval		Tp-e/QT Ratio		Tp-e/QTc Ratio	
	<i>r</i>	<i>p value</i>	<i>r</i>	<i>p</i>	<i>r</i>	<i>p value</i>
GH	0.612	< 0.001	0.523	< 0.001	0.549	< 0.001
IGF-1	0.456	< 0.001	0.478	< 0.001	0.449	< 0.001
LVMI	0.502	< 0.001	0.487	< 0.001	0.479	< 0.001
Disease duration	0.506	0.002	0.496	0.002	0.530	< 0.001

GH = growth hormone, IGF-1 = Insulin-like growth factor 1, LVMI = left ventricular mass index

ratio and Tp-e/QTc ratio were significant higher in patients with active disease (Table 3).

A significant positive correlation was observed between Tp-e, Tp-e/QT, Tp-e/QTc values and GH level, IGF-1 level and LVMI values (Table 3). Also a significant positive correlation was observed between Tp-e interval, Tp-e/QT ratio, Tp-e/QTc ratio values and disease duration (Table 4).

DISCUSSION

In this study, we focused on determining the Tp-e interval, Tp-e/QT ratio, and Tp-e/QTc ratio in patients with acromegaly. We found out that the Tp-e, Tp-e/QT, Tp-e/QTc, QT, QTc, dQT, and dQTc values were measured for the acromegaly patients were significantly longer compared to the control group. In addition, while there was no difference between the QT, QTc, dQT and dQTc values in patients with the active phase and remission, we found that the Tp-e interval, Tp-e/QT, Tp-e/QTc ratio to be significantly higher in patients with the active phase. Therefore, we demonstrated that new generation parameters are superior to traditional methods in evaluating ventricular repolarization, especially in patients with acromegaly in the active phase. Furthermore, we have seen a significant correlation between Tp-e interval, Tp-e/QT ratio, Tp-e/QTc ratio, and disease duration. This study is the first study that evaluates Tp-e, Tp-e/QT ratio, and Tp-e/QTc ratio in patients with acromegaly.

In this study, we have found out that QT, QTc, dQT, and dQTc values of the acromegaly patients are significantly longer compared to the control group.

QT, QTc, dQT, and dQTc are reported to be associated with sudden cardiac death and the development of ventricular arrhythmia in different clinical circumstances [8, 19]. QT, QTc, dQT, and dQTc are the traditionally well-known markers of ventricular repolarization [8, 19]. Similarly, it has been shown that QT, QTc, dQT, and dQTc values are prolonged in patients with acromegaly [15, 20, 21]. That the changes occurring in the ventricle after acromegalic CMP causes prolongation in ventricular repolarization and ventricular dishomogeneity can explain the increased QT, QTc, dQT, and dQTc intervals [21, 22]. Recently, the use of Tp-e interval, Tp-e/QT ratio, and Tp-e/QTc ratio as the new markers of ventricular repolarization dispersion are becoming more and more common [14, 23]. In our study, we have found that Tp-e interval, Tp-e/QT, and Tp-e/QTc ratios were significantly higher in patients with acromegaly than control subjects. According to the results of our study, we have revealed that acromegaly disorder causes impaired repolarization anomalies. Furthermore, prolonged Tp-e interval and increased Tp-e/QT ratio and Tp-e/QTc ratio have been shown to be associated with increased mortality in various diseases such as, firstly, Brugada syndrome, long QT syndrome, hypertrophic cardiomyopathy syndrome, and acute ST-segment elevation myocardial infarction, and the ventricular repolarization anomalies [9, 10, 14, 24, 25]. It is well known that pathologic left ventricular hypertrophy is a risk factor for the development of ventricular arrhythmia and sudden cardiac death [22, 26]. Pathological hypertrophy developing in patients with acromegaly makes the ventricle more susceptible to malign tachycardias by causing electrical instability in

cardiomyocytes [4-6]. Furthermore, it has been shown that the presence of LVH increases ventricular repolarization time [24, 25].

In our study, we have found the left ventricular wall thickness, as well as LVMI values in patients with acromegaly significantly higher compared to the control group. Furthermore, in our study, the finding of a significant correlation between Tp-e interval, Tp-e/QT, Tpe/QTc values, and LVMI is supported by the mechanisms above. Zhao *et al.* demonstrated that LVH was closely related to increased QT interval, Tp-e interval, and Tp-e/QT ratio [25]. Similarly, in a previous study, a correlation was found between cardiac arrhythmia frequency and echocardiographic LVM in patients with acromegaly [1]. In the same study, it was also shown that the severity of ventricular arrhythmias increases with the increase in left ventricular mass [1]. Our results support that the increased LVMI is closely associated with prolonged Tp-e interval, Tp-e/QT ratio, and Tp-e/QTc ratio values that signify ventricular repolarization anomalies. The receptors of GH and IGF-1 hormones are present in cardiomyocytes as well, and these hormones form the basis of cardiovascular complications by affecting the myocardial structure and function via endocrine, autocrine, paracrine systems [6, 27]. As a result of these impacts, a complication like myocarditis occurs with the development of increased myocardial collagen tissue, impairment of myocyte necrosis areas, lymphonuclear myocarditis, and as a consequence, a gradual impairment occurs in the structure of the heart [28].

Another important finding of our study is that we found a significant relationship between disease duration and Tpe, Tpe/QT and Tpe/QTc values at follow-up. This shows that the longer the disease duration, the more risky the patients are in terms of developing arrhythmia. It was shown that ventricular arrhythmia occurs more frequently and in a more complex manner in patients with acromegaly [1, 5, 6]. It was also shown that ventricular arrhythmias among in patients with acromegaly affect life quality and even are the most significant cause of death [1, 3, 4]. Therefore, early detection of the parameters that may be related to the development of arrhythmia is crucial for acromegaly patients.

In addition, while there was no difference between

the QT, QTc, dQT and dQTc values in patients with the active phase and remission, we found that the Tp-e interval, Tp-e/QT, Tp-e/QTc ratio to be significantly higher in patients with the active phase. In other words, we determined that the risk of arrhythmia is still high in patients with active disease and traditional repolarization parameters are insufficient in this case. Therefore, we demonstrated that new generation parameters are superior to traditional methods in evaluating ventricular repolarization, especially in patients with acromegaly in the active phase.

When we consider the effects of GH and IGF-1 hormones on cardiomyocytes, our results are not surprising and according to our study, closer follow-up may be required for the development of arrhythmia. When we evaluate all our findings, we recommend measuring the next generation ventricular repolarization parameters to determine the risk of cardiac arrhythmia in all patients with acromegaly.

Limitations

The main limitations of our study are that it is a retrospective study. Another limitation is that we have not evaluated the relation between ventricular arrhythmia and Tp-e interval, Tp-e/QT, and Tp-e/cQT ratio, as the patients were not followed up for a long time. Furthermore, the study population was not monitored for ventricular arrhythmic episodes or mortality prospectively. Large-scale prospective studies are needed to determine the predicted value of prolonged Tp-e interval and increased Tp-e/QT, and Tp-e/cQT.

CONCLUSION

For the first time, we have shown that Tp-e interval, Tp-e/QT, and Tp-e/cQT ratios are longer in patients with acromegaly. Our results show the increased ventricular repolarization heterogeneity in these patients and may contribute to understanding the pathophysiologic mechanisms of ventricular arrhythmia prevalence and cardiovascular mortality risk. Increased ventricular arrhythmia and sudden cardiac death frequency can be explained by transmural dispersion. Improvement in new ventricular repolarization parameters in patients with remission phase suggests

that mortality can be reduced with treatment in patients with acromegaly.

Ethical Approval

İnönü University Scientific Research and Publication Ethics Committee, Health Sciences Non-Invasive Clinical Research Ethics Committee. Date : 22-12-2020, Decision no.: 2020/1406

Authors' Contribution

Study Conception: HE, SG, BE, İŞ; Study Design: HE, SG, BE, İŞ; Supervision: HE, SG, BE, İŞ; Funding: HE, SG, BE, İŞ; Materials: HE, SG, BE, İŞ; Data Collection and/or Processing: HE, SG, BE, İŞ; Statistical Analysis and/or Data Interpretation: HE, SG, BE, İŞ; Literature Review: HE, SG, BE, İŞ; Manuscript Preparation: HE, SG, BE, İŞ and Critical Review: HE, SG, BE, İŞ.

Conflict of interest

The authors disclosed no conflict of interest during the preparation or publication of this manuscript.

Financing

The authors disclosed that they did not receive any grant during conduction or writing of this study.

REFERENCES

- Kahaly G, Olshausen KV, Mohr-Kahaly S, Erbel R, Boor S, Beyer J, et al. Arrhythmia profile in acromegaly. *Eur Heart J* 1992;13:51-6.
- Colao A, Ferone D, Marzullo P, Lombardi G. Systemic complications of acromegaly: epidemiology, pathogenesis, and management. *Endocr Rev* 2004;25:102-52.
- Matturri L, Varesi C, Nappo A, Cuttin MS, Rossi L. [Sudden cardiac death in acromegaly. Anatomopathological observation of a case]. *Minerva Med* 1998;89:287-91. [Article in Italian]
- Arias MA, Pachón M, Rodríguez-Padial L. Ventricular tachycardia in acromegaly. *Rev Port Cardiol* 2011;30:223-6.
- Saccà L, Cittadini A, Fazio S. Growth hormone and the heart. *Endocr Rev* 1994;15:555-73.
- Colao A, Marzullo P, Di Somma C, Lombardi G. Growth hormone and the heart. *Clin Endocrinol (Oxf)* 2001;54:137-54.
- Colao A. Are patients with acromegaly at high risk for dysrhythmias? *Clin Endocrinol* 2001;55:305-69.
- Galinier M, Vialette JC, Fourcade J, Cabrol P, Dongay B, Massabuau P, et al. QT interval dispersion as a predictor of arrhythmic events in congestive heart failure. Importance of aetiology. *Eur Heart J* 1998;19:1054-62.
- Kors JA, Ritsema van Eck HJ, van Herpen G. The meaning of the Tp-Te interval and its diagnostic value. *J Electrocardiol* 2008;41:575-80.
- Antzelevitch C, Sicouri S, Di Diego JM, Burashnikov A, Viskin S, Shimizu W, et al. Does Tpeak-Tend provide an index of transmural dispersion of repolarization? *Heart Rhythm* 2007;4:1114-6.
- Castro Hevia J, Antzelevitch C, Tornés Bárzaga F, Dorantes Sánchez M, Dorticós Balea F, Zayas Molina R, et al. Tpeak-Tend and Tpeak-Tend dispersion as risk factors for ventricular tachycardia/ventricular fibrillation in patients with the Brugada syndrome. *J Am Coll Cardiol* 2006;47:1828-34.
- Erikssen G, Liestøl K, Gullestad L, Haugaa KH, Bendz B, Amlie JP. The terminal part of the QT interval (T peak to T end): a predictor of mortality after acute myocardial infarction. *Ann Noninvasive Electrocardiol* 2012;17:85-94.
- Watanabe N, Kobayashi Y, Tanno K, Miyoshi F, Asano T, Kawamura M, et al. Transmural dispersion of repolarization and ventricular tachyarrhythmias. *J Electrocardiol* 2004;37:191-200.
- Gupta P, Patel C, Patel H, Narayanaswamy S, Malhotra B, Green JT, et al. T(p-e)/QT ratio as an index of arrhythmogenesis. *J Electrocardiol* 2008;41:567-74.
- Baser H, Akar BN, Polat B, Evranos B, Ersoy R, Bozkurt E, et al. The evaluation of QT intervals during diagnosis and after follow-up in acromegaly patients. *Acta Med Port* 2014;27:428-32.
- Melmed S, Bronstein MD, Chanson P, Klibanski A, Casanueva FF, Wass JAH, et al. A Consensus Statement on acromegaly therapeutic outcomes. *Nat Rev Endocrinol* 2018;14:552-56.
- Devereux RB, de Simone G, Koren MJ, Roman MJ, Laragh JH. Left ventricular mass as a predictor of development of hypertension. *Am J Hypertens* 1991;4:603S-7S.
- Lang RM, Bierig M, Devereux RB, Flachskampf FA, Foster E, Pellikka PA, et al. Chamber Quantification Writing Group; American Society of Echocardiography's Guidelines and Standards Committee; European Association of Echocardiography. *J Am Soc Echocardiogr* 2005;18:1440-63.
- Hintenseer M, Beckmann BM, Thomsen MB, Pfeufer A, Dalla Pozza R, Loeff M, et al. Relation of increased short-term variability of QT interval to congenital long-QT syndrome. *Am J Cardiol* 2009;103:1244-8.
- Mohamed AL, Yusoff K, Muttalif AR, Khalid BA. Markers of ventricular tachyarrhythmias in patients with acromegaly. *Med J Malaysia* 1999;54:338-45.
- Unubol M, Eryilmaz U, Guney E, Ture M, Akgullu C. QT dispersion in patients with acromegaly. *Endocrine* 2013;43:419-23.
- Mayet J, Shahi M, McGrath K, Poulter NR, Sever PS, Foale RA, et al. Left ventricular hypertrophy and QT dispersion in hypertension. *Hypertension* 1996;28:791-6.
- Zhao X, Xie Z, Chu Y, Yang L, Xu W, Yang X, et al. Association between Tp-e/QT ratio and prognosis in patients undergoing primary percutaneous coronary intervention for ST-segment elevation myocardial infarction. *Clin Cardiol* 2012;35:559-64.
- Yayla Ç, Bilgin M, Akboğa MK, Gayretli Yayla K, Canpolat U, Dinç Asarcikli L, et al. Evaluation of Tp-E interval and Tp-

E/QT ratio in patients with aortic stenosis. *Ann Noninvasive Electrocardiol* 2016;21:287-93.

25. Zhao Z, Yuan Z, Ji Y, Wu Y, Qi Y. Left ventricular hypertrophy amplifies the QT, and Tp-e intervals and the Tp-e/QT ratio of left chest ECG. *J Biomed Res* 2010;24:69-72.

26. Ijiri H, Kohno I, Yin D, Iwasaki H, Takusagawa M, Iida T, et al. Cardiac arrhythmias and left ventricular hypertrophy in dipper and nondipper patients with essential hypertension. *Jpn Circ J*

2000;64:499-504.

27. Ito H, Hiroe M, Hirata Y, Tsujino M, Adachi S, Shichiri M, et al. Insulin-like growth factor-I induces hypertrophy with enhanced expression of muscle specific genes in cultured rat cardiomyocytes. *Circulation* 1993;87:1715-21.

28. Lie JT. Pathology of the heart in acromegaly: anatomic findings in 27 autopsied patients. *Am Heart J* 1980;100:41-52.



This is an open access article distributed under the terms of [Creative Commons Attribution-NonCommercial-NoDerivatives 4.0 International License](https://creativecommons.org/licenses/by-nc-nd/4.0/).

The mechanism of mindfulness meditation on pain by functional magnetic resonance imaging method

Yasemin Yıldız¹, Sayad Kocahan¹, Alp Eren Çelenlioğlu², Mehmet Özler¹

¹Department of Physiology, University of Health Sciences, Gülhane Faculty of Medicine, Ankara, Turkey; ²Department of Algology, University of Health Sciences, Gülhane Training and Research Hospital, Ankara, Turkey

ABSTRACT

Pain is a subjective feeling having sensory, cognitive and emotional components. Brain regions that cognitively and affectively contribute to pain sensation are the anterior cingulate cortex (ACC), insula, prefrontal cortex (PFC) and the default mode network (DMN). Depression and anxiety may accompany pain and they may exaggerate the pain via cognitive and affective disturbance. As a complementary treatment of pain, mindfulness meditation which is a therapeutic technique may be described as “non-judgmental awareness of the present moment”. Mindfulness meditation aims to focus on the experiences of bodily sensations and breathing in a non-judgmental and accepting manner. The functional magnetic resonance imaging (fMRI) is one of the tools that can explain the mechanism of action of mindfulness meditation on pain intensity, pain unpleasantness and the cognitive and affective disorders which accompanying pain. This study compiles studies examining the mechanism of action of mindfulness meditation on pain and pain accompanying pain unpleasantness, depression, anxiety with fMRI.

Keywords: Pain, mindfulness meditation, functional magnetic resonance imaging

Pain is a clinical symptom that causes suffering making life sometimes unbearable. The generally accepted definition of pain has been made by the International Association for the Study of Pain as “an unpleasant sensory and emotional experience associated with or similar to actual or potential tissue damage” [1]. The sensory and the emotional aspect of the pain sensation is described by the parameters of "pain intensity" and "pain unpleasantness" determined by various scales that are validated and reliable [2, 3]. Due to the pain-related quality of life impairment, psychological comorbidity, reduction of productivity and other negative social and economic consequences pain needs to be treated [4]. Many pharmacological (such

as tricyclic antidepressants, anticonvulsants such as gabapentin, opioids) and non-pharmacological (such as Cognitive Behavioral Therapy, Transcutaneous Electrical Nerve Stimulation) methods are used in the treatment of pain [5, 6]. Mindfulness meditation is one of the non-pharmacological treatment methods offered in the treatment of pain. There are many studies in the literature demonstrating the ameliorative effects of mindfulness meditation for the treatment of pain, depression and anxiety [7-12]. In some studies, the mechanisms underlying the ameliorating effect of mindfulness meditation on pain, depression and anxiety were examined with functional Magnetic Resonance Imaging (fMRI). In this review, a

Received: February 1, 2023; Accepted: April 5, 2023; Published Online: April 12, 2023



e-ISSN: 2149-3189

How to cite this article: Yıldız Y, Kocahan S, Çelenlioğlu AE, Özler M. The mechanism of mindfulness meditation on pain by functional magnetic resonance imaging method. Eur Res J 2023;9(3):591-599. DOI: 10.18621/eurj.1245845

Address for correspondence: Yasemin Yıldız, MD., University of Health Sciences, Gülhane Faculty of Medicine, Department of Physiology, Gülhane Külliyesi, Emrah Mah., 06018 Etilik, Keçiören, Ankara, Turkey. E-mail: yasemin.yildiz1@sbu.edu.tr, Phone: +90 312 304 61 71



©Copyright © 2023 by Prusa Medical Publishing
Available at <http://dergipark.org.tr/eurj>
info@prusamp.com

comprehensive compilation is conducted using a combination of the keywords "pain, mindfulness meditation and fMRI". The purpose of this review is to evaluate the fMRI findings that could explain underlying neural mechanisms of mindfulness meditation for the patients with pain.

TRANSMISSION AND PROCESSING OF PAIN SENSATION

The pain receptors (nociceptor) are specialized sensory receptors that convert noxious stimulus to pain sensation in the form of free nerve endings. The nociceptors transmit the painful stimuli to the Central Nervous System (CNS) via action potential. Sensory neurons that receive the sensation of pain from the nociceptors and transmit it to the CNS, are primary afferent neurons. The processing of pain sensation in the central nervous system is a complex process. Primary afferent neurons that receive pain sensation with nociceptors (C type and A delta type fibers) reach the posterior horn of the spinal cord and synapse here. They innervate the second neuron with the neurotransmitters (glutamate and substance P) secreted into the synaptic gap via the spinothalamic pathways to transmit the pain sensation to the thalamus. The spinothalamic pathway is divided into two as the neospinothalamic pathway which transmits fast and sharp pain and the paleospinothalamic pathway which transmits slow, dull pain. Via these two pathways, the third neurons that receive the sensation of pain from thalamus reach the primary and secondary somatosensory cortex in the parietal cortex. These neurons are represented topographically in the sensory homunculus region that are corresponding to them and pain is perceived in the body region that topographically fits its location [6, 13].

In addition to the pathway that the pain is carried, it is clinically divided into acute and chronic pain according to its duration. "Acute pain" defines pain that lasts less than 30 days, while pain that lasts longer than 6 months is called "chronic pain". Acute pain is self-limiting and is attenuated when nociceptive input is blocked by medications. However, the patients suffer more from chronic pain due to comorbidities such as depression and anxiety [14].

COGNITIVE AND EMOTIONAL ASPECTS OF PAIN

Pain is not a simple somatosensory sensation perceived by nociceptors and transmitted by spinothalamic pathways. There are also cerebral cortex regions that affect the perception of pain by cognitive and affective factors [13]. Among the neuroimaging methods, fMRI is an important tool in determination of the effect of the psychology, cognitive and emotional status of a patient on the changes in the structure and functions of the brain during pain. In fMRI studies it has been reported that regions in the brain such as the insula, anterior cingulate cortex (ACC), prefrontal cortex (PFC), amygdala and hippocampus where the pain is processed cognitively and affectively contribute to pain sensation [15-19]. Animal studies have shown that the ACC and amygdala play an important role in pain avoidance behavior and the affective/motivational aspect of pain [15, 16]. It has been reported that the PFC, primarily responsible for executive functions such as "decision making", may also be responsible for the cognitive and affective aspects of pain [17, 18].

In addition, Default Mode Network (DMN) activity reveals during pain. DMN is a neural network characterized by oscillatory activity in certain brain regions (medial prefrontal cortex, posterior cingulate cortex, precuneus, inferior and lateral temporal cortex). This network is activated by self-referential processes (mind-wandering and ruminations) and pain [20-22]. Pathways as "top-down control" that reflect on the horn of the Periaqueductal Gray Matter (PAG) and the posterior medulla spinalis are also effective in terms of painful sensory and emotional aspects. In this pathway, the main transmitters are serotonin and noradrenaline that may modify the perception of pain via cognitive and emotional factors by cortical control, indicating the importance of the psychological aspect of pain [23-25].

The depression and anxiety are among the most common diseases in primary care diseases in which cognitive and affective disorders are seen [26]. In the "Netherlands Study of Depression and Anxiety", a large sample study, a significant relationship was found between depression-anxiety and pain severity in patients with pain and with depression and anxiety [27]. It has been reported that the reason for the strong

relationship between pain, depression and anxiety may be that they share the same pathophysiological mechanisms. Pain, depression and anxiety may share the same cognitive and behavioral processes and they can occur with a change in activation in the same brain areas (ACC, PFC, insula) [27, 28]. Since cognitive and emotional factors affect the pain intensity, the offered treatment method should improve depression and anxiety to relieve the patients with pain. At this point, mindfulness meditation emerges as a complementary treatment approach for pain, pain unpleasantness, depression and anxiety that may accompany pain [29].

EFFECT OF MINDFULNESS MEDITATION ON PAIN

Mindfulness meditation has its origins in Ancient Eastern culture. Although it is originated from 2500 years of Buddhism tradition, it is a cognitive and behavioral therapeutic technique used for medical practices in the West medicine. Basically, mindfulness can be defined as “*moment-by-moment awareness*”. However, mindfulness is purely experiential [29, 30]. During the mindfulness meditation process, people intentionally direct their attention and awareness to a certain focus by often breathing or arising physical sensations. People are encouraged to experience their mental stance (thoughts and emotions) and sensations in a non-judgemental, accepting manner and nonelaborative attitude. Meditators who are aware of the transience of thoughts, feelings and sensations reduce their stress and rumination [31, 32].

Although there are different mindfulness practices, mindfulness meditation is basically divided into two as “Focused Attention” and “Open Monitoring” in terms of the quality of the practice. In “Focus Attention”, the meditators focus on a certain object such as breathing and bodily sensation, by repeatedly shifting their attention from thought / emotion / external stimuli focuses to the selected object. Via “Open Monitoring”, on the other hand, the meditators become aware of their sensory/cognitive/emotional experience observing them with an openness attitude, non-judgement and nondetailed evaluation. It can be defined as “awareness of awareness”. Through the continuity of these practices, the meditators reach the ability to become aware of the thoughts, emotions in their mind

and somatosensory experiences (trait mindfulness), even when they do not practice meditation [12, 33]. Recently, the effect of mindfulness meditation on pain, depression and anxiety which may accompany pain have been the most common research topic. Kabat-Zinn [29], who has an important role in the widely acceptance of mindfulness, carried out an important study at Massachusetts Medical Center, in which patients experienced pain and stress for various reasons. As a result of this study, it was determined that pain, depression and anxiety decreased, after mindfulness meditation and this improvement – excluding pain – continued for 15-months follow-up [29]. This was MBSR (Mindfulness-Based Stress Reduction) used as a method in many clinical pain studies. MBSR is a structured and standardized program that includes a variety of practices such as breath focusing, yoga, body scanning and silence retreats [34]. After Kabat-Zinn *et al.* [29], scientific studies investigating the therapeutic effect and underlying mechanism of mindfulness meditation and MBSR on pain, depression and anxiety have increased over the years [7, 35-37]. Reiner *et al.* [38], reported that mindfulness-based practices reduced pain severity and this reduction continued for a long time through learned techniques.

PAIN, MINDFULNESS and fMRI

fMRI is a non-invasive method that investigates the effects of cognitive processes on neural activity in the brain. It is based on hemodynamic changes due to alterations in local neural activity [39]. In various studies, the pain-relieving effect of mindfulness meditation was demonstrated using fMRI that can determine the underlying neural mechanism. In the study of Gard *et al.* [40], painful stimuli were applied to expert meditators and novices (control group)(Table 1). They determined that the intensity of pain did not change in both groups via mindfulness meditation. However, in expert meditators, the decrease in pain unpleasantness was accompanied by a decrease in bilateral lateral prefrontal cortex activity. During mindfulness meditation, “accepting the pain non-judgementally” is related to decreased lateral PFC activity. In addition, an increase in posterior insula and seconder somatosensory cortex activity was accompanied by the decrease in anxiety about pain expectation. Because “focusing the atten-

tion to the sensory aspect of pain” is related to the insula activity through interoceptive attention (awareness of inner bodily sensations). Also, it has been reported that frontal top-down control was decreased in this process [40]. In this study, the increase in right anterior cingulate cortex and ventromedial prefrontal cortex activity may be related to the effect of reducing pain unpleasantness and anxiety expectation about pain in the positive emotional state created by mindfulness meditation. These are areas where the pain is processed cognitively and affectively. Because the pain and anxiety modulation through mindfulness is associated with decreased sensory processing of the pain in the brain [40].

Lutz *et al.* [9] showed that expert meditators had less pain unpleasantness during painful stimuli and stronger activity in left anterior insula and anterior midcingulate cortex by mindfulness meditation. In addition, it was reported that the activation of the amygdala decreased in experienced meditators anxiety during anticipation of pain. Amygdala activity is related with anxiety and decreased activity may be due to decreased anxiety [9].

In a study, a reduction in pain catastrophizing (negative, destructive thoughts about the pain itself) was accompanied by a decrease in connectivity in DMN nuclei and an increase in connectivity between the DMN and the somatosensory cortex [10]. It was attributed to the increased focus on the sensory stimulus (pain) and the lack of detail of emotional processes. This may lead to the fact that the “state of being mindful” in daily life, which can be improved with formal mindfulness meditation, is also effective in reducing pain [10]. Supporting this result, Zeidan *et al.* [11] suggested that mindfulness meditation during painful stimulus caused in increased “awareness”, decreased pain intensity, pain unpleasantness, and dorsal posterior cingulate cortex and precuneus deactivation in the brain in participants who had no previous meditation experience (novice). Mindfulness meditation can be a complementary treatment method in pain symptom via decreasing posterior cingulate cortex and precuneus activity by reducing self-referential and ruminative thoughts [119]. Because the posterior cingulate cortex and precuneus, which is the nucleus of the DMN, plays significant role in the processing of pain along with self-referential and ruminative thoughts.

Recently, there are studies by novice and expert

mediators on the effect of mindfulness meditation on pain. Wang *et al.* [41] presented that mindfulness meditation reduced pain unpleasantness in expert mediators and that the reason was the separation of the sensory and cognitive/affective aspects of pain. Painful stimuli were accompanied by increased activity in the secondary somatosensory cortex and posterior insula in experts, and decreased activity in the primary somatosensory cortex in novices. The reason may be the difference in the applied meditation directives. Thus; somatosensory activity is modulated by cognitive factors. Shifting attention from the painful stimulus to another thing decreases the activity in the somatosensory region while focusing on the painful stimulus increases the activity. In this respect, it is similar to the results of the study of Harrison *et al.* [10]. Expert mediators could improve pain through decreased activity in the ACC, PFC, and Orbitofrontal Cortex (OFC) (one of the areas responsible for sensory discrimination and emotional reaction), modulation of cognitive functions and decreased emotional reactivity. This once again points to the cognitive and affective aspects of analgesia developed by mindfulness meditation. Attenuation of the pain signal by mindfulness meditation before it reaches the thalamus, may decrease the activity in the thalamus and prevent the pain from reaching the somatosensory cortex as a strong signal. Reduction of self-referential thoughts in expert mediators may alleviate the pain by reducing DMN activity [41]. Considering the role of DMN in pain sensation, this is an expected feature.

Zeidan *et al.* [20] reported that the decrease in pain intensity by mindfulness meditation (Focus Attention) was accompanied by a decreased in ACC and right anterior insula activity which is responsible for the cognitive modulation of pain and interoceptive awareness. In this respect, “Focus Attention” has a different mechanism from “Open Monitoring” mindfulness meditation [20]. In a comprehensive study of Zeidan *et al.* [42] individuals who applied during a painful stimulus were divided into mindfulness meditation, sham and placebo. These groups were compared with fMRI imaging methods in terms of the effect of mindfulness meditation during the painful stimulus. Consequently, it was determined that “the level of awareness” (assessed by a scale) increased only in the group that applied mindfulness meditation and it was reported that although pain intensity and pain unpleasantness de-

Table 1. The effect of mindfulness meditation on pain and the results of the fMRI method

Authors	Areas	Effect	Comments
Gard et al. [40]	PFC, Insula, SII	Decreased pain unpleasantness, anxiety expectation	Interoceptive attention, accepting the pain non-judgementally
Lutz et al. [9]	Insula, Amygdala, MCC	Decreased anxiety of pain expectation	Decreased of amygdala activity may due to decreased anxiety
Harrison et al. [10]	DMN, Somatosensory Cortex	Reduction in pain catastrophizing	“State of being mindful” is effective in reducing pain
Zeidan et al. [11]	PCC, Precuneus	Decreased pain intensity and pain unpleasantness	Reduced ruminative and self-referential thoughts
Wang et al. [41]	ACC, Insula, OFC, Amygdala, PFC, DMN	Decreased pain unpleasantness	Reduced mind-wandering and emotional reaction
Zeidan et al. [42]	ACC, Insula, OFC, PAG	Decreased pain intensity and pain unpleasantness	Mindfulness meditation group’s mechanism is different from sham and control groups
Zeidan et al. [20]	ACC, Insula	Decreased pain intensity	“Focus Attention” and “Open Monitoring” has different mechanism on pain
Riegner et al. [43]	Precuneus, PFC, Amygdala	Decreased pain intensity and pain unpleasantness	“Focus Attention” result in precuneus deactivation, reduced emotional reaction
Seminowicz et al. [45]	Insula, Parietal Cortex	Headache frequency was reduced	MBSR; practice should continue
Braden et al. [46]	ACC, PFC	Back pain intensity and depression was reduced	Short-term MBSR is presented
Smith et al. [47]	ACC, PCC, PFC	Decreased pain intensity	MBSR is effective by shifting ruminative thoughts from pain
Mioduszewski et al. [48]	Brain White matter	Decreased chronic neuropathic pain	MBSR; white matter could new target for investigations
Hatchard et al. [49]	Primer Somatosensory Cortex, Precuneus	Decreased pain perception	MBSR; decreased emotional reactivity and pain expectation
Medina et al. [51]	Amygdala, ACC, Insula	Nondecreased pain intensity in groups	MBSR; VAS doesn’t reflect general pain intensity

fMRI = functional Magnetic Resonance Imaging, PFC = Prefrontal Cortex, SII = Secondary Somatosensory Cortex, MCC = Midcingulate Cortex, DMN = Default Mode Network, PCC = Posterior Cingulate Cortex, ACC = Anterior Cingulate Cortex, OFC = Orbitofrontal Cortex, PAG = Periaqueductal Gray Matter, MBSR = Mindfulness-Based Stress Reduction

creased in all three groups. However, it was determined that the neural analgesic mechanisms accompanying the decreased of pain intensity and pain unpleasantness in the group that practice mindfulness meditation were different from those in the sham and placebo groups. It was reported that the increase in the activity of the subgenual ACC, anterior insula and OFC responsible for the cognitive modulation of pain, was due to the non-judgmental awareness that takes place in mindfulness meditation. Also, significantly reduced neural activity was observed in the thalamus and PAG, where nociceptive information is facilitated and modulated by mindfulness meditation [42].

In a study, people who were applied painful stimuli and practiced mindfulness meditation (Focus Attention) had significantly decreased pain intensity and pain unpleasantness compared to the control group (reading an audiobook). The improvement in pain parameters was accompanied by decreased connectivity between the contralateral thalamus and precuneus and decreased activation of the ventromedial PFC, amygdala, and hippocampus [43]. The areas in which activity changes were observed in the study are similar to the study of Lutz *et al.* [9], Harrison *et al.* [10], Zeidan *et al.* [11] and Wang *et al.* [41]. Precuneus refers to the ‘‘awareness of one’s self and the surrounding sensory environment’’; pain increases with its activation [43, 44]. ‘‘Awareness of breath’’ through ‘‘Focus Attention’’ may explain the decreased activation of precuneus and improvement of pain parameters. In addition, mediators did not abandon oneself to the self-referential thoughts related to the painful stimulus, thanks to their ‘‘non-judgmental refocusing on their breath when their attention is disengaged from their breath without reacting emotionally’’. In the study, changes in ventromedial PFC can have a positive effect on pain by controlling affective processes [19]. The decrease in the emotional reaction to pain may explain the positive effect of these regions on the sensation of pain.

In addition to experimental painful stimuli, the underlying mechanism of mindfulness meditation on the patients with clinical pain was investigated by fMRI imaging method.

In these studies, MBSR, a structured program based on mindfulness meditation, was offered as a method to observe the activity changes in the insula, ACC, PFC and DMN playing an important role in the

effect of mindfulness meditation on pain [45-48].

Headache frequency was significantly reduced at 20th weeks compared to the active control group who applied MBSR in migraine patients who were administered two consecutive Stress Management for Headache programs, each lasting 8 weeks. In fMRI analyzes, it was found that connectivity decreased in the left dorsal anterior insula and the right posterior parietal cortex, which are responsible for the cognitive functions of the brain. These effects did not persist in the study at 52nd week. This points to the importance of continuity as well as the effectiveness of mindfulness meditation-based practices [45]. MBSR is a grueling and expensive program. For this reason, it was hypothesized that shorter-term MBSR (4-week) studies could also be done in the clinic. In a study [46], emotional awareness of patients who were given sadness-inducing visual stimuli and music to patients with back pain was determined and graded instantly. After the practices, pain intensity, depression and somatic-emotional symptoms of depression decreased compared to before (compared to the control group) and there was no change in the level of anxiety. In fMRI, right and left subgenual ACC, left ventrolateral PFC activity increased (compared to before) in the MBSR group. In addition, a positive correlation was found between the severity of sadness and left subgenual ACC activity. According to this study, although short-term MBSR programs are presented as a therapeutic method for pain intensity and depression in back pain patients, further research can be conducted with a larger sample and different meditation procedures, since their effects on anxiety are contradictory [46]. One of the painful syndromes is chronic neuropathic pain that does not respond to pharmacological treatments. So as to, the effectiveness of mindfulness-based practices and the underlying neural mechanisms in patients have been investigated via fMRI in many studies.

In a study, MBSR was applied for the management of chronic neuropathy in patients with breast cancer. The decrease in pain intensity in the MBSR group (compared to the wait-list group) was accompanied by an increase in PCC, medial PFC activity and ACC connectivity of the DMN. This finding was attributed to shifting the focus of attention from ruminative thoughts about pain and emotional evaluation of pain [47]. In this study, fMRI findings accompany-

ing the decrease in pain intensity contradict with the studies of Zeidan *et al.* [11] and Harrison *et al.* [10]. The reason for this result may be the difference in the mindfulness meditation procedure practiced. In addition to the ACC, insula, PFC and DMN imaged with fMRI in mindfulness meditation, there is another study in which brain white matter is also imaged as a new approach. In that study, it was reported that in patients with breast cancer after the MBSR program, the intensity of chronic neuropathic pain was decreased. The development was observed in the left lateralized uncinate fascicle, hippocampus, amygdala and outer capsule. These regions are responsible for executive functions, attention, emotional state and pain perception targeted by MBSR. As a result, it was presented as a non-pharmacological method for chronic neuropathic pain, which is a treatment-limiting factor in breast cancer [48]. Also in the patient group with chronic neuropathic pain, visual stimulus (compared to the control group) after MBSR was accompanied by a decrease in pain perception, accompanied by decreased activity in the primary somatosensory cortex (activated in chronic pain). A decrease in activity was observed in the precuneus. This finding points to the "mindful trait (ability of being aware of one's self and the surrounding sensory stimuli)". The decrease in activity seen in the dorsolateral PFC has been attributed to a decrease in pain expectation and reduced effort to control emotions. This study is one of the studies reporting the role of decreased emotional reactivity developed via mindfulness meditation in its improved effect on pain [49].

Fibromyalgia Syndrome is a pain disorder characterized by widespread skeletal-muscular pain and tenderness by palpation. It is accompanied by cognitive and affective disorders [50]. For this reason, mindfulness meditation, one of the treatments offered, has taken part in an approach that also targets these psychological comorbidities. In the study of Medina *et al.* [51], pain intensity and accompanying fMRI findings were compared in patients who continued their routine treatment (TAU), healthy lifestyle recommendations added to their routine treatment (TAU+FibroQoL) and in addition to MBSR (TAU+MBSR). In the TAU+FibroQoL group, amygdala activation was decreased in fMRI and it was reported that the patients were not engaged in negative emotions. Amygdala has the role in the top-down processes and the contribution of top-

down control to the affective aspect of pain can explain this result. However, no significant reduction in pain perception was reported in any of the three groups. This may indicate that mindfulness-based practices have no effect on chronic pain. However, measurement of pain intensity by VAS (Visual Analog Scale), which is an instant assessment, may not provide information about the pain in general of patients with chronic pain [51].

CONCLUSIONS

The fMRI findings about the effects of mindfulness meditation on pain intensity, pain unpleasantness and depression and anxiety may accompany pain are similar. During pain, activity changes in the ACC, insula, amygdala, PFC and DMN are observed with mindfulness meditation. This may indicate that the effect of mindfulness meditation on pain intensity occurs by affecting the areas where pain is processed cognitively and affectively. So that, mindfulness meditation can be offered as a complementary treatment method for pain intensity and accompanying psychological comorbidities such as pain unpleasantness, depression and anxiety.

In future studies, it may be aimed to determine the underlying neurophysiological abnormalities in patients with pain with different clinical diagnoses by fMRI and to determine the optimum meditation protocol and duration. In addition, the mechanism of action of mindfulness meditation in pain treatment can be investigated by using neurophysiological methods such as PET (Positron Emission Tomography), EEG (Electroencephalography) and Heart Rate Variability, as well as fMRI.

Authors' Contribution

Study Conception: YY; Study Design: N/A; Supervision: SK, MÖ, AEÇ; Funding: N/A; Materials: N/A; Data Collection and/or Processing: N/A; Statistical Analysis and/or Data Interpretation: N/A; Literature Review: YY; Manuscript Preparation: YY and Critical Review: YY, SK.

Conflict of interest

The authors disclosed no conflict of interest during the preparation or publication of this manuscript.

Financing

The authors disclosed that they did not receive any grant during conduction or writing of this study.

Acknowledgement

We would like to thank Hacettepe University Faculty of Medicine, Department of Physiology, Ass. Prof. Okan Arihan, for his contributions.

REFERENCES

- Raja SN, Carr DB, Cohen M, Finnerup NB, Flor H, Gibson S, et al. The revised International Association for the Study of Pain definition of pain: concepts, challenges, and compromises. *Pain* 2020;161:1976-82.
- Price DD. Psychological and neural mechanisms of the affective dimension of pain. *Science* 2000;288:1769-72.
- Pagé MG, Katz J, Stinson J, Isaac L, Martin-Pichora AL, Campbell F. Validation of the numerical rating scale for pain intensity and unpleasantness in pediatric acute postoperative pain: sensitivity to change over time. *J Pain* 2012;13:359-69.
- Henschke N, Kamper SJ, Maher CG. The epidemiology and economic consequences of pain. *Mayo Clin Proc* 2015;90:139-47.
- Finnerup NB, Otto M, McQuay H, Jensen T, Sindrup SH. Algorithm for neuropathic pain treatment: an evidence based proposal. *Pain* 2005;118:289-305.
- JE H. Guyton ve Hall Tibbi Fizyoloji (12. Baskı). Nobel Tıp Kitabevleri, İstanbul; 2013: pp. 721-5.
- Ball EF, Muhammad Sharizan ENS, Franklin G, Rogozińska E. Does mindfulness meditation improve chronic pain? A systematic review. *Curr Opin Obstet Gynecol* 2017;29:359-66.
- Song Y, Lu H, Chen H, Geng G, Wang J. Mindfulness intervention in the management of chronic pain and psychological comorbidity: a meta-analysis. *Int J Nurs Sci* 2014;1:215-23.
- Lutz A, McFarlin DR, Perlman DM, Salomons TV, Davidson RJ. Altered anterior insula activation during anticipation and experience of painful stimuli in expert meditators. *Neuroimage* 2013;64:538-46.
- Harrison R, Zeidan F, Kitsaras G, Ozcelik D, Salomons TV. Trait mindfulness is associated with lower pain reactivity and connectivity of the default mode network. *J Pain* 2019;20:645-54.
- Zeidan F, Salomons T, Farris SR, Emerson NM, Adler-Neal A, Jung Y, et al. Neural mechanisms supporting the relationship between dispositional mindfulness and pain. *Pain* 2018;159:2477-85.
- Zeidan F, Baumgartner JN, Coghill RC. The neural mechanisms of mindfulness-based pain relief: a functional magnetic resonance imaging-based review and primer. *Pain Rep* 2019;4:e749.
- Kandel ER, Schwartz JH, Jassel TM, Siegelbaum SA, Hudspeth AJ. Eds., *Principles Of Neurosciences*, 5th ed. McGraw-Hill Education/Medical, 2013.
- Weiner RS. *Pain management: A practical guide for clinicians*: CRC press; 2001.
- Fuchs PN, Peng YB, Boyette-Davis JA, Uhelski ML. The anterior cingulate cortex and pain processing. *Front Integr Neurosci* 2014;8:35.
- Derbyshire SW, Jones AK, Gyulai F, Clark S, Townsend D, Firestone LL. Pain processing during three levels of noxious stimulation produces differential patterns of central activity. *Pain* 1997;73:431-45.
- Thompson JM, Neugebauer V. Cortico-limbic pain mechanisms. *Neurosci Lett* 2019;702:15-23.
- Ong W-Y, Stohler CS, Herr DR. Role of the prefrontal cortex in pain processing. *Mol Neurobiol* 2019;56:1137-66.
- Roy M, Shohamy D, Wager TD. Ventromedial prefrontal-subcortical systems and the generation of affective meaning. *Trends Cogn Sci* 2012;16:147-56.
- Zeidan F, Martucci KT, Kraft RA, Gordon NS, McHaffie JG, Coghill RC. Brain mechanisms supporting the modulation of pain by mindfulness meditation. *J Neurosci* 2011;31:5540-8.
- Baliki MN, Mansour AR, Baria AT, Apkarian AV. Functional reorganization of the default mode network across chronic pain conditions. *PloS One* 2014;9:e106133.
- Kucyi A, Moayed M, Weissman-Fogel I, Goldberg MB, Freeman BV, Tenenbaum HC, et al. Enhanced medial prefrontal-default mode network functional connectivity in chronic pain and its association with pain rumination. *J Neurosci* 2014;34:3969-75.
- Donaldson LF, Lumb BM. Top-down control of pain. *J Physiol* 2017;595:4139-40.
- Bannister K, Dickenson A. The plasticity of descending controls in pain: translational probing. *Journal Physiol* 2017;595:4159-66.
- Chen Q, Heinricher MM. Descending control mechanisms and chronic pain. *Curr Rheumatol Rep* 2019;21:13.
- Lépine J-P. The epidemiology of anxiety disorders: prevalence and societal costs. *J Clin Psychiatr* 2002;63:4-8.
- de Heer EW, Gerrits MM, Beekman AT, Dekker J, Van Marwijk HW, De Waal MW, et al. The association of depression and anxiety with pain: a study from NESDA. *PloS One* 2014;9:e106907.
- Hooten WM. Chronic pain and mental health disorders: shared neural mechanisms, epidemiology, and treatment. *Mayo Clin Proc* 2016;91:955-70.
- Kabat-Zinn J, Lipworth L, Burney R. The clinical use of mindfulness meditation for the self-regulation of chronic pain. *J Behav Med* 1985;8:163-90.
- Germer C. What is mindfulness. *Insight Journal* 2004;22:24-9.
- Gordon DJ. *A critical history of mindfulness-based psychology*. 2009.
- Dreyfus G. Is mindfulness present-centred and non-judgmental? A discussion of the cognitive dimensions of mindfulness. *Contemporary Buddhism* 2011;12:41-54.
- Zeidan F, Vago D. Mindfulness meditation-based pain relief: a mechanistic account. *Ann N Y Acad Sci* 2016;1373:114-27.
- Kabat-Zinn J. Mindfulness-based stress reduction (MBSR). *Construct Hum Sci* 2003;8:73.

35. Deng Y-Q, Li S, Tang Y-Y. The relationship between wandering mind, depression and mindfulness. *Mindfulness* 2014;5:124-8.
36. Rod K. Observing the effects of mindfulness-based meditation on anxiety and depression in chronic pain patients. *Psychiatr Danub* 2015;27(Suppl 1):S209-11.
37. Hilton L, Hempel S, Ewing BA, Apaydin E, Xenakis L, Newberry S, et al. Mindfulness meditation for chronic pain: systematic review and meta-analysis. *Ann Behav Med* 2017;51:199-213.
38. Reiner K, Tibi L, Lipsitz JD. Do mindfulness-based interventions reduce pain intensity? A critical review of the literature. *Pain Med* 2013;14:230-42.
39. Heeger DJ, Ress D. What does fMRI tell us about neuronal activity? *Nat Rev Neurosci* 2002;3:142-51.
40. Gard T, Hölzel BK, Sack AT, Hempel H, Lazar SW, Vaitl D, et al. Pain attenuation through mindfulness is associated with decreased cognitive control and increased sensory processing in the brain. *Cereb Cortex* 2012;22:2692-702.
41. Wang MY, Bailey NW, Payne JE, Fitzgerald PB, Fitzgibbon BM. A systematic review of pain-related neural processes in expert and novice meditator. *Mindfulness* 2021;12:799-814.
42. Zeidan F, Emerson NM, Farris SR, Ray JN, Jung Y, McHaffie JG, et al. Mindfulness meditation-based pain relief employs different neural mechanisms than placebo and sham mindfulness meditation-induced analgesia. *J Neurosci* 2015;35:15307-25.
43. Riegner G, Posey G, Oliva V, Jung Y, Mobley W, Zeidan F. Disentangling self from pain: mindfulness meditation-induced pain relief is driven by thalamic-default mode network decoupling. *Pain* 2023;164:280-91.
44. Vago DR, Silbersweig DA. Self-awareness, self-regulation, and self-transcendence (S-ART): a framework for understanding the neurobiological mechanisms of mindfulness. *Front Hum Neurosci* 2012;6:296.
45. Seminowicz DA, Burrowes SA, Kearson A, Zhang J, Krimmel SR, Samawi L, et al. Enhanced mindfulness-based stress reduction in episodic migraine: a randomized clinical trial with magnetic resonance imaging outcomes. *Pain* 2020;161:1837-46.
46. Braden BB, Pipe TB, Smith R, Glaspy TK, Deatherage BR, Baxter LC. Brain and behavior changes associated with an abbreviated 4-week mindfulness-based stress reduction course in back pain patients. *Brain Behav* 2016;6:e00443.
47. Smith A, Leeming A, Fang Z, Hatchard T, Mioduszewski O, Schneider M, et al. Mindfulness-based stress reduction alters brain activity for breast cancer survivors with chronic neuropathic pain: preliminary evidence from resting-state fMRI. *J Cancer Surviv* 2021;15:518-25.
48. Mioduszewski O, Hatchard T, Fang Z, Poulin P, Khoo E-L, Romanow H, et al. Breast cancer survivors living with chronic neuropathic pain show improved brain health following mindfulness-based stress reduction: a preliminary diffusion tensor imaging study. *J Cancer Surviv* 2020;14:915-22.
49. Hatchard T, Mioduszewski O, Khoo E-L, Romanow H, Shergill Y, Tennant E, et al. Reduced emotional reactivity in breast cancer survivors with chronic neuropathic pain following mindfulness-based stress reduction (MBSR): an fMRI Pilot investigation. *Mindfulness* 2021;12:751-62.
50. Vago DR, Nakamura Y. Selective attentional bias towards pain-related threat in fibromyalgia: preliminary evidence for effects of mindfulness meditation training. *Cogn Ther Res* 2011;35:581-94.
51. Medina S, O'Daly OG, Howard MA, Feliu-Soler A, Luciano JV. Differential brain perfusion changes following two mind-body interventions for fibromyalgia patients: an Arterial Spin Labelling fMRI Study. *Mindfulness (N Y)* 2022;13:449-61.



This is an open access article distributed under the terms of [Creative Commons Attribution-NonCommercial-NoDerivatives 4.0 International License](https://creativecommons.org/licenses/by-nc-nd/4.0/).

Primary bone diffuse B cell lymphoma of the thoracic spine: a rare entity

Emrah Akçay¹, Hüseyin Berk Benek¹, Hakan Yılmaz¹, Alper Tabanlı¹, Alaattin Yurt¹

Department of Neurosurgery, University of Health Sciences, İzmir Bozyaka Training and Research Hospital, İzmir, Turkey

ABSTRACT

Primary bone lymphoma is a rare entity, accounting for approximately 3-7% of malignant bone tumors, 5% of extra-nodal lymphomas and < 1% of all non-Hodgkin lymphomas. Primary spine localized lymphoma is 1.7% of all primary bone lymphomas. A 73 year-old female presented with a two month history of severe backache. T1W and T2W MRI showed a hypointense soft tissue component extending from the left posterior elements to Th7 corpus. The patient underwent Th6-7-8 total laminectomy. Th7-8 extradural mass was totally resected. Excisional biopsy was performed through Th7 left pedicle and vertebroplasty was applied. Significant reduction in pain was seen postoperatively. The patient was diagnosed with diffuse large B cell lymphoma. The patient received combined treatment with R-CHOP chemotherapy and local radiotherapy. Any other lesions were not detected after the examinations following 6 months period and it was accepted as primary bone lymphoma.

Keywords: Primary bone lymphoma, diffuse large B cell lymphoma, thoracic spine, excisional biopsy, vertebroplasty

Primary bone lymphoma (PBL) involving the spine is an extremely rare tumor and therefore may be missed in diagnosis. It could cause pain and neurological symptoms, and affect the quality of life negatively, especially in elderly and comorbidized patients [1]. Following a well-planned surgery, it is possible to control the tumor with chemotherapy and radiotherapy applications [1, 2].

CASE PRESENTATION

A 73 year old woman presented with a two month history of severe backache started without any trauma. She had primary hypertension, hypercholesterolemia, type 2 diabetes and chronic obstructive pulmonary dis-

ease. Localized tenderness and percussion pain were observed at Th6-8 levels. T1W and T2W MRI showed a hypointense soft tissue component extending from the left posterior elements to Th7 corpus (Fig. 1). The patient was considered primarily plasmacytoma or metastasis in differential diagnosis. No other focus or suspicious lymph nodes were observed in thorax CT, abdominal CT, dynamic abdominal MR, whole body bone scintigraphy, and all spinal MRI.

The patient was operated under general anesthesia. Th6-7-8 total laminectomy performed. The extradural lesion at Th7-8 totally excised. The tumor extending into the corpus was curetted through the T7 left pedicle, and vertebroplasty was applied (Fig. 2). As a result of histopathological and immunohistochemical analysis, lymphoid cells CD 20 (+), Bcl-2 (+), CD10 (+),

Received: August 3, 2022; Accepted: December 5, 2022; Published Online: January 18, 2023



How to cite this article: Akçay E, Benek HB, Yılmaz H, Tabanlı A, Yurt A. Primary bone diffuse B cell lymphoma of the thoracic spine: a rare entity. Eur Res J 2023. DOI: 10.18621/eurj.1153678

Address for correspondence: Hüseyin Berk Benek, MD., University of Health Sciences, İzmir Bozyaka Training and Research Hospital, Department of Neurosurgery, Saim Çıkırıkçı Cad., No: 59, 35170 Karabağlar, İzmir, Turkey. E-mail: benekberk@gmail.com, Phone: +90 232 250 50 50



©Copyright © 2023 by Prusa Medical Publishing
Available at <http://dergipark.org.tr/eurj>
info@prusamp.com

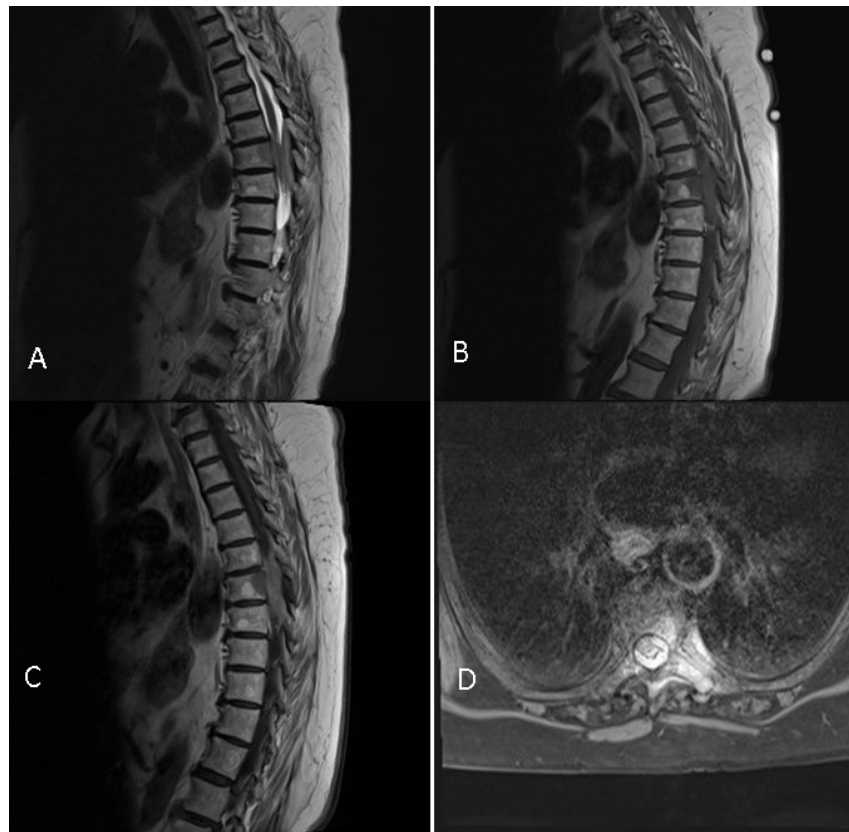


Fig. 1. (A) Preoperative sagittal T1W, (B) sagittal T2W, (C) post-contrast sagittal and (D) post-contrast axial MR images of the patient showing a soft tissue component with T1W and T2W hypointense signal characteristics, and extending from the left posterior elements and Th6-7 and Th7-8 foramens, posterior to the Th7 vertebral corpus.

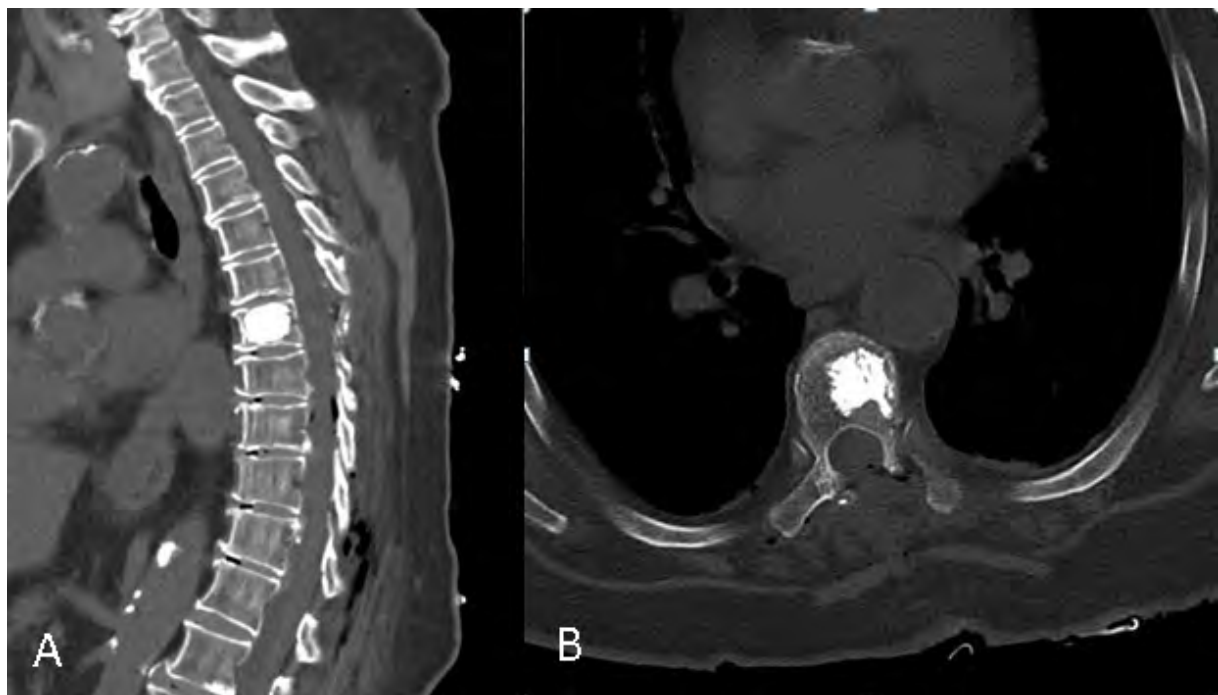


Fig. 2. (A) sagittal and (B) axial early postoperative control thoracic CT showing the mass was totally excised and the polymethylmethacrylate (PMMA) applied to the 7. thoracic vertebra.

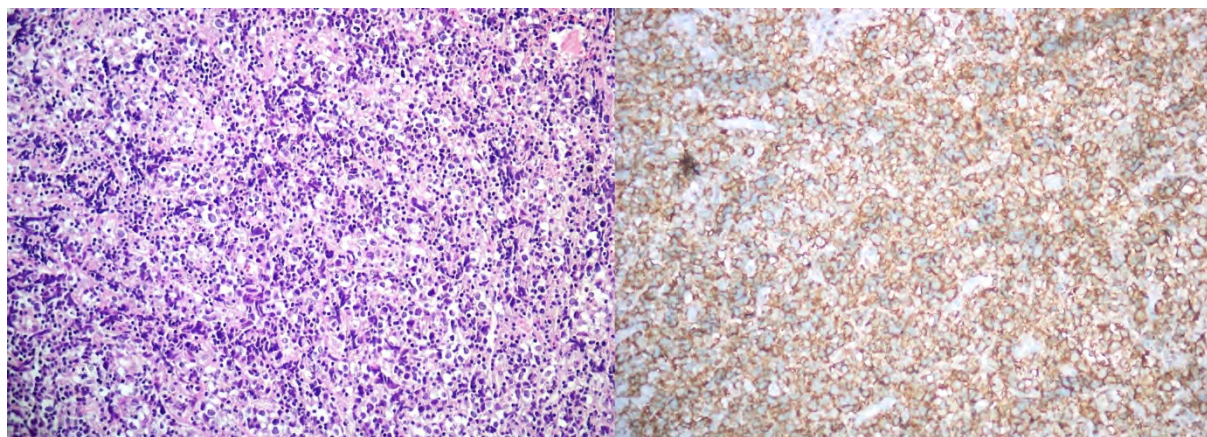


Fig. 3. Histopathology: (A) Diffuse infiltration of large atypical lymphoid cells (HE $\times 200$) and (B) diffuse CD20 positivity in atypical lymphoid cells (CD20 $\times 200$).

PAX-5 (+), Bcl-6 30% (+), Mum-1 (-). Ki67 proliferation index detected around 70%. It was thought "Germinal Center Originated" B cell phenotype with Hans algorithm. It was accepted as diffuse large B-cell lymphoma (Fig. 3). The patient received combined treatment with four cycles of R-CHOP chemotherapy (rituximab, cyclophosphamide, doxorubicin, vincristine, prednisone), and radiotherapy in a dose of 46 Gy in 15 sessions.

The patient was diagnosed with primary bone lymphoma, with no local or systemic extra involvement at the post-op control within six months. The patient has no complaints or neurological deficits 15

months postoperatively. No local recurrence was observed in control spinal MRI (Fig. 4).

DISCUSSION

Primary bone lymphoma is a rare entity; and constitutes 3-7% of all malignant bone tumors, less than 1% of all non-hodgkin lymphomas and 5% of all extranodal lymphomas [3,4]. Primary bone lymphomas are mostly reported in the femur or pelvis (50%) and upper extremities long bones (20%). The remaining 30% cases include rare localizations such as costa,

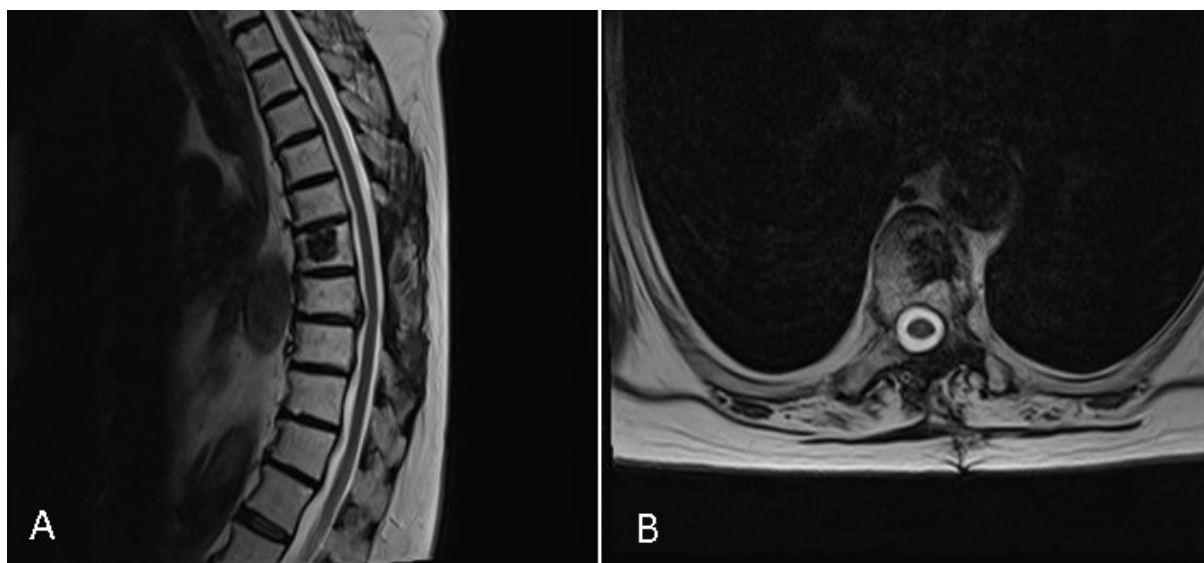


Fig. 4. (A) T2W sagittal and (B) T2W axial control MRI sections at the postoperative 15th month, showing the mass was completely excised and no local recurrence was seen.

mandible or scapula. 1.7% of all primary bone lymphomas involve the spine, mostly thoracic or lumbar spine [5]. World Health Organization classification of neoplasms of the hematopoietic and lymphoid tissues in 2022 characterized PBL as an independent disease [2].

Following four criteria should be met in the detection of primary bone lymphoma today: (1) primary involvement site of the bone; (2) no evidence of extra-bone lesion; (3) no evidence of any other extra-bone lesion six months after bone lesion is diagnosed; and (4) the diagnosis is confirmed by both pathological morphology and immunochemistry [2].

The most common histological type (90%) of primary bone lymphomas is diffuse large B-cell lymphoma [4]. It is moderately higher in men, most common age is 45-60, it peaks around the age of 50 [6]. Pain is the most common symptom (80-95%). Pathological fractures (15-20%), hypoesthesia, paraplegia, bladder and anal sphincter dysfunction could be determined [7].

MRI provides clear information about soft tissue spread, and spinal cord compression. PET CT provides insight into disease spread and involvement sites [8]. Primary bone lymphoma as a rare entity should be kept in mind in the differential diagnosis of metastatic carcinoma, Ewing sarcoma, osteosarcoma, plasmacytoma and chronic osteomyelitis [9]. The definitive diagnosis of primary bone lymphoma is based on histopathological and immunohistochemical examinations, such as MUM1 positivity and BCL6 mutation compared to other extranodal lymphomas. MUM1 expression > 10%, low CD10 expression and non-germinal center origin are signs of poor prognosis. Patients initially presented with a pathological fractures were also associated with a poor prognosis [10].

Emergency surgery is indicated for spinal cord compression presenting with neurological deficits. Stabilization prevents instability and increases the quality of life, especially in multiple level pathological fractures. Percutaneous vertebroplasty preferred as a minimally invasive procedure for pain palliation in patients with only corpus involvement [1, 10]. With systemic chemotherapy (R-CHOP protocol) and local radiotherapy following surgical resection, five year survival range is from 62% to 88% [3, 4, 11].

CONCLUSION

Primary bone lymphoma involving the spine is an extremely rare entity. Histopathological and immunohistochemical examination is important in the differential diagnosis of diseases such as metastasis, osteomyelitis, plasmacytoma, and osteosarcoma. Treatment options include percutaneous vertebroplasty, resection with open surgery, and resection + stabilization following systemic chemotherapy and local radiotherapy.

Authors' Contribution

Study Conception: EA, HBB, HY, AT, AY; Study Design: EA, HBB, HY, AT, AY; Supervision: EA, HBB, HY, AT, AY; Funding: EA, HBB, HY, AT, AY; Materials: EA, HBB, HY, AT, AY; Data Collection and/or Processing: EA, HBB, HY, AT, AY; Statistical Analysis and/or Data Interpretation: EA, HBB, HY, AT, AY; Literature Review: EA, HBB, HY, AT, AY; Manuscript Preparation: EA, HBB, HY, AT, AY and Critical Review: EA, HBB, HY, AT, AY.

Conflict of interest

The authors disclosed no conflict of interest during the preparation or publication of this manuscript.

Financing

The authors disclosed that they did not receive any grant during conduction or writing of this study.

REFERENCES

1. Jia P, Li JJ, Chen H, Bao L, Feng F, Tang H. Percutaneous vertebroplasty for primary non-Hodgkin's lymphoma of the thoracic spine: case report and review of the literature. *Pain Physician* 2017;20:E727-35.
2. Alaggio R, Amador C, Anagnostopoulos I, Attygalle AD, Araujo IBO, Berti E, et al. The 5th edition of the World Health Organization Classification of Haematolymphoid Tumours: Lymphoid Neoplasms. *Leukemia* 2022;36:1720-48.
3. Beal K, Allen L, Yahalom J (2006) Primary bone lymphoma: treatment results and prognostic factors with long-term follow-up of 82 patients. *Cancer* 2006;106:2652-6.
4. Ramadan KM, Shenkier T, Sehn LH, Gaycoyne RD, Connors JM. A clinicopathological retrospective study of 131 patients with primary bone lymphoma: a population-based study of successively treated cohorts from the British Columbia Cancer Agency. *Ann Oncol* 2007;18:129-35.

5. Ahmadi SA, Frank S, Hanggi D, Eicker SO. Primary spinal marginal zone lymphoma: Case report and review of the literature. *Neurosurgery* 2012;71:E495-508.
6. Messina C, Christie D, Zucca E, Gospodarowicz M, Ferreri AJ. Primary and secondary bone lymphomas. *Cancer Treat Rev* 2015;41:235-46.
7. Undabeitia J, Noboa R, Boix M, Garcia T, Panades MJ, Nogues P. Primary bone non-Hodgkin lymphoma of the cervical spine: case report and review. *Turk Neurosurg* 2014;24:438-42.
8. Paes FM, Kalkanis DG, Sideras PA, Serafini AN. FDG PET/CT of extranodal involvement in non-Hodgkin lymphoma and Hodgkin disease. *Radiographics* 2010;30:269-91.
9. Fidas P, Spiro I, Sobczak ML, Nielsen GP, Ruffolo EF, Mankin H, et al. Long-term results of combined modality therapy in primary bone lymphomas. *Int J Radiat Oncol Biol Phys* 1999;45:1213-8.
10. Kaifa G, Didangelos T, Bobos M, Karlafti E, Ztriva E, Kanellos I, et al. Primary bone diffuse large B-cell lymphoma with multifocal osteolytic lesions: a rare entity. *Gen Med (Los Angeles)* 2018;6(1):1-3.
11. Zhang X, Chang CK, Song LX, Xu L, Wu LY, Li X. Primary lymphoma of bone: a case report and review of the literature. *Med Oncol* 2011;28:202-6.



This is an open access article distributed under the terms of [Creative Commons Attribution-NonCommercial-NoDerivatives 4.0 International License](https://creativecommons.org/licenses/by-nc-nd/4.0/).

Ovarian malignant melanoma metastasized from skin mimicking a benign cyst: a rare case report and mini-review of the literature

Fatma Ketenci Gencer¹, Bülent Babaoğlu², Zeynep Kübra Usta Kurt¹, Hatice Yaşat Nacar¹, Sibel Bektaş³

¹Department of Obstetrics and Gynecology, University of Health Sciences, Istanbul Gaziosmanpasa Training and Research Hospital, İstanbul, Turkey; ²Department of Obstetrics and Gynecology, Division of Perinatology, Manisa Celal Bayar University Faculty of Medicine, Manisa, Turkey; ³Department of Pathology, University of Health Sciences, Istanbul Gaziosmanpasa Training and Research Hospital, İstanbul, Turkey

ABSTRACT

Malignant melanomas, often appearing on the skin, rarely metastasize to internal organs and the ovaries are the least affected site. A 45-year-old female patient presenting with a skin lesion on the right side of the neck and diagnosed with malignant melanoma through excision biopsy also appeared to have lung metastasis and a nonspecific ovarian cystic mass of 6 cm after PET-CT scan was performed. Examination revealed a mass with the widest diameter of 9 cm and a surgical decision was made due to the rapid growth pattern. Tumor markers appeared to be within the normal range. Laparoscopic right salpingoophorectomy was performed and frozen section biopsy was obtained. The result was found to be malignant and complementary surgery was performed. Pathological examination of the cystic mass, which was detected to have only nonspecific findings on radiological exam, revealed tiny solid areas in its capsule. The patient was started on postoperative Dabrafenib + Trametinib treatment by oncology and was followed up without recurrence until the 24th postoperative month. At month 24, the brain metastasis with no response to radiotherapy occurred and the patient was lost on the 15th day after decompression surgery. It is important to send adnexal masses to the frozen even if they appear to have a benign character. In patients with a known history of primary cancer, the possibility of the metastasis from the primary tumor site to the ovary should be considered in those whose peroperative frozen section result is in favor of malignancy. Our case is the first case of ovarian malignant melanoma metastasis with a completely cystic and septa-free character in the literature.

Keywords: Metastasis, ovarian malignant melanoma, ovary cyst, survey

Malignant melanoma (MM) is a malignant tumor of melanocytes with the skin being the most important site of localization [1]. Rarely, eye mucosa and internal organ involvement can also be seen. This type

of cancer is known to have the most rapidly increasing incidence worldwide. Genetic mutations such as CDKN2A, PTEN, TP53, and ARID2, atypical/dysplastic nevi, overexposure to UV and sunlight, FAMM

Received: April 9, 2022; Accepted: June 21, 2022; Published Online: January 14, 2023



e-ISSN: 2149-3189

How to cite this article: Ketenci Gencer F, Babaoğlu B, Usta Kurt ZK, Yaşat Nacar H, Bektaş S. Ovarian malignant melanoma metastasized from skin mimicking a benign cyst: a rare case report and mini-review of the literature. *Eur Res J* 2023. DOI: 10.18621/eurj.1100943

Address for correspondence: Fatma Ketenci Gencer, MD., University of Health Sciences, Istanbul Gaziosmanpasa Training and Research Hospital, Department of Obstetrics and Gynecology, Karayolları Mah., Osmanbey Cad., 621. Sk., Gaziosmanpasa 34255, Istanbul, Turkey. E-mail: fathma_k@hotmail.com, Phone: +90 212 945 30 00, Fax: +90 212 945 31 78



©Copyright © 2023 by Prusa Medical Publishing
Available at <http://dergipark.org.tr/eurj>
info@prusamp.com

(Familial atypical multiple mole melanoma syndrome), and immunosuppression are among the risk factors [2, 3]. Gynecologically, the most common site of metastasis is the endometrium; much more rarely, it is seen to metastasize to the ovary [4]. Female genital tract MM constitutes 3% of all melanomas [5]. MM of the ovary may be a metastasis of a melanoma originating from the skin or elsewhere, as well as it may be a primary site of disease [6]. Primary ovarian malignant melanoma is a rarely seen presentation. Although generally originated from mature cystic teratoma, it appears to be a rare malignant transformation of this tumor [6]. Clinically, it usually appears as a solid ovarian mass, although additional metastases may be seen during the operation [7]. MM may spread via lymphatic and hematogenous routes, and metastases often occur to regional lymph nodes, lung, liver, central nervous system, bone, and more rarely other visceral organs [8].

In this report it was aimed to present our experience of management for malignant melanoma case metastasize to ovary without any signs of malignancy. A 45-year-old female patient with a prior skin excision biopsy-confirmed diagnosis of malignant melanoma, with lung metastases detected on PET-CT is presented. In the same PET-CT session, a right ovarian cyst of 6 cm, which was considered to show physiological uptake, was reported, and further referral to obstetrics and gynecology was made. The patient, whose lung lesion was also surgically removed, was operated on after the ovarian cyst progression to 12 cm, and the final pathology result was reported as malignant melanoma for both sites.

CASE PRESENTATION

A 45-year-old climacteric period female, gravida 1, parity 1, was referred to our clinic after a 6 cm non-specific cystic mass originating from the right ovary was detected on PET-CT performed in an external medical center. There was no known history of chronic disease, she has been smoking ½ pack/day (5 packs/year) for 10 years and had a lateral neck mass of 1.5 × 1.5 × 0.8 cm excised at external center 5 months ago; as a result, a diagnosis of malignant melanoma was established. Immunohistochemical examination was focally positive for HMB45 genemed,

positive for vimentin clone V9 genemed, while microscopic examination showed poorly differentiated malignant tumoral infiltration. Following the diagnosis, a PET-CT scan revealed masses each one the size of 1 cm in the apical region of the right lung upper lobe and the middle lobe; therefore, wedge resection of the upper and middle lobes was performed. The pathology results were reported to be compatible with malignant melanoma metastasis; she was followed up by a thoracic surgeon.

In addition, on the PET-CT scan taken upon the diagnosis, a 6 cm mass structure with a mild FDG uptake in the right adnexal area suggesting a nonspecific ovarian cyst was distinguished, and a 3 cm mass suggesting physiological ovarian tissue with heterogeneous and minimal FDG uptake at the anterosuperior junction was observed. Referral to obstetrics and gynecology has been made and approximately 9 cm in length cystic mass was observed on gynecological examination on the right adnexal locus. On MRI the endometrium and uterine cavity appeared to be normal, a few fibroids of 1,5 cm was found in the uterus corpus and fundus; in the pelvic entrance, a 7 × 8 × 9 cm thin-walled cystic mass with a slight thickening on the anterior wall was observed. Surgical excision was recommended.

After the decision of the patient for the surgery, on the gynecological examination, performed 4 months after the initial PET-CT, the uterus and left ovary were normal, and a homogeneous cystic mass of 12 × 9 cm



Fig. 1. Ultrasonographic image of a homogeneous cystic mass of 12×9 cm without septa in the right adnexal locus.

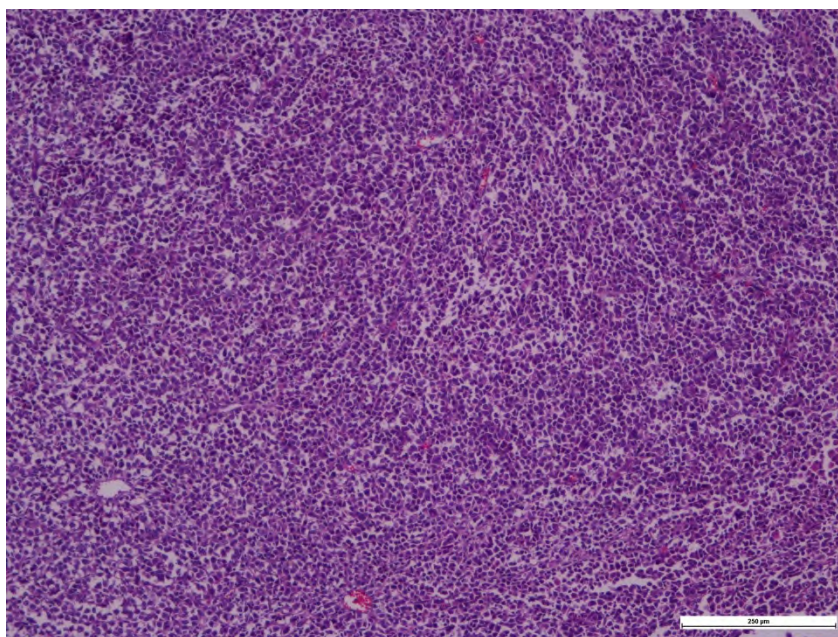


Fig. 2. Diffuse atypical proliferation of polygonal cells (H&E ×100)

without septa in the right adnexal locus was observed (Fig. 1). The patient in the climacteric period sees a period every 45 days; bleeding lasts for 4 days and changes 3-4 pads a day on average. Tumour marker levels were CA125 = 36.3- CA15.3 =14.1 – CA19.9 = 4.6 – CEA = 1.18 and considered normal. The cystic mass was considered benign in the foreground, and L/S right salpingo-oophorectomy was planned. Preoperative endometrial biopsy results were reported as irregular endometrial tissue fragments, and mammography was normal. During the operation, the cyst, approximately 13-15 cm in size, was taken into the endobag, and after the bag was mouthed out, it was ruptured and aspirated into the bag; the remaining material was taken out of the abdomen and sent to the frozen. It was observed that the aspiration fluid was slightly yellowish, attributed to the cyst's semitorcion. After the frozen section result was reported as malignant, the patient was reopened with a median incision above and below the umbilicus, and complementary surgery was performed with hysterectomy, left salpingo-oophorectomy, bilateral pelvic/paraortic/obturator lymphadenectomy, omentectomy, and peritoneal biopsy; the patient was discharged on the 5th-day postoperatively with no complications. In the final pathology report, the cystic mass originating from the right ovary was described as 2 tissue pieces with macroscopic dimensions of $8.5 \times 6 \times 2$ cm and $10.5 \times 8 \times 1$

cm. On the larger piece of tissue, tiny solid areas were reported; the size was not specified. No metastasis was observed in the removed lymph nodes, and no adverse features were observed in the uterus, left ovary, left and right tuba. Immunohistochemical study was positive for S100, HMB45, Melan A, MART1; pan-cytokeratin and PAX were reported negative. In addition, after the BRAF mutation studied in the malignant mass sample was reported positive, the pathologic diagnosis of malignant melanoma metastasized to the ovary was established. Diffuse atypical proliferation consisting of polygonal cells (H&E × 100) is shown in Fig. 2, and a cross-section (× 100) in which positivity was detected in atypical cells with Melan A immunostain is shown in Fig. 3.

After the final pathology report, the patient proceeded to oncology follow-up, and dual-targeted therapy (dabrafenib + trametinib) was initiated. Regression prevailed on the PET-CT performed at 6th month after surgery in contrast to the initial one, and routine follow-up continued.

Consecutive PET-CT scan taken at the 12th month postoperatively revealed hypermetabolic nodular formation in the upper inner quadrant of the right breast suggestive of malignancy (second primary?) and minimal hypermetabolic lymph node in the right upper axillary fossa, suggestive of metastasis. No hypermetabolic area was observed in the lungs and pelvis. On further

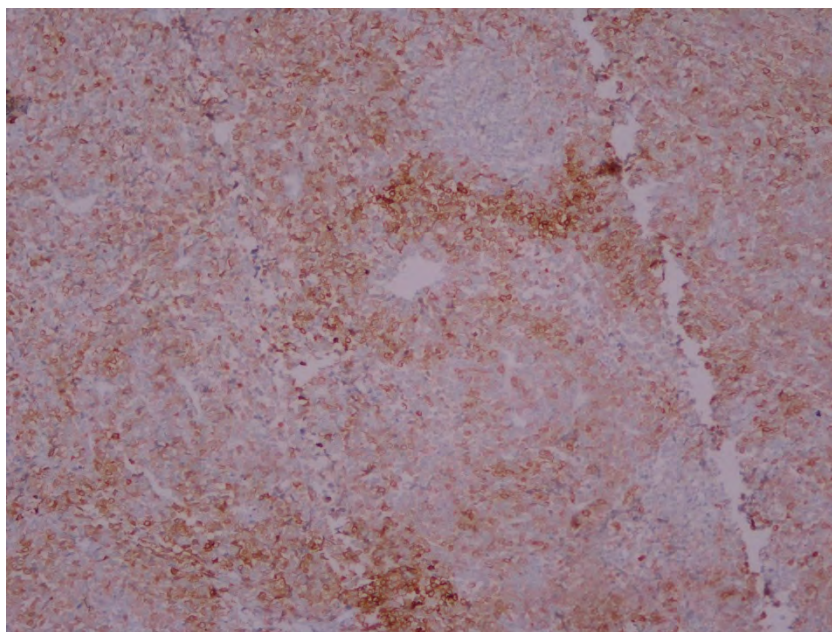


Fig. 3. Melan A immunostaining revealed positivity in atypical cells ($\times 100$).

investigation, no malignancy of the breast and axillary region was detected. Partial regression was observed in the hypermetabolic area of the breast on the 18th week postoperative PET-CT scan.

The patient was followed up with no recurrence till the 24th month. At the 24th month after surgery headache and convulsion attacks started to appear, and neurological follow up were initiated. Increased intracranial pressure and cerebral masses were seen on the MRI, and epilepsy was ruled out by neurology. Whole brain radiotherapy in 10 fractions was performed. Minimal regression of cerebral masses was observed on the control MRI after treatment. Convulsions recurred and intracranial pressure findings reappeared on the 27th month postoperatively. The neurosurgical evaluation took place and decompressive surgery was performed. The patient died on postoperative day 15 during the intensive care unit follow-up.

DISCUSSION

Ovarian metastases account for about 5% of all ovarian cancer cases, and usually, stomach, lung, and liver cancers metastasize to the ovary [8, 9]. Ovary metastasis from malignant melanoma is extremely rare [8].

Metastasis to the ovary occurs within an average

of 7 years after the diagnosis of primary malignant melanoma [9]. In our case, the patient was diagnosed with primary skin MM 5 months before referral, her treatment was completed and she was followed up for MM. From this perspective, in contrast to the time predicted in the literature, the time to ovarian metastasis in our patient was considerably shorter. According to the literature, the mean age of patients with MM metastasis in the ovary is 35.7 years, with extremities being the most common site of tumor spread [7]. Our patient is 45 years old and the primary tumor was detected in the left lateral part of the neck. In this context, our patient appears to be diagnosed with MM 10 years later than the predicted mean age of metastasis, and the localization is the neck - instead of the commonly seen extremities. It is known that malignant melanoma most commonly spreads to the lung and liver [10]. Consistent with the literature, the lung metastases were seen on PET-CT following the primary diagnosis, and the patient was under thorough follow-up after the tumor resection. Since the patient stated that she did not delay the visit to the doctor after the neck mass resection, it is clear that the tumor may have had an aggressive course in the patient. Thus, metastasis to the lung must have occurred at the time of the first diagnosis, and metastasis to the ovary was observed at the 5th month afterward.

Clinically, the solid component predominates in

malignant melanoma metastases, and they have an appearance suggestive of ovarian cancer on ultrasound [11]. First imaging is done with transvaginal ultrasound, though this modality only detects an ovarian mass, and it is not possible to detect clinical findings that would suggest malignant melanoma [12]. A pure cystic lesion with a maximum size of 12 cm was detected in the right adnexal area on the first transvaginal ultrasound examination performed in our patient, and since the tumor marker levels were within the normal range, the patient was initially considered to have a benign ovarian cystic mass. Among other imaging studies, PET-CT and MRI usually reveal nonspecific findings rather than those suggestive of MM [8, 12]. It is mentioned in the literature that ovarian malignant melanoma can be detected on MRI if the tumor contains melanin pigment, which may not always be present [9]. On the first PET-CT imaging of our patient, a nonspecific cyst of 6 cm and a 3 cm cyst suggestive of physiological ovarian involvement were detected, which was considered nonspecific, and consecutive MRI showed the cyst progression to $7 \times 8 \times 9$ cm. It is known from the literature that ovarian MM may have a partially cystic appearance, though a pure cystic lesion has not been shown in any case so far. In our case, no solid mass lesion was detected on any imaging modality, but tiny solid areas were found on the capsule on the paraffin section.

Patients may present with pain due to malignant metastases in the ovary, but the cases may also be asymptomatic, as is stated in the literature [4]. There was no pelvic pain in our case, and the patient appeared to be in an asymptomatic group in gynecological terms. Most cases are unilateral, with a minority of cases being bilateral [7, 13, 14]. In our patient, a cystic mass without septa, reaching a size of 12 cm, was seen in the right adnexal area, while the other ovary looked completely normal.

The diagnosis is made immunohistochemically according to proteins S-100, human melanoma black-45 and MART-1 positivity, and the absence of coexpression of the antibody vimentin: cytokeratins 8 and 18. Our case was diagnosed with MM by being reported positive for S100, HMB45, Melan A and MART1, and negative for pan-cytokeratin and PAX-8.

Although there is a common opinion that the treatment is surgical, there is no consensus on the type of surgery. As it is emphasized, surgery options are oophorectomy alone, TAH+BSO or, especially in advanced cases, pelvic and para-aortic lymphadenectomy with infracolic omentectomy in adjunction to TAH+BSO [9]. Since the findings suggestive of malignancy were insufficient in our patient, laparoscopic right salpingo-oophorectomy was performed first, and after frozen was found suggestive of malignancy, the operation was continued considering MM. Wide surgical excision, which is routinely applied to patients whose frozen results are found to be malignant, was also performed on our patient.

Survival remains poor despite new targeted treatments developed; even though there are cases reported with patients followed for as long as 96th month without recurrence after bilateral oophorectomy for ovarian metastasis was performed, the median overall survival is 2 years after metastasis [7]. Our patient died 27 months after ovarian metastasis was detected, which is consistent with these data.

CONCLUSION

Malignant melanoma has a worse prognosis compared to other ovarian cancers. As seen in our case, ovarian involvement is generally due to metastasis. In general, they manifest as solid lesions, but it should not be forgotten that they can also present as masses with a cystic appearance, as seen in our case. Our case is the first case of ovarian malignant melanoma metastasis with a completely cystic and septa-free character in the literature. It is important to evaluate adnexal masses histopathologically with frozen, even if they seem benign on ultrasonographic and radiological images. The possibility of tumor metastasis to the ovary should be kept in mind for patients whose frozen results are suggestive of malignancy if there is a known history of primary cancer.

Authors' Contribution

Study Conception: FKG; Study Design: FKG, BB; Supervision: SB; Funding: FKG, BB, HY, ZKUK; Materials: FKG, BB, SB; Data Collection and/or Processing: FKG; Statistical Analysis and/or Data Interpretation: FKG; Literature Review: FKG, BB, ZKUK;

Manuscript Preparation: FKG, BB, SB and Critical Review: FKG.

Informed Consent

Written informed consent was obtained from the patient for publication of this case and any accompanying images or data.

Conflict of interest

The authors disclosed no conflict of interest during the preparation or publication of this manuscript.

Financing

The authors disclosed that they did not receive any grant during conduction or writing of this study.

Acknowledgement

This case report was orally presented at 2nd International and 17th National Gynecological Oncology Congress, December 20, 2021, CVK Park Bosphorus Hotel, İstanbul.

REFERENCES

- Schadendorf D, van Akkooi ACJ, Berking C, Griewank KG, Gutzmer R, Hauschild A, et al. Melanoma. *Lancet* 2018;392:971-84.
- Cancer Genome Atlas Network. Genomic Classification of cutaneous melanoma. *Cell* 2015;161:1681-96.
- Lynch HT, Fusaro RM, Danes BS, Kimberling WJ, Lynch JF. A review of hereditary malignant melanoma including biomarkers in familial atypical multiple mole melanoma syndromes. *Cancer Genet Cytogenet* 1983;8:325-58.
- Piura B, Kedar I, Ariad S, Meirovitz M, Yanai-Inbar I. Malignant melanoma metastatic to the ovary. *Gynecol Oncol* 1998;68:201-5.
- Oliver R, Dasgupta C, Coker A, Al-Okati D, Weekes ARL. Ovarian malignant melanoma: unusual presentation of a solitary metastasis. *Gynecol Oncol* 2005;99:412-4.
- Choi WK, Lee DH, Cho DH, Jang KY, Kim KM. Primary malignant melanoma arising from ruptured ovarian mature cystic teratoma with elevated serum CA 19-9: a case report and review of the literature. *BMC Women Health* 2019;27:149.
- Young RH, Scully RE. Malignant melanoma metastatic to the right ovary. A clinicopathologic analysis of 20 cases. *Am J Surg Pathol* 1991;15:849-60.
- Mendel A, Terzibachian JJ, Aubin F, Malicenco L, Ramanah R, Riethmuller D. Ovarian metastasis of malignant melanoma: a case report. *J Gynecol Obstet Hum Reprod* 2017;46:461-2.
- Gupta D, Deavers MT, Silva EG, Malpica A. Malignant melanoma involving the ovary: a clinicopathologic and immunohistochemical study of 23 cases. *Am Surg Pathol* 2004;28:771-80.
- Pavri SN, Clune J, Ariyan S, Narayan D. Malignant melanoma: beyond the basics. *Plast Reconstr Surg* 2016;138:330e-40e.
- Karateke A, Tuğ N, Sahin D. Metastatic ovarian malignant melanoma with no obvious primary. *J Turk Ger Gynecol Assoc* 2011;12:181-2.
- Sabban F, Boukerrou M, Mubiayi N, Houpeau JL, Robert Y, Vinatier D. [Malignant melanoma metastatic to the ovary. A case report]. *Gynecol Obstet Fertil* 2005;33:409-11. [Article in French]
- Fitzgibbons PL, Martin SE, Simmons TJ. Malignant melanoma metastatic to the ovary. *Am J Surg Pathol* 1987;12:959-64.
- Sbitti Y, Fadoukhair Z, Kadiri H, Oukabli M, Essadi I, Kharroum S, et al. Diagnostic challenge for ovarian malignant melanoma in premenopausal women: primary or metastatic? *World J Surg Oncol* 2011;9:65.



This is an open access article distributed under the terms of [Creative Commons Attribution-NonCommercial-NoDerivatives 4.0 International License](https://creativecommons.org/licenses/by-nc-nd/4.0/).

Surgical approach to neglected giant cervical fibroids

Cagdas Nurettin Emeklioglu¹, Emine Aydin¹, Merve Konal², Hicran Acar Sirinoglu¹, Erhan Akturk¹, Ozgur Akbayir²

¹Department of Obstetrics and Gynecology, Prof. Dr. Cemil Tascioglu City Hospital, Istanbul, Turkey; ²Department of Obstetrics and Gynecology, Gynecologic Oncology Unit, Prof. Dr. Cemil Tascioglu City Hospital, Istanbul, Turkey

ABSTRACT

Cervical fibroids are rare neoplasms of uterine origin whose management has not been standardized. Cervical fibroids, which can be challenging in surgical management, can become a difficult problem for the surgeon when neglected or asymptomatic and reach gigantic dimensions. Suspending the aorta abdominalis or arteria iliaca communis with vascular tapes and balloting the uterus with the help of vaginal taping while searching for the correct cleavage may reduce the risk of intraoperative hemorrhage and adjacent organ injury, as well as may be guide for the steps of the operation. Management of neglected giant cervical fibroids may not be suitable for testing alternative treatment methods to surgery used in the treatment of uterine neoplasms. However, surgical management will also be challenging. For this reason, the technique we describe can help the surgeon with clues that should be considered in the surgical management of these patients.

Keywords: Gynecological surgery, uterine fibroid, neglected, cervical leiomyoma

Uterine leiomyomas are one of the most common benign neoplasms in women. 95% of myomas, the frequency of which reaches 70% in women of reproductive age, originate from the uterine corpus [1]. Cervical fibroids are seen less than 5 percent of the time. [2]. Although it is usually asymptomatic, in symptomatic cases, the patient is most often admitted to the hospital with abnormal uterine bleeding, chronic pelvic pain, urinary and gastrointestinal complaints associated with pressure.

In the subclassification of leiomyomas published by FIGO in 2011 regarding abnormal uterine bleeding, cervical myomas were included in the other group, which is type 8 [3]. Over the years, cervical fibroids have been examined as classified into subserosal (extracervical) and intracervical (intracervical) fibroids.

Location is one of the most important parameters in choosing a surgical method [2, 4].

Surgical procedures applied to cervical fibroids may be more difficult than fibroids originating from the corpus uteri. This, increased intraoperative hemorrhage, is due to an increased risk of adjacent organ injury related to impaired pelvic anatomy caused by dislocated pelvic organs because of cervical myoma. For these reasons, it would be better to involve experienced surgeons who have knowledge of retroperitoneal anatomy and, if possible, experience in gynecological oncology in operations related to neglected giant cervical fibroids [5]. The preoperative diagnosis of our patients was made by ultrasound and contrast-enhanced lower-upper abdomen MR imaging. Preoperative diagnosis of cervical myoma was made

Received: August 26, 2022; Accepted: February 28, 2023; Published Online: March 27, 2023



e-ISSN: 2149-3189

How to cite this article: Emeklioglu CN, Aydin E, Konal M, Sirinoglu HA, Akturk E, Akbayir O. Surgical approach to neglected giant cervical fibroids. Eur Res J 2023;9(3):611-617. DOI: 10.18621/eurj.1167105

Address for correspondence: Cagdas Nurettin Emeklioglu, MD., Prof. Dr. Cemil Tascioglu City Hospital, Department of Obstetrics and Gynecology, Kaptanpaşa Mah. Darülaceze Cad. No:27, Şişli, Istanbul, Turkey. E-mail: c.n.emeklioglu@gmail.com, Phone: +90 212 314 55 55, Fax: +90 212 221 78 00



©Copyright © 2023 by Prusa Medical Publishing
Available at <http://dergipark.org.tr/eurj>
info@prusamp.com

by the same gynecological oncologist (ÖA).

Currently, there is no standardized approach or technique in the treatment of cervical fibroids. This causes the change in the chosen treatment according to the experience of the center and the surgeon, the accessibility of current techniques, and patient-related variables. Therefore, the size of the fibroid, its location in the cervix, its relationship with neighboring organs are other factors that determine the operation technique and the difficulty coefficient. In recent years, with increased uterus-sparing approaches, there has been a tendency towards uterus-sparing surgical procedures and radiological techniques. However, uterine-sparing surgeries may not be possible in neglected giant fibroids due to insufficient surgical field, increased risk of intraoperative bleeding and impaired pelvic anatomy. With this study, we aimed to give surgeons an alternative idea to deal with such large cervical fibroids and to share our approach to management.

CASE PRESENTATIONS

CASE 1

The 37-year-old patient, gravida 3, parity 2, abortus 1, had no known disease other than lumbar disc herniation and gastroesophageal reflux, and had no additional features in her history, had complaints of men-

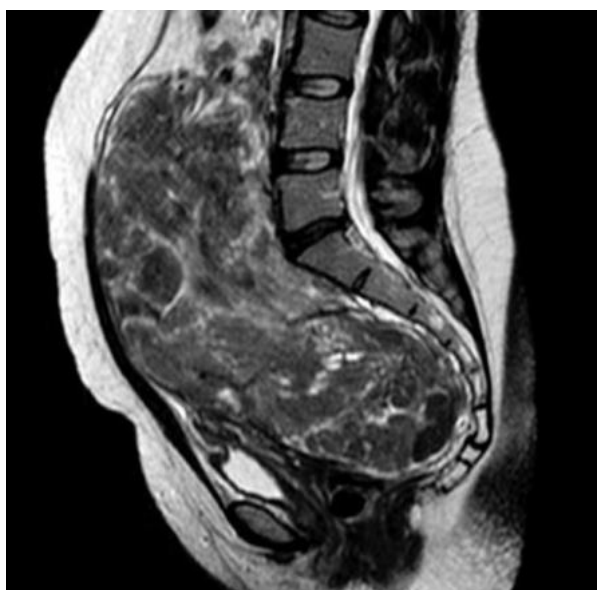


Fig. 1. Sagittal plane MRI of the giant cervical fibroid.

orrhagia and abdominal bloating. On examination, there was approximately 25 cm multiple myomatous uterus extending to the umbilicus. In order to reduce the risk of bleeding during the operation, the abdominal aorta was turned approximately 1 cm above the aortic bifurcation with vascular tape and suspended for approximately 15 minutes. There was no need for intraoperative transfusion. Postoperatively, one unit of erythrocyte suspension was transfused. The pathology result was reported as 25×15×10 cm leiomyoma starting from the lateral cervix and extending to the uterus corpus (Fig. 1).

CASE 2

The patient, who was 46 years old, had gravida 5, parity 2 and abortus 3, had a known chronic hypertension disease and was using amlodipine for this reason, and had no additional features in her history, had a complaint of urinary incontinence. In her routine examination, myoma uteri with a diameter of 13×14 cm, which was thought to originate from the cervix, was detected. Before the specimen was removed during the operation, bilateral arteria iliaca communis were suspended for approximately 12 minutes with the help of vascular tapes in order to reduce bleeding. No massive



Fig. 2. Degenerated leiomyoma extending from the cervix.

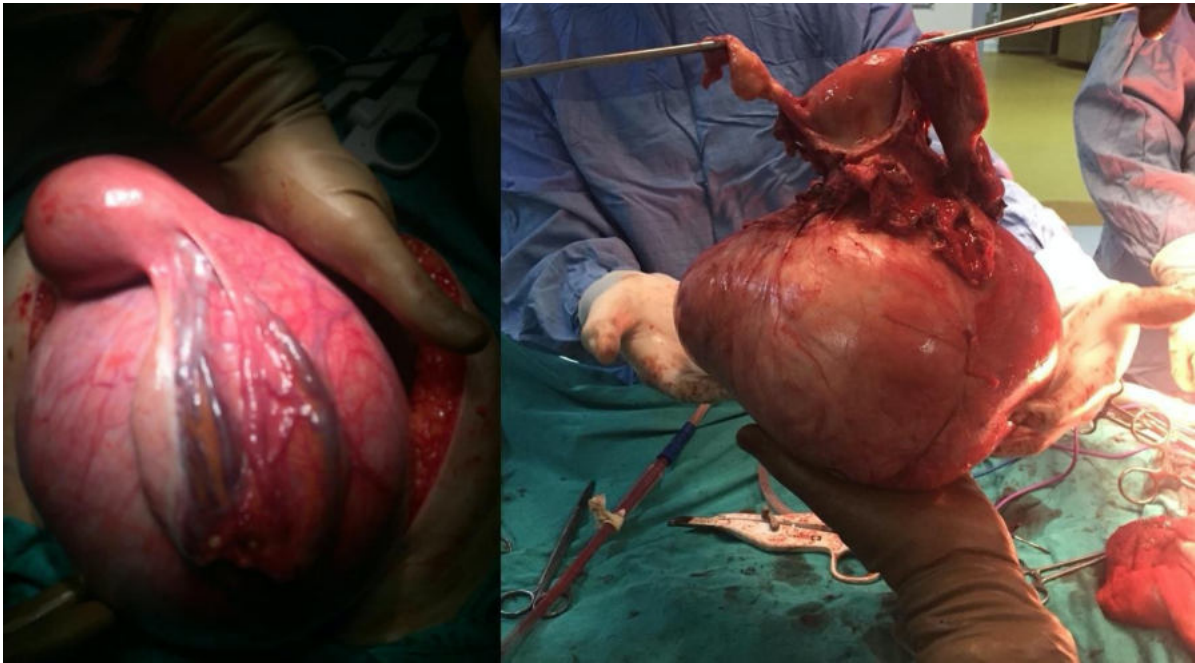


Fig. 3. Intraoperative view of giant cervical myoma.

bleeding was observed during the operation and no need for blood transfusion occurred during the post-operative period. In the pathology report, a degenerate myoma nodule with a diameter of approximately 13 cm, localized on the anterior wall extending from the cervix, which was visible when the uterus was cut, was observed (Figs. 2 and 3).

CASE 3

The 44-year-old patient, who was gravid 0, parity 0, had no features other than being a Hepatitis B carrier in her history, had no additional complaints other than abdominal swelling. On examination, giant myoma uteri, which was thought to be of cervical origin, enlarged the uterus to the xiphoid, bilateral grade

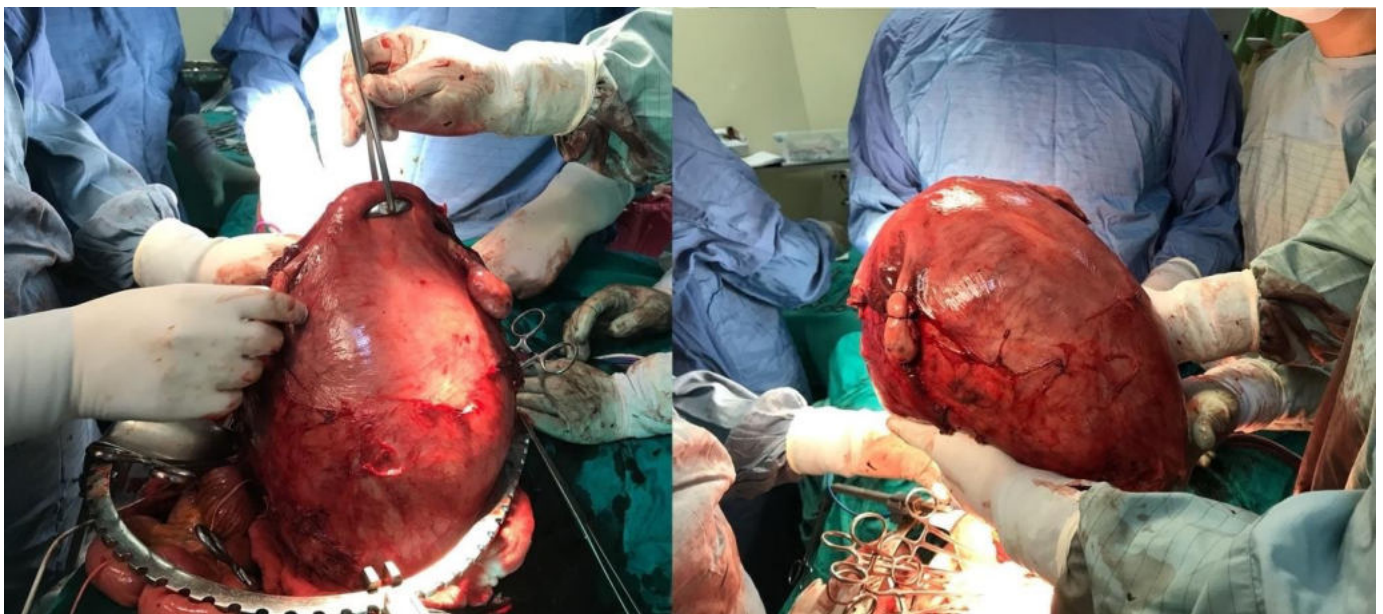


Fig. 4. Intraoperative image of cervical myoma measuring approximately 33 × 17 cm.

3-4 hydronephrosis was observed. Due to preoperative anemia, 2 units of erythrocyte suspension and 2 units of fresh frozen plasma were transfused. Horseshoe kidney and bilaterally dilated ureters were present on exploration. Urology consultation was requested, and it was said that no additional intraoperative intervention was required. In order to reduce the risk of bleeding during the operation, the abdominal aorta was turned approximately 2 cm above the aortic bifurcation with vascular tape and suspended for approximately 25 minutes. At the end of 25 minutes, the aortic tape was cut and removed (Fig. 4). There was no need for additional post-operative blood transfusion. Although the cervix could not be observed separately in the pathology report, a giant myoma measuring approximately 33 × 17 cm was observed.

For these cases, we prepared the patients in the dorsal lithotomy position, and we also stained the vaginal and vulvar areas during routine povidone iodide staining. We always started the operation with a median incision below and above the umbilicus, and we always kept an extra person ready in the operation area in case there is a need for vaginal manipulation. Before proceeding to the surgical steps before entering the abdomen, suspending the aorta abdominalis approximately 1 cm above the aortic bifurcation if possible, and if not possible, suspending the arteria iliaca communis with vascular tapes is the most appropriate precaution that can be taken to prevent possible vascular complications and to reduce intraoperative hemorrhage. In case 2, we applied tape to the bilateral arteria communis because of the mass, and in the other two cases, we applied tape over the aortic bifurcation.

In these 3 cases, the tapes were left loose throughout the operation, and in the presence of possible bleeding, they were tightened without knotting. We had dissected bilateral ureters in the retroperitoneal space and lateralized. After the arteria uterinae were ligated at the cervico isthmic junction, the anterior and posterior fornix were balloted with the touch of the 3rd person, who was take place between the legs; and the vagina was entered in the relevant region by palpating the fingers on the abdominal vaginal touch and guiding to find the right cleavage.

DISCUSSION

Our aim to share this study is, with the approach we will describe, to reduce the need for postoperative blood transfusion related to intraoperative hemorrhage, and to minimize adjacent organ damage in the anatomically overturned pelvic area by the traction method we will explain. We did not encounter any unusual intraoperative bleeding in 3 cases performed with this method, blood transfusion was not required in 2 of our patients, and no adjacent organ damage was reported.

In a literature review in which studies on all cervical fibroids were examined, the rate of complication development was reported as 5.6% [5]. It is inevitable that this rate stated in this review, which is reported independently of myoma size, will increase as the size of myoma increases. Since the surgical technique will be difficult in cervical fibroids larger than 4 cm, the approach we present in neglected giant fibroids can reduce the risk of surgical complications and prevent the risk of accompanying mortality. In our clinic, we prepare the patient in the dorsal lithotomy position for giant cervical myoma surgery, and we also stain the vaginal and vulvar areas during routine povidone iodide staining. We always start the operation with a median incision below and above the umbilicus, and we always keep an extra person ready in the operation area in case there is a need for vaginal manipulation. Before proceeding to the surgical steps before entering the abdomen, suspending the aorta abdominalis approximately 1 cm above the aortic bifurcation if possible, and if not possible, suspending the arteria iliaca communis with vascular tapes is the most appropriate precaution that can be taken to prevent possible vascular complications and to reduce intraoperative hemorrhage (Fig. 5). The tapes should be left loose throughout the operation, and in the presence of possible bleeding, they are tightened without knotting and fixed with instruments (Fig. 6). In an animal experiment, it was reported that after 1 hour of the abdominal aorta tourniquet method in pigs (swine), all functions returned and no ischemic damage occurred [6]. We suggest that the tapes can be loosened for 1-2 minutes in order to avoid ischemic damage in patients

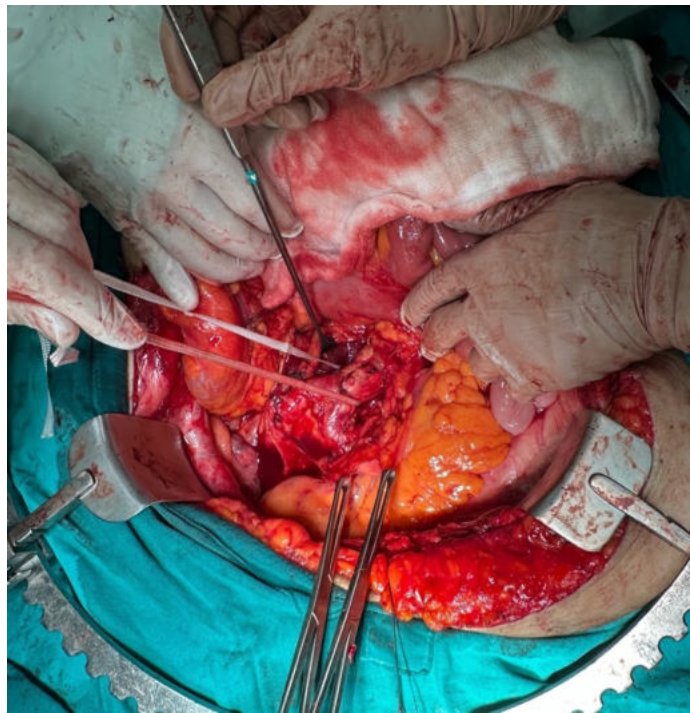


Fig. 5. Suspending the aorta abdominalis approximately 1 cm above the aortic bifurcation.

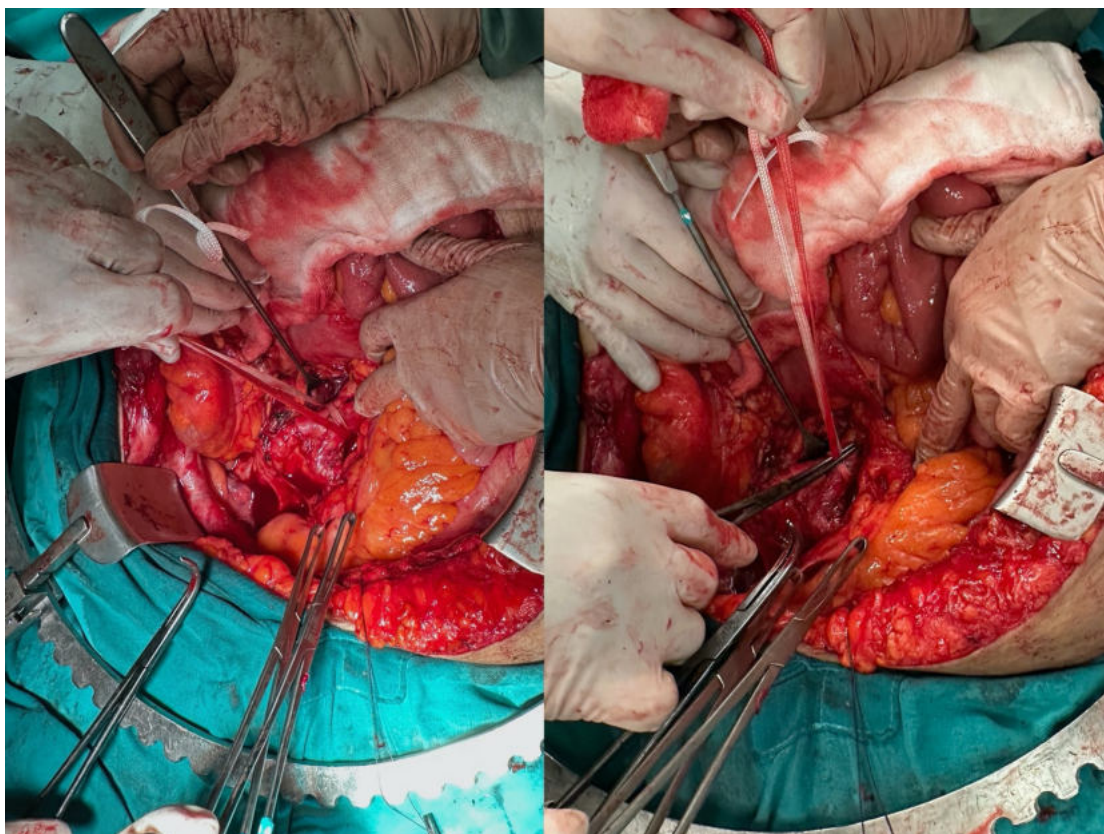


Fig. 6. Intraoperative image of cervical myoma measuring approximately 33 × 17 cm.

who need vascular sling for periods longer than 30 minutes.

Uterine manipulators conventionally placed before surgery may be preferred to facilitate the abdominal approach; however, it may not be possible to use in the presence of masses where the cervix has been eroded and the cervix is bulging towards the vagina. After the arteria uterinae are ligated at the cervico-isthmic junction, the anterior and posterior fornix are balled with the touch of the 3rd person, who will take place between the legs; and the vagina is entered in the relevant region by palpating the fingers on the abdominal vaginal touch and guiding to find the right cleavage. If the fingers cannot be reached, as the sacrouterine ligaments are cut and ligated in classical hysterectomy; after the uterine arteries are ligated, the tissues from the appropriate area are continued to be dissected until they reach the fingers in the vagina. This surgical approach which seems to be simple, can be life-saving when it is considered, as the risk of complications will increase if it is not considered. We called all 3 patients, whom we operated with the method we described, for control 3 times in the 1st year following the operation, and no complications were observed in the post-operative follow-up. The largest reported cervical myomas that we could reach in the literature is the case series published by Tian and Hu [7], which includes 3 cases with a diameter greater than 20 cm. Cervical myoma measuring 20 × 10 cm, which was also published by Wong *et al.*, was one of the largest cervical myomas we could reach [8]. Therefore, with this article, we describe a surgical approach, but also present the neglected cervical fibroids larger than the cervical fibroids in the literature. In the three cases we presented, no malignancy was observed in the pathology report.

Preoperative GnRH agonist, intraoperative vasopressin injection and uterine artery ligation are other methods that can be used to reduce the risk of intraoperative hemorrhage, especially in patients who will undergo myomectomy [9]. As the size of the fibroid increases, it is fed from the surrounding vessels due to increased neovascularization, which may render uterine artery ligation dysfunctional or insufficient in such neglected giant fibroids.

In addition to surgical treatment, radiological techniques are among the alternative treatment options. It seems to be an option that can be preferred especially

in patients who do not want hysterectomy or who want to preserve their fertility. However, a 6-10% failure rate for uterine artery embolization has been reported [10, 11]. In another study, 89% of the patients had post-procedure pain, which they described as severe [12]. In a study published by Kim *et al.* [13], the rate of complete necrosis was reported as only 20%, and the probable cause of this was stated as difficulty in catheterization, feeding of myoma from collaterals coming from the ovarian artery, and the presence of concomitant adenomyosis. Balloon occlusion of the abdominal aorta, which is applied before cesarean sections with a high risk of bleeding, is another alternative to surgery that can be preferred [14]. However, we think that studies on this subject are needed due to risks such as vascular injury, pseudoaneurysm, aortic dissection or rupture, ischemic nerve damage that increase mortality and morbidity [15].

CONCLUSION

For all these reasons and due to the impossibility of applicability of these alternative methods in neglected giant fibroids, we suggest the surgical approach we have described as an alternative method. We think that more studies are needed to standardize the treatment of all cervical myomas and to develop systematic algorithms.

Ethical Approval

These Case Series were approved by İstanbul Prof. Dr. Cemil Tascioglu City Hospital Clinical Research Ethics Committee (Date:20/06/2022, Decision no:206).

Informed Consent

Written informed consent was obtained from the patients for publication of these case series and any accompanying images or data.

Authors' Contribution

Study Conception: CNE, EAY, HAS, OA; Study Design: CNE, MK, HAS, EAK, OA; Supervision: HAS, EAK, OA; Funding: CNE, EAY, MK; Materials: CNE, MK, OA; Data Collection and/or Processing: CNE, EAY, EAK, OA; Statistical Analysis and/or Data Interpretation: CNE, MK, HAS, OA; Literature Re-

view: CNE, EAY, EAK; Manuscript Preparation: CNE, HAS, OA and Critical Review: CNE, OA.

Conflict of interest

The authors disclosed no conflict of interest during the preparation or publication of this manuscript.

Financing

The authors disclosed that they did not receive any grant during conduction or writing of this study.

REFERENCES

1. Stewart EA, Cookson CL, Gandolfo RA, Schulze-Rath R. Epidemiology of uterine fibroids: a systematic review. *BJOG* 2017;124:1501-12.
2. Patel P, Banker M, Munshi S, Bhalla A. Handling cervical myomas. *J Gynecol Endosc Surg* 2011;2:30-2.
3. Munro MG, Critchley HO, Broder MS, Fraser IS; FIGO Working Group on Menstrual Disorders. FIGO classification system (PALM-COEIN) for causes of abnormal uterine bleeding in non-gravid women of reproductive age. *Int J Gynaecol Obstetrics* 2011;113:3-13.
4. Ferrari F, Forte S, Valenti G, Ardighieri L, Barra F, Esposito V, et al. Current treatment options for cervical leiomyomas: a systematic review of literature. *Medicina (Kaunas)* 2021;57:92.
5. Ferrari F, Gubbala K, Campanile RG, Tozzi R. Latest developments and techniques in gynaecological oncology surgery. *Curr Opin Obstet Gynecol* 2015;27:291-6.
6. Kheirabadi BS, Terrazas IB, Miranda N, Voelker AN, Klemcke HG, Brown AW, et al. Long-term consequences of abdominal aortic and junctional tourniquet for hemorrhage control. *J Surg Res* 2018;231:99-108.
7. Tian J, Hu W. Cervical leiomyomas in pregnancy: report of 17 cases. *Aust N Z J Obstet Gynaecol* 2012;52:258-61.
8. Wong J, Tan GHC, Nadarajah R, Teo M. Novel management of a giant cervical myoma in a premenopausal patient. *BMJ Case Rep* 2017;2017:bcr2017221408.
9. Liu WM, Wang PH, Chou CS, Tang WL, Wang IT, Tzeng CR. Efficacy of combined laparoscopic uterine artery occlusion and myomectomy via minilaparotomy in the treatment of recurrent uterine myomas. *Fertil Steril* 2007;87:356-61.
10. Walker WJ, Pelage JP. Uterine artery embolisation for symptomatic fibroids: clinical results in 400 women with imaging follow up. *BJOG* 2002;109:1262-72.
11. Ambekar A, Vogelzang RL. Aberrant uterine artery as a cause of uterine artery embolization treatment failure. *Int J Gynaecol Obstet* 2001;74:59-60.
12. Pelage JP, Jacob D, Fazel A, Namur J, Laurent A, Rymer R, et al. Midterm results of uterine artery embolization for symptomatic adenomyosis: initial experience. *Radiology* 2005;234:948-53.
13. Kim MD, Lee M, Jung DC, Park SI, Lee MS, Won JY, et al. Limited efficacy of uterine artery embolization for cervical leiomyomas. *J Vasc Interv Radiol* 2012;23:236-40.
14. Zhu B, Yang K, Cai L. Discussion on the timing of balloon occlusion of the abdominal aorta during a caesarean section in patients with pernicious placenta previa complicated with placenta accreta. *BioMed Res Int* 2017;2017:8604849.
15. Bishop S, Butler K, Monaghan S, Chan K, Murphy G, Edozien L. Multiple complications following the use of prophylactic internal iliac artery balloon catheterisation in a patient with placenta percreta. *Int J Obstet Anesth* 2011;20:70-3.



This is an open access article distributed under the terms of [Creative Commons Attribution-NonCommercial-NoDerivatives 4.0 International License](https://creativecommons.org/licenses/by-nc-nd/4.0/).